

# *PhD Dissertation 01/2015*

Understanding toxicity as processes in time - Analyzing and modeling effects on algae cell-cycle processes exposed to organic chemicals

Carolina Vogts

---

Understanding toxicity as processes in time

—

Analyzing and modeling effects on algae  
cell-cycle processes exposed to organic  
chemicals

---

Von der Fakultät für Mathematik, Informatik und  
Naturwissenschaften der RWTH Aachen University  
vorgelegte Dissertation zur Erlangung des akademischen Grades  
einer Doktorin der Naturwissenschaften

von

Diplom-Geoökologin Carolina Vogs

aus Wernigerode, Deutschland

Berichter:

Universitätsprofessor Dr. Henner Hollert  
Universitätsprofessor Dr. Rolf Altenburger

Tag der mündlichen Prüfung: 20.10.2015



# Erklärung

Die vorliegende Dissertation wurde im Department Bioanalytische Ökotoxikologie vom UFZ – Helmholtz-Zentrum für Umweltforschung in Zusammenarbeit mit dem Lehr- und Forschungsgebiet für Ökosystemanalyse des Instituts für Umweltforschung (Biologie V) der RWTH Aachen University unter Betreuung von Herrn Prof. Dr. Rolf Altenburger und Herrn Prof. Dr. Henner Hollert angefertigt.

Hiermit versichere ich, dass ich die vorliegende Doktorarbeit selbstständig verfasst und keine anderen als die angegebenen Hilfsmittel verwendet habe. Alle Textauszüge und Grafiken, die sinngemäß oder wörtlich aus veröffentlichten Schriften entnommen wurden, sind durch Referenzen gekennzeichnet.

Diplom-Geoökologin Carolina Vogs

Aachen, den 18. März 2015



”Du siehst die Welt nicht so wie sie ist, du siehst die Welt so wie du bist”

Anthony Paul Moo-Young



# ABSTRACT

The occurrence of agricultural and industrial chemicals in the environment likely causes effects on aquatic organism (Malaj et al., 2014). To assess and estimate the probability of the chemical risk to organisms in the environment, effect models might be able to face major challenges in risk assessment. Effect models, especially modeling toxicokinetic-toxicodynamic (TKTD) processes, have been used to describe and simulate toxicity over time (Lee et al., 2002a; Legierse et al., 1999; Verhaar et al., 1999), the carry-over toxicity following sequential exposure (Ashauer et al., 2007c, 2010; Nyman et al., 2012) and the joint effect on organism exposed to sequential concentrations of a chemical mixture (Ashauer et al., 2007a).

TKTD models abstract toxicological processes by linking the accumulated internal concentration over time to the temporal dynamic of adverse effect like the temporal pattern of survival probability. Toxicokinetic processes describe the time-course of the internal concentration in the entire body by the sum of the chemical mass fluxes uptake in the organism, distribution to the target site, potential biotransformation and elimination back into the ambient exposure medium (Ashauer et al., 2007b, 2013; Jager et al., 2011). The toxicodynamic processes encompass the underlying mechanisms of biologically significant perturbations as sum of the overall damage injury and damage recovery/repair to describe the temporal dynamics of adverse effects (Ashauer et al., 2007b, 2013; Jager et al., 2011). TKTD models have been proposed for different ecotoxicological standard organisms like amphipod and fish species, but have not been established for unicellular algae cells yet. Thus, the first objective of this thesis was to formulate a TKTD model for describing the perturbed growth of the algae *Scenedesmus vacuolatus* causally related to the internal concentration in the entire organism over time (**Chapter 2**). The model formulation based on a pharmacological model that simulated tumor growth kinetics after drug administration (Simeoni et al., 2004). The TKTD model included a total of eleven parameters for characterizing the processes of unperturbed algae growth, kinetics of bioconcentration and toxicodynamic processes. For calibrating purposes, unperturbed and perturbed algae growth changes over one generation cell-cycle (24 h) were measured every two hours for two time-shifted cultures of synchronized *S. vacuolatus* population (**Chapter 2**). Both cultures were exposed to six concentrations of triclosan, norflurazone and n-phenyl-2-naphthylamine (PNA). Internal concentrations over time were simulated by using literature-derived kinetic rates (Sijm et al., 1998). Affected algae cell growth was described well by the developed algae TKTD model. One global toxicodynamic parameter set was estimated for each chemical by global numerical methods. The interpretation of toxicodynamic parameters was limited, because internal concentrations were guessed in the first place. Thus, measuring the internal concentration over time would likely increase the estimation accuracy of toxicodynamic parameters and therefore the models scope for inference.

In comparison to the exposure concentration, the internal concentration is assumed to better reflect the intrinsic toxic potency of a chemical by accounting for variability of toxicokinetic

processes. Internal concentrations have been measured for different ecotoxicological model organisms like fish (Könemann and van Leeuwen, 1980), amphipods (Ashauer et al., 2006b), and fish embryos (Kühnert et al., 2013). To measure concentrations in small-volume organisms, like algae cells, remains still challenging due to the limits of analytical quantification. So far, internal concentrations were analytically determined in batches of large algae biomass for highly accumulative organic chemicals ( $\log K_{OW} > 5$ ) with nonspecific mode of action. Nevertheless, bioconcentration kinetics in algae cells have rarely been studied for structurally diverse chemicals and different physicochemical properties that may differ in their binding affinities toward different classes of lipids and proteins. Thus, the second objective of this thesis was to determine the chemicals accumulation in *S. vacuolatus* over time (**Chapter 3**). Kinetics of bioconcentration in algae cells were examined for chemicals of one group with lower hydrophobicity ( $\log K_{OW} < 3$ : isoproturon, metazachlor, paraquat) and one group with moderate hydrophobicity ( $\log K_{OW} > 4$ : irgarol, triclosan, PNA) by using an indirect approach (Fahl et al., 1995; Manthey et al., 1993). The indirect method reported by Fahl et al. (1995); Manthey et al. (1993) was modified in order to measure the exposure concentration in the ambient medium which was assumed to decline as a consequence of chemical uptake in algae cells over time. To this end, a sufficient high algae biomass spanning from  $1 \times 10^{10}$  to  $1 \times 10^{12}$  cells  $L^{-1}$  was adjusted according to the hydrophobicity of the chemical. Nearly equilibrium concentrations were reached within minutes due to partitioning-driven distribution processes. Altered kinetics of bioconcentration occurred, which could not be explained by partitioning-driven distribution processes only. Here, other influential factors like ionization of chemicals, the ion trapping mechanism, or the potential susceptibility for biotransformation were discussed. The toxicokinetic parameters were successfully estimated by fitting a one-compartment model to the measured concentration decline. The intrinsic potency of a chemical was derived by the estimated internal concentration causing 50% inhibition of *S. vacuolatus* reproduction and spanned from 0.05 to 7.61  $mmol\ kg^{-1}$ . Knowing the kinetics of bioconcentration of structurally diverse chemicals with lower and moderate hydrophobicity further allows for investigating how toxicokinetic processes contribute to the overall damage development over time in algae cells.

A few studies have shown that damage on algae photosynthesis or growth cumulatively increases over hours (Altenburger et al., 2006; Franz et al., 2008; Vogs et al., 2013). By contrast, the internal concentration in the unicellular green algae reaches equilibrium very fast, namely within minutes supposedly due to hydrophobicity-driven partitioning processes (Vogs et al., 2015). Thus, the observed time-gap of hours between steady state of internal concentration and the development of damage in algae cells might be explainable assuming another rate-limiting toxicodynamic step. Moreover, a rate-limiting toxicodynamic step might vary depending on the progress of effect towards an adverse outcome for different adverse outcome pathways (AOPs). An AOP is a proposed theoretical framework for portraying existing toxicological knowledge to provide the mechanistic linkage of an initial molecular event over key events to an adverse outcome (Ankley et al., 2010). In this thesis, a joint approach between experimentation and TKTD modeling was provided to (i) analyze the contribution of toxicokinetic and toxicodynamic processes of chemicals to toxicity over time and to (ii) estimate rates that characterize the rate-limiting toxicodynamic step for different types of AOPs (**Chapter 4**). Six model chemicals were chosen in order to represent two hydrophobicity groups ( $\log K_{OW} < 3$ : isoproturon, metazachlor, paraquat and  $\log K_{OW} > 4$ : irgarol, triclosan, PNA) as well as three groups of different AOPs. Isoproturon and irgarol are known to inhibit the functioning of photosynthesis, metazachlor and triclosan block the lipid biosynthesis, and paraquat and PNA

represent reactive chemicals. The dynamics of estimated internal concentrations were linked to the algae growth affected by specifically acting and reactive chemicals through the algae TKTD model. As one result, toxicities were mainly driven by the rate-limiting step for the progress of the effect towards the adverse outcome on the organism level. Furthermore, the estimated rates of effect progression spanned over six orders of magnitude between all six chemicals, but less than one order of magnitude between chemicals of similar biological activity. To conclude, the function of effect progression towards an adverse outcome can be aggregated by process parameters. Process parameters were estimated by calibrating effect models to time- and concentration-dependent responses. Parameter values aggregating toxicokinetic and toxicodynamic processes were quantified within a biological meaningful range in respect of the previous formulated hypotheses.

Based on the dissertations' results, subsequent research is suggested that anchors changes of molecular responses to the adverse outcome on algae growth or reproduction by using an extended algae TKTD model based on physiologic indirect response models (Jin et al., 2003; Jusko, 2013; Ramakrishnan et al., 2002). Furthermore, known bioconcentration kinetics as well as toxicodynamic parameters (no-effect concentration, injury rate constant, repair/recovery rate constant, effect progression rates for different types of AOPs) enables to assess and estimate combined effects on the unicellular green algae over time and carry-over toxicity following a sequential exposure of a chemical cocktail of low concentrations.



# Zusammenfassung

Anthropogene, organische Spurenchemikalien stehen im Verdacht Effekte auf aquatische Organismen zu verursachen (Malaj et al., 2014). Modelle zur Beschreibung von Effekten auf Organismen, wie z.B. toxikokinetische-toxikodynamische (TKTD) Modelle, könnten wesentliche Schwierigkeiten bei der Risikobewertung von Chemikalien unter Umweltbedingungen bewältigen. TKTD Modelle werden angewendet um die Toxizität über die Zeit (Lee et al., 2002a; Legierse et al., 1999; Verhaar et al., 1999), den "Carryover"-Effekt in Folge einer sequentiellen Exposition (Ashauer et al., 2007c, 2010; Nyman et al., 2012) und die Kombinationswirkung in Folge der sequentiellen Exposition einer Chemikalienmischung auf den Organismus (Ashauer et al., 2007a) zu beschreiben und zu simulieren.

Bei TKTD Modellen wird die Expositionskonzentration mit den Dynamiken der adversen Effekte über die aufgenommene Chemikalienmenge verbunden. Hierbei beschreiben die toxikokinetische Prozesse den zeitlichen Verlauf der internen Konzentration im Organismus, welches das Ergebnis der summierten Massenflüsse Absorption, Verteilung, Biotransformation und Ausscheidung ist (Ashauer et al., 2007b, 2013; Jager et al., 2011). Des Weiteren werden toxikodynamische Prozesse durch die zwei Prozessparameter Schädigungs- und Erholungsrate zur Simulation von Effektdynamiken zusammengefasst (Ashauer et al., 2007b, 2013; Jager et al., 2011). TKTD Modelle wurden für verschiedene ökotoxikologische Standardorganismen (wie z.B. Fische oder wirbellose Tiere) vorgeschlagen, jedoch existiert bisher kein TKTD Modell für die Grünalge. Daher bestand das erste Ziel der vorliegenden Dissertation in der Formulierung eines TKTD Modelles, welches das gestörte Algenwachstum der einzelligen Grünalge *Scenedesmus vacuolatus* im Bezug zur jeweiligen aufgenommenen Chemikalienmenge beschreibt (**Kapitel 2**). Die Modellformulierung basierte auf einem pharmakologisches Modell, welches das Wachstum von Krebszellen nach medikamentöser Behandlung charakterisiert (Simeoni et al., 2004). Das entwickelte TKTD Modell besteht aus insgesamt elf Parametern, mit welchen das ungestörte Algenwachstum, die Biokonzentrationskinetiken und die toxikodynamischen Prozesse abgebildet werden. Zur Modellkalibration wurde das ungestörte sowie das gestörte Algenwachstum eines Generationszyklus (24) von zwei zeitverschobenen, synchronisierten *S. vacuolatus* Populationen alle zwei Stunden gemessen (**Kapitel 2**). Dabei wurde das gestörte Wachstum in Abhängigkeit von sechs Konzentrationen pro Chemikalie (Triclosan, Norflurazon, N-Phenyl-2-Naphthylamin (PNA)) beobachtet. Obwohl die Biokonzentrationskinetiken auf einer ersten groben Schätzung anhand Literaturangaben basierte, wurde das gestörte Algenwachstum durch das TKTD Modell korrekt beschrieben. Ein globaler toxikodynamischer Parametersatz je Chemikalie wurde unter Verwendung von globalen numerischen Methoden geschätzt. Schätzungsgenauigkeit und -sicherheit der Parameter würden jedoch durch die Bestimmung der internen Konzentrationsverläufe in der Grünalge gesteigert werden und könnten damit zur Interpretation der Wirkungsweise einer Chemikalie auf die biologische Aktivitäten in aquatischen Organismen herangezogen werden.

Die Konzentration der Chemikalie in der Zelle ist ein besseres Maß zur Beschreibung

der spezifisch-chemikalischen Wirksamkeit als die Konzentration im Expositionsmedium, weil die Nutzung der interne Konzentration die durch toxikokinetische Prozesse verursachte Datenvariabilität bereits einbezieht. Daher wurde der Zeitverlauf der interne Chemikalienkonzentration in verschiedenen Organismen wie z.B. Fische (Könemann and van Leeuwen, 1980), wirbellosen Tiere (Ashauer et al., 2006b) oder Fischembryonen (Kühnert et al., 2013) bestimmt. Aufgrund von analytischen Bestimmungslimits stellt die Quantifizierung geringer aufgenommener Konzentrationen in kleinvolumigen Organismen wie Algenzellen eine Herausforderung dar. Bisher wurden interne Konzentrationen für anreichernde Substanzen ( $\log K_{OW} > 5$ ) mit nicht-spezifischer Wirkung in Algensuspension mit hoher Biomasse quantifiziert. Dagegen gibt es wenige Studien über Biokonzentrationskinetiken von Chemikalien komplexer Struktur unterschiedlicher physikochemischer Eigenschaften in Algenzellen, obwohl diese Chemikalien verschiedene Bindungsaffinitäten mit diversen Protein- und Lipidklassen aufweisen können. Aus diesem Grund wurde ein toxikokinetischer Assay zur Bestimmung von Biokonzentrationskinetiken in der Grünalge entwickelt (**Kapitel 3**). Hierfür wurde eine indirekte Methode von Fahl et al. (1995) und Manthey et al. (1993) zur Bestimmung der Biokonzentrationskinetik modifiziert. Die Abnahme der Expositionskonzentration im Umgebungsmedium eines statischen Systems resultierte aus der aufgenommenen Chemikalienmengen über die Zeit in den Algenzellen. Die eingesetzten Algenmassen variierten entsprechend den Hydrophobizitäten der Chemikalien von  $1 \times 10^{10}$  bis  $1 \times 10^{12}$  Zellen  $L^{-1}$ . Biokonzentrationskinetiken wurden erfolgreich für Chemikalien mit geringer Hydrophobizität ( $\log K_{OW} < 3$ : Isoproturon, Metazachlor, Paraquat) und für Chemikalien mit moderater Hydrophobizität ( $\log K_{OW} > 4$ : Irgarol, Triclosan, PNA) bestimmt. Gleichgewichtskonzentrationen wurden bereits nach einigen Minuten erreicht, wobei die Geschwindigkeit der Gleichgewichtseinstellung von der Hydrophobizität gesteuert wurde. Andere Prozesse wie die extra- und intrazelluläre chemikalische Dissoziation, der "ion trapping" Mechanismus oder die Fähigkeit zur Biotransformation wurden als beeinflussende Prozesse diskutiert, die einen veränderten Zeitverlauf der Konzentrationsabnahme erklären könnten. Die toxikokinetische Parameter wurden erfolgreich durch die inverse Modellierung der gemessenen Konzentrationsverläufe mit einem Einkompartiment-Modell geschätzt. Die inhärente Wirksamkeit der Chemikalien wurde durch die geschätzte interne Konzentration bestimmt und variierte von 0.05 bis  $7.61 \text{ mmol kg}^{-1}$ . Mit der Bestimmung der Biokonzentrationskinetiken von Chemikalien unterschiedlicher Struktur und physikochemischer Eigenschaften wurde in einer weiteren Studie der Beitrag von toxikokinetischen Prozessen zu der Toxizitätsentwicklung bei Algenzellen untersucht.

Einige Studien zeigten, dass Schädigungen auf photosynthetischen Funktionen und Algenwachstums über Stunden kumulativ ansteigen (Altenburger et al., 2006; Franz et al., 2008; Vogs et al., 2013). Im Gegensatz dazu erreicht die interne Konzentration einer Chemikalie innerhalb weniger Minuten den Gleichgewichtszustand (Vogs et al., 2015). Der Zeitverlauf des internen Konzentrationanstieges kann die Schädigungsentwicklung über mehrere Stunden alleine nicht erklären. Daher könnte ein weiterer zeitlimitierender Prozess die beobachtete Effektverzögerung beschreiben. In **Kapitel 5** wurde untersucht, ob der zeitlimitierende Prozess von den verschiedenen Wirkungsweisen der Chemikalien auf die Algenzelle abhängt. Es wurde angenommen, dass die Fortpflanzung eines Effektes von der Interaktion einer Chemikalie mit einem biologischen Zielmolekül hin zur negativen Wirkung zeitabhängig ist (Ankley et al., 2010). Ferner wurde untersucht, ob diese Effektfortpflanzung verschiedener Wirkungsweisen von Chemikalien auf der Basis von Prozessparameter unterscheidbar ist. Deswegen wurde

zuerst analysiert in welchem zeitlichen Maß toxikokinetische und toxikodynamische Prozesse von spezifisch-wirkenden und reaktiven Chemikalien auf die Effektdynamiken auswirken. Der Einfluß verschiedener Hydrophobizitäten und Wirkungsweisen auf das gestörte Algenwachstum wurde für sechs Chemikalien betrachtet. Hierfür wurden Chemikalien ausgewählt, welche einerseits zwei Hydrophobizitätsgruppen ( $\log K_{OW} < 3$ : Isoproturon, Metazachlor, Paraquat und  $\log K_{OW} > 4$ : Irgarol, Triclosan, PNA) und andererseits drei Wirkungsweisen auf Algenzellen repräsentieren. Isoproturon und Irgarol hemmen spezifisch die photosynthetische Funktion, Metazachlor und Triclosan blockieren die Lipidbiosynthese und Paraquat und PNA sind reaktive Chemikalien. In einem zweiten Schritt wurden die Prozessparameter des TKTD Modelles anhand der gemessenen Wachstumsstörungen bestimmt. Hierzu wurden die Veränderungen der internen Chemikalienkonzentration mit dem gestörten Algenwachstum durch das entwickelte TKTD Modell verbunden. Diese Studie zeigte, dass der Toxizitätsverlauf hauptsächlich durch den zeitlimitierenden Prozess der Effekfortpflanzung zwischen den verschiedenen biologischen Ebenen bei Algen dominiert wird. Ferner wurde dargestellt, dass die geschätzten Effekfortpflanzungsraten über sechs Größenordnungen variieren, sich die Parametervariabilität zwischen den Chemikalien ähnlicher Wirkweisen aber auf einer Größenordnung reduziert ist (**Kapitel 5**). Demnach konnten toxikodynamische Prozessparameter durch die Modellkalibrierung von zeit- und konzentrationsabhängigen Wirkungsantworten bestimmt werden.

Basierend auf den Dissertationsergebnissen wird für zukünftige Forschungsvorhaben vorgeschlagen, Änderungen von molekularen Antworten hin zu dem adversen Effekt auf das Algenwachstum oder -reproduktion mit Hilfe eines erweiterten Algenmodelles zu untersuchen und zu verbinden. Hierfür können Modelle aus der Pharmakologie zur Beschreibung von physiologisch indirekten Effekten herangezogen werden (Jin et al., 2003; Jusko, 2013; Ramakrishnan et al., 2002). Weiterhin kann durch die Bestimmung von Biokonzentrationskinetiken und toxikodynamischer Parametersets (Schädigungs- und Erholungsrate, Nichteffektkonzentration, Effekfortpflanzungsrate) ermöglicht, die Kombinationswirkung bei sequentieller Mischungsexposition geringer Konzentrationen zu erforschen und zu bewerten.



# Contents

<b>List of Figures</b>	<b>xx</b>
<b>List of Tables</b>	<b>xxii</b>
<b>Abbreviations and Symbols</b>	<b>xxiii</b>
<b>1 Introduction to effect modeling in ecotoxicology</b>	<b>1</b>
1.1 Chemical pollution in the environment . . . . .	1
1.2 Risk assessment processes . . . . .	2
1.3 Understanding toxicity as time- and concentration-dependent processes . . . . .	4
1.4 One-step model: The critical body residue as dose surrogate for narcotic mode of action . . . . .	5
1.5 One-step model: The critical area under the curve as dose surrogate for specifically acting and reactive chemicals . . . . .	7
1.6 The two-step model "Damage Assessment Model": Linking a constant exposure to effects through modeling of toxicokinetic-toxicodynamic processes . . . . .	8
1.7 The two-step model "Threshold Damage Model": Estimation of an effect on aquatic organisms from fluctuating and pulsed exposure to chemicals . . . . .	9
1.8 Lessons learned of applied model concepts for the estimation of effects on aquatic organisms . . . . .	10
1.9 The unicellular algae <i>Scenedesmus vacuolatus</i> as model organism . . . . .	13
1.10 Goals and structure of this dissertation . . . . .	15
<b>2 Effect progression in a toxicokinetic-toxicodynamic model explains delayed effects on the growth of unicellular green algae <i>Scenedesmus vacuolatus</i></b>	<b>17</b>
2.1 INTRODUCTION . . . . .	18
2.2 METHODOLOGY . . . . .	19
2.2.1 Algae cultivation . . . . .	19
2.2.2 Algae growth assay . . . . .	20
2.2.3 Statistical analysis . . . . .	20
2.2.4 Modeling of the concentration-response relationship for different exposure times . . . . .	20
2.2.5 Determination of n-phenyl-2-naphthylamine uptake kinetics . . . . .	21
2.2.6 The toxicokinetic-toxicodynamic model . . . . .	21
2.2.7 Estimation of model parameters and model analysis . . . . .	24
2.3 RESULTS . . . . .	27
2.3.1 Unperturbed algae growth . . . . .	27
2.3.2 Perturbed algae growth pattern in dependency of exposure concentration and exposure time . . . . .	29

2.3.3	Time dependence of toxicity . . . . .	31
2.3.4	Toxicokinetic-toxicodynamic modeling . . . . .	32
2.4	DISCUSSION . . . . .	34
2.4.1	Data quality assessment . . . . .	34
2.4.2	Toxicokinetic-toxicodynamic modeling framework . . . . .	35
2.4.3	Modeling of algae growth . . . . .	36
2.4.4	Toxicokinetic Modeling . . . . .	36
2.4.5	Toxicodynamic Modeling . . . . .	38
2.5	CONCLUDING REMARKS & OUTLOOK . . . . .	40
<b>3</b>	<b>A toxicokinetic study of specifically acting and reactive organic chemicals for the prediction of internal effect concentrations in <i>Scenedesmus vacuolatus</i></b>	<b>43</b>
3.1	INTRODUCTION . . . . .	44
3.2	METHODOLOGY . . . . .	46
3.2.1	Algae cultivation . . . . .	46
3.2.2	Experimental design for measuring the chemical depletion in the ambient medium . . . . .	46
3.2.3	Quantification of the ambient concentration over time . . . . .	48
3.2.4	The toxicokinetic model . . . . .	49
3.2.5	Parameter estimation and Mathematica settings . . . . .	49
3.2.6	Prediction of internal effect concentration . . . . .	50
3.3	RESULTS . . . . .	50
3.3.1	Quantification of concentration decline in the ambient medium and pH-dependent molecular speciation of the chemicals . . . . .	50
3.3.2	Toxicokinetic modeling . . . . .	52
3.3.3	From measured external exposure concentration to predicted internal effect concentration . . . . .	56
3.4	DISCUSSION . . . . .	58
3.4.1	Data quality assessment . . . . .	58
3.4.2	Time for reaching chemical equilibration between ambient medium and algae biomass . . . . .	59
3.4.3	Estimated toxicokinetic parameters . . . . .	61
3.4.4	From measured external exposure to predicted internal effect concentrations	63
3.5	CONCLUDING REMARKS & OUTLOOK . . . . .	63
<b>4</b>	<b>How toxicokinetic and toxicodynamic processes in <i>Scenedesmus vacuolatus</i> contribute to the time dependence of toxicity? - A modeling case study for different adverse outcome pathways</b>	<b>65</b>
4.1	INTRODUCTION . . . . .	66
4.2	METHODOLOGY . . . . .	68
4.2.1	Algae cultivation . . . . .	68
4.2.2	Modeling of the concentration-response relationship for different exposure times . . . . .	68
4.2.3	Toxicokinetic and toxicodynamic modeling . . . . .	69
4.2.4	Model calibration and parameter estimation . . . . .	70
4.3	RESULTS . . . . .	71
4.3.1	Unperturbed algae growth . . . . .	71

4.3.2	Perturbed algae growth pattern in dependence of exposure concentration and exposure time . . . . .	71
4.3.3	Time dependence of toxicity . . . . .	73
4.3.4	Contribution of toxicokinetic processes to the toxicity development over time . . . . .	75
4.3.5	Toxicokinetic-toxicodynamic modeling . . . . .	75
4.4	DISCUSSION . . . . .	77
4.4.1	Data quality assessment . . . . .	77
4.4.2	Time dependence of median effect concentrations . . . . .	78
4.4.3	Toxicokinetic-toxicodynamic modeling framework . . . . .	79
4.4.4	Estimated no-effect concentration . . . . .	80
4.4.5	Estimated injury rate constant and repair/recovery rate constant . . . . .	80
4.4.6	Estimated effect progression rate constants for different adverse outcome pathway . . . . .	82
4.5	CONCLUDING REMARKS & OUTLOOK . . . . .	83
<b>5</b>	<b>Synthesis</b>	<b>85</b>
5.1	Developed tool: toxicokinetic-toxicodynamic modeling of <i>S. vacuolatus</i> growth .	86
5.2	"How fast accumulate structurally diverse chemicals with different physicochemical properties in algae cells?" . . . . .	88
5.3	"How toxicokinetic and toxicodynamic processes contribute to the overall toxicity development in algae cells over time?" . . . . .	89
5.4	Implication of toxicokinetic-toxicodynamic modeling in current risk assessment .	90
<b>6</b>	<b>Implementation challenges</b>	<b>93</b>
6.1	Refinement and modeling of toxicokinetic processes in algae cells . . . . .	93
6.2	Extrapolation concepts for dealing with multiple contamination . . . . .	94
6.3	Linkage of effects across multiple biological levels towards an adverse outcome at the individual or population level . . . . .	95
	<b>Bibliography</b>	<b>97</b>
<b>A</b>	<b>Supplementary information for Chapter 2</b>	<b>111</b>
<b>B</b>	<b>Supplementary information for Chapter 3</b>	<b>119</b>
<b>C</b>	<b>Supplementary information for Chapter 4</b>	<b>133</b>
	<b>Acknowledgment</b>	<b>145</b>
	<b>Curriculum Vitae</b>	<b>147</b>
	<b>List of Publications</b>	<b>149</b>



# List of Figures

1.1	A simplified scheme of the relationship between toxicokinetic and toxicodynamic processes as implemented in current effect models. . . . .	11
2.1	Conceptual scheme of the algae toxicokinetic-toxicodynamic model. . . . .	22
2.2	Two-dimensional example of the "Differential Evolution" method. . . . .	26
2.3	Unperturbed growth of the synchronized <i>S. vacuolatus</i> algae cell. . . . .	28
2.4	Measured effect parameter cell volume and cell number over time in dependence of six triclosan, norflurazone and PNA concentrations, respectively. . . . .	29
2.5	Concentration-dependent relationship of inhibited effect parameters. . . . .	30
2.6	The time-course of estimated $EC_{50}(t)$ -values and slope-values $\theta(t)$ for triclosan, norflurazon and PNA, respectively. . . . .	31
2.7	Observed and model-fitted toxicokinetic and toxicodynamic processes for triclosan, norflurazon, and PNA. . . . .	34
2.8	Consideration of the PNA uptake kinetic in <i>S. vacuolatus</i> cells derived by analytical measured concentrations for TKTD modeling. . . . .	40
3.1	General scheme illustrating kinetics of bioconcentration processes for basic and acid chemicals in a green algae cell <i>S. vacuolatus</i> . . . . .	45
3.2	Time-dependent exposure concentrations of individual experiments measured in exposure medium without algae and in exposure medium with different algae densities. . . . .	52
3.3	Estimated uptake rate constants in dependency of the chemical's hydrophobicity. . . . .	53
3.4	Estimated uptake rate constants related to the used cell densities. . . . .	55
3.5	Estimated overall elimination rate constants in dependency of the chemical's hydrophobicity. . . . .	56
3.6	Estimated overall elimination rate constants related to the used cell densities. . . . .	57
3.7	Calculated bioconcentration factor ( $\log BCF_{kin}$ ) related to the chemical's $\log K_{OW}$ . . . . .	57
4.1	Conceptual scheme illustrating toxicokinetic and toxicodynamic processes for an adverse outcome pathway. . . . .	67
4.2	Concentration-response curves of inhibited algae growth at $t_{14}$ and algae reproduction at $t_{24}$ as result of the preliminary range-finding test for all chemicals. . . . .	72
4.3	Measured and simulated perturbed algae growth pattern affected by six concentrations per chemical. . . . .	73
4.4	Time-course of the effect concentrations in comparison to the time-course of the estimated internal concentration for all analyzed chemicals. . . . .	74
C.1	Measured and simulated unperturbed growth of <i>S. vacuolatus</i> synchronized cultures. . . . .	142

C.2	Measured cell volumes of the first- and second-generation algae cycle at different time points affected by six different concentrations per chemical . . . . .	143
C.3	Measured cell numbers of the first- and second-generation algae cycle at different time points affected by six different concentrations per chemical . . . . .	144

# List of Tables

1.1	Overview about the various toxicokinetic-toxicodynamic models that have been used to explain the mortality dynamics for different biosystems. . . . .	12
2.1	Parameter estimates, their 95% confidence intervals, and goodness-of-fit parameters of the cell-cycle model and the TKTD model. . . . .	33
3.1	Chemical identity, sources, molecular structure, and relevant physicochemical properties of the chemicals used as well as the biological processes known to be affected by the chemicals are listed. . . . .	47
3.2	Estimated toxicokinetic parameters and bioconcentration factors . . . . .	54
3.3	Estimated internal effect concentrations $IEC_{50}$ . . . . .	58
4.1	Estimated parameters to characterize unperturbed algae growth, toxicokinetic and toxicodynamic parameters as well as as goodness-of-fit indicators . . . . .	76
A.1	Measured cell number for two untreated algae cell cultures, two DMSO-treated algae cell cultures (DMSO1/DMSO2) and norflurzon-treated algae cultures exposed to six concentrations. . . . .	112
A.2	Measured cell volume for two untreated algae cell cultures, two DMSO-treated algae cell cultures (DMSO1/DMSO2) and norflurzon-treated algae cultures exposed to six concentrations. . . . .	113
A.3	Measured cell number for two untreated algae cell cultures, two DMSO-treated algae cell cultures (DMSO1/DMSO2) and PNA-treated algae cultures exposed to six concentrations. . . . .	114
A.4	Measured cell volume for two untreated algae cell cultures, two DMSO-treated algae cell cultures (DMSO1/DMSO2) and PNA-treated algae cultures exposed to six concentrations. . . . .	115
A.5	Measured cell number for two untreated algae cell cultures, two DMSO-treated algae cell cultures (DMSO1/DMSO2) and triclosan-treated algae cultures exposed to six concentrations. . . . .	116
A.6	Measured cell volume for two untreated algae cell cultures, two DMSO-treated algae cell cultures (DMSO1/DMSO2) and triclosan-treated algae cultures exposed to six concentrations. . . . .	117
A.7	Analytical determined PNA concentrations in GB-medium without algae and in algae suspension over 256 minutes. . . . .	118
A.8	Estimated effect concentrations ( $EC_{50}(c,t)$ values) and slopes ( $\theta$ )(c,t) for triclosan, norflurazon and PNA, respectively . . . . .	118

B.1	Analytical concentrations measured in the ambient medium with algae and without algae (C) for irgarol, isoproturon, triclosan, metazachlor, paraquat, and n-phenyl-2-naphthylamine. . . . .	120
B.2	Calculated fraction of neutral irgarol species in dependency of measured ambient medium pH as well as in dependency of cytoplasmatic pH measured under aerobic and anaerobic conditions. . . . .	129
B.3	Calculated fraction of neutral isoproturon species in dependency of measured ambient medium pH as well as in dependency of cytoplasmatic pH measured under aerobic and anaerobic conditions. . . . .	129
B.4	Calculated fraction of neutral triclosan species in dependency of measured ambient medium pH as well as in dependency of cytoplasmatic pH measured under aerobic and anaerobic conditions. . . . .	130
B.5	Calculated fraction of neutral metazachlor species in dependency of measured ambient medium pH as well as in dependency of cytoplasmatic pH measured under aerobic and anaerobic conditions. . . . .	130
B.6	Calculated fraction of neutral PNA species in dependency of measured ambient medium pH as well as in dependency of cytoplasmatic pH measured under aerobic and anaerobic conditions. . . . .	131
C.1	The cell volume measured every two hours for two untreated algae cell cultures, two DMSO-treated algae cell cultures and PNA-treated algae cultures exposed to six concentrations. . . . .	134
C.2	The cell volume measured every two hours for two untreated algae cell cultures, two DMSO-treated algae cell cultures and irgarol-treated algae cultures exposed to six concentrations. . . . .	135
C.3	The cell volume measured every two hours for two untreated algae cell cultures, two DMSO-treated algae cell cultures and isoproturon-treated algae cultures exposed to six concentrations. . . . .	136
C.4	The cell volume measured every two hours for two untreated algae cell cultures, two DMSO-treated algae cell cultures and metazachlor-treated algae cultures exposed to six concentrations. . . . .	137
C.5	The cell volume measured every two hours for two untreated algae cell cultures, two DMSO-treated algae cell cultures and paraquat-treated algae cultures exposed to six concentrations. . . . .	138
C.6	The cell volume measured every two hours for two untreated algae cell cultures, two DMSO-treated algae cell cultures and triclosan-treated algae cultures exposed to six concentrations. . . . .	139
C.7	Estimated mean values and standard errors of parameters for the concentration-response relationships . . . . .	140
C.8	Estimated mean values and their standard errors ( $EC_{50}$ ) and ( $\theta$ ) for different exposure times. . . . .	140
C.9	Coefficient of variation calculated for the estimated algae growth and toxicodynamic parameters. . . . .	141
C.10	Values of measured effect concentrations and predicted internal effect concentrations for algae growth at $t_{14}$ and algae reproduction at $t_{24}$ from this study compared to values from literature for all six model chemicals. . . . .	141

# Abbreviations and Symbols

## Abbreviations

AChE	Acetylcholinesterase
AOP	Adverse Outcome Pathway
BCF	Bioconcentration Factor
CAS RN	Chemical Abstract Service Register Number
CAUC	Critical Area Under the Curve
CBR	Critical Body Burden
CI	Confidence Interval
CoV	Coefficient of Variance
CTO	Critical Target Occupation
DAM	Damage Assessment Model
DMSO	Dimethyl Sulfoxide
E	Effect
GB-medium	Grimme-Boardman-Medium
GC-MS	Gas Chromatography-Mass Spectrometry
GUTS	General Unified Threshold Model of Survival
HPLC	High-Performance Liquid Chromatography
IEC	Internal Effect Concentration
ISO	International Organization for Standardization
MEA	Mean Absolute Error
NEC	No-Effect Concentration
NOEC	No Observed Effect Concentration
OECD	Organization of Economic Cooperation and Development
PEC	Predicted Environmental Concentration
PKPD model	Pharmacokinetic-Pharmacodynamic Model
PNA	N-phenyl-2-naphthylamine
PNEC	Predicted No Effect Concentration
QSAR	Quantitative Structure-Activity Relationship
R <sup>2</sup>	Regression Coefficient
RA	Risk Assessment
RMSE	Root Mean Squared Error
<i>S. vacuolatus</i>	<i>Scenedesmus vacuolatus</i>
SETAC	Society of Environmental Toxicology and Chemistry
TDM	Threshold Damage Model
TKTD model	Toxicokinetic-Toxicodynamic Model
WFD	EU Water Framework Directive

## Symbols

$BCF_{kin}$	Kinetic Bioconcentration Factor
$BCF_{ss}$	Steady State Bioconcentration Factor
$C(t)$	Exposure Concentration of the Ambient Medium
$C_{int}(t)$	Internal Concentration in the Entire Organism
$CAUC_{oxon}$	Critical Area Under the Curve of the Oxon Analog
$D(t)$	Damage
$D_n$	Damage Stage n
$E_{max}$	Maximum Effect Level
$E_{min}$	Minimum Effect Level
$EC_{50}$	Median Effect Concentration
$EP_{Control}$	Effect Measures of Untreated Samples
$EP_{Treatment}$	Effect Measures of Treated Samples
$I(t)$	Inhibition
$k_3$	Dimensionless Coefficient
$k_{act}$	Metabolic Activation Rate Constant
$K_{Crit}$	Cell Volume of the Commitment Point
$k_I$	Injury Rate Constant
$k_i$	Inhibition Rate Constant
$k_{in}$	Uptake Rate Constant
$k_{out}$	Overall Elimination Rate Constant
$K_{OW}$	Octanol-Water Partition Coefficient
$k_R$	Recovery/Repair Rate Constant
$LC_{50}$	Median Lethal Concentration
$S(t)$	Survival Probability
$t_i$	Time Point $i$
$V_0$	Initial Cell Volume
$V_{Control}(t)$	Cell Volume of Unperturbed Algae Growth
$V_{th}(t)$	Threshold Cell Volume
$V(t)$	Mean Cell Volume
$\mu_C$	Cell-clock Growth Rate
$\mu_E$	Exponential Growth Rate
$\mu_L$	Linear Growth Rate
$\Phi$	Force the Switch from Exponential to Linear Growth Phase
$\tau$	Effect Progression Rate
$\theta$	Slope of the Concentration-Response Curve

# Introduction to effect modeling in ecotoxicology

## 1.1 Chemical pollution in the environment

Human activities like land cover change, urbanization and industrialization have impaired ecosystems since several decades in order to increase the access to natural resources for an exponential growing population (Carpenter et al., 2011; Vörösmarty et al., 2010). The impairment of human interventions on earth-system processes transgressed planetary boundaries for biodiversity loss, nitrogen and phosphorus cycle and climate change (Rockström et al., 2009; Steffen et al., 2015). The boundaries for global freshwater use, change in land use and ocean acidification seems to approach towards the threshold values when keeping the current human activity (Rockström et al., 2009). Furthermore, Rockström et al. (2009) analyzed that the planetary boundaries of atmospheric aerosol loading and chemical pollution have not been quantified yet. Nevertheless, humanity is facing an increasing worldwide contamination of freshwater ecosystems with an unknown threat to human water security and biodiversity (Schwarzenbach et al., 2006, 2010; Vörösmarty et al., 2010).

More than 30% of the accessible global freshwater resources are used for agricultural, industrial and domestic purposes (Jackson et al., 2001; Schwarzenbach et al., 2006). The anthropogenic activities lead to water contamination with diverse inorganic and organic chemicals. Agrochemicals, pharmaceuticals, hormones, industrial and consumer products, acids, alkalis, and heavy metals have been reported to occur in aquatic ecosystems (Daughton and Ternes, 1999; Eriksson et al., 2002; Kolpin et al., 2002; Reinert et al., 2002; Schwarzenbach et al., 2006, 2010; Wittmer et al., 2010). Around 14 million chemicals exist, from which more than 100,000 synthetic chemicals are daily used in consumer products in the European Union (Hartung and Rovida, 2009; Schwarzenbach et al., 2010; von der Ohe et al., 2009). Thus, an uncertain number of chemicals may potentially be released into the aquatic environment by diverse routes like point sources, remobilization from contaminated sediments and groundwater input (Ritter et al., 2002). Moreover, agrochemicals may enter the aquatic environment by soil run-off, spray drift, surface runoff, or drainage (Ashauer et al., 2006a; Brock et al., 2006). Depending on the physicochemical properties, a chemical can persist in the aquatic environment (e.g., polychlorinated biphenyls, polychlorinated dibenzofurans, hexachlorobenzene), can be distributed via water or air over long distances (e.g., polychlorinated biphenyls), can be transformed to even more toxic products (e.g. the biocide triclosan degrades to methyl-triclosan) as well as degraded to nontoxic forms (Ritter et al., 2002). Additionally to the diverse exposure routes in the environment, chemicals may be accumulated along up food web and/or may adversely affect freshwater organisms and human

health. A cause-effect relation between chemical exposure and the adverse ecological effects have been explored in several remarking case studies. For instance, water contamination of pesticides are suspected to be responsible for the global amphibian decline (Alford and Richards, 1999; Houlihan et al., 2000). Furthermore, the bumble bee colony growth and queen production is likely reduced due to exposure to neonicotinoid pesticides (Whitehorn et al., 2012). Endocrine disrupting chemicals, which disturb the endocrine system development and the organs that respond to endocrine signals, might be responsible for gonadal aberration and skewed sex ratios in fish populations and a decline of amphibian populations (Colborn et al., 1993; Larsson and Förlin, 2002; Munkittrick et al., 1991). Moreover, pharmaceuticals like antibiotics or steroid drugs may cause resistance among natural bacterial populations (Kolpin et al., 2002; Richardson et al., 2005). Aquatic ecosystems are contaminated with a mixture of different chemicals. Therefore, it is challenging to find the trigger for adverse effects on ecosystems and the establishment of cause-effect relationships is like looking for "the needle in a haystack". Thus, the assessment of the likelihood of risk for freshwater ecosystems exposed to a mixture of diverse chemicals with low and fluctuating concentrations remains a formidable task (Altenburger et al., 2015).

## 1.2 Risk assessment processes

The EU Water Framework Directive (WFD) commences with the words "Water is not a commercial product like any other but, rather a heritage which must be protected, defended and treated as such" (European Commission, 2000). The main objective of the WFD is to achieve good ecological and chemical status of the European river basin and groundwater and to prevent deterioration of the water status. To this end, a common European river basin management has been established to regularly monitor aquatic organisms as well as various stressors including chemicals. This enabled a comprehensive data analysis of the monitored chemical concentrations in the European river basins indicating that 14% of the monitoring sites were likely to be acutely affected by organic chemicals and 42% of the monitoring sites were likely to be chronically affected by organic chemicals for at least one of the three major organism groups in freshwater ecosystems (fish, invertebrates, and unicellular algae) (Malaj et al., 2014). The analysis of the retrospective chemical risk assessment conducted by Malaj et al. (2014) strengthened the general consensus that the aim of "good ecological status" according to the WFD definition will not be achieved for the majority European river basins until 2015 (European Environment Agency, 2012). Further, Malaj et al. (2014) pointed out that the retrospective chemical risk assessment in their study likely underestimates the real risk. One uncertainty relies in the limited number of monitored chemicals, even for the only EU-wide monitored 33 priority substances. Consequently, an unknown chemical status for about 40% of European river basins still exists (European Commission, 2012). Further, chemical monitoring in freshwater systems is confronted with low chemical concentrations of a chemical cocktail varying in time and space (Ohe et al., 2004). The monitoring is even aggravated by high limits of quantification (Brack et al., 2015).

In opposition to the retrospective risk assessment (RA), prospective risk assessment of chemicals aims to protect populations, communities or entire ecosystems before chemicals are daily used (Hommen et al., 2010). For this purpose, several European directives and regulations have been formulated referring to the use of chemicals, e.g. for plant protection products, biocidal products, pharmaceuticals, or industrial products. Chemical risk is generally defined as "the probability of an adverse effect in an organism, system, or (sub)population caused under specified

circumstances by exposure to the agent” (World Health Organization, 2004). RA consists of exposure and effect assessment of a chemical for which risk can be characterized in different environmental compartments (Jager et al., 2006). The risk characterization approach bases on the quotient of a predicted environmental concentration (*PEC*) or a measured concentration and on an ecological threshold value, referred to as predicted no-effect concentration (*PNEC*) (Hommen et al., 2010). For the exposure assessment, the *PEC* value is commonly estimated by process-based fate models which include physicochemical properties of the chemical as well as the physical properties of the various environmental compartments (Jager et al., 2006). For the effect assessment, the *PNEC* value is derived from the endpoint of the most sensitive single-species laboratory test in a first stage, usually for species of the standard organisms fish, invertebrates and algae used in ecotoxicology. The effect assessment process typically follows a tiered approach. Lower-tier tests of RA are based on single-species laboratory tests conducted according to guidelines from the Organisation of Economic Cooperation and Development (OECD) and International Organization for Standardization (ISO). Here, individuals are exposed to continuous concentrations for a predefined duration in order to determine the concentration dependence of an organism response, e.g. the concentration where 50% of individuals are death ( $LC_{50}$ ). Acute toxicity data are provided for a limited number of standard fish, crustacean, and algae species. Besides the effect assessment, the potential for bioconcentration and secondary poisoning is also tested according to OECD guidelines (Hommen et al., 2010). Higher-tier test systems aim to better reflect the complexity of ecosystems by accounting for instance for species interaction or interaction with the physical and biological environment. Therefore, higher-tier tests include additional single-species laboratory tests, microcosm or mesocosm studies. Moreover, higher-tier testing may also provide information on long-term effects (chronic toxicity data), include different life stages (e.g. juveniles and adults), or indicate the concentration which induces 50% of sublethal effects like growth and reproduction ( $EC_{50}$ ) (Forbes and Calow, 2002). Nevertheless, acute toxicity data are the most abundant ecotoxicological data available for the risk assessment process due to the fast, easy, and inexpensive generation of comparable data (Forbes and Calow, 2002). Additionally, the endpoint measured may not represent a direct indicator of an effect on the population density (Forbes and Calow, 2002). Moreover, responses on standard species to acute exposure of a high and constant concentration may probably not reflect responses of communities of species within ecosystems exposed to low and fluctuating concentrations (Forbes and Calow, 2002). Currently, a safety factor for acute toxicity data is included into the estimate of risk to account for uncertainties resulting from experimental testing between lower-tier and higher-tier test systems (e.g. laboratory vs. field conditions, acute vs. chronic conditions, sensitivity differences between species, toxicities, or chemicals). In conclusion, current RA faces various challenges to estimate the real risk on freshwater ecosystems exposed to a chemical mixture under realistic circumstances (Galic et al., 2010; Hommen et al., 2010; Jager et al., 2006). To meet the challenges in current RA, toxicity processes need to be understood in order to link untested exposure scenarios to the probability of an adverse response on different biological levels through modeling approaches (Eggen et al., 2004; Forbes and Calow, 2012; Jager et al., 2006; Villeneuve and Garcia-Reyero, 2011).

### 1.3 Understanding toxicity as time- and concentration-dependent processes

Ecotoxicological studies traditionally provide concentration-response relationships for chemicals. To this end, the probability of a response on the organism level is quantified for various exposure concentrations at a fixed test duration. The response generally follows a cumulative distribution function that describes the dependence of toxicity on concentration until a maximum effect is reached. Modeling of concentration-response relationships allows parameter estimations like the exposure concentration at which 50% of response can be expected ( $EC_{50}$ ) or the slope of the curve ( $\theta$ ).  $EC_{50}$  values are used to compare the sensitivity differences between organism groups or species and different toxicities between chemicals. Verhaar et al. (1992), for instance, related  $EC_{50}$  values of a large number of organic chemicals to the chemical's hydrophobicities, characterized by octanol-water partition coefficient ( $\log K_{OW}$ ). The authors showed that  $EC_{50}$  values of half of all organic compounds clearly decreased with an increase of the chemical's hydrophobicity. That quantitative structure-activity relationship (QSAR) enables the estimation of a baseline or minimum toxicity of a chemical, defined as baseline toxicity or narcotic mode of action. Thus, baseline toxicity of narcotics is assumed to be mainly driven by chemical-specific descriptors like hydrophobicity. Depending on the determined  $EC_{50}$  value difference to the baseline toxicity estimated by QSAR, more potent chemicals were classified to show reactive or specific modes of toxic action. Consequently, the hydrophobicity of a chemical gives a hint but does not entirely explain the effect contributions of specifically acting and reactive chemicals. Differences in toxicity may be further caused by biological-specific parameters like the abundance of target sites, the ability to biotransform the parent compound or to recover from the internal exposure.

Already hundred years ago, Haber (1924) demonstrated that toxicity depends on a time-integrated concentration. According to Haber's rule (1924), an equivalent toxicological response ( $k$ ) depends on the grouping of the product of exposure concentration ( $c$ ) and the exposure time duration ( $t$ ), simplified by the mathematical expression  $c \times t = k$ . Consequently, an equal response can be achieved either by a long-term exposure of a low concentration or a short-term exposure of a high concentration. Thus, the injury accumulation in an organism is a function of both the exposure time and the bioavailable concentration in the exposure medium (Ashauer et al., 2006a; McCarty et al., 2011; McCarty and Mackay, 1993; Rozman and Doull, 2000). The intrinsic sensitivity of an organism to a chemical is the integrated result of several internal processes and threshold values (Rubach et al., 2012). The internal processes in an organism are aggregated toxicokinetic and toxicodynamic processes which describe the effect development depending on the variables time and concentration in a quantitative manner (Rozman and Doull, 2000). The toxicokinetic and toxicodynamic processes leading to the the adverse outcome on the organism and/or population level are depicted in Figure 1.1.

First, the toxicokinetic processes characterize the chemical's potency in the organism (**What does the body to the chemical?**) (Rozman and Doull, 2000). Toxicokinetic processes describe the time-course of the internal concentration by encompassing the chemical mass fluxes absorption of the external freely dissolved concentration into the organism, the distribution to the biological sites due to partitioning processes, the potential susceptibility for biotransformation and the elimination back into the ambient medium (Ashauer et al., 2006a; Escher and Hermens, 2002, 2004). How the internal concentration behaves over time depends on physicochemical properties of the chemical (e.g. hydrophobicity, speciation, water solubility) and physiological parameters of the organism

(e.g. organism size, lipid content, growth) (Arnot and Gobas, 2006; McCarty et al., 2013; Rubach et al., 2012). Thus, the internal effect concentration more directly reflects the intrinsic potency of a chemical and enables to reduce of the toxicity variability between chemicals and species (Escher and Hermens, 2002; McCarty and Mackay, 1993; McCarty et al., 2013; Meador et al., 2008; Rubach et al., 2010). The internal concentration remains stable when the mass balance is equalized. Then, the ratio of internal concentration at steady state to the exposure concentration at the same time point results into the steady state bioconcentration factor ( $BCF_{ss}$ ) (Arnot and Gobas, 2006). Similarly, the kinetic bioconcentration factor ( $BCF_{kk}$ ) results from uptake and elimination kinetic rates derived from the time-course of the internal concentration (Ashauer et al., 2006b; Kühnert et al., 2013). The bioconcentration factors indicate the accumulation potential of a chemical in the organism, which generally increases with the chemical's hydrophobicity (Arnot and Gobas, 2006).

Second, the toxicodynamic processes describe the organism dependent vulnerability when exposed to a chemical (**What does the chemical do to the body?**) (Rozman and Doull, 2000). Toxicodynamic processes are described by injury and recovery dynamics which driving the adverse developmental outcome on the organism or population level (Ashauer et al., 2006a). Traditionally, the mechanistic principles underlying the toxicodynamic processes are explained by mechanisms and modes of toxic action (Escher and Hermens, 2002). The mechanism of action defines crucial chemical-biological interactions that are classified for different target sites (membranes, proteins, peptides, DNA) and interaction types (e.g., van der Waals interaction, H-donor/acceptor interaction, ionic interaction or formation of covalent binding) according to Escher and Hermens (2002). These interactions might cause biological responses leading to different classes of effects (e.g., non-specific effects, receptor-mediated effects, damage of biomolecules), called modes of action (Escher and Hermens, 2002). Thus, the behavior and the sensitivity of various endpoints give indication of mechanisms and modes of toxic action of a chemical and can explain differences in species sensitivities.

Over the last decades, various effect models have been developed that translate the mechanistic understanding of toxicological process into mathematical equations. Compartment models have commonly been used in order to describe the transfer of masses or energy fluxes between interacting subsystems. Nowadays, an increasing application of effect models is noticeable and the benefit of modeling tools in chemical risk assessment is under discussion (Eggen et al., 2004; Forbes and Calow, 2012; Jager et al., 2006; Villeneuve and Garcia-Reyero, 2011). In the following, concepts of one and two-step effect models with their applicabilities and limitations will be introduced that focus on the description of toxicity development in individual organism exposed to continuous or pulsed concentrations. Table 1.1 list the assumptions and the parameters behind the various effect models that have been used to explain the mortality dynamics for different biosystems. Furthermore, the parameters implemented in the current effect model frameworks are depicted in Figure 1.1.

#### **1.4 One-step model: The critical body residue as dose surrogate for narcotic mode of action**

Narcotic chemicals are thought to nonspecifically disturb the integrity and functioning of cell membranes due to partitioning into biological cell membranes (Escher et al., 2011; Könemann,

1981; van Wezel and Opperhuizen, 1995; Veith et al., 1983). The interaction of narcotic acting chemicals with the lipid bilayers of the membrane is instantaneous and completely reversible due to the non-covalent binding character (Escher et al., 2011). McCarty (1986) showed for narcotics that the relationship between the bioconcentration factor ( $BCF$ ) and the physicochemical descriptor  $\log K_{OW}$  is inversely related to the relationship between the  $LC_{50}(\infty)$  values and the chemical's  $\log K_{OW}$ . Thus, McCarty and Mackay (1993) derived that a critical effect occurs when the total concentration in an organism reaches a certain threshold level, the so-called critical body residues (CBR). The critical concentration in the entire organism is assumed to cause an equal intrinsic activity over a broad hydrophobicity range of the baseline toxicants. A constant membrane concentration CBR value of  $2.5 \text{ mmol kg}_{\text{wet wt}}^{-1}$  has been estimated by the linear relationship between bioconcentration factor and the lethal concentration at which 50% of organisms die

$$CBR = BCF \times LC_{50}(\infty) = BCF \times C \times \left(1 - \exp^{-k_{\text{out}} \times t}\right) \quad (1.1)$$

The predicted CBR of  $2.5 \text{ mmol kg}_{\text{wet wt}}^{-1}$  was afterward confirmed with measured CBR values which ranged between  $2 - 8 \text{ mmol kg}_{\text{wet wt}}^{-1}$  in the whole organism (McCarty and Mackay, 1993; Van Hoogen and Opperhuizen, 1988). For this purpose, the total concentration in an organism was quantified at steady state indicating the dose surrogate of the critical effect (Escher and Hermens, 2002; McCarty and Mackay, 1993). The terms internal effect concentration (IEC), body burden, or body residue have equivalently been used in literature (Escher et al., 2011). The dose surrogate has been further refined by normalizing the IEC values to an average lipid content of 5% of the total organism which is assumed to be the target for baseline toxicants. Thus, IEC values spanned between  $40$  and  $160 \text{ mmol kg}_{\text{Lipid}}^{-1}$  (McCarty and Mackay, 1993; van Wezel and Opperhuizen, 1995). A refinement of the internal effect concentration aims to reduce variances of toxicokinetic processes. Thus, the dose surrogate of a constant threshold enables an improved comparison of the chemical's intrinsic potencies between different species. For that reason, chemical body residues have been suggested to be a better metric of the target concentration than exposure-based dose metrics, as they reflect the bioavailable and effective concentration in the organism (Landrum et al., 2005; McCarty and Mackay, 1993; Meador et al., 2008). However, the CBR concept is only valid when narcotic chemicals reach equilibrium of internal exposure in the organism. Hence, time dependence of baseline toxicity mainly depends on hydrophobicity-driven partitioning processes. Furthermore, chemical interaction with the biological membrane is assumed to be completely reversible and instantaneous. However, the time-course of narcotic toxicity has been observed to be not only driven by bioconcentration kinetics, but also by the cumulative damage resulting from toxicodynamic processes (de Maagd et al., 1997; Lee et al., 2002b; van Wezel and Opperhuizen, 1995). Moreover, the CBR concept is limited (i) to describe time-dependent toxicity of specifically acting and reactive chemicals that irreversibly interact with the biological target sites (Verhaar et al., 1999), (ii) to explain temporal changes of body burdens (Chaisuksant et al., 1997; Mortimer and Connell, 1994; Yu et al., 1999), and (iii) to estimate effects on organisms from sequential exposure (Ashauer et al., 2006a, 2007b).

## 1.5 One-step model: The critical area under the curve as dose surrogate for specifically acting and reactive chemicals

Verhaar et al. (1999) demonstrated that the time-dependent toxicities in guppy exposed to reactive chemicals are misfitted by the CBR approach, which would overestimate effects at short exposure times or underestimate effect at long exposure times. In contrast to narcotics, reactive and receptor-mediated chemicals instantaneously and irreversibly interact with the biological target sites (Legierse et al., 1999; Verhaar et al., 1999). Therefore, the critical area under curve (CAUC) approach was proposed to determine the dose surrogate of a constant threshold for reactive chemicals (Verhaar et al., 1999). The toxicity of reactive chemicals is assumed to be constant when a critical area under the curve (CAUC) is reached. The dose surrogate CAUC [amount time mass<sup>-1</sup>] is defined as the time integral of the internal concentration change in the whole organism:

$$CAUC = \int_0^t C_{\text{int}}(t)dt = \int_0^t BCF \times C(t) \times (1 - \exp^{-k_{\text{out}} \times t}) dt \quad (1.2)$$

The critical threshold (CAUC) is a chemical-specific value. The effect occurs when the critical threshold value is exceeded that is independent of the time when the steady state concentration in the organism is reached. Integration of Eq.1.2 and replacement of the exposure concentration  $C(t)$  with  $EC_{50}$  value leads to the following mathematical expression with the effect depending on the exposure time:

$$EC_{50} = \frac{CAUC}{BCF} \times \frac{1}{t - \frac{(1 - \exp^{-k_{\text{out}}})}{k_{\text{out}}}} + EC_{50}(\infty) \quad (1.3)$$

Legierse et al. (1999) suggested the critical target occupation model (CTO) to analyze the time-dependent toxicity of specifically acting chemicals. Organophosphorus pesticides need to be first biotransformed to their oxon analogues, which then irreversibly inhibit the enzyme acetylcholinesterase (AChE). Similar to the CAUC approach, the critical target occupation CTO [amount mass<sup>-1</sup>] is defined as time-integrated concentration of the oxon analogue ( $CAUC_{\text{oxon}} \times k_{\text{act}}$ ) and the AChE inhibition rate constant  $k_i$  [time<sup>-1</sup>]

$$CTO = \int_0^t C_{\text{oxon}}(t)dt = k_{\text{act}} \times k_i \times CAUC_{\text{oxon}} \quad (1.4)$$

The parameter  $k_{\text{act}}$  is a first-order rate constant [time<sup>-1</sup>] to account for the metabolic activation of the oxon analogue by cytochrome P-450. The critical amount of "covalently occupied" target sites is associated to mortality by Eq.1.3. The time-course of the measured internal effect concentrations in guppy and pond snail were accurately described by the CTO model. Measured body residue values varied from 0.0025 mmol kg<sub>wetwt</sub><sup>-1</sup> to 0.632 mmol kg<sub>wetwt</sub><sup>-1</sup> depending on the organism, the chemical and the exposure time. Verhaar et al. (1999) and Legierse et al. (1999) showed that the assumptions of the CAUC approach and the CTO model are valid for completely irreversible mechanisms of toxic action and when recovery or repair does not occur.

## 1.6 The two-step model "Damage Assessment Model": Linking a constant exposure to effects through modeling of toxicokinetic-toxicodynamic processes

Lee et al. (2002b) discovered that the time-dependent toxicity of narcotics in the *Hyalella azteca* is regulated not only by toxicokinetic processes but also by a cumulative damage increase over time. An incompletely reversible interaction of narcotics with the biological target site might, for instance, potentially be caused by a biotransformation product with a different affinity to the target site (Landrum et al., 2005; Lee et al., 2002a; Schuler et al., 2004). Lee et al. (2002a) proposed the damage assessment model (DAM) that describes the observed time dependence of narcotic toxicity. The DAM model consists of two time-limiting steps representing toxicokinetic and toxicodynamic processes (based on conceptual ideas of Ankley et al. (1995)). The accumulated chemical concentration over time in an organism ( $C_{\text{int}}(t)$ ) is assumed to follow a first-order kinetic

$$\frac{dC_{\text{int}}(t)}{dt} = k_{\text{in}} \times C(t) - k_{\text{out}} \times C_{\text{int}}(t) \quad (1.5)$$

The time-course of the internal concentration is characterized by the uptake rate constant  $k_{\text{in}}$  [ $\text{time}^{-1}$ ] and the overall elimination rate constant  $k_{\text{out}}$  [ $\text{volume mass}^{-1} \text{time}^{-1}$ ]. Furthermore, (Lee et al., 2002a) assumed that the effect is characterized by the dose surrogate damage and time-dependent toxicity is proportional to damage recovery:

$$\frac{dD(t)}{dt} = k_{\text{I}} \times C_{\text{int}}(t) - k_{\text{R}} \times D(t) \quad (1.6)$$

The aggregated processes of damage  $D(t)$  [-] is parametrized by the injury rate constant  $k_{\text{I}}$  [ $\text{mass amount}^{-1} \text{time}^{-1}$ ] and the repair/recovery rate constant  $k_{\text{R}}$  [ $\text{time}^{-1}$ ]. The injury rate constant can be interpreted as an integrated parameter of chemical potency that quantifies effectiveness of the toxicity. The DAM model is applicable for reversible binding ( $k_{\text{R}} \approx \infty$  for very fast, instant recovery) or irreversible binding ( $k_{\text{R}} \approx 0$  for very slow recovery) of a chemical to its biological target site and thus generalizes the assumptions of the extreme cases of the CBR and CAUC approaches. A hazard model was adapted that links the effect metric damage to the survival probability  $S(t)$  of an organism (Ashauer et al., 2006a, 2007b).

$$\frac{dH(t)}{dt} = k_3 \times D(t, c) \quad (1.7)$$

where  $H(t)$  is the hazard function [-] and  $k_3$  is a dimensionless coefficient [-]. The exponential of the negative cumulative hazard in the individual describes the temporal pattern of the survival probability  $S(t)$  [-] (Ashauer et al., 2007b).

$$S(t) = \exp^{-H(t)} \times S_{\text{Background}} \quad (1.8)$$

The term  $S_{\text{Background}}(t)$  [-] accounts for the background mortality observed in the untreated samples. However, the DAM approach has been shown to be inappropriate to simulate effects from sequential exposure, because damage can decrease after the end of an exposure pulse governed by  $k_{\text{R}}$  (Ashauer et al., 2007b). To accurately estimate the survival probability of an organism exposed to fluctuating and pulsed concentrations from the existing evidence (Péry et al., 2001, 2002), Ashauer et al. (2006a) suggested to measure toxicokinetic and toxicodynamic processes separately from each other.

## 1.7 The two-step model "Threshold Damage Model": Estimation of an effect on aquatic organisms from fluctuating and pulsed exposure to chemicals

The effect on organisms exposed to subsequent chemical pulses may be significantly higher compared to the effect on organisms without prior stress. The resulting toxicity is defined as carry-over toxicity (Ashauer et al., 2010). Current risk assessment approaches do not consider pulse exposure and would thus underestimate the likelihood of chemical risk for such cases. Therefore, the Threshold Damage Model (TDM) has been suggested that combines assumptions for toxicokinetic and toxicodynamic processes formulated in the DAM approach with the threshold principle (based on the threshold hazard model from Kooijman and Bedaux (1996)) (Ashauer et al., 2006a, 2007b). Thus, the TDM approach assumes that the internal concentration ( $C_{int}$ ) accumulates in the entire organism according to the first-order toxicokinetic model (Eq.1.5). Further, the time-course of accumulated internal damage ( $D(t)$ ) is described by Eq. 1.6, which consists of an injury rate constant and a recovery/repair rate constant. If a certain damage threshold [-] is exceeded, internal damage is linked to the probability of an organism to die over time through the hazard function  $dH(t)/dt$  (Kooijman and Bedaux, 1996; Péry et al., 2001)

$$\frac{dH(t)}{dt} = \max [D(t, c) - \text{threshold}, 0] \quad (1.9)$$

The differential of Eq.1.9 is defined as hazard rate, which proportionally increases with a changing damage level. The exponential of the negative cumulative hazard in the individual is linked to the hazard rate to describe the temporal pattern of the survival probability  $S(t)$  [-]. The killing process itself is therefore assumed to be more a stochastic description rather than a mechanistic-based process (Jager et al., 2011).

The TDM model was verified by temporal patterns of measured survival data for the aquatic invertebrate *Gammarus pulex* exposed to fluctuating and sequential pulses of the pesticides pentachlorophenol, carbaryl, and chlorpyrifos (Ashauer et al., 2007b,c,a). The TDM model was successfully calibrated to the measured survival data indicated by a mean error varying from 5% to 15% for various exposure scenarios. Furthermore, the estimated toxicokinetic and toxicodynamic parameters could be analyzed with regard to aggregated toxicity processes depending on chemical-specific and biological-specific system properties. The observed carry-over toxicity between two sequential pulses was explained by either an incomplete elimination into the exposure medium in the case of carbaryl or a slow recovery of internal damage in the case of chlorpyrifos (Ashauer et al., 2007a). In contrast, carry-over toxicity was not observed for a sequential exposure of pentachlorophenol, because the simulated internal damage level of pentachlorophenol decreased fast below a certain threshold within the recovery phase between two pulses. Ashauer et al. (2007a) further showed that it does matter that organisms were previously exposed to another chemical. The authors studied the combined effect on *Gammarus pulex* from pulsed exposure of two chemicals. A combined mortality of 45% was observed when a one day exposure of carbaryl was followed by a chlorpyrifos exposure (14 days later). In contrast, 60% combined mortality was reached when the organisms were firstly exposed to chlorpyrifos and subsequently exposed to carbaryl. The resulting difference in combined effects is unexplainable by the combined internal concentrations of carbaryl and chlorpyrifos that were the same in both treatments. Also carbaryl and chlorpyrifos were both eliminated by 95% within the recovery phase between the two pulses of

14 days according to the simulated internal concentration. However, the simulated internal damage level of carbaryl decreased faster below a certain threshold (8 days) than the internal damage of chlorpyrifos after the first pulse. To conclude, carry-over toxicity is a function of aggregated toxicokinetic and toxicodynamic processes that depends on the exposure duration, the recovery time between two pulses and the height of the exposure peak.

**The understanding of aggregated processes leading to combined effects from sequential exposure of a chemical mixture would be improved by characterizing chemically and biologically relevant parameters of toxicokinetic and toxicodynamic processes.**

## **1.8 Lessons learned of applied model concepts for the estimation of effects on aquatic organisms**

During the last two decades, different effect models have been proposed to describe the temporal changes of effects mainly on fish and invertebrates. Ashauer and Brown (2008) mathematically proofed that the specific assumptions for the different effect models can be generalized by the TDM approach. Nowadays, the TDM approach has been broadly applied as interpretation and extrapolation tool. For instance, the use of the TDM approach explained variations in species sensitivities. Rubach et al. (2010) investigated that 50 to 60% of the intrinsic sensitivity variation between 15 freshwater arthropods exposed to chlorpyrifos is interpretable by uptake and elimination processes. That finding is in agreement to measured internal effect concentrations at specific target tissues in three invertebrates (Nyman et al., 2014). The remaining variation of 40 to 50% might be attributed to other processes like biotransformation or toxicodynamic processes (Nyman et al., 2014; Rubach et al., 2010). Another TDM application investigated that the lower toxicity of diazinon to *Gammarus pulex* in comparison to the diazinon toxicity to *Daphnia magna* was ascribed to toxicodynamic processes of receptor-mediated toxicity (Kretschmann et al., 2012). Although the estimated activation of diazinon to diazoxon was two times faster in *Gammarus pulex* than in *Daphnia magna* (Kretschmann et al., 2011b), diazoxon activation differences are overcompensated by a six-times faster detoxification of diazinon and diazoxon and a 400-times lower injury rate constant in *Gammarus pulex* than in *Daphnia magna* (Kretschmann et al., 2012). Other studies linked the chemical-receptor interaction at the biological target site (also initial molecular event) to the survival probability (Jager and Kooijman, 2005; Kretschmann et al., 2011a). However, the model results indicate that the aggregated toxicodynamic processes might not be correctly reflected by the effect model. One reason might be that toxicokinetic and toxicodynamic processes overlap over time. Thus, it is unclear whether toxicity is a result of internal exposure to or effect of chemicals (Forbes et al., 2006; van Straalen and Feder, 2011). Additionally, damage has been aggregated as an integrative state variable that lumps all kinds of biochemical and physiological processes involved in toxicity manifestation in the individual organism (Ashauer and Brown, 2008; Jager et al., 2011). Nevertheless, toxicodynamic processes encompass an effect cascade from the initial molecular event progressed over key events (e.g. changes in gene expression by toxicogenomics) towards the adverse outcome of higher effect levels such as immobilization and mortality (Ankley et al., 2010).

As discussed by Jager et al. (2011), the effect models described the likelihood of individual survival by applying two different assumptions. First, the concept about "individual tolerance" assumes that not all organism die at the same time due to different sensitivities. Second,

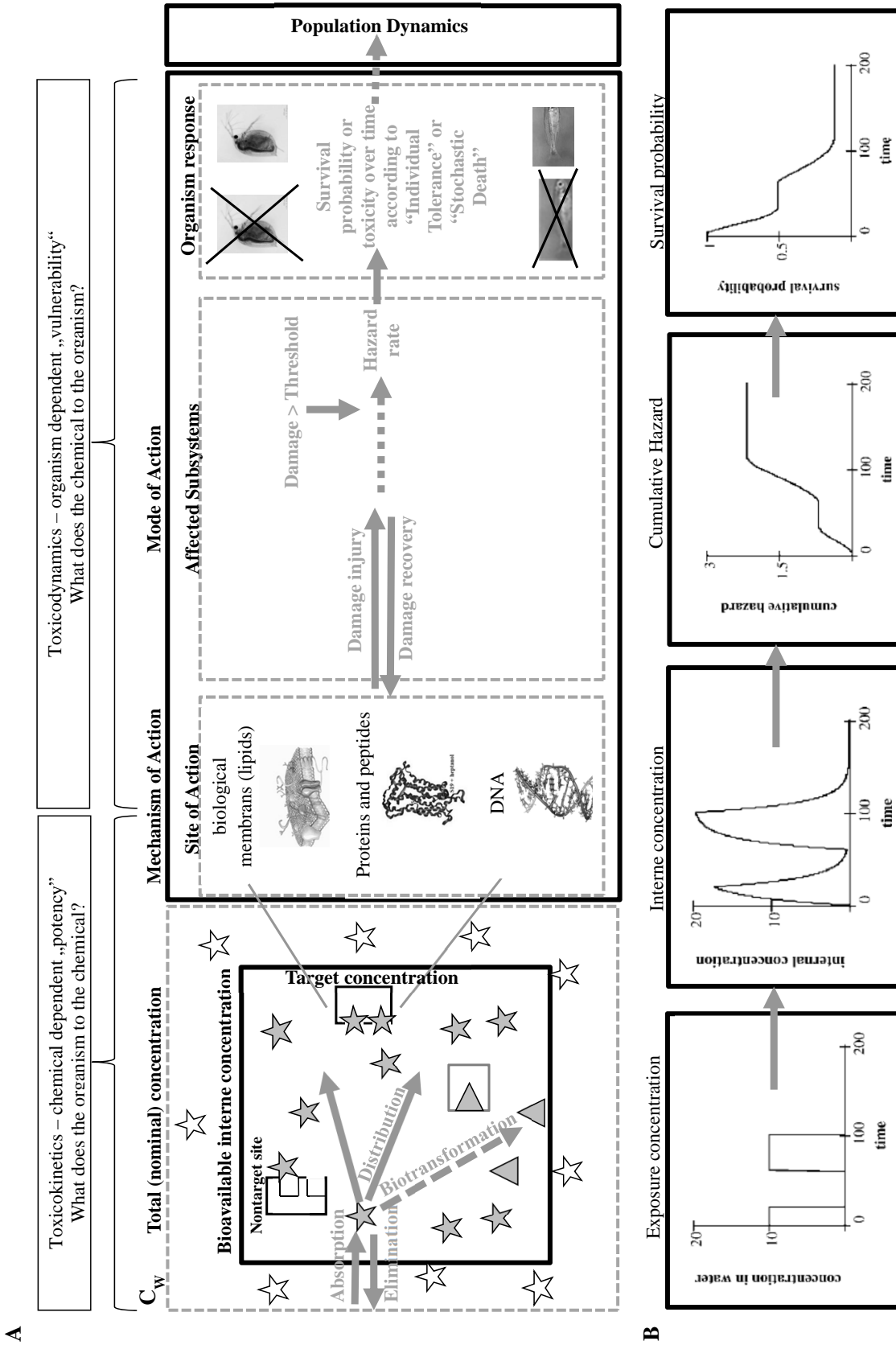


**Figure 1.1:** A: A simplified scheme of the relationship between toxicokinetic and toxicodynamic processes as implemented in current effect models modified after Ashauer et al. (2006a), Escher and Hermens (2002), Escher et al. (2011) and Jager et al. (2011). B: A simulation example of the survival probability of organisms exposed to a sequential concentration  $C_{int}$  and cumulative damage  $D$  are system variables of the toxicokinetic-toxicodynamic model which link exposure concentration  $C$  to mortality  $S(t)$ .

**Table 1.1:** Overview about the various toxicokinetic-toxicodynamic models that have been used to explain the mortality dynamics for different biosystems. Abbreviations: model (CBR - Critical Body Burden, CAUC - Critical Area under the Curve, CTO - Critical Target Occupation, DAM - Damage Assessment Model, TDM - Threshold Damage Model, GUTS - General Unified Threshold Model of Survival); SoA: site of action (AChE - acetylcholin esterase); MoA: mode of action (n - narcosis, r - reactive, s - specific); NEC: no-effect concentration; death: assumptions about the survival (IT - individual tolerance, SD - stochastic death); total number: total number of parameters incorporated in effect models (+ parameters estimated by dose-response relationships DR); effect model parameters (BCF - bioconcentration factor,  $LC_{50}(\infty)$  - unlimited median effect concentration,  $k_1$  - inhibition rate,  $k_{act}$  - activation rate,  $k_{out}$  - overall elimination rate constant,  $k_m$  - uptake rate constant,  $k_r$  - recovery/repair rate constant,  $k_I$  - injury rate constant, NEC - no-effect concentration); dose metric (CBR - critical body burden, CAUC - critical area under the curve, D - damage)

model	organism	endpoints	chemicals	SoA	MoA	recovery	NEC	death	total number	effect model parameters	dose metric
CBR	<i>Fathead minnow</i>	$LC_{50}$	chlorobenzene	membrane	n	$k_r \rightarrow \infty$	No	IT	3 + DR	BCF, $LC_{50}(\infty)$	CBR
CAUC	Guppy	$LC_{50}$	benzyllic compounds	proteine & peptide	r	$k_r \rightarrow 0$	No	IT	3 + DR	$k_{out}$ , BCF, $LC_{50}(\infty)$	CAUC
CTO	Pond snail, Guppy	$LC_{50}$	organo-phosphates	AChE	s	$k_r \rightarrow 0$	No	IT	5 + DR	$k_{out}$ , $k_I$ , $k_{act}$ , BCF, $EC_{50}(\infty)$	CAUC
DAM	<i>Hyalella azteca</i>	$LC_{50}$	PAHs	membrane	n	$0 < k_r < \infty$	No	IT	4	$k_{in}$ , $k_{out}$ , $k_r$ , $k_I$	D
TDM	<i>Gammarus pulex</i>	S(t)	organo-phosphates	AChE	s	$0 < k_r < \infty$	Yes	SD	5	$k_{in}$ , $k_{out}$ , $k_r$ , $k_I$ , NEC	D
GUTS	<i>Gammarus pulex</i> , <i>Fathead minnows</i>	S(t)	PAHs, organo-phosphates	membrane, AChE	n, s	$0 < k_r < \infty$	Yes	SD/IT	5	$k_{in}$ , $k_{out}$ , $k_r$ , $k_I$ , NEC	D

mortality is supposed to be a stochastic process for all identical individuals, known as "stochastic death" (Jager et al., 2011). To clarify the underlying hypotheses and assumptions of survival, Jager et al. (2011) suggested a general unified threshold model of survival (GUTS). GUTS combines the assumptions of the "individual tolerance" and the "stochastic death" within the TDM approach (Jager et al., 2011). Nyman et al. (2012) showed that the survival of *Gammarus pulex* in multiple pulse exposures to propiconazole was slightly different described depending on the implementation of the individual tolerance model or the stochastic death model in GUTS. However, the simulations resulted into very different parameter estimations, which is consistent with results from Jager et al. (2011). Furthermore, TKTD models have been used to basically describe the survival probability of fish or invertebrates, which is a quantal endpoint (Ashauer et al., 2011). There exist just a few toxicodynamic approaches with different effect mechanism and connect different endpoints to each other, e.g. the dynamic energy budget theory (DEBtox) (Kooijman and Bedaux, 1996; Kooijman, 2000; Martin et al., 2013b; Nisbet et al., 2000). To conclude, TKTD models have to be further refined in order to simulate and emphasises linkages between graded and quantal endpoints describing sublethal and lethal effects for multiple untested scenarios (Ashauer et al., 2011). Based on the understood and described effect development for various graded and quantal endpoints generated by single-species laboratory tests, effect modeling has been used as a tool to extrapolate effects on the population level and on untested exposure patterns (Galic et al., 2010, 2014; Hommen et al., 2010; Martin et al., 2013).

**TKTD models are crucial to understand toxic effects on fish and invertebrates over time, interpret differences between chemical toxicities and specie sensitivities and understand chemical interaction in order to extrapolate toxic effects to untested scenarios (Jager et al., 2011). To my knowledge, however, a TKTD model for unicellular algae toxicity has not been developed yet.**

## **1.9 The unicellular algae *Scenedesmus vacuolatus* as model organism**

Effect assessment is typically conducted for the three representative taxonomic groups fish, invertebrate and algae (Brock et al., 2006). Malaj et al. (2014) investigated that the maximum concentrations of monitored chemicals exceeded the acute risk threshold for algae at 9% of the European-river basin sites and the mean chemical concentration exceeded the chronic risk threshold for algae at 13% of sites. Hereby, algae were most sensitive to herbicides that potentially changes structural and functional parameters (Malaj et al., 2014; Rotter et al., 2013). Thus, the algae organism groups are suitable diagnostic systems for assessing phytotoxic effects. The unicellular green freshwater algae *Scenedesmus vacuolatus* (*S. vacuolatus*) is a model organism in ecotoxicology. The adverse outcome on photosynthesis, growth, or reproduction of the unicellular algae has commonly been evaluated based on a descriptive concentration-effect relationship to a defined exposure time (Altenburger and Greco, 2009). A standardized bioassay of the synchronized algae culture was applied as tool to analyze effects on the metabolome level (Kluender et al., 2009; Sans-Piché et al., 2010) and combined effects of a chemical mixture (Altenburger et al., 2004; Faust et al., 2001, 2003), to determine time dependence of toxicity (Altenburger et al., 2006; Franz et al., 2008) or to investigate modes of action of chemicals (Adler

et al., 2007; Neuwoehner et al., 2008). A purely empirical description of concentration-response relationships is, nevertheless, neither helpful to understand the process of damage development nor suitable to predict effects on algae for different exposure scenarios from the existing evidence (Heckmann et al., 2010; Baas et al., 2009; Jager et al., 2006). To overcome these limitations, the determination of toxicokinetic and toxicodynamic process parameters incorporated in the TKTD model would improve our understanding of the damage development in algae cells (Altenburger and Greco, 2009). How toxicokinetic and toxicodynamic processes contribute to the overall dynamic of toxicity has not yet been investigated in *S. vacuolatus*.

Based on bioconcentration tests of sulfonylurea herbicides and photosystem II inhibitors in *S. vacuolatus*, there is evidence that the steady state internal concentration is reached very fast in algae cells, namely within minutes likely driven by hydrophobicity-depending partitioning processes (Fahl et al., 1995; Manthey et al., 1993). By contrast, damage in *S. vacuolatus* cells is assumed to be progressed over hours until effect equilibration is reached (Altenburger et al., 2006; Franz et al., 2008). Thus, it is hypothesized that the time-gap between a steady state internal concentration and an equilibrium of toxicity in algae cells might be related to a rate-limiting toxicodynamic step. The rate-limiting toxicodynamic step supposedly depends on the progress of the effect over a chain of events from the initiating molecular event over key events across various biological levels towards an adverse outcome on the organism, which is defined as adverse outcome pathway (AOP) (Ankley et al., 2010). The unicellular algae system might be valid to study the progress of the effect towards the adverse outcome on algae growth, because the bias of the internal exposure change in the algae cell is assumed to be small with respect to the overall development of damage.

Ankley et al. (2010) suggested the theoretical framework AOP for a few model chemicals with known modes of action (e.g.; narcosis, aryl hydrocarbon receptor related effects, activation of estrogen receptor) that portrays the existing knowledge of the chain of events leading to toxicity. Various AOP frameworks have qualitatively been designed based on comprehensive information of critical (eco)toxicological endpoints organized for multiple biological levels. By contrast to the descriptive AOP frameworks, pharmacological studies proposed to abstract the progress of an effect towards an adverse outcome as a rate constant incorporated in a pharmacokinetic-pharmacodynamic model (PKPD model) like a transit compartment model (Danhof et al., 2008; Jusko et al., 1995). Here, effect progression is assumed to aggregate all biological activities leading to damage development after inhibiting or stimulating the production or loss of endogenous substances or mediators as a consequence of a chemical-target interaction (Mager et al., 2003). Simeoni et al. (2004) successfully applied a transit compartment model that simulate perturbed and unperturbed tumor growth kinetics after drug administration. It was suggested that perturbed and unperturbed algae growth kinetics can be described by adapting such a PKPD model formulation. Thus, rate-limiting toxicodynamic steps driving the development of algae damage could be quantified by linking the internal concentration of the chemical in algae cells to the change of algae growth through an adapted PKPD model. Further, the time-gap between a steady state internal concentration and an effect equilibration is hypothesized to vary between different AOPs.

**The use of TKTD modeling may give insights into rate-limiting steps in the whole chain of events from chemical exposure to an adverse outcome of sublethal and lethal endpoints (Escher and Hermens, 2002).**

## 1.10 Goals and structure of this dissertation

The main goals of this thesis were to (i) mechanistically describe the time dependence of toxicity on algae exposed to different chemicals through a TKTD model and (ii) to quantify the time-limiting toxicodynamic step in the whole chain of events from exposure to an adverse outcome by toxicokinetic and toxicodynamic process parameters. To this end, this thesis addresses the toxicokinetic and toxicodynamic processes of seven model chemicals in the unicellular algae *S. vacuolatus*: the photosystem II inhibitors irgarol and isoproturon, the lipid biosynthesis inhibitors triclosan and metazachlor, the reactive chemicals n-phenyl-2-naphthylamine and paraquat as well as the carotenoid synthesis inhibitor norflurazon. The impact of structurally complex chemicals was studied on growth of the model organism *S. vacuolatus* considering several reasons: The hydrophobicity-driven partitioning process of a chemical into an organism is potentially influenced by other processes like the dissociation in the ambient medium and biotransformation (Fahl et al., 1995; Neuwoehner and Escher, 2011). Influential processes may significantly alter the time-course of internal concentration and damage development. Structurally complex chemicals are further known to have different binding affinities towards diverse classes of proteins and lipids (Endo et al., 2011, 2012). Thus, chemicals of complex structures are expected to interact specifically or reactively with biological target sites, potentially causing excess toxicity of receptor-mediated or reactive mechanisms (Escher and Hermens, 2002; Escher et al., 2011). These processes are further assumed to lead to different time-courses of toxicity on algae growth which is dominated by the slowest toxicokinetic or toxicodynamic process (Jager et al., 2011).

The first research objective was the development of an algae TKTD model, that is addressed in **Chapter 2**. Hereby, an algae TKTD model was developed based on hypotheses and assumptions of effect models from pharmacology and ecotoxicology. The standardized bioassay of synchronized *S. vacuolatus* cultures has been modified in order to study unperturbed and perturbed algae growth over time. For calibration purposes, the kinetic of algae growth was determined over a one generation cell-cycle (24 h). Algae growth was perturbed by six concentrations of the specifically acting chemicals.

The question "How fast accumulate structurally diverse chemicals with different hydrophobicities in algae cells?" was answered in **Chapter 3**. To this end, a toxicokinetic assay was established for measuring bioconcentration kinetics of structurally complex chemicals with diverse hydrophobicities in *S. vacuolatus*. Toxicokinetic parameters are estimated by fitting a one-compartment toxicokinetic model to the time series of the analytical determined concentration. Known toxicokinetic parameters enabled the estimation of the bioconcentration potential of chemicals with diverse hydrophobicities, the comparison of estimated critical body burdens between the investigated chemicals, and the estimation of internal concentrations for every environmental concentration potentially causing an effect.

**Chapter 4** addresses the research question "How toxicokinetic and toxicodynamic processes contribute to the overall toxicity over time?" Based on the studies presented in **Chapter 2** and **3**, a joint approach between experimentation and effect modeling was applied (i) to define the time-limiting steps of algae toxicity for six model chemicals and (ii) to estimate rates of effect progression for different types of AOPs in dependency of bioconcentration kinetics. It was hypothesized that time-gaps between steady state internal concentration and effect equilibration vary between different AOPs. To this end, estimated internal concentrations were linked to the affected algae growth through the developed algae TKTD model in order to determine chemically and biologically relevant parameters of toxicokinetic and toxicodynamic processes.

To achieve the main goals, the research of this thesis is guided through five chapters addressing the individual research questions. **Chapter 2** and **3** were published in the international peer-reviewed journal *Environmental Toxicology & Chemistry*. **Chapter 4** provides a joint approach based on results of **Chapter 2** and **3**, so far unpublished. This thesis further allocates a synthesis of the main results related to the research questions (**Chapter 5**) and completes with recommendations for further research directions (**Chapter 6**).

# Effect progression in a toxicokinetic-toxicodynamic model explains delayed effects on the growth of unicellular green algae *Scenedesmus vacuolatus*

## ABSTRACT

Ecotoxicological standard tests assess toxic effects by exposing an organism with high concentrations over short defined periods of times. To evaluate toxicity under field conditions such as fluctuating and pulsed exposures, process-based toxicokinetic-toxicodynamic (TKTD) models may be used for extrapolation from the existing evidence. A TKTD model was developed that simulates the effect on growth of the green algae *Scenedesmus vacuolatus* continuously exposed to the model chemicals norflurazon, triclosan, and n-phenyl-2-naphthylamine. A pharmacological time-response model describing the effects of anticancer treatments to cancer cell growth was adapted and modified to model the affected growth of synchronized algae cells. The TKTD model simulates the temporal effect course by linking the ambient concentration of a chemical to the observable adverse effect via an internal concentration and a sequence of biological events in the organism. The parameters of the toxicodynamic model are related to growth characteristics of algae cells, a no-effect concentration, the chemical efficacy as well as the ability for recovery/repair, and the delay during damage progression. The TKTD model fitted well to the observed algae growth. The effect progression through cumulative cell damage explained the observed delayed responses better than just the toxicokinetics. The TKTD model could facilitate the link between several effect levels within damage progression which, prospectively, may be helpful to model adverse outcome pathways and time-dependent mixture effects.

---

Published in a slightly modified form as:

Vogs, C., Bandow, N., Altenburger, R., (2013): Effect propagation in a toxicokinetic/toxicodynamic model explains delayed effects on the growth of unicellular green algae *Scenedesmus vacuolatus*. *Environ. Toxicol. Chem.* 32 (5), 1161 - 1172.

---

## 2.1 INTRODUCTION

Chemicals such as pesticides, pharmaceuticals, and industrial chemicals are reported to occur in the aquatic environment due to anthropogenic activities and are potentially toxic to aquatic organisms (Schwarzenbach et al., 2006). To assess the toxicity on organisms, standard toxicity tests have been established in which the organism is typically exposed to high and constant concentrations over short defined exposure times (Jager et al., 2006). However, under field conditions chronic toxic effects to the organism are expected due to long-term exposure of sequential pulses with low fluctuating concentrations (Reinert et al., 2002).

To extrapolate from acute toxic effects in standard toxicity tests to chronic toxic effects under field conditions, process-based models are thought to provide powerful tools (Ashauer et al., 2007b; Jager et al., 2006). Toxicokinetic-toxicodynamic (TKTD) models are process-based models that simulate the time-course of the observed adverse effect on the organism, which is exposed to a certain chemical concentration over time (Ashauer and Brown, 2008; Jager et al., 2011). The toxicokinetic processes define the time-course of the chemicals' internal concentration inside the entire organism, which is mathematically linked to the ambient chemical concentration by the law of mass action (Spacie and Hamelink, 1982). The time-course of the internal concentration is equivalent to the sum of the chemical fluxes uptake, internal distribution, biotransformation, and elimination (Ashauer et al., 2007b; Escher et al., 2011). The toxicodynamic processes determine the time-course of the observable toxic effect, such as survival of an organism, over time. The assumed underlying toxicodynamic processes are described by the state variable damage, which consists of the temporal dynamics of injury and recovery when exceeding a threshold (Ashauer et al., 2007b; Rozman and Doull, 2000). To quantify survival over time, damage is translated into a hazard rate, which is the probability of an organism dying at a given time.

Two fundamentally different approaches have been used in various TKTD models, which mechanistically describe the survival probability of an organism in time: the individual tolerance distribution concept and the assumption that death is stochastic (hazard models) (Ashauer et al., 2007b). These TKTD models additionally differ in their underlying hypotheses and assumptions for toxicodynamic processes such as speed of damage recovery or threshold distribution (Ashauer and Brown, 2008; Jager et al., 2011). Recently, Jager et al. (2011) proposed a general unified threshold model for survival (GUTS). GUTS combines the underlying hypotheses and assumptions of the specific TKTD models to a general mixed model, which comprises individual tolerance models and stochastic death models. A process-based interpretation hence exists, which describes survival of an organism over time. Nevertheless, Ashauer et al. (2011) stated that TKTD models are still lacking, which simulate the effects on life history traits such as growth, development, or reproduction of an organism.

The independent variables of TKTD models are exposure concentration and exposure time leading to the dynamics of an effect in the organism. Although the exposure time is of particular importance, it has often been neglected as a factor in ecotoxicology (Heckmann et al., 2010). First, from the chemical point of view, three separate time scales (exposure time, toxicokinetic time, and toxicodynamic time) have to be considered when interpreting the observed effect (Rozman and Doull, 2000). Second, from the biological point of view, an organism is a dynamic system with possible altered life-cycle processes when exposed to a chemical (Heckmann et al., 2010). Finally, the state variable damage in TKTD models implicitly describes an effect progression triggered by the target concentration at the molecular target site and comprises a sequential series of effects on

molecular, cellular, organ, and organism level (Ankley et al., 2010; Escher et al., 2011). However, time-dependent effect progression has mostly been neglected in the description of toxicodynamic processes up to now.

By contrast, pharmacological research has focused on time-dependent toxicodynamic processes, which are described as explicit effect progression in various pharmacokinetic-pharmacodynamic models (PKPD) (e.g., Mager and Jusko (2001); Simeoni et al. (2004); Sun and Jusko (1998)). One of these PKPD models has been proposed by Simeoni et al. (2004) who linked the impact of different administration regimes of anticancer treatments to cancer cell growth. They applied a transit compartment model to explicitly characterize the time-dependent progression of cancer cell damage stages. The cell-cycle of cancer cells has been extensively studied in pharmacology to evaluate the effect of anticancer treatment on cancer cell growth (Simeoni et al., 2004). Cancer cell growth can be mathematically described by functional models, which base on a set of assumptions about biological growth involving cell-cycle mechanism. Altenburger et al. (2008) showed that the synchronized growth of unicellular green algae can be modeled with a modified model based on cancer cell growth. The cell-cycle of a unicellular green algae cell consists of three distinguishable phases, namely interphase, mitosis, and multiple divisions (Krupinska and Humbeck, 1994).

Chemicals may potentially affect basic biological processes of green algae cells such as growth or division (Krupinska and Humbeck, 1994; Ševčovičová et al., 2008). To evaluate adverse effects on algae growth or division, suitable biological assays with model organisms are essential in ecotoxicology. A 24 hours bioassay with a synchronized *Scenedesmus vacuolatus* cell population as a model organism has been shown to be a suitable diagnostic system assessing adverse effects on unicellular green algae (e.g., Adler et al. (2007); Altenburger et al. (2006); Franz et al. (2008); Neuwoehner et al. (2008)). A descriptive concentration-effect relationship for a fixed exposure time is usually employed to quantify the potential toxicity on individual cell growth ( $t_{14}$ ) or reproduction ( $t_{24}$ ). However, a purely descriptive concentration-effect relationship for a predefined exposure time is neither helpful to understand the processes behind the change of toxicity in time nor it is possible to translate the observed effect to different circumstances such as varying exposure concentrations (Jager et al., 2006). A process-based TKTD model for effect prediction on algae growth might address some of these limitations.

Therefore, the objective of the present study was to establish a specific TKTD model based on the description of time-dependent toxicodynamic processes leading to inhibition of individual algae cell growth. For this purpose, we performed bioassays with synchronized *Scenedesmus vacuolatus* suspensions exposed to various concentrations of model compounds with different modes of action, namely norflurazon, triclosan, and n-phenyl-2-naphthylamine. To predict the time-dependent effect progression on synchronized algae growth, we adopted and modified the PKPD model from Simeoni et al. (2004). Thus, a process-based TKTD model with focus on time-dependent effect progression during the synchronized growth of unicellular green algae has been developed.

## 2.2 METHODOLOGY

### 2.2.1 Algae cultivation

A synchronous culture of the unicellular green algae *Scenedesmus vacuolatus* (*S. vacuolatus*) (strain 211-215 SAG, Göttingen, Germany) was grown photoautotrophically in a climate

chamber at  $28 \pm 0.5$  °C. The liquid culture of the incubated algae grew in an inorganic, sterilized Grimme-Boardman-medium (GB-medium) adjusted to the pH of 6.4 (Altenburger et al., 2004). Algae cells were synchronized by a light/dark rhythm of 14/10 h. The *S. vacuolatus* suspensions were periodically diluted to a standard cell density of  $1 \times 10^6$  cells mL<sup>-1</sup> after every 24 h generation cycle. Synchronized algae cultures started to grow with the homogeneous algae size distribution within the light phase of the growth cycle.

### 2.2.2 Algae growth assay

Algae growth assays were performed with synchronized cultures of *S. vacuolatus* populations to determine the effect of chemicals on algae growth. The algae cells were exposed to the model chemicals norflurazon (CAS RN: 27314-13-2, purity 95%, Dr. Ehrenstorfer, Germany), triclosan (CAS RN: 3380-34-5, purity 99.8%, Calibochem, Switzerland), and n-phenyl-2-naphthylamine (PNA, CAS RN: 135-88-6, purity 97%, Aldrich, Germany) for one-generation cell-cycle. For preparation of the stock solutions, the chemicals were dissolved in 0.1% dimethyl sulfoxide (DMSO, CAS RN: 67-68-5, Merck, Germany) prior to the performance of the algae growth assay. Six different concentrations of each chemical were added to the algae cultures. Additionally, two negative controls and two DMSO controls were tested using the algae growth assay. The initial cell density was set to approximately  $7.5 \times 10^4$  cells mL<sup>-1</sup>, which was controlled by an electronic particle counter (CASYII, Schärfe System, Reutlingen, Germany). The algae growth assay was subsequently conducted in a closed 20 mL pyrex glass tube under permanent fluorescent light. Cell volume distribution and cell number of the algae cell population were measured with the electronic particle counter every two hours. For every observation time point, two technical replicates were taken. Two time-shifted algae synchronized cultures were treated with chemicals in parallel. Cell volume and cell number of the first algae culture were measured between 2 h and 14 h and of the second culture between 14 h and at least 24 h.

### 2.2.3 Statistical analysis

We used a two-tailed t-test of independent paired two-samples with a significance level of 5% to test the null hypothesis whether the effect parameters of the time-shifted cultures can be combined to one data set representing one-generation cell-cycle. Moreover, we investigated whether an influence of DMSO solvent on the control growth can be rejected.

### 2.2.4 Modeling of the concentration-response relationship for different exposure times

The concentration-response relationships were evaluated by using the values for the effect parameters cell volume and cell number for every sample time. The inhibition of cell volume or cell number ( $I(t)$  [%]) were calculated by

$$I(t) = 100 \times \frac{EP_{\text{Control}}(t) - EP_{\text{Treatment}}(t)}{EP_{\text{Control}}(t)} \quad (2.1)$$

where  $EP_{\text{Control}}(t)$  [fL or counts mL<sup>-1</sup>] and  $EP_{\text{Treatment}}(t)$  [fL or counts mL<sup>-1</sup>] reflect the effect measures for the chemical-untreated and chemical-treated algae cultures, respectively, which were measured at the same time points. A two parametric log-logistic nonlinear model was applied to the effect measures

$$E = \frac{1}{1 + \left(\frac{C}{EC_{50}}\right)^\theta} \quad (2.2)$$

where  $C$  [ $\mu\text{g L}^{-1}$ ] is the exposure concentration,  $EC_{50}$  [ $\mu\text{g L}^{-1}$ ] means the effect concentration causing 50% inhibition of algae growth or reproduction, and  $\theta$  [-] indicates the slope of the nonlinear function. The parameters  $EC_{50}$  and  $\theta$  were inversely estimated by minimizing the sum of squares of the nonlinear regression to the inhibited cell volume values, while at the same time keeping the minimum and the maximum effect level fixed to 0 and 100%, respectively, unless otherwise stated. In general, six chemical concentrations via 12 measured cell volume data points per time point were considered to determine the concentration-response relationship, except for the time point  $t_{14}$  where double the amount of data was fitted to the function due to the measurement of the time-shifted cultures in parallel. Statistical analyzes and concentration-response relationships were performed in the environment R by using the add-on package *drc* (Ritz and Streibig, 2005).

### 2.2.5 Determination of n-phenyl-2-naphthylamine uptake kinetics

At the time of harvest, the algae suspension had a density of approximately  $1 \times 10^7$  cells  $\text{mL}^{-1}$ . The algae suspension was concentrated by centrifuging at 2000 g and  $4^\circ\text{C}$  for three minutes. The supernatant was discarded and the pellet re-suspended in GB-medium. The algae suspension ( $3.2 \times 10^7$  cells  $\text{mL}^{-1}$ ) was divided in aliquots of 20 mL. All experiments were performed in amber vials to prevent degradation of the PNA by light. 20  $\mu\text{L}$  of standard stock solution of PNA in methanol was added, the solution was stirred at  $28^\circ\text{C}$  and 200 r.p.m with a glass covered stirrer bar. PNA concentrations were measured after 0, 1, 2, 4, 8, 16, 32, 64, 128, and 256 min in two replicates. A new sample was used for every sampling time. The experiment was conducted in duplicates. PNA concentrations in the algae suspension were measured with solid phase microextraction in combination with GC-MS (Bandow et al., 2010) (detailed description is given in **Chapter 3**, raw data Table A.7). To demonstrate that the decrease in the concentration was caused by algae uptake kinetics solely, three samples without algae were additionally prepared with 20 ml GB-medium and 20  $\mu\text{L}$  PNA stock solution. These samples were treated analogous to the algae samples and the concentration was measured after 0 min and 256 min, respectively.

### 2.2.6 The toxicokinetic-toxicodynamic model

A TKTD model was adopted and modified from Simeoni et al. (2004) to simulate the affected *S. vacuolatus* growth. A system of ordinary differential equations was connected to each other, which consisted of a (i) cell-cycle model, (ii) a toxicokinetic model, and (iii) a toxicodynamic model (Figure 2.1).

#### (i) The algae growth model

The dynamic of the unperturbed algae growth was mathematically described by an exponential growth phase ( $\approx 0 - 8$  h) which was followed by a linear growth phase ( $\approx 8 - 16$  h). The change of the mean cell volume  $V(t)$  [fL] at time point  $t$  resulted in the overall equation

$$V(t) = \begin{cases} V_0 \times \exp^{\mu_E \times t} & V(t) \leq V_{th} \\ \mu_L \times t + V_{th} & V(t) > V_{th} \end{cases} \quad (2.3)$$

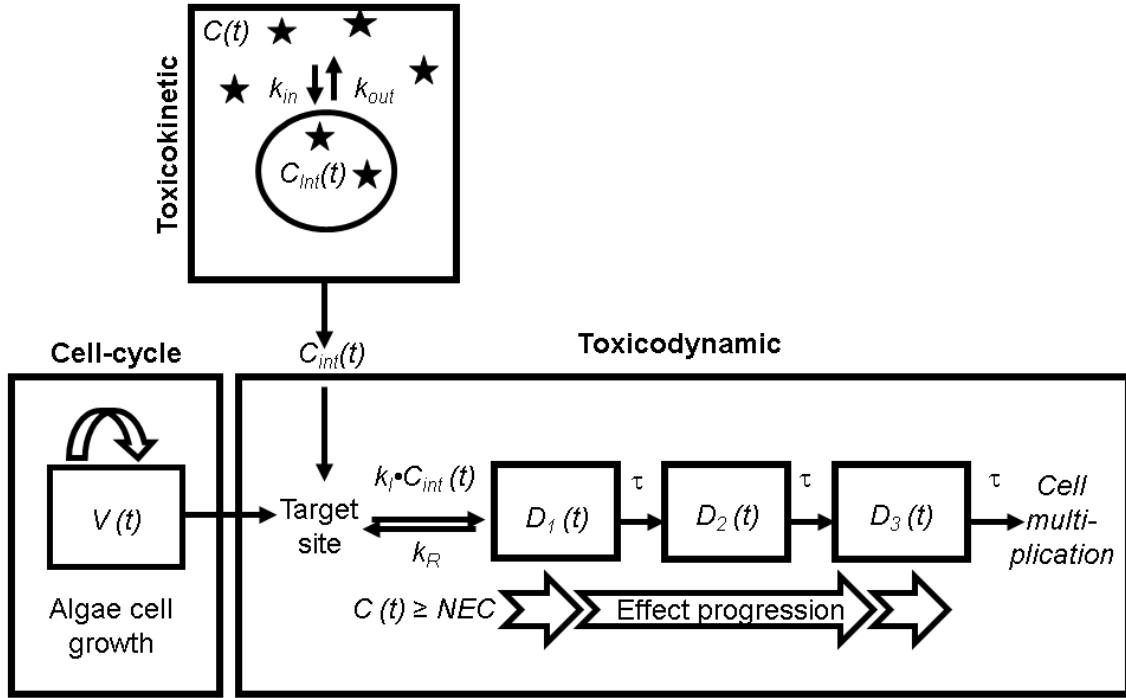


**Figure 2.1:** Conceptual scheme of the toxicokinetic-toxicodynamic model.  $C(t)$  denotes the ambient chemical concentration,  $C_{int}(t)$  is the internal concentration of the chemical in the algae cell,  $V(t)$  means the cell volume of the untreated algae cells,  $D_1(t) - D_3(t)$  are cell damage stages within the effect progression. Constants for uptake and elimination of a chemical in the algae cell are  $k_{in}$  and  $k_{out}$ , respectively.  $NEC$  represents the no-effect concentration,  $k_1$  is the kinetic rate constant to describe the chemical injury,  $k_R$  denotes the recovery/repair rate, and  $\tau$  means the effect progression time between two cell damage stages.

where the exponential growth rate is given by  $\mu_E$  [ $h^{-1}$ ] and the linear growth rate by  $\mu_L$  [ $fL h^{-1}$ ].  $V_0$  [ $fL$ ] represents the initial cell volume. The threshold volume value  $V_{th}$  [ $fL$ ] is calculated by  $\mu_L/\mu_E$  and indicates the switch from the exponential to the linear growth phase. To ensure a limited growth phase at the end of the one-generation algae cell-cycle, a cell-clock function was additionally included to the growth model of human cancer cells (Altenburger et al., 2008). To sum up, the differential equation characterizing the unperturbed growth of unicellular green algae is expressed as

$$\frac{dV(t)}{dt} = \frac{\mu_E \times V(t)}{\left[1 + \left(\frac{\mu_E}{\mu_L} \times V(t)\right)^\psi\right]^{\frac{1}{\psi}}} \times \left(1 - \mu_C \times \frac{V(t)}{K_{Crit}}\right) \quad (2.4)$$

The parameter  $\psi$  [-] is included into the growth model to force the switch from exponential to linear growth phase and, consequently, from a first-order to a zero-order growth process as clearly shown in Equation 2.3. Altenburger et al. (2008) proposed a value of  $\psi = 20$  for an elegant switch, which we also used in our study.  $K_{Crit}$  [ $fL$ ] represents the critical size for a commitment point and  $\mu_C$  [ $fL h^{-1}$ ] stands for the cell-clock rate.

**(ii) The toxicokinetic model**

The time-course of the internal chemical concentration  $C_{\text{int}}(t)$  [ $\mu\text{g kg}_{\text{wet}}^{-1}$ ] in *S. vacuolatus* cells was explicitly simulated by using a one-compartment model with a first-order kinetic

$$\frac{dC_{\text{int}}(t)}{dt} = k_{\text{in}} \times C(t) - k_{\text{out}} \times C_{\text{int}}(t) \quad (2.5)$$

$k_{\text{in}}$  [ $\text{L kg}_{\text{wet}}^{-1} \text{h}^{-1}$ ] represents the uptake rate constant and  $k_{\text{out}}$  [ $\text{h}^{-1}$ ] is the overall elimination rate constant. The parameters  $k_{\text{in}}$  and  $k_{\text{out}}$  could be estimated by fitting Equation 2.5 to the measured internal chemical concentration in algae cells  $C_{\text{int}}(t)$ . However, it is not straightforward to measure  $C_{\text{int}}(t)$  in algae cells. To overcome this issue, the parameters  $k_{\text{in}}$  and  $k_{\text{out}}$  were predicted by applying the linear log-log relationship between the hydrophobicity ( $K_{\text{OW}}$  [-]) of 41 organic chemicals and the measured bioconcentration factor (BCF [ $\text{L kg}_{\text{wet}}^{-1}$ ]) for the algae *Chlorella fusca* (Geyer et al., 1984)

$$\log BCF = \log \left( \frac{k_{\text{in}}}{k_{\text{out}}} \right) = 0.681 \times \log K_{\text{OW}} + 0.164 \quad (n = 41, r = 0.902) \quad (2.6)$$

The uptake rate was predicted using Equation 2.6 while at the same time considering a constant elimination rate of  $0.646 \pm 1.892 \text{h}^{-1}$  according to Sijm et al. (1998). The simulated internal concentration for the entire algae body was assumed to be approximately or proportional to the effect concentration at the target site triggering the effect. However, how many molecules ultimately induced an effect at the target site may depend on further features.

**(iii) The toxicodynamic model**

The toxicodynamic model was mathematically expressed as a continuous-time Markov process to simulate an inhibited cell growth caused by a certain chemical's internal concentration. Equation 2.7 reflects the initial state of the Markov chain where the predicted effect concentration of a chemical interacts with the target site that initiates the cumulative cell damage

$$\frac{D_1(t)}{dt} = \begin{cases} \frac{\mu_E \times V(t)}{\left[1 + \left(\frac{\mu_E}{\mu_L} \times V(t)\right)^\psi\right]^{\frac{1}{\psi}}} \times \left(1 - \mu_C \times \frac{V(t)}{K_{\text{Crit}}}\right) & \text{for } C(t) \leq NEC \\ \frac{\mu_E \times V(t)}{\left[1 + \left(\frac{\mu_E}{\mu_L} \times V(t)\right)^\psi\right]^{\frac{1}{\psi}}} \times \left(1 - \mu_C \times \frac{V(t)}{K_{\text{Crit}}}\right) - (k_I \times C_{\text{int}}(t) \times D_1(t) - k_R \times D_1) & \text{for } C(t) > NEC \end{cases} \quad (2.7)$$

where  $D_1(t)$  [fL] means the first damage stage of the inhibited cell volume within the damage progression. Effect progression was assumed to be induced when the exposure concentration  $C(t)$  is higher than a certain threshold concentration, the so-called no-effect concentration  $NEC$  [ $\mu\text{g L}^{-1}$ ]. For the index of chemical efficacy, the model assumes that the chemical elicits its effect decreasing the algae growth rate by a factor proportional to  $C_{\text{int}} \times D_1(t)$  through a second-order chemical injury rate constant  $k_I$  [ $\text{kg}_{\text{wet}} \mu\text{g}^{-1} \text{h}^{-1}$ ]. A repair/recovery rate constant  $k_R$  [ $\text{h}^{-1}$ ] was included to quantify the reversibility of damage at the target site. If the exposure concentration  $C(t)$  is less than a certain  $NEC$ , the algae cell population grows unperturbed. The toxicodynamic model was applied to display an effect progression from the interaction of a chemical with a target site to the observed effect parameter cell volume by explicitly assuming a sequence of damage steps within an effect progression. A simplified effect progression chain is expressed as

$$\frac{D_2(t)}{dt} = (k_1 \times C_{\text{int}}(t) \times D_1(t) - k_r \times D_1(t)) - D_2(t) \times \tau \quad (2.8)$$

$$\frac{D_3(t)}{dt} = \tau \times (D_2(t) - D_3(t)) \quad (2.9)$$

where the stages of progressive cell damage are represented by the three compartments  $D_1(t)$ ,  $D_2(t)$ , and  $D_3(t)$ . This Markov chain model represented three degrees of damage (n) described with an average time-to-event of  $n \times \tau$ . In general, one might include as many compartments in the Markov chain model, as involved cell damage steps in the effect progression processes

$$\frac{D_n(t)}{dt} = \tau \times (D_{n-1}(t) - D_n(t)) \quad (2.10)$$

The compartment  $D_n(t)$  at the end of the effect progression chain depicts here the observable phenotypic effect parameter cell volume. In the present study, the algae cell volume growth inhibition was expected to be the result of an effect progression process initiated by an interaction between the chemical and the biological target. We assumed three compartments in the toxicodynamic model to represent three observed cell damage stages within an effect progression process: the first compartment  $D_1$  reflected the molecular interaction of the chemical with the biological target site; the second compartment  $D_2$  demonstrated the physiological effect progression process e.g. on the physiological level; and the third compartment  $D_3$  represented the observed phenotypic endpoint cell growth distribution. The time to progress the effect between cell damage stages was characterized by the effect progression time  $\tau$  [ $\text{h}^{-1}$ ]. The effect progression times were assumed to be identical between the damage stages. Finally, the overall inhibited cell volume was described by:

$$\frac{D(t)}{dt} = V_0 + D_1(t) + D_2(t) + D_3(t) \quad (2.11)$$

### 2.2.7 Estimation of model parameters and model analysis

The TKTD model was implemented into the software Mathematica (Version 8.0, Wolfram Research) in which the model was inversely fitted to the cell volume measurements. Parameter optimization was achieved by minimizing the least-squares objective function. According to the maximum-likelihood theory, we assumed normal independent distribution for the errors with a mean of zero and an unknown standard deviation. The least-squares objective function was numerically minimized by the genetic algorithm named Differential Evolution. The Differential Evolution addresses the problem of predicting parameters by a global optimization approach, which should find the true global minimum of the objective function. Assuming all initial parameter values to be  $\geq 0$ , we found one robust parameter set which minimized the objective function. The 95% uncertainty intervals of the estimated best-fit parameter values were quantified using the standard error and the proper quantiles of the appropriate Student's  $t$ -distribution. To determine the model's accuracy, goodness-of-fit parameters such as the mean absolute error  $MAE$  [fL] and the coefficient of determination  $R^2$  [%] were calculated (Table 2.1). In the following, detailed information on the modeling and optimization settings in Mathematica as well as an excursion to the inverse modeling techniques are given.

### Modeling and optimization settings in Mathematica

- Time discretization: 0.01
- Iteration criteria: Maximum number of iterations 100
- Initial condition:
  - cell volume ( $V_0$ ) = 20;
  - cell volume damages  $D_1, D_2, D_3 = 0$ ;
  - external concentrations were set according to the six exposure concentrations of each chemical;
  - internal concentrations of triclosan, norflurazon and PNA = 0;
  - initial parameter region  $\mu_E, \mu_L, \mu_C \geq 0$ ;  
 $k_I, k_R, \tau, NEC \geq 0$
- Estimation method: Mathematica function "NonlinearModelFit"
- Numerical algorithm for constrained nonlinear optimization: "NMinimize" with special option to use the estimator algorithm Differential Evolution

### Objective function

Model parameters are determined by systematically minimizing the differences between measured ( $Y_i$ ) and simulated data ( $\hat{Y}_i$ ) of  $n$  values, the so-called residuals. To minimize the residuals, we applied the least-squares estimator as objective function  $\Theta(\beta_p)$ . The least-squares estimator squares and sums all residuals, which is mathematically described as follows

$$\Theta(\beta_p) = \sum_{i=1}^n (Y_i - \hat{Y}_i(\beta_p))^2 \quad (2.12)$$

$\beta_p$  means the array of parameter values in the form of an optimized parameter set that minimizes the objective function. To this end, the best solution for the array of parameter values is generated. However, deviations between model and data exist due to measurement errors, systematic errors and random errors. The assumptions of the deviations between measured and fitted data in the model error are:

- The error between data and simulation follow a normal distribution with mean zero and an unknown standard deviation.
- The standard deviation is the same for all data points.
- The normal distributions are uncorrelated (independent trials).

### Likelihood-Function

The defined likelihood distribution has to be maximized in order to estimate the value of one or more parameters. Assuming normal distributed errors with the mean  $\mu$  and the standard deviation  $\sigma$ , the likelihood function  $L(\Theta|Y)$  can be written as

$$L(\Theta(\beta_p)|Y) = P(\Theta(Y|\beta_p)) = \prod_{i=1}^n \frac{n}{\sqrt{2\pi}\sigma^2} \exp\left(-\frac{(Y_i - \hat{Y}_i(\beta_p))^2}{2\sigma^2}\right) \quad (2.13)$$

According to Equation 2.13, the maximum-likelihood estimate is the value of the unknown parameter vector  $\beta$  that maximizes the value of the likelihood function.

### Global parameter optimization algorithm "Differential Evolution"

The objective function was minimized by the "Differential Evolution", which is a genetic algorithm developed by Storn and Price (1995). It is a parallel search techniques which running several vectors simultaneously. It follows a typical pattern including the four stages (i) initialize population, (ii) mutation, (iii) crossover and (iv) evaluation and selection (Figure 2.2).

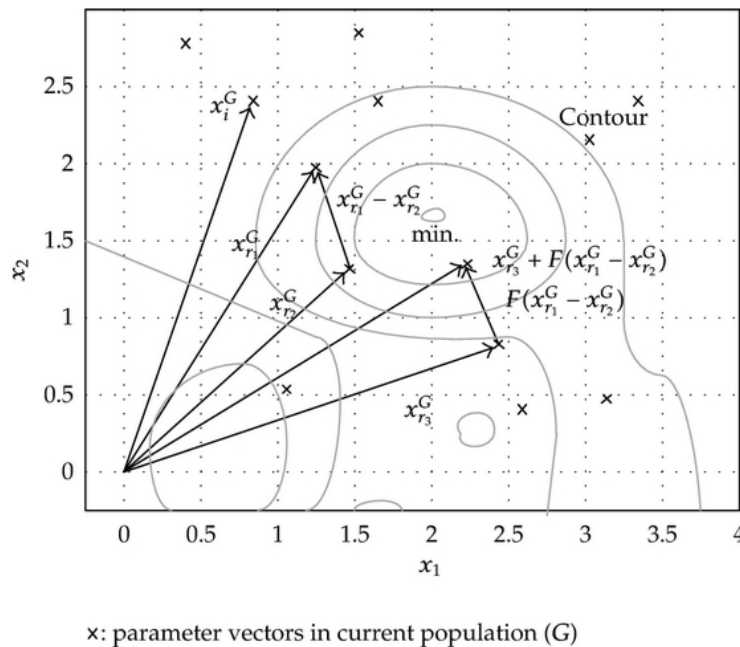


**Figure 2.2:** Two-dimensional example of the "Differential Evolution" method – creation of new generation from current generation (adapted from Taher and Afsari (2012)).

1. Initialize population with size NP: The initial vector population ( $x_{i;G} = 1, 2, \dots, NP$ ) chosen randomly in the limited D-dimensional parameter space
2. Mutation: Creation of new parameter vectors from each member  $i$  by adding the weighted difference ( $\Delta$ ) between two population vectors, the so-called mutated vector  $v_{i,G+1}$

$$v_{i,G+1} = x_{r3,G} + \Delta(x_{r1,G} - x_{r2,G}) \quad (2.14)$$

where the subscripts  $r_1$ ,  $r_2$ , and  $r_3$  represent the randomly selected vectors of the generation G.

3. **Crossover:** In order to increase the diversity of the perturbed parameter vectors, the crossover is introduced. The mutated vector's  $V_{i,G+1}$  are mixed with the parameters of the predetermined target vector  $X_{i,G}$  in order to form the trial vector  $u_{i,G+1}$ .

$$\begin{cases} u_{i,G+1} = v_i^k \text{if rand} \leq CR \text{ or } k = JRand \\ u_{i,G+1} = x_{i,G} \text{if rand} > CR \text{ or } k \neq JRand \end{cases} \quad (2.15)$$

where the subscript k indicates the kth component of the trial vector, rand is a random scalar between 0 and 1, JRand is a randomly chosen integer between 1 and the dimension.

4. **Evaluation and Selection:** To decide whether or not it should become a member of the new generation
- If the trial vector  $u_{i,G+1}$  yields a smaller objective function than the target vector  $x_{i,G}$ , then create a new generation with the vector population  $u_{i,G+1}$  and restart with the genetic algorithm
  - If the trial vector  $u_{i,G+1}$  yields a larger objective function than the target vector  $x_{i,G}$ , then stop the the genetic algorithm running as the objective function has not improved for a certain number of iterations.

The "Differential Evolution" is a heuristic approach which minimizes nonlinear, non-differentiable and multimodal continuous objective functions. It is a computationally expensive method, but is relatively robust and tends to work well for problems that have more than one local minimum. Therefore, it is a suitable method supposed to find the global parameters.

### Calculation of parameter uncertainty

The uncertainties of the estimated parameters were quantified using the standard error and the proper quantiles of the appropriate Student's  $t$ -distribution. The Student's  $t$ -distribution was used to calculate the prediction interval for an unobserved sample from a normal distribution with unknown mean and variance.

$$t \equiv \frac{\bar{x} - \mu}{\frac{s}{\sqrt{n}}} \quad (2.16)$$

where  $\bar{x}$  is the sample,  $\mu$  means the population mean, and  $s$  is the standard error. The 95% parameter confidence interval follows the subsequent calculation if normal distributed errors of the optimized parameters with the mean  $\mu$  and the standard error  $s$  is assumed

$$P\left(\bar{x} - 1.96 \frac{s}{\sqrt{n}} \leq \mu \leq \bar{x} + 1.96 \frac{s}{\sqrt{n}}\right) \quad (2.17)$$

where n is the sample size and 1.96 means the z-value of the Students'  $t$ -distribution when the confidence is assumed to be 95%.

## 2.3 RESULTS

### 2.3.1 Unperturbed algae growth

First, we investigated the unperturbed growth behavior of the synchronized suspension cultures of *S. vacuolatus* populations (Figure 2.3). Because we did not find a significant difference between

measured cell volume of the negative control groups and the DMSO-solvent control groups (two-tailed paired t-Test,  $p \geq 0.05$ ,  $n = 4$ ), we combined both groups to a pooled control group including eight data per time point. The growth pattern of a one-generation cell-cycle can be described as follows: starting with autospores, a first lag-phase of slow growth was followed by a second phase of fast growth, and finally finishing into a plateau (Figure 2.3). The plateau state was reached for the control groups between time points 18 h and 20 h. After reaching the plateaus, the cell volumes decreased to almost the initial cell size within two hours. This indicated the synchronous release of autospores after the multiple divisions of the mother cells (Figure 2.3; closed symbols). Due to the multiple divisions of the mother cells, the number of autospores increased at the same time as the cell volume decreased (Figure 2.4A–C). In total, an increase of 22-fold cell volume was observed within the one-generation cell-cycle for the pooled controls when testing the influence of triclosan and PNA on algae growth and even a 27-fold increase for the control group tested in parallel to the growth assay with norflurazon. The growth rates  $\mu_E$ ,  $\mu_L$ , and  $\mu_C$  were estimated by fitting the cell-cycle model to the measured cell volume of the pooled control groups (Equation 2.4). Table 2.1 itemizes the estimated parameters  $\mu_E$ ,  $\mu_L$ , and  $\mu_C$  while at the same time the parameters  $K_{\text{Crit}}$  and  $\psi$  were fixed to 80 fL and 20, respectively, according to Altenburger et al. (2008). Only the cell volume data of one-generation cell-cycle were incorporated into the minimization of the objective function by the global estimator (Figure 2.3; open symbols). The cell-cycle model fitted the cell volume measurements of the pooled control groups very well, as can be deduced from the goodness-of-fit parameters (Table 2.1).

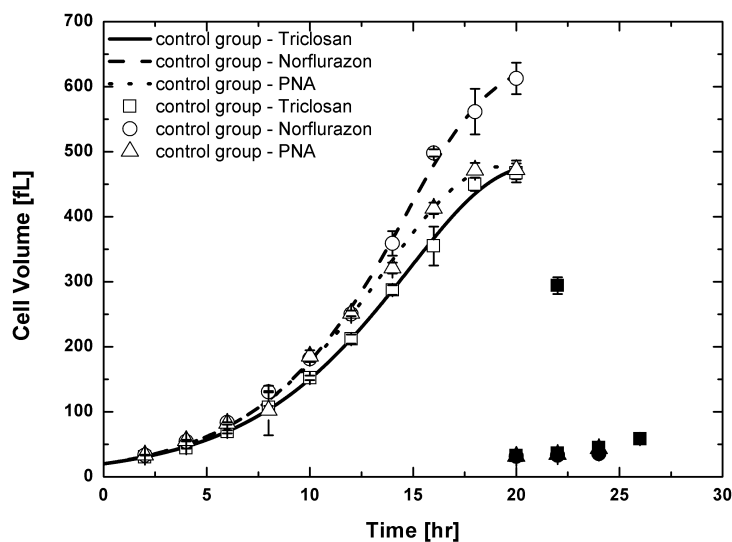


**Figure 2.3:** Cell volume of the unperturbed *S. vacuolatus* synchronized cultures was measured in parallel to each algae growth assay with triclosan, nrflurazon, and PNA. The symbols represent the mean cell volume measurements ( $\pm 95\%$  CI) of the first generation (open) and second generation (closed). Each control group consists of eight measurements per time point except time point  $t_{14}$  with 16 measurements. The lines show the simulations of the predicted time-course of the first generation cell volume. For modeling the measurements of the second algae generation have been neglected.

### 2.3.2 Perturbed algae growth pattern in dependency of exposure concentration and exposure time

Next, we investigated the influence of model chemicals with different modes of action on individual and population growth (raw data Table A.1 – Table A.6). We found chemical-specific concentration-time-response patterns for the effect parameter cell volume (Figure 2.5A–C) and concentration-response relationships for the effect parameter cell number (Figure 2.5D–F) of *S. vacuolatus* cell populations exposed to six different concentrations of triclosan, norflurazon, and PNA, respectively. In general, the averaged volume of *S. vacuolatus* cells decreased with increasing concentration. The response gradients of the cell volumes between the simulated growth patterns of the control groups (Figure 2.4; solid line) and the triclosan and norflurazon treated algae cells increased with both exposure time and chemical concentration in a nonlinear relationship. Also, the earliest responses were observed with the highest norflurazon and triclosan exposure concentrations. Inversely, the lower the ambient concentrations of the chemicals were, the later the chemicals caused an observable inhibition of the cell volumes. In contrast to the concentration and time-driven response gradients for triclosan and norflurazon, the response

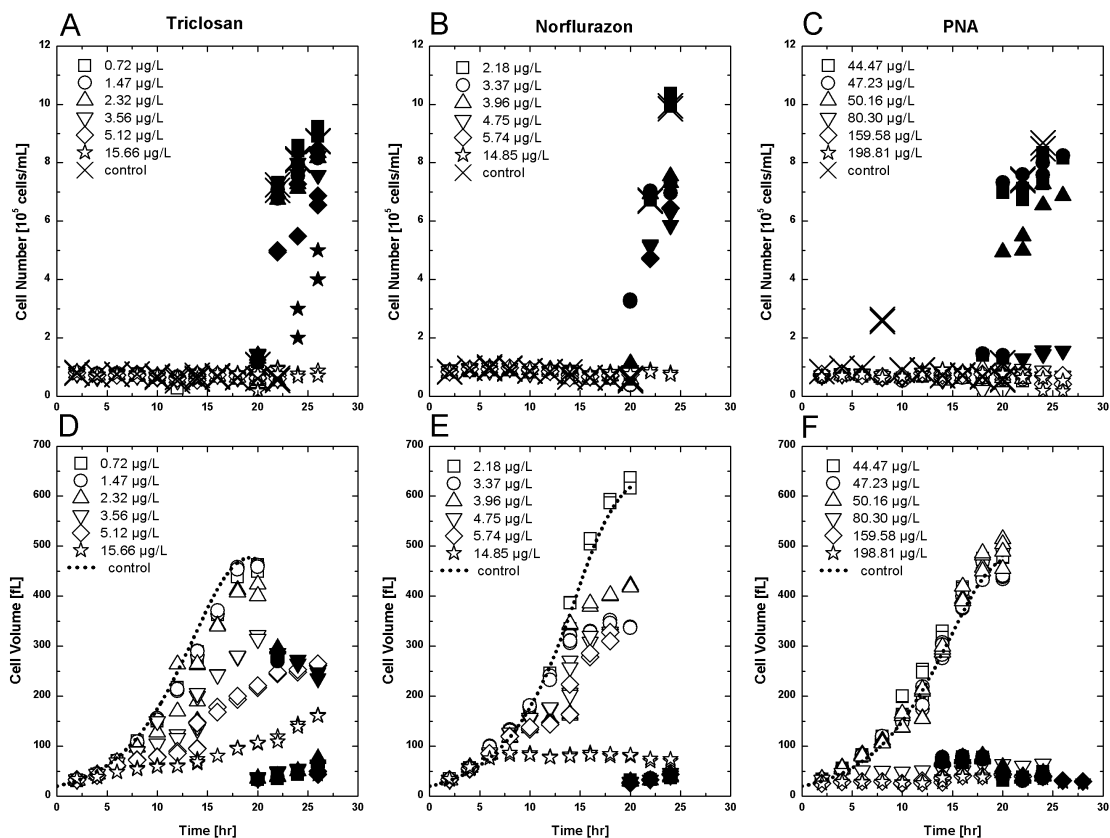


**Figure 2.4:** Measurements of the effect parameter cell number (A–C) and cell volume (D–F) of *S. vacuolatus* cells. The algae cell populations were treated with six different concentrations of the chemicals triclosan, norflurazon, and PNA, respectively. The cell volumes of the first algae cell generation (open symbols) have been used for TKTD modeling, whereas the cell volumes of the second generation (closed symbols) have been neglected. Note that instead of two replicates four replicates were generated only at time point 14 due to two time-shifted algae cultures tested in parallel.

gradients between the cell volumes of PNA treated *S. vacuolatus* cells and the simulated growth of the control groups seemed to be mainly driven by the PNA exposure concentrations. Either there was no response as observed for the three lowest PNA concentrations, or there was a high response as observed for the three highest PNA concentrations compared to the control group growth. Moreover, we observed two subpopulations differentiated during the linear growth phase for the *S. vacuolatus* population treated with the three lowest PNA concentrations. One sub-population was not growing characterized by a constant cell volume, while at the same time the second coexisting cell sub-population grow with the same rate as the control group.

Finally, we found chemical concentrations for all three investigated chemicals, which do not affect the cell volume over exposure time. The lowest norflurazon concentration ( $2.18 \mu\text{g L}^{-1}$ ) and the three lowest triclosan exposure concentrations ( $0.72 \mu\text{g L}^{-1}$ ,  $1.47 \mu\text{g L}^{-1}$ , and  $2.32 \mu\text{g L}^{-1}$ ) did not affect the algae cell growth compared to the control growth. The three lowest PNA exposure concentrations ( $44.47 \mu\text{g L}^{-1}$ ,  $47.23 \mu\text{g L}^{-1}$ , and  $50.16 \mu\text{g L}^{-1}$ ) affected cell growth of one sub-population.

The inhibition of algae cell volume affected the number of released autospores (Figure 2.5). All norflurazon treated algae cells divided between 20 h and 24 h of continuous exposure, except for algae cells exposed to the highest concentration of  $14.85 \mu\text{g L}^{-1}$ , which did not divide over

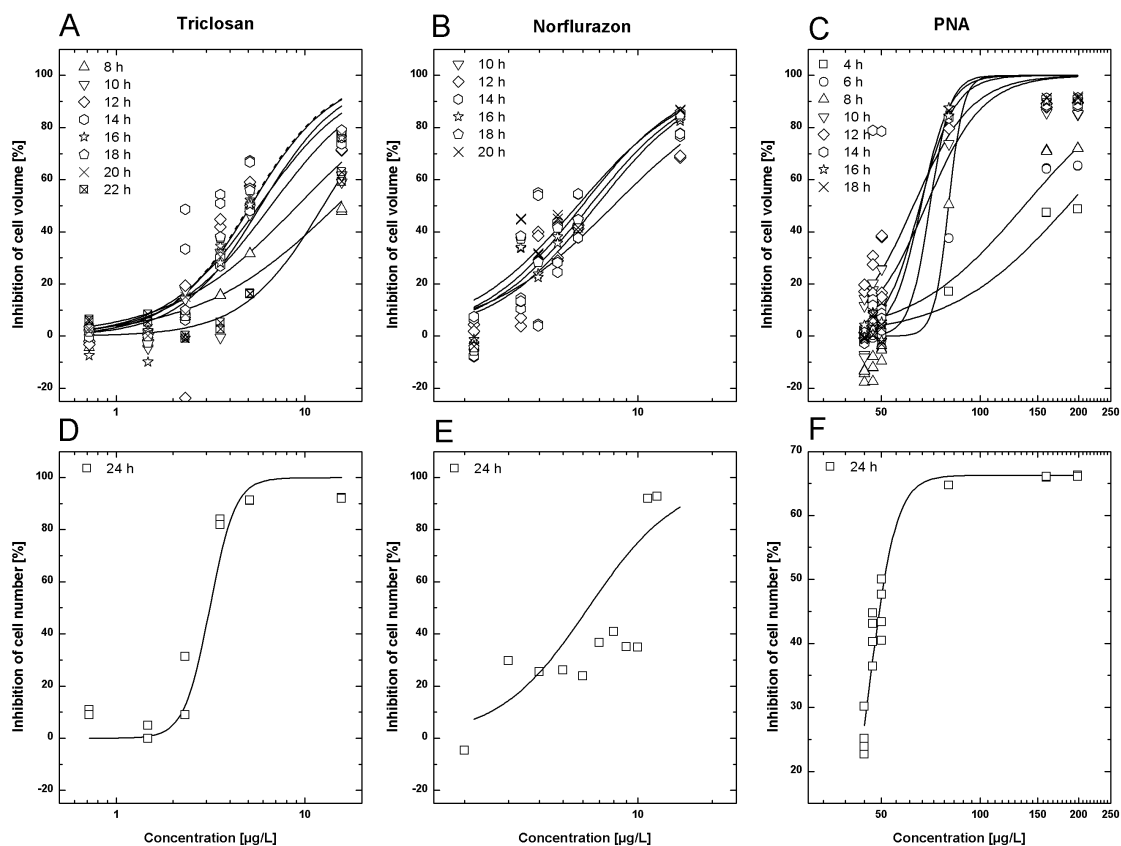


**Figure 2.5:** The two-parametric log-logistic model (lines) fitted to the concentration-depending inhibited effect parameters cell volume (A–C) and cell number (D–F) for Triclosan, Norflurazon, and PNA, respectively. Please notice that the maximum inhibition of cell number for PNA was fitted to 65.66% (95% CI [61.978%, 69.35%]).

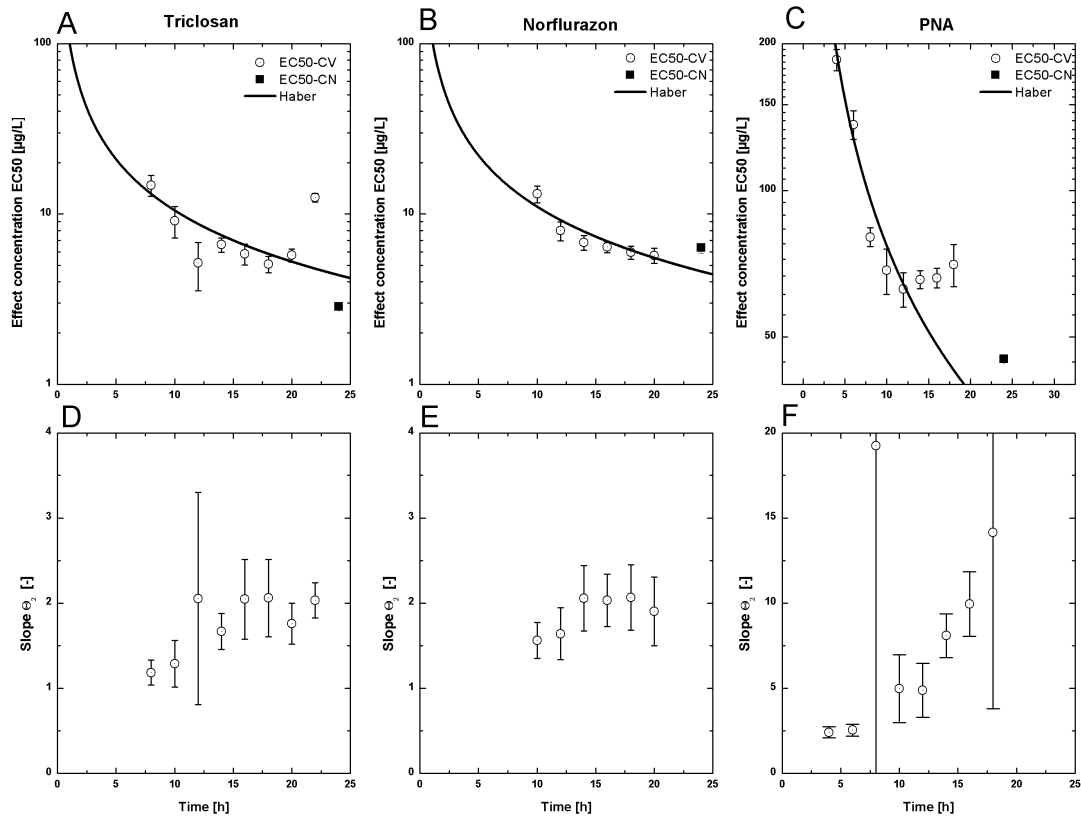


**Figure 2.6:** The time-course of estimated  $EC_{50}(t)$ -values  $\pm 95\%$  CI (A–C) and slope-values  $\theta(t) \pm 95\%$  CI (D–F) are represented for triclosan, norflurazon, and PNA, respectively. The solid line demonstrate the simulation of the time-effect relationship by Haber's law (A–C).

26 h exposure. (Figure 2.4A–C). The algae cells of the control group and of the norflurazon treated group with the lowest concentration of  $2.18 \mu\text{g L}^{-1}$  multiplied both eight times on average. The number of divisions generally decreased with increasing norflurazon concentration. By comparison, algae cells exposed to the three highest triclosan concentrations did not divide within the 26 h experiment duration, although the non-treated and the three lowest exposed algae cells started to divide after 20 h. Additionally, a reduced number of autospores after multiple divisions compared to the control was observed for the treated algae cells of  $2.32 \mu\text{g L}^{-1}$  triclosan, although growth of algae cells was not inhibited. We did not find an inhibition of the growing sub-population of PNA treated *S. vacuolatus* culture compared to the control growth, but the numbers of autospores were reduced within the multiple division phases at the end of the first generation of the cell-cycle. In general, the cell growth inhibited by higher chemical concentrations (norflurazon =  $14.85 \mu\text{g L}^{-1}$ , triclosan =  $3.56 \mu\text{g L}^{-1}$ ,  $5.11 \mu\text{g L}^{-1}$ ,  $15.65 \mu\text{g L}^{-1}$ ) induced a retarded growth characterized by a delayed cell division in comparison with the control groups.

### 2.3.3 Time dependence of toxicity

The observed temporal growth patterns resulted in time-dependent median effect concentrations (Table A.8). To describe the toxicities over time, at least 14 parameters had

to be estimated (Figure 2.5). Figure 2.6 displays the time-courses of the estimated parameters  $EC_{50}(t)$ -values as well as slope values  $\theta$  and their 95% confidence intervals for triclosan, norflurazon, and PNA, respectively. Norflurazon and triclosan inhibited the cell volume and cell number in the same range of exposure concentrations, whereas PNA was clearly 5-fold less effective. The estimated  $EC_{50}(t)$ -values decreased with time (Figure 2.6). Consequently, the toxicity increased over time until a steady-state of toxicity was reached. For norflurazon and PNA, the time-dependent effect concentrations  $EC_{50}(t)$  reached the steady-state within the exposure time. By contrast, steady-state toxicity was not reached for triclosan. Instead, a slight detoxification was observed after 20 h continuous exposure, which was indicated by an increase of the  $EC_{50}(t)$  values measured at 24 h. A generalized form of Haber's law was used as an empirical model to describe the observed toxicities over exposure duration (Figure 2.6).

### 2.3.4 Toxicokinetic-toxicodynamic modeling

Using the experimental observations, we adopted the represented TKTD model (Figure 2.1) to test the models' applicability. In Figure 2.7 (A–C) the predicted time-courses of the internal concentrations depending on the exposure concentrations for each chemical as applied in the growth assay is shown. Corresponding to the hydrophobicities of triclosan and PNA, the uptake rate constants were predicted as  $1643.59 \text{ L kg}^{-1} \text{ h}^{-1}$  and  $905.76 \text{ L kg}^{-1} \text{ h}^{-1}$ , respectively, which were much higher than the predicted uptake rate constant for norflurazon ( $34.72 \text{ L kg}^{-1} \text{ h}^{-1}$ ). However, the concentration-independent steady-state of the internal concentrations in the algae cell for the three chemicals was predicted to occur after approximately 5 h of exposure, which was characterized as chemical-unspecific. The chemical-unspecific time to reach steady-state of the internal concentration results from the constant elimination rate of  $0.646 \pm 1.892 \text{ h}^{-1}$  for all chemicals according to Sijm et al. (1998).

In Figure 2.7(D–F) the measurements of cell volumes are depicted compared to the corresponding simulations of the estimated *S. vacuolatus* growth as affected by various concentrations of triclosan, norflurazon, and PNA. In general, the TKTD model successfully fitted the measured cell volumes over time for the various tested concentrations of triclosan, norflurazon, and PNA as can be deduced by low mean absolute errors (MAE) with respect to the mean absolute errors gained for the control groups as well as by high correlation coefficients  $R^2 \leq 98\%$  (Table 2.1). The predicted cell volume time-courses for various concentrations of triclosan fitted the measured cell volumes for all concentrations well except for the highest concentration, where the cell volumes until 22 h exposure time were overestimated. Also, the time-course of the predicted cell growth for the highest norflurazon concentration of  $14.85 \mu\text{g L}^{-1}$  overestimated the measurements. Moreover, the simulations for the norflurazon concentrations  $3.37 \mu\text{g L}^{-1}$  and  $3.96 \mu\text{g L}^{-1}$  mismatched the observed cell volumes systematically. The delayed observed effect of cell volume inhibitions agreed with the simulations for triclosan and norflurazon. The time-course of the predicted cell growth for PNA accurately simulated either no observable responses for the three lowest PNA concentrations or high responses for the three highest PNA concentrations. To model the individual cell growth, notice that the non-growing subpopulation observed for the three highest PNA concentrations was excluded from the parameter estimation procedure. The delayed effect of the PNA inhibited cell volumes were matched by the simulations of the TKTD model, which were observed independent of the tested PNA concentrations.

The individual cell growth was simulated according to the estimated chemical-specific global toxicodynamic parameter sets (Table 2.1). The effect progression rate of  $1.018 \times 10^{-3} \text{ h}^{-1}$  for

**Table 2.1:** Parameter estimates, their 95% confidence intervals, and goodness-of-fit parameters of the cell-cycle model and the TKTD model.

	tricolosan				norflurazon				PNA <sup>a</sup>				PNA <sup>b</sup>			
	estimated mean [95% CI]	SE	df	MAE [FL] [FL]	R <sup>2</sup> [%] [%]	estimated mean [95% CI]	SE	df	MAE [FL] [FL]	R <sup>2</sup> [%] [%]	estimated mean [95% CI]	SE	df	MAE [FL] [FL]	R <sup>2</sup> [%] [%]	
$\mu_E$ [h <sup>-1</sup> ]	0.213 [0.209, 0.217]	2.016 × 10 <sup>-3</sup>	93	6.18	99.80	0.228 [0.222, 0.234]	3.027 × 10 <sup>-3</sup>	77	10.14	99.82	0.231 [0.229, 0.232]	0.780 × 10 <sup>-3</sup>	83	6.72	99.89	
$\mu_L$ [FL h <sup>-1</sup> ]	91.586 [17.122, 166.051]	37.498				99.511 [60.225, 138.798]	19.73				192.314 [0.5358 × 10 <sup>6</sup> ]	2.694 × 10 <sup>6</sup>				
$\mu_C$ [h <sup>-1</sup> ]	0.018 [0.016, 0.020]	1.070 × 10 <sup>-3</sup>				0.014 [0.105, 0.018]	1.794 × 10 <sup>-3</sup>				0.0202 [0.197, 0.0207]	0.250 × <sup>-3</sup>				
$K_{Ccrit}$ [FL]	80	-				80	-				80	-				
$\psi$ [-]	20	-				20	-				20	-				
$k_{in}$ [L kg <sub>wet</sub> <sup>-1</sup> h <sup>-1</sup> ]	1643.586	-	-	-	-	34.720	-	-	-	-	905.759	-	-	-	8.63	
$k_{out}$ [h <sup>-1</sup> ]	0.646	-	-	-	-	0.646	-	-	-	-	0.646	-	-	-	6.347	
NEC [μg L <sup>-1</sup> ]	3.459 [3.459, 3.459]	0	140	14.56	98.63	3.286 [3.286, 3.286]	0	128	23.15	98.23	69.865 [69.865, 69.865]	0	192	14.38	99.15	
$k_I$ [kg <sub>wet</sub> μg <sup>-1</sup> h <sup>-1</sup> ]	23.26 × 10 <sup>-6</sup> [21.965 × 10 <sup>-6</sup> , 24.561 × 10 <sup>-6</sup> ]	0.656 × 10 <sup>-6</sup>				3.593 × 10 <sup>-4</sup> [3.041 × 10 <sup>-4</sup> , 4.146 × 10 <sup>-4</sup> ]	2.787 × 10 <sup>-5</sup>				0.144 [0.080, 0.208]	0.032				
$k_R$ [h <sup>-1</sup> ]	0.104 [0.099, 0.109]	0.002				0.013 [0.002, 0.025]	0.006				0.453 [0.258, 0.647]	0.098				
$\tau$ [h <sup>-1</sup> ]	1.018 × 10 <sup>-3</sup> [0, 13.152 × 10 <sup>-3</sup> ]	6.173 × 10 <sup>-3</sup>				0.458 [0.423, 0.494]	0.018				0.309 [0.245, 0.372]	0.032				

<sup>a</sup>PNA - Toxicodynamic parameter estimations for PNA based on toxicokinetic parameters derived from literature (2.6)

<sup>b</sup>PNA - Toxicodynamic parameter estimations for PNA based on measured PNA uptake kinetics (see also Figure 2.8)

Abbreviations:  $\mu_E$ -exponential growth rate,  $\mu_L$ -linear growth rate,  $\mu_C$ -cell-clock rate,  $K_{Ccrit}$ -critical size as a commitment point,  $\psi$ -parameter to force switch from exponential to linear growth,

$k_{in}$ -uptake rate constant,  $k_{out}$ -elimination rate constant, NEC-no-effect concentration,  $k_I$ -chemicals injury rate constant,  $k_R$ -repair/recovery rate constant,  $\tau$ -effect progression time,

CI-confidence interval, df-degrees of freedom, MAE-mean absolute error, R<sup>2</sup>-correlation coefficient

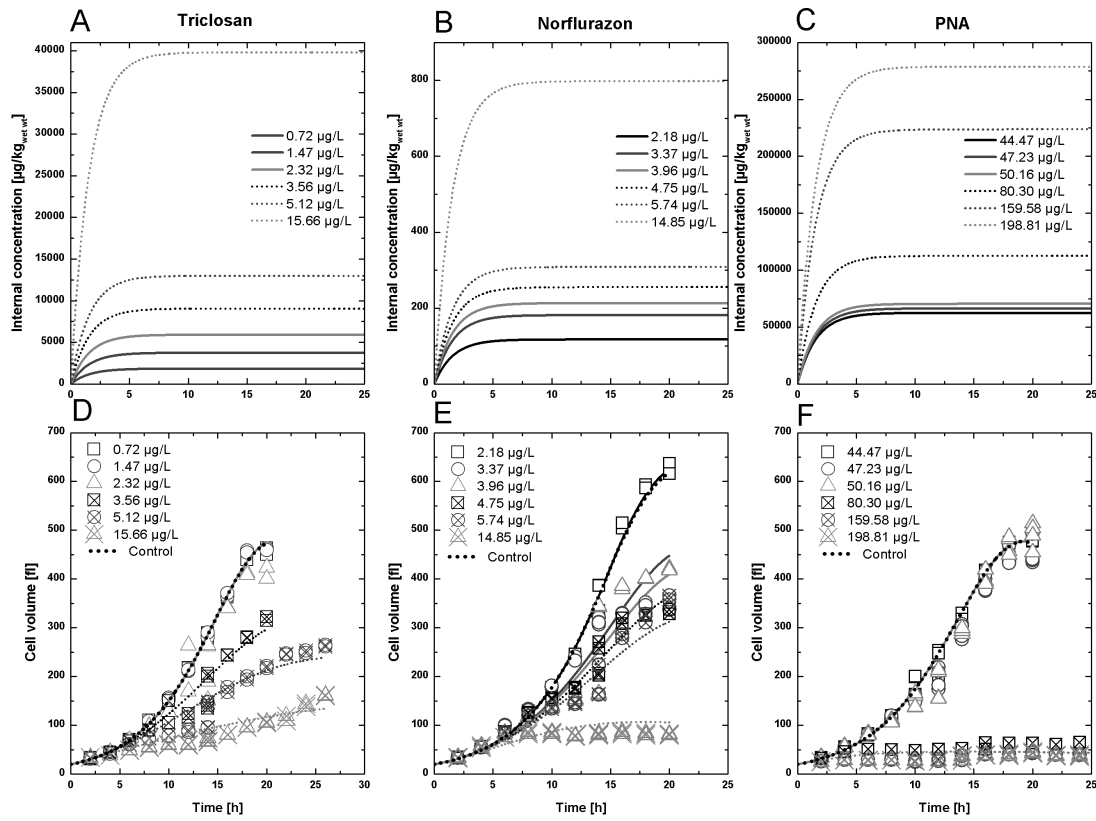


**Figure 2.7:** Observed and model-fitted toxicokinetic (A–C) and toxicodynamic (D–F) processes for triclosan, norflurazon, and PNA. The predicted internal algae concentrations (lines) depend on the tested exposure concentrations of each chemical (A–C). The simulations of the toxicodynamic model are represented by the lines (D–F). The measurements of the cell volume are depicted as symbols. The dashed lines represent the cell volume simulation for the control groups.

triclosan was estimated to be 450-fold lower than for norflurazon and 300-fold lower than for PNA. Furthermore, we predicted a chemical injury rate  $k_I$  of  $23.26 \times 10^{-6} \text{ kg}_{\text{wet}} \mu\text{g}^{-1} \text{ h}^{-1}$  for triclosan, which was 15-fold lower for norflurazon and even 6200-fold lower for PNA. The estimated recovery/repair rates did not vary between the chemicals as widely as the previous mentioned toxicodynamic parameters. We estimated for triclosan an 8-fold higher and a 4.35-fold lower recovery/repair rate compared to norflurazon and PNA, respectively. In addition, we estimated the no-effect concentrations  $NEC$  for triclosan ( $1.97 \mu\text{g L}^{-1}$ ), norflurazon ( $2.81 \mu\text{g L}^{-1}$ ), and PNA ( $69.86 \mu\text{g L}^{-1}$ ).

## 2.4 DISCUSSION

### 2.4.1 Data quality assessment

*S. vacuolatus* growth assays with norflurazon, triclosan, and PNA showed differences in sensitivity regarding their time-dependent toxicities (Figure 2.6). The effect concentration  $EC_{50}$  for growth over time ranged from  $13.13 \mu\text{g L}^{-1}$  to  $5.70 \mu\text{g L}^{-1}$  for norflurazon, from  $14.77 \mu\text{g L}^{-1}$  to  $5.09 \mu\text{g L}^{-1}$  for triclosan, and from  $185.31 \mu\text{g L}^{-1}$  to  $62.69 \mu\text{g L}^{-1}$  for PNA. All three model

chemicals have shown excess toxicity in unicellular algae (Altenburger et al., 2006; Adler et al., 2007; Franz et al., 2008; Neuwoehner et al., 2008). Norflurazon is known to specifically inhibit the carotenoid biosynthesis (Neuwoehner et al., 2008). It reversibly binds to the phytoene desaturase within the carotenoid biosynthesis pathway, which is located in the lipid-rich chloroplast. The effect concentration indicating 50% inhibition of *S. vacuolatus* reproduction has been found to range between  $2.00 \mu\text{g L}^{-1}$  (Adler et al., 2007) and  $12.45 \mu\text{g L}^{-1}$  (Neuwoehner et al., 2008) when continuously exposed to norflurazon for 24 h, which is consistent with our findings. Thies et al. (1996) detected slightly higher norflurazon effect concentrations  $EC_{50}$  of  $12.15 \mu\text{L}^{-1}(t_{14})$  and  $182.20 \mu\text{g L}^{-1}(t_{14})$  for *Chlorella fusca* and *Chlorella sorokiniana* growth, respectively, than found in the present study ( $EC_{50}(t_{14}) = 6.80 \mu\text{g L}^{-1}$ ). Triclosan is thought to interact with multiple target sites in *S. vacuolatus* and may provoke multiple modes of action (Franz et al., 2008). Triclosan has been reported to destabilize the cell membrane, causing structural perturbations with resultant loss of permeability barrier functions, and inhibit the enzyme enoyl-acyl carrier protein reductase (FabI) (Franz et al., 2008). Franz et al. (2008) reported  $EC_{50}$  values of  $1.90 \mu\text{g L}^{-1}$  for the inhibition of reproduction of *S. vacuolatus* and of  $5.42 \mu\text{L}^{-1}$  for the inhibition of the photosynthetic activity, which are comparable to the effect concentrations found in the present study (individual cell growth:  $EC_{50}(t_{14}) = 6.60 \mu\text{g L}^{-1}$ ). Altenburger et al. (2006) suggested that PNA acts as a reactive chemical in membrane-rich compartments such as algae chloroplasts. Altenburger et al. (2006) have shown that *S. vacuolatus* was the most sensitive species to PNA in terms of reproduction ( $EC_{50}(t_{24}) = 33.5 \mu\text{g L}^{-1}$ ). They also observed time-shifted  $EC_{50}$  values from  $790 \mu\text{g L}^{-1}(t_2)$  to  $80 \mu\text{g L}^{-1}(t_{14})$  for the inhibition of cell volume, which again is reasonably similar to what was found here. TKTD modeling could help to derive clearer insights into the reasons for temporal-shifted toxicities such as the distinction of the time scales of toxicokinetic and toxicodynamic processes. Therefore, the question can be addressed whether the time-dependent toxicity is controlled mainly by toxicokinetic processes or is rather due to another rate-limiting step such as an effect progression process. Moreover, TKTD models are able to predict a no-effect concentration of a chemical below which no observable effects to the organism occur over the exposure duration.

## 2.4.2 Toxicokinetic-toxicodynamic modeling framework

To characterize time-dependent toxicities descriptive models such as concentration-response models with many parameters to be optimized have been usually used (Altenburger et al., 2006; Franz et al., 2008). Here, the concentration-response model was fitted to the measurements of inhibited cell volume and at least 14 parameters would be needed to describe toxicity over time without giving an insight into the underlying driving processes (Jager et al., 2006) (Figure 2.6, Table A.8). In the present study, a process-based TKTD model was established to model and estimate unicellular *S. vacuolatus* growth of synchronous cultures and the observed delayed effects of triclosan, norflurazon, and PNA on algae growth. The TKTD model successfully fitted the different patterns of *S. vacuolatus* growth by estimating just four toxicodynamic parameters, while at the same time keeping fixed parameters describing cell-cycle and toxicokinetics (Figure 2.7, Table 2.1). The TKTD model simulated internal concentration and time-dependent responses of chemicals with three different modes of action. This model robustness might be due to the attempt to model the damage kinetics instead of the specific molecular mechanism by which the *S. vacuolatus* cell population is damaged (Simeoni et al., 2004). Nevertheless, the chemicals differently affected the algae growth process resulting in chemical-specific cell growth patterns. Even if the interpretation of toxicity remains a challenge associated with the complexity of

multiple processes, a TKTD model may help to understand the underlying driving processes that affect *S. vacuolatus* growth, including cell-cycle, toxicokinetic, and toxicodynamic processes (Rozman and Doull, 2000).

### 2.4.3 Modeling of algae growth

First, a simple exponential growth model was fitted to the measurements of algae cell volume as it is usually done in ecotoxicological hazard assessment. The exponential growth rates for the control groups were estimated to be  $0.167 \pm 0.004 \text{ h}^{-1}$  for triclosan,  $0.180 \pm 0.004 \text{ h}^{-1}$  for norflurazon, and  $0.170 \pm 0.005 \text{ h}^{-1}$  for PNA. However, a more complex algae growth pattern has been reported by Altenburger:2008, who described different growth phases of *Desmodesmus subspicatus* cultures. We confirmed this growth pattern by measuring the mean cell volume within a one-generation *S. vacuolatus* cell-cycle over time and fitted a mechanism-based model for algae growth to the measurements (Altenburger et al., 2008). The cell-cycle model fits very well to the time course of the cell volume measurements, although the critical size of commitment point  $K_{\text{Crit}}$  and the parameter  $\Psi$  were fixed to 80 fL and 20, respectively, based on current thinking in cell growth theory (Table 2.1) (Krupinska and Humbeck, 1994; Ševčovičová et al., 2008; Simeoni et al., 2004). Altenburger et al. (2008) have inversely estimated the parameters  $\mu_E$  ( $0.1 \text{ h}^{-1}$ ) and  $\mu_C$  ( $0.011 \text{ fL h}^{-1}$ ) to the mean cell volume measurements of *Desmodesmus subspicatus* suspension in the same order of magnitude as we found here, while at the same time  $\mu_L$  has been fixed to double the volume at commitment  $K_{\text{Crit}}$ . The cell-cycle model reflects the growth of *S. vacuolatus* synchronous cultures based on basic cellular mechanisms of well-understood biological principles (Krupinska and Humbeck, 1994; Mittag et al., 2005; Ševčovičová et al., 2008). The cell-cycle model is able to fit the observed time lag in growth due to a dominant exponential growth phase  $V(t) = V_0 \times \exp^{\mu_E \times t}$  with a low exponential growth rate  $\mu_E$  during the first six to eight hours. Growth smoothly changes from the exponential growth phase to linear growth phase. The linear growth phase  $V(t) = \mu_L \times t + V_{\text{th}}$  indicates a constant increase of cell volume with the slope  $\mu_L$  due to a continuous photosynthetic activity during the interphase. The maximum capacity of the photosynthetic yield is reached after six to eight hours of linear growth (Altenburger et al., 2006). The last term of the cell-cycle model then converges to zero during the last four to six hours of the 24 h cell-cycle. This phase represents limited growth where nuclear DNA replication process mainly proceeds within the mitosis phase (Krupinska and Humbeck, 1994). Although permanent light was applied during the 24 h growth experiment, a subsequent synchronous multiple division of algae cells lead to autospores formation and liberation. Mittag et al. (2005) found that cell division of *Chlamydomonas reinhardtii* cells is independent of an external trigger like absence of gravity, magnetism, and cyclic light-dark changes. The trigger for multiple cell fissions has been reported to be an endogenous biological phenomenon controlled by several clock-controlled genes and a RNA-binding protein (Mittag et al., 2005). Complex cellular mechanisms lead to the here observed growth behavior of *S. vacuolatus* synchronous cultures.

### 2.4.4 Toxicokinetic Modeling

Another consideration, when interpreting the process of toxicity in time, is the relation of the exposure duration to the time, which is required to reach a steady-state between concentrations in the algae and the ambient water. The time to steady-state might be sufficient to explain the delayed responses such as inhibition of cell volume. By using the toxicokinetic model the

time to reach steady-state was predicted within approximately 5 h of continuous exposure (Figure 2.6A–C). The predicted time to reach steady-state highly depends on the elimination rate constant  $k_{out}$ , which was assumed to be independent from the chemical's hydrophobicity with an average rate of  $0.646 \pm 1.892 \text{ h}^{-1}$  according to Sijm et al. (1998). Elimination rate constants have been reported to be influenced by other factors such as growth dilution, algae density, the physiology of the algae cell including the lipid content and lipid composition, elimination by exudates, and exudates-independent excretion process (Sijm et al., 1998). However, the internal concentration in the algae was supposed to be constant after the steady-state was reached as any internal loss is assumed to be instantaneously absorbed from the ambient medium with an infinite number of molecules. This exchange is assumed to take place much faster compared to the algae growth process.

We additionally assumed that the influence of algae density is negligible for our test system, because the algae density stays constant until the number of autospores increases at  $t_{22}$ . However, the observed delayed responses in growth inhibition of four to eight hours are inexplicable based on toxicokinetics only. The uptake rate constant in green algae has been reported to increase with increasing hydrophobicity of the chemical (Sijm et al., 1998; Skoglund et al., 1996; Swackhamer and Skoglund, 1993). The chemicals triclosan ( $\log K_{OW} = 4.38$ ) and PNA ( $\log K_{OW} = 4.76$ ) are regarded to show a considerable bioaccumulation potential in green algae due to their high lipophilicities. Consequently, the uptake rate constants from triclosan and PNA were predicted to be higher when compared to norflurazon ( $\log K_{OW} = 2.19$ ). The intracellular distribution of PNA and triclosan will be favored in membrane-rich compartments (Altenburger et al., 2006). Membrane-rich compartments in algae cells such as chloroplasts may represent specific target sites for chemicals (Escher et al., 2011).

The toxicities of the used chemicals increased over continuous exposure time, even though the predicted times to steady state were already reached. The temporal variations might be due to a continued accumulation of metabolites. Thies et al. (1996) showed that norflurazon is the more toxic biotransformation product of the pyridazinone pro-herbicide metflurazon. But norflurazon itself may be biotransformed to five intermediates, including a subsequent n-demethylation step toward the less toxic SAN 9774 (Thies et al., 1996). There is evidence that triclosan may interact with cytochrome P450 enzymes in liver microsomes (Dann and Hontela, 2011). However, triclosan has not been found to be biotransformed to another metabolite in algae cells. Algae body residues of PNA and potential metabolites have not yet been analyzed in green algae cells. But PNA is reported to be biotransformed to epoxides and hydroxylated derivatives as well as n-dephenylated to 2-naphthylamine, which is catalyzed by the cytochrome system and the prostaglandin endoperoxide synthetase in mammals (Laham and Potvin, 1984). Further research is, however, necessary to investigate the internal concentrations of parent compounds and their biotransformation potential as well as their biological activities in algae cells over time. The potential of the parent compound to be biotransformed may be an important quality to consider for a time-resolved interpretation of toxic effects. Ashauer et al. (2012) found that biotransformation of organic chemicals in *Gammarus pulex* dominated toxicokinetic processes and strongly affected internal concentrations of parent compounds and metabolites. Furthermore, Kretschmann et al. (2011b) showed that the predicted buildup of the more toxic metabolite diazoxon mediated a time-delayed immobilization to *Daphnia magna* based on a TKTD model.

### 2.4.5 Toxicodynamic Modeling

Another important factor concerning the temporal variation of toxicity is the accumulation of damage including sequential progress of cell damage over continuous exposure time. The toxicodynamic process in the TKTD model represents a chemical induced effect progression without any assumption about the specific mode of chemical action or the reversibility of receptor binding (Simeoni et al., 2004).

The toxic potential of a chemical to the individual growth of algae cells was described by the toxicodynamic parameter  $k_I$ . PNA had the largest inherent toxic potential compared to the toxic potentials of triclosan and norflurazon, which agrees with the highest  $k_I$  value. The estimated high  $k_I$  value resulted from the large response gradient for PNA leading to either no observed responses for low concentrations or high observed responses for high concentrations compared to the control group. The large inherent toxic potential was consistent with a steep concentration-response curve characterized by a large slope parameter over time (i.e.  $\theta(t_{14})$  of 8.09 (Table A.8)). Also, the higher estimated  $k_I$  value of norflurazon compared to the  $k_I$  value of triclosan corresponded to a steeper concentration-response curve modeled for norflurazon ( $\theta(t_{14}) = 2.06$ ) than for triclosan ( $\theta(t_{14}) = 1.67$ ).

A repair/recovery rate  $k_R$  in the TKTD quantifies the reversibility of damage at the target site (Ashauer and Brown, 2008). We additionally assumed that the induced mechanism of action at postreceptor events is irreversible leading to a continuous progression of cell damage. The toxic actions of PNA, triclosan, and norflurazon were predicted to be reversible at the target sites when continuous exposure takes place due to estimated repair/recovery rates higher than zero. However, to correctly identify the repair/recovery rate one has to evaluate sequential chemical pulses including recovery periods (Ashauer et al., 2007b). Vallotton et al. (2008a) reported that the effect at the target site was highly reversible when photosystem II inhibitors isoproturon and atrazine were removed, even after multiple pulses to *S. vacuolatus* (Vallotton et al., 2009).

The *NEC* value for triclosan was predicted as  $1.97 \mu\text{g L}^{-1}$  meaning that the tested concentrations of  $0.72 \mu\text{g L}^{-1}$  and  $1.47 \mu\text{g L}^{-1}$  were simulated to be not effective on the cell volume. The cell volume measurements of *S. vacuolatus* cell population exposed to the lowest concentration of norflurazon was fitted to be not compromising to algae growth corresponding to an estimated *NEC* of  $2.81 \mu\text{g L}^{-1}$ . We also estimated a *NEC* value of  $69.86 \mu\text{g L}^{-1}$  for PNA, which comprised the growing sub-population found for the three lowest PNA concentrations.

The observed delayed cell growth might be the result of chemical-mediated sequential series of events within an effect progression (Ankley et al., 2010). The effect progression time  $\tau$  addressed the behavior of delayed effects due to a rate-limiting effect progression step within the sequential series of events (Simeoni et al., 2004). A low value of  $\tau$  generally characterized a slow effect progression and *vice versa* (Sun and Jusko, 1998). The lowest  $\tau$  value of  $1.018 \times 10^{-3} \text{ h}^{-1}$  was estimated for triclosan. Triclosan seems to attribute multiple modes of action such as baseline toxicity, uncoupling mode of action, and the block of lipid biosynthesis in *S. vacuolatus* (Franz et al., 2008). A blocked lipid biosynthesis leads to a reduced synthesis of endogenous lipids, which are for instance components of cell membranes. The observed delayed individual cell growth might consequently be a tertiary action within the effect progression caused by triclosan (Escher et al., 2011). Inversely, the highest  $\tau$  value of  $0.458 \text{ h}^{-1}$  was estimated for norflurazon, even though we did not observe the fastest response to cell volume inhibition. Norflurazon inhibits the carotenoid biosynthesis, which we assumed to have a fast effect progression towards

growth processes. However, norflurazon might capture delayed effect on *S. vacuolatus* growth due to the time consuming toxicokinetic process of intracellular distribution caused by the low hydrophobicity of norflurazon ( $\log K_{OW} = 2.19$ ). We observed the fastest cell volume response for PNA as compared to triclosan and norflurazon. However, the effect progression rate  $\tau$  was estimated to be lower for PNA as for norflurazon, which differs with our observations. The estimated value of effect progression rate for PNA may depend on the time-scale of the toxicokinetic processes.

The accessibility of time-course of the internal concentration in the algae cell would be a major contribution to the understanding of the toxicity process in time. However, a straightforward method has not yet been developed which allows to directly measure the internal concentration in the algae cell. To overcome the technical problems, we applied a method developed by Bandow et al. (2010). This phase represents limited growth where nuclear DNA replication process mainly proceeds within the mitosis phase who measured freely dissolved concentrations in the *S. vacuolatus* bioassay for realistic analyzed effect concentrations but also to extrapolate indirectly the chemical doses reached in the algae cell. As an example, we examined the PNA exposure concentration in the algae suspension over a time period of 256 min (Figure 2.8A) and extrapolated the corresponding PNA dose in the algae (Figure 2.8B). By using a 420-fold higher initial biomass of *S. vacuolatus* as in the algae growth bioassays we were able to detect a 62-fold decrease of the initial PNA concentration in the ambient medium. The steady-state of PNA exposure in the algae suspension was reached within 30 min which demonstrated a very fast PNA uptake kinetic by *S. vacuolatus* according to the law of mass action (Figure 2.8A). Additionally, we measured a stable PNA concentration in GB-media without algae over 256 min excluding confounding PNA degradation/transformation processes. Neglecting PNA degradation/transformation processes the observed PNA concentration decrease in algae suspension is due to only PNA uptake in *S. vacuolatus* cell (Figure 2.8A). Please note that the extrapolated dose in the algae cell according to the measured PNA kinetics (Figure 2.8B) was predicted to be 1000-fold lower compared to the lipophilicity-based estimation (Figure 2.7C). The steady state condition was reached within the first 30 min of continuous PNA exposure reflected by a 10-fold higher estimated value for the elimination rate constant according to the toxicokinetic model (Table 2.1). The estimated toxicokinetic parameters fitted to the measured PNA exposure concentration represented the much faster chemical uptake as derived from the quantitative structure-activity relationships (Geyer et al., 1984) and bioconcentration kinetics of hydrophobic chemicals (Sijm et al., 1998). This observation agrees with various other studies, which shows that the time to steady-state was reached within one hour continue exposure during the algae growth assay (Sijm et al., 1998; Tang et al., 1998; Weiner et al., 2004). Consequently, the fast toxicokinetic process does not only explain the time-dependent toxicity, but rather indicates the relevance of another time-limiting toxicodynamic step.

To verify the high parameter uncertainties of the literature derived kinetic rates to the estimations of the toxicodynamic parameters we included the predicted PNA kinetic parameters fitted to the kinetic measurements in the TKTD model. This resulted into a total different PNA toxicodynamic parameter set (Table 2.1). Although we included more information in the TKTD model, we lost in agreement between the observations and simulations reflected by a lower  $R^2$  of 98.59 (Figure 2.8C, Table 2.1). The faster toxicokinetic process leads to a much higher effect progression time value of  $1.742 \text{ h}^{-1}$  compared to the estimated PNA effect progression time based on toxicokinetic parameters derived from literature (Table 2.1). The high effect progression time indicated the fastest observed cell volume response for PNA. Moreover, the injury rate constant

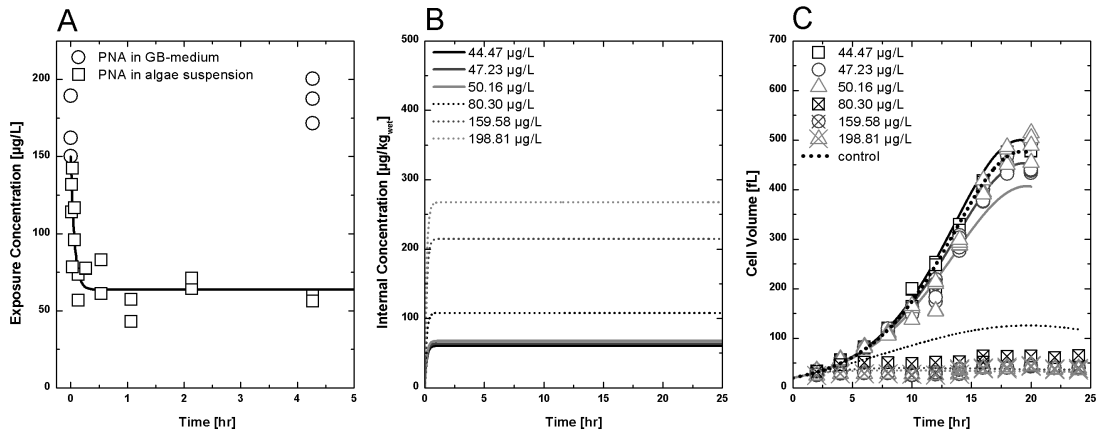


**Figure 2.8:** Consideration of the PNA uptake kinetic in *S. vacuolatus* cells derived by analytical measured concentrations for TKTD modeling. (A) The symbols show the measured PNA concentration in GB-medium and in algae suspension over time. The line is the simulated time-course of the PNA exposure concentration. (B) The simulations of the estimated time-courses of the internal PNA concentrations derived from the PNA bioconcentration kinetic parameters. (C) The simulations of the toxicodynamic model represent the estimated cell volume time-courses (lines) for the tested exposure concentrations of PNA. The measurements of the cell volume are depicted as symbols. The dashed line represents the cell volume simulation for the control groups.

for PNA was estimated to be lower than the recovery/repair rate constant (Table 2.1) leading to the estimated no-effect concentration of zero.

The effect progression rates were estimated to be different between the chemicals indicating different types of effect progressions within the toxicodynamic processes. The effect progression rates might help to differentiate toxicodynamic processes related to adverse outcome pathways within different signal cascades from toxic mechanism, adaptive detoxification and defense mechanisms, or from mode of action to tertiary action (Ankley et al., 2010; Escher et al., 2011). Nevertheless, time-dependent toxicity has to be interpreted with caution to the complexity of multiple processes. Hence, covariates such as parameters of the cell-cycle model and toxicokinetic processes have to be identified that explain and predict the frequency distribution of  $\tau$  values (Mager and Jusko, 2001).

## 2.5 CONCLUDING REMARKS & OUTLOOK

In the present study, a TKTD model based on a modified cancer cell model correctly describes the synchronous growth of *S. vacuolatus* cells affected by chemicals with different modes of action. By including an effect progression rate in the TKTD model, we successfully represented the observed delayed inhibition of cell volume caused by postreceptor events (Mager and Jusko, 2001). We discussed that the effect progression through cumulative cell damage in algae cells might explain the increase of toxicity in time for all three model chemicals. To conclude, in comparison to published methods just one additional toxicodynamic parameter was used to describe time-dependent toxicodynamic processes as a rate-limiting step. Moreover, the TKTD model might have the potential to link several effect levels within damage progression, which may be helpful to comprehend and simulate observed time-dependent effects (Sun and

Jusko, 1998). Therefore, observations of different time-concentration-response relationships from molecular effect scale such as transcriptomics, proteomics, or metabolomics but also from the physiological effect scale such as photosynthetic yield or oxygen consumption could in future help to substantiate these compartments with information from observations. A step further would be the distinction of biological system-dependent parameters and chemicals-associated parameters by incorporating physiological and biochemical mechanisms into TKTD modeling (Dahl et al., 2010). A deeper understanding of underlying mechanism would also improve the attempt to set up predictive models with interpretable parameters (Escher et al., 2011). A mechanistic understanding of biologic processes would be helpful when extrapolating observed time-dependent effect of a single chemical to an aquatic organism under laboratory condition to field conditions such as fluctuating and pulsed mixture exposures.



# A toxicokinetic study of specifically acting and reactive organic chemicals for the prediction of internal effect concentrations in *Scenedesmus vacuolatus*

## ABSTRACT

The toxic potency of chemicals is determined well by using the internal effect concentration accounting for differences in toxicokinetic processes and mechanisms of toxic action. This present study examines toxicokinetics of specifically acting and reactive chemicals in the green algae *Scenedesmus vacuolatus* by using an indirect method. Concentration depletion in the exposure medium was measured for chemicals of lower ( $\log K_{OW} < 3$ : isoproturon, metazachlor, paraquat) and moderate ( $\log K_{OW}$  4-5: irgarol, triclosan, n-phenyl-2-naphthylamine) hydrophobicity at seven time points over 240 min or 360 min. Uptake and overall elimination rates were estimated by fitting a toxicokinetic model to the observed concentration depletions. The equilibrium of exposure concentrations was reached within minutes to hours or was even not observed within the exposure time. Kinetics of bioconcentration cannot be explained by the chemical's hydrophobicity only, but influencing factors such as the ionization of chemicals, the ion-trapping mechanism or the potential susceptibility for biotransformation are discussed. Internal effect concentrations associated to 50% inhibition of *Scenedesmus vacuolatus* reproduction were predicted by linking the bioconcentration kinetics to the effect concentrations and ranged from 0.048 to 7.61 mmol kg<sub>wetweight</sub><sup>-1</sup> for specifically acting and reactive chemicals. Knowing the time-course of the internal effect concentration may help to understand toxicity processes like delayed toxicity, carry-over toxicity or mixture toxicity in future studies.

---

Published in a slightly modified form as:

Vogs, C., Kühnert, A., Hug, C., Küster, E., Altenburger, R., (2015): A toxicokinetic study of specifically acting and reactive organic chemicals for the prediction of internal effect concentrations in *Scenedesmus vacuolatus*. *Environ. Toxicol. Chem.*, 32(5), 1161 - 1172.

---

### 3.1 INTRODUCTION

Various pollutants such as pesticides, industrial chemicals, biocides, or pharmaceuticals occur ubiquitously in the aquatic environment and may cause effects in aquatic organisms. The potential hazards of chemicals for organisms are typically assessed by linking the observed effect to the ambient exposure concentration in a standard bioassay. However, relating the apparent exposure concentration as dose metric to the effect may lead to a misjudgment of the chemical's intrinsic potency (Escher and Hermens, 2002; Escher et al., 2011; McCarty and Mackay, 1993).

For toxicity assessment, a more accurate dose descriptor than the exposure-based dose metric is the internal concentration in the whole body as suggested by the body-residue approach. The internal concentration is assumed to better reflect the chemical's potency by accounting for the variability of toxicokinetics (Escher and Hermens, 2002; McCarty et al., 2011). Toxicokinetics comprise the uptake of the bioavailable fraction of a chemical in the organism, its distribution to the biological target site, the biotransformation and elimination from the organism. The sum of these mass fluxes results in the time-course of the internal concentration in the whole body. The time to reach internal equilibrium concentration generally increases with the chemical's hydrophobicity as long as processes such as changes in the chemical's bioavailability, ion trapping mechanism or biotransformation are negligible. Internal concentrations over exposure time have been measured in different ecotoxicological model organisms such as fish (Könemann and van Leeuwen, 1980), amphipods (Ashauer et al., 2006b), and fish embryos (Kühnert et al., 2013). The chemical analysis of the internal concentration in smaller organisms like phytoplankton remains, however, challenging.

Phytoplankton is a primary producer in the food chain of the aquatic ecosystem and is consumed by higher organisms. In order to predict food-chain magnification through the primary producer, the bioconcentration of very hydrophobic, non-reactive organic chemicals ( $\log K_{OW} > 5$ ) in different algae species have been analyzed (Gerofke et al., 2005; Geyer et al., 1984; Jabusch and Swackhamer, 2004; Mayer et al., 1998; Skoglund et al., 1996; Swackhamer and Skoglund, 1993). The bioconcentration factor of a chemical is determined by relating the accumulated amount in algae cells to the ambient water concentration. The limits of analytical quantifications of the internal concentration in small volume organisms have been overcome by applying different approaches. On the one hand, the internal concentrations of chemicals' in algae were quantified by using radio-labeled chemicals (Gerofke et al., 2005; Geyer et al., 1984; Jabusch and Swackhamer, 2004; Mayer et al., 1998). The measurement of concentrations of radio-labeled chemicals is restricted to the total amount without distinguishing between the parent chemical and possible biotransformation products (Arnot and Gobas, 2006). On the other hand, analytical methods have been applied to measure the accumulated amount of non-specific organic chemicals with high hydrophobicities in batches of large algae biomass (Sijm et al., 1998; Skoglund et al., 1996; Swackhamer and Skoglund, 1993). Sijm et al. (1998) determined bioconcentration kinetics of hydrophobic chemicals ( $\log K_{OW} > 5$ ) in different algae densities of *Chlorella pyrenoidosa* by relating the analytically measured concentration in algae to the freely dissolved chemical fraction in the ambient medium. However, bioconcentration kinetics have rarely been studied for specifically acting and reactive chemicals with wider physicochemical properties that may influence the time-dependent accumulation and toxicity to phytoplankton.

Chemical uptake across the algae cell membrane for instance is hampered for dissociating species which leads to a decrease of toxicity (Escher and Hermens, 2004; Fahl et al., 1995; Neuwoehner and Escher, 2011). Moreover, chemicals with complex structures may have

different binding affinities towards different classes of lipids and proteins (Endo et al., 2011, 2012). Those chemicals may interact specifically or reactively with the biological target site in the organism, which potentially cause excess toxicity. Moreover, biotransformation of parent chemicals might change toxicity (Figure 3.1). Internal effect concentrations (or critical body burden CBR) have been investigated for photosystem II inhibitors and sulfonylurea herbicides in *Scenedesmus vacuolatus* (*S. vacuolatus*), respectively (Fahl et al., 1995; Manthey et al., 1993). Instead of measuring the internal effect concentrations directly, effect concentrations were related to the steady-state bioconcentration factors of the chemicals. Hereby, the bioconcentration factor was determined as difference in the measured concentration in the ambient exposure medium which was depleted as a consequence of the accumulated amount by a sufficiently high algae biomass. Moreover, knowing the kinetics of bioconcentration for predicting internal effect concentrations over time of specifically acting and reactive chemicals in organisms may improve our understanding of toxicity phenomena such as delayed toxicity by cumulative exposure (Altenburger et al., 2006; Franz et al., 2008; Vogs et al., 2013) (**Chapter 2**), carry-over toxicity after sequential pulses (Ashauer et al., 2007c) and mixture toxicity (Faust et al., 2003).

The aims of the present study were to quantify the time-dependent chemical depletion in the ambient medium of *S. vacuolatus* suspension for the determination of bioconcentration kinetics described by a toxicokinetic model. Internal effect concentrations were predicted in order to compare the chemicals intrinsic potencies of chemicals interacting specifically and reactively with different biological target sites in *S. vacuolatus*. To this end, kinetics of bioconcentration were studied for a group of chemicals with lower hydrophobicity of  $\log K_{OW} < 3$  (isoproturon, metazachlor, and paraquat) and chemicals with moderate hydrophobicity of  $\log K_{OW} > 4$  (irgarol,

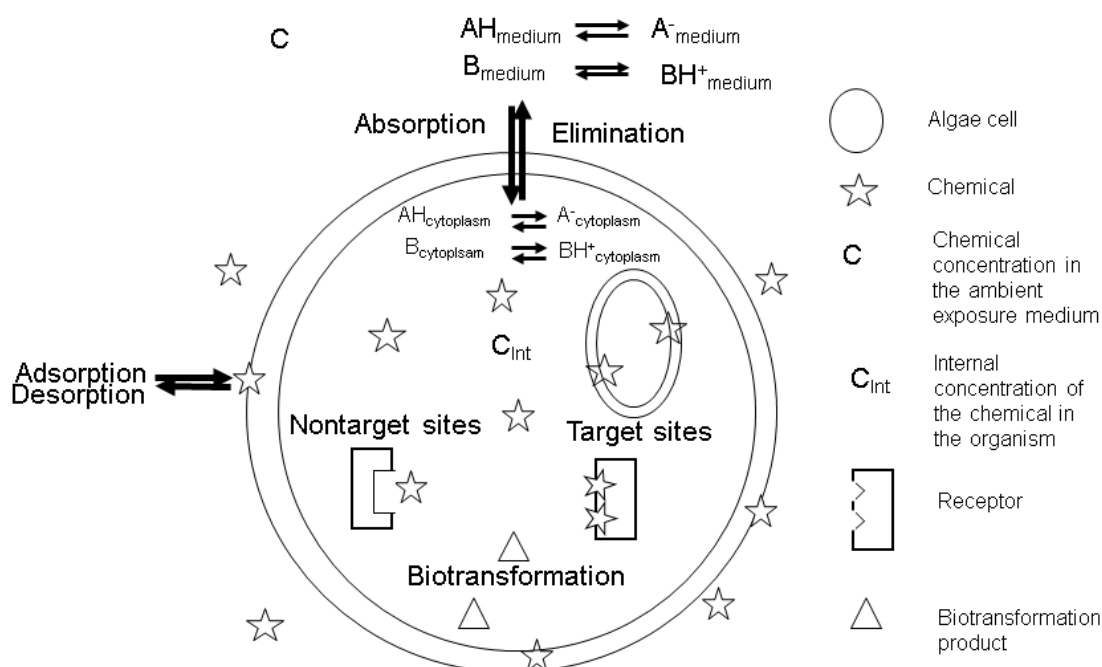


**Figure 3.1:** General scheme illustrating kinetics of bioconcentration processes for basic and acid chemicals in a green algae cell *S. vacuolatus*.  $BH^{+}$  charged species of the basic chemical,  $A^{-}$  charged species of the acid species

triclosan, and n-phenyl-2-naphthylamine). Furthermore, representatives of three modes of action are considered in each hydrophobicity group. Isoproturon (Manthey et al., 1993) and irgarol (Arrhenius et al., 2006; Hock et al., 1995) represent photosystem II inhibitors, metazachlor (Böger et al., 2000) and triclosan (Franz et al., 2008) are lipid biosynthesis inhibitors and paraquat (Faust et al., 2003) and PNA (Altenburger et al., 2006) represent reactive chemicals.

## 3.2 METHODOLOGY

### 3.2.1 Algae cultivation

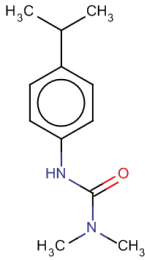
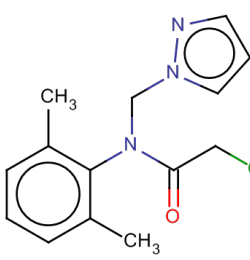
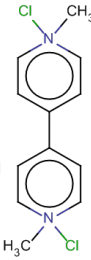
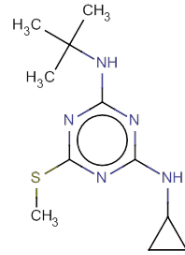
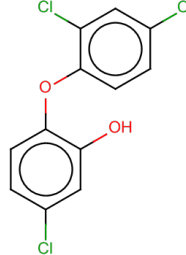
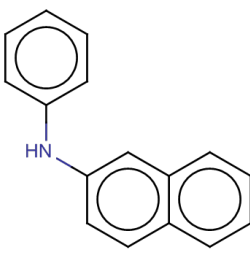
Synchronized *S. vacuolatus* (strain 211-215 SAG, Göttingen, Germany) was cultured in a modified inorganic, sterilized Grimme-Boardman medium (GB-medium) adjusted to pH 6.4 at  $28 \pm 0.5^\circ\text{C}$ . The unicellular green algae were grown photoautotrophically. The cultures of *S. vacuolatus* suspension were synchronized by a light/dark rhythm of 14/10 h and diluted to a cell density of  $1 \times 10^9$  cells  $\text{L}^{-1}$  after every 24 h generation cycle (Altenburger et al., 2004; Faust et al., 2003).

### 3.2.2 Experimental design for measuring the chemical depletion in the ambient medium

Toxicokinetic assays were performed for irgarol, isoproturon, triclosan, metazachlor, paraquat, and n-phenyl-2-naphthylamine (PNA). CAS Registry Number, supplier, molecular structure, and relevant physicochemical properties of the chemicals used as well as the biological processes in algae known to be affected by the chemicals are listed in Table 3.1. Irgarol, isoproturon, metazachlor, triclosan, and PNA were dissolved in dimethyl sulfoxide (DMSO, CAS RN: 67-68-5, Merck, Germany) for preparing the stock solutions and paraquat was freshly dissolved in GB-medium prior to the algae toxicokinetic assay.

The cell density was adjusted according to the ratio of exposure volume to the product of the cell volume of autospores ( $2 \times 10^{-14}$  L) and the octanol-water partition coefficient ( $K_{OW}$ ) of the respective chemical in order to achieve approximately 50% chemical depletion in the static exposure system (Table 3.1). To this end, the algae biomass was enriched from a synchronous autospore suspension of *S. vacuolatus* with a homogeneous algae size distribution and a cell density of about  $2.5 \times 10^{10}$  cells  $\text{L}^{-1}$  after 24 h of growth. This algae suspension was immediately centrifuged at 3,000 g and  $5^\circ\text{C}$  for 5 min (Megafuge 2.R, Heraeus Instruments). The supernatant was removed and the algae pellet was re-suspended in a reduced volume of GB-medium until a sufficiently high enough cell density was reached. The cell density and size were controlled using an electronic particle counter (CASYII, Schärfe System, Reutlingen, Germany). After the transfer of 10 mL of concentrated autospore suspension in a 20 mL closed pyrex glass tube, the algae suspension was continuously agitated with a glass covered stirrer during the experiment. The experiments were conducted without introducing oxygen to the algae suspension and without illumination. One to three replicates were prepared for each experiment. Initial exposure concentrations were chosen to be quantifiable for all sampling times and exceeded median effect concentration one to three orders of magnitude. After dosing irgarol, isoproturon, metazachlor, triclosan or paraquat to the algae suspension, one mL aliquots were sampled at 0, 7, 15, 30, 60, 120 and 240 min (and 360 min for triclosan). Then, one mL of each aliquot was transferred to

**Table 3.1:** Chemical identity, sources, molecular structure, and relevant physicochemical properties of the chemicals used as well as the biological processes known to be affected by the chemicals are listed.

mode of action	photosystem II Inhibitor	lipid inhibitor	biosynthesis	oxidative stress
common name	isoproturon	metazachlor		paraquat
CAS RN	34123-59-6	6717-08-2		1910-42-5
Source	Riedle	Riedle-de-Haen		Fluka
log $K_{OW}$ < 3	Molecular structure <sup>1</sup>			
				
	Chemical group <sup>2</sup>	substitutes Urea/Amide	Chloroacetanilide	Neutral Organics
	Molecular target site (t) or mechanism (m)	(t) D1 protein of photosystem II <sup>4</sup>	(t) Elongase catalyzing the formation of very-long-chain fatty acids <sup>3/5</sup>	(m) Redox catalyst at photosystem I <sup>3/4</sup>
	pK <sub>a</sub> <sup>1</sup>	13.79	16.65	∞
	pK <sub>b</sub> <sup>1</sup>	-3.11	1.84	∞
	log $K_{OW}$ <sup>1</sup>	2.87	2.13	-2.71
	Molar mass [g mol <sup>-1</sup> ] <sup>1</sup>	206.12	277.10	256.05
	Water solubility at 25 °C [mg L <sup>-1</sup> ] <sup>1</sup>	143.8	250.4	1 × 10 <sup>6</sup>
	common name	irgarol	triclosan	
CAS RN	28159-98-0	3380-34-5		135-88-6
Source	Sigma	CalbioChem		Aldrich
log $K_{OW}$ > 4	Molecular structure <sup>1</sup>			
				
	Chemical group <sup>2</sup>	Triazine	Phenol	Neutral Organics
	Molecular target site (t) or mechanism (m)	(t) D1 protein of photosystem II <sup>4</sup>	?	?
	pK <sub>a</sub> <sup>1</sup>	14.13	7.68	∞
	pK <sub>b</sub> <sup>1</sup>	5.68	-6.67	0.52
	log $K_{OW}$ <sup>1</sup>	4.07	4.76	4.47
	Molar mass [g mol <sup>-1</sup> ] <sup>1</sup>	253.14	287.95	219.10
	Water solubility at 25 °C [mg L <sup>-1</sup> ] <sup>1</sup>	7.52	4.62	6.31

<sup>1</sup>ChemAxon, <sup>2</sup>EpuiSuit, <sup>3</sup>Faust et al. (2001), <sup>4</sup>Hock et al. (1995), <sup>5</sup>Böger et al. (2000), <sup>6</sup>Arrhenius et al. (2006)

a tube (Eppendorf) and centrifuged at 20,000 rpm and 4 °C for 5 min (2K15, Sigma, Germany). The supernatant without algae was removed and stored in a 4 mL amber vial (VWR International, Germany) until chemical analysis. Storage in a -20 °C freezer never exceeded two days. Two replicates of GB-medium without algae suspension were additionally prepared and treated in an analog manner in order to confirm that only the chemical uptake by algae causes the depletion of the exposure concentrations. All controls consisted of 10 µL chemical stock solution dissolved in 10 mL GB-medium. The controls for paraquat were prepared by using 9 mL GB-medium and one mL stock solution. The experiments were independently repeated two to three times for each chemical. The toxicokinetic study of PNA was similarly conducted using aliquots of 20 mL algae suspensions. PNA concentrations in the ambient exposure medium were measured after 0, 1, 2, 4, 8, 16, 32, 64, 128 and 256 min in two replicates. We measured the pH of the ambient medium with and without algae over time for calculating the fractions of neutral and dissociated molecules of the chemicals. The neutral fraction of the basic chemicals irgarol, PNA, and metazachlor were calculated by

$$f_B = \frac{1}{1 + 10^{(pK_b - pH)}} \quad (3.1)$$

and the neutral fraction of the acidic chemicals triclosan and isoproturon by

$$f_{AH} = \frac{1}{1 + 10^{(pH - pK_a)}} \quad (3.2)$$

where  $pK_b$  is the base constant and  $pK_a$  the acidity constant estimated by the software ChemAxon (<http://www.chemaxon.com>). The charged fraction equals to the difference of the neutral fraction to one. Paraquat exists as dication in the aqueous medium independent of the pH ( $pK_a = pK_b = \infty$ ).

### 3.2.3 Quantification of the ambient concentration over time

Exposure concentrations over time were analyzed from samples with and without algae suspensions in the toxicokinetic studies. Concentrations of isoproturon, irgarol, triclosan, paraquat and metazachlor were determined in the supernatant by a reversed-phase high-performance liquid chromatography (RP-HPLC) using an UV-detector (Hitachi UV Detector, L-7400) at wavelengths of 226 nm (irgarol), 240 nm (isoproturon), 220 nm (metazachlor), 205 nm (triclosan), and 253 nm (paraquat). Samples were analyzed on a LiChrospher 100 RP-18 (Merck, Germany) endcapped column (125 mm × 4 mm, 5 µm particle size). The column temperature was set at 25 °C. The flow rate was 0.5 mL min<sup>-1</sup> for irgarol, isoproturon, triclosan, and paraquat and to 0.3 mL min<sup>-1</sup> for metazachlor. Isocratic elution was conducted with a mobile phase of acetonitrile/water mixture (50/50 v/v) for irgarol, (70/30 v/v) for isoproturon and triclosan, and acetonitrile/phosphoric acid (0.2%) (49/51 v/v) for metazachlor. HPLC was carried out using 75% heptafluorobutyric acid (15 mM)-ammonium formate buffer (20 mM) adjusted to pH 3.30 by formic acid and 25% acetonitrile for paraquat analysis (Ariffin and Anderson, 2006). A volume of 30 µL was injected for metazachlor, isoproturon, and paraquat and 50 µL for triclosan and irgarol, for each of the three technical replicates. Acetonitrile (ACN, gradient grade) and water (HPLC, ultragradient grade) were provided by J.T. Baker (United States) and Merck (Germany), respectively.

PNA concentrations in the supernatant were quantified with pre-equilibrium solid-phase microextraction in combination with gas chromatography - mass spectrometry (GC-MS) (Vogs et al., 2013) (**Chapter 2**). An Agilent 6890 GC coupled to an Agilent 5973 N mass selective

detector was equipped with a DB-17 MS capillary column (30 m × 0.25 mm I.D., 0.25 μm) all from Agilent Technologies (Santa Clara, USA). The 85 μm polyacrylate (PA) fibre was purchased from Supelco (Bellefonte, USA). An external calibration was used for quantification with the fibre. The fibre was loaded for one minute at 28 °C and 200 r.p.m. in the sample and was desorbed in the inlet of the GC-MS for two minutes in the splitless mode at 300 °C. The carrier gas was helium at a constant flow of 1.2 mL<sup>-1</sup>. The following oven program was used: The oven was held for two minutes at 60 °C and heated with a rate of 120 °C min<sup>-1</sup> to the final temperature of 280 °C, which was held for 4.5 minutes.

### 3.2.4 The toxicokinetic model

The decrease of the concentration in the algae suspension  $C(t)$  [μmol L<sup>-1</sup>] was considered to be caused by the hydrophobicity-driven bioconcentration to algae cells in a static exposure system. The toxicokinetic processes were mathematically described by a one-compartment model with a first-order kinetic according to the law of mass action

$$\frac{dC(t)}{dt} = k_{\text{out}} \times C_{\text{int}}(t) - k_{\text{in}} \times C(t) \times F \quad (3.3)$$

where  $k_{\text{in}}$  [h<sup>-1</sup>] means the uptake rate constant,  $k_{\text{out}}$  [h<sup>-1</sup>] represents the overall elimination rate constant of the chemical,  $C_{\text{int}}(t)$  [μmol biovolume<sup>-1</sup>] reflects the internal amount of substance accumulated in *S. vacuolatus* cells, and  $F$  [-] is the ratio of the algae biovolume to the exposure volume. The kinetic rate constants  $k_{\text{in}}$  and  $k_{\text{out}}$  were estimated by fitting the toxicokinetic model to the measured exposure concentrations in the algae suspension. Parameter estimations were conducted separately for each independent experiment as well as globally for each chemical measurement series (Table 3.2). The steady-state bioconcentration factor ( $BCF_{\text{ss}}$ ) was calculated by the quotient of the accumulated amount in the algae cell and the chemical concentration in the ambient medium at equilibrium. The kinetic bioconcentration factor ( $BCF_{\text{kin}}$ ) is the ratio of  $k_{\text{in}}$  to  $k_{\text{out}}$ . The time to reach 95% of the equilibrium concentration  $t_{95}$  [h] was determined by the ratio of  $-\ln(0.05)$  to  $k_{\text{out}}$  (Table 3.2).

### 3.2.5 Parameter estimation and Mathematica settings

Inverse modeling and parameter estimations of the toxicokinetic model were conducted in the software Mathematica (Version 8.0, Wolfram Research). To find one global parameter set, the least-squares objective function was numerically minimized by the genetic algorithm named Differential Evolution. If the predicted kinetic parameters were not meaningful in a biological sense or residue plots showed systematic bias, then the numeric algorithm Random Search was additionally applied. Although all initial parameter values were set to  $\geq 0$  without reflecting a biological meaning, one robust parameter set for each optimization procedure was achieved. The errors were assumed to be normally distributed with a mean of zero and an unknown standard deviation in accordance to the maximum-likelihood theory (excursion of the numerical method used is given in **Chapter 2**). The 95% uncertainty intervals of the estimated best-fit parameter values were quantified using the standard error and the quantiles of the Student's *t*-distribution. Goodness-of-fit parameters such as the mean absolute error  $MAE$  [μmol L<sup>-1</sup>] and the coefficient of determination  $R^2$  [%] were calculated (Table 3.2).

- Time discretization: 0.01

- Iteration criteria: Maximum number of iterations 100
- Initial condition:
  - external concentrations were set according to the measured exposure concentrations of each chemical;
  - internal concentrations of irgarol, isoproturon, triclosan, metazachlor, PNA and paraquat = 0;
  - initial parameter region for the estimation of the individual and global parameter set per chemical  
 $k_{in}, k_{out} \geq 0$
- Estimation method: Mathematica function "NonlinearModelFit"
- Numerical algorithm for constrained nonlinear optimization: "NMinimize" with special option to use the estimator algorithm "Differential Evolution" or "Random Search" (if no solution was found by the "Differential Evolution")

### 3.2.6 Prediction of internal effect concentration

Effect concentrations inhibiting 50% of the reproduction of *S. vacuolatus* ( $EC_{50}(t_{24})[\mu\text{mol L}^{-1}]$ ) were multiplied by the bioconcentration factor  $BCF_{kin}$  in order to estimate the internal effect concentration of a chemical in the whole organism ( $IEC$  [ $\text{mmol kg}_{\text{wet weight}}^{-1}$ ]), To this end, data of effect concentrations on synchronized *S. vacuolatus* reproduction exposed to the six chemicals were collected from the literature (Table 3.3). Effect concentrations in the exposure medium were assumed to be stable over the whole exposure time in the standard bioassay. The number of chemical molecules accumulated in a single algae cell of a given cell size ( $CV = 2 \times 10^{-14}$  L) was further calculated by the relationship

$$IEC_{50} = \frac{BCF_{kin} \times EC_{50} \times N_a}{CN} \quad (3.4)$$

where  $IEC_{50}$  is the median number of accumulated molecules causing 50% inhibition [number of molecules algae cell<sup>-1</sup>],  $CN$  means the algae cell density of  $5 \times 10^{13}$  cells in one liter biovolume and  $N_a$  represents the Avogadro constant [ $\text{mol}^{-1}$ ].

## 3.3 RESULTS

### 3.3.1 Quantification of concentration decline in the ambient medium and pH-dependent molecular speciation of the chemicals

To indirectly determine the kinetics of chemical bioconcentration in the green algae *S. vacuolatus*, the ambient concentration was analyzed in the algae suspension over a maximum time period of six hours. Figure 3.2 depicts the decline of the ambient concentration in the algae suspension for all analyzed chemicals (Table B.1). The exposure concentrations in pure GB-medium without algae remained stable within a variation range of < 10% for irgarol, isoproturon, metazachlor, PNA and paraquat and within a variation range of < 20% for triclosan (Figure 3.2). Therefore, chemical depletion due to an adsorption to the exposure vessel, abiotic transformation of the chemical, or evaporation into the head space can be neglected. The

observed decline of exposure concentration was consequently assumed to be solely caused by the bioconcentration into algae cells.

The measured chemical decline ranged from 15% to 90% of the initial concentrations depending on the analyzed chemicals (Table 3.2). The depleted amount was assumed to be accumulated in the algae cells, although this method does not allow for distinguishing between adsorption at the algae cell wall and absorption into the algae cell. A decrease of chemical concentration in the ambient exposure media was achieved for all chemicals by adjusting a sufficiently high biomass. Algae biomass was enriched to 10 to 100-fold higher algae cell densities for the chemicals with a  $\log K_{OW} < 3$  compared to the biomass used for the chemicals with a  $\log K_{OW} > 4$ . Compared to cell densities of  $7.5 \times 10^7$  cells  $L^{-1}$  used in the standard bioassay, 1000 to 10000-fold higher algae cell densities were utilized in the toxicokinetic assay for the chemicals with a  $\log K_{OW} < 3$ . A concentration decline of  $\geq 50\%$  was observed for the chemicals metazachlor ( $\log K_{OW} = 2.13$ ) and isoproturon ( $\log K_{OW} = 2.87$ ) at algae densities of approximately  $1 \times 10^{12}$  cells  $L^{-1}$ . The maximum metazachlor decline of 86% of the initial concentration was observed at an algae cell density of  $1.49 \times 10^{12}$  cells  $L^{-1}$ , while the smallest depletion of 64% was detected at a cell density of  $1.24 \times 10^{12}$  cells  $L^{-1}$ . The maximum decline of the isoproturon ambient concentration was 58% and 54% at algae cell densities of  $2.11 \times 10^{12}$  cells  $L^{-1}$  and  $1.23 \times 10^{12}$  cells  $L^{-1}$ , respectively. A concentration decline of maximum 33% at a cell density of  $2.44 \times 10^{12}$  cells  $L^{-1}$  was achieved for paraquat ( $\log K_{OW} = -2.71$ ). The smallest loss of 15% of the initial paraquat concentration was determined at a 2.5-fold lower algae cell density of  $9.80 \times 10^{11}$  cells  $L^{-1}$ . Concentration depletion of  $\geq 50\%$  were observed for the chemicals irgarol ( $\log K_{OW} = 4.07$ ), triclosan ( $\log K_{OW} = 4.76$ ) and PNA ( $\log K_{OW} = 4.47$ ) at algae densities spanning from  $10^{10}$  cells  $L^{-1}$  to  $10^{11}$  cells  $L^{-1}$ . The concentration of irgarol declined to 82% of the initial concentration at an algae density of  $2.14 \times 10^{11}$  cells  $L^{-1}$  and 50% at an algae density of  $1.38 \times 10^{11}$  cells  $L^{-1}$ . The maximum depletion of triclosan was reached after 30 min and varied between 78% at an algae density of  $2 \times 10^{10}$  cells  $L^{-1}$  and 83% at algae density of  $7.11 \times 10^{10}$  cells  $L^{-1}$ . A PNA depletion of 67% was measured at an algae density of  $3.15 \times 10^{10}$  cells  $L^{-1}$ .

The time to reach intracellular and extracellular equilibrium concentrations in *S. vacuolatus* suspension spanned over minutes to hours or was even not observed within the exposure time (Figure 3.2). The ambient concentrations of the chemicals isoproturon and paraquat with  $\log K_{OW} < 3$  reached almost immediate equilibrium within the first observation time point of seven minutes, while concentrations for metazachlor continuously declined over the exposure period of four hours. In the group of chemicals with moderate hydrophobicity ( $\log K_{OW} 4-5$ ), only the concentration of PNA quickly reached steady-state after 30 min exposure. The exposure concentration of triclosan also depleted until approximately 30 min comparable to PNA. After 120 min of continuous exposure, the triclosan exposure increased again up to approximately 90% of the initial exposure concentration until 390 min. The ambient concentration of irgarol slowly decreased over the exposure time without achieving equilibrium, which is similar to the observation of the toxicokinetics for metazachlor. The estimated times to reach 95% of steady-state concentration  $t_{95}$  follows the order isoproturon > paraquat > PNA > triclosan > irgarol > metazachlor (Table 3.2).

Speciation of chemicals depends on the pH value in the ambient medium. The fractions of neutral and charged species were calculated by using Equation 3.1 or Equation 3.2 for the basic or acidic chemicals according to the measured medium pH in the toxicokinetic assay over the exposure time (Table B.2-B.6). Paraquat, PNA, isoproturon, and metazachlor did not dissociate at

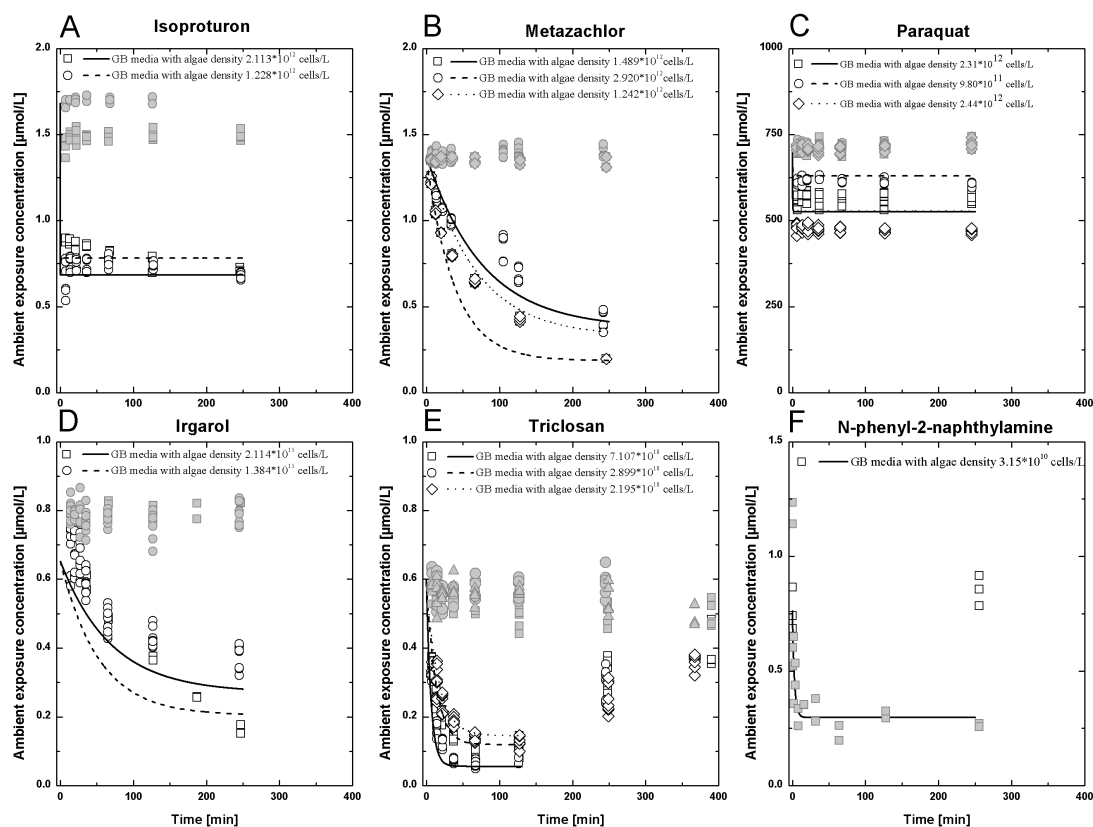


**Figure 3.2:** Time-dependent exposure concentrations [ $\mu\text{molL}^{-1}$ ] of individual experiments measured in exposure medium without algae (closed symbols) and in exposure medium with different algae densities (open symbols) for the chemicals with  $\log K_{\text{OW}} < 3$  (A) isoproturon, (B) metazachlor, (C) paraquat and for the chemicals with  $\log K_{\text{OW}} 4-5$  (D) irgarol, (E) triclosan, (F) n-phenyl-2-naphthylamine, respectively. The lines represent the global toxicokinetic model fitted to the chemical depleted concentration of the ambient medium based on one estimated toxicokinetic parameter set for each chemical globally.

an ambient medium pH of approximately 6.5, while the fraction of neutral triclosan species and neutral irgarol species amounted to 94% and 86%, respectively. The pH in the ambient medium remained stable over the exposure time (Table B.2-B.6). The fraction of chemical speciation in the ambient medium can differ from one inside the algae cell depending on the cytoplasmatic pH. The shift from ambient medium pH of 6.5 to cytoplasmatic pH of 7.6 in *S. vacuolatus* (Küsel et al., 1990) would not be expected to induce a change in molecular speciation of the chemicals paraquat, PNA, isoproturon, and metazachlor. However, the fraction of neutral irgarol would be expected to increase to 99% in the algae cell (Table B.2) and the pH change leads to a shift to an anionic triclosan fraction from 0.5% to 45% inside the algae cell (Table B.4).

### 3.3.2 Toxicokinetic modeling

The decrease of the chemical's concentrations was accurately simulated by using a one-compartment toxicokinetic model fitted to the measurement series for each chemical globally (Figure 3.2). The simulations of the toxicokinetic model represented the measured decline of the

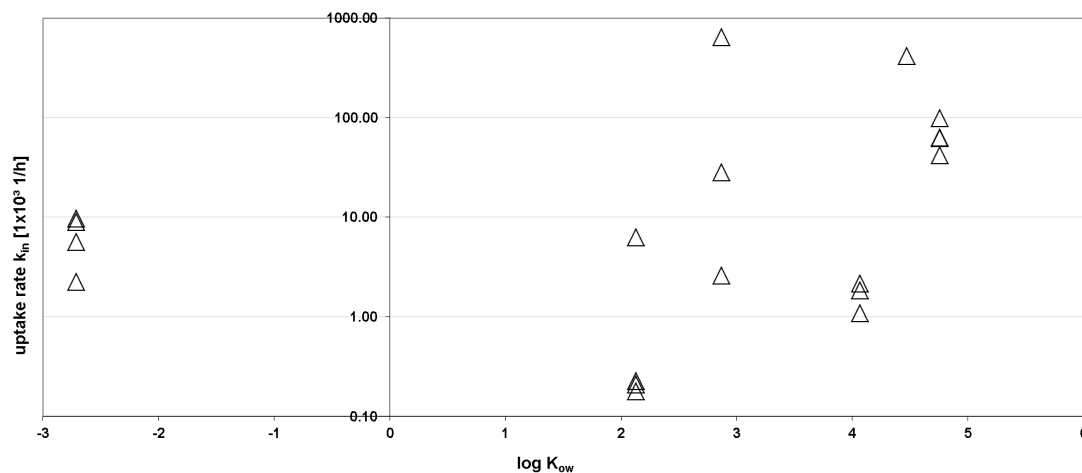


**Figure 3.3:** Estimated uptake rate constants for each independent experiment separately as well as for each chemical measurement series globally as a function of  $\log K_{OW}$  (paraquat  $\log K_{OW} = -2.71$ , metazachlor  $\log K_{OW} = 2.13$ , isoproturon  $\log K_{OW} = 2.87$ , irgarol  $\log K_{OW} = 4.07$ , PNA  $\log K_{OW} = 4.47$ , triclosan  $\log K_{OW} = 4.76$ ).

chemicals concentrations with a coefficient of determination  $R^2 > 95\%$  and the highest  $MAE$  was  $0.106 \mu\text{mol L}^{-1}$  for metazachlor (Table 3.2). One kinetic parameter set was estimated by multiple fitting Equation 3.3 to all measurements for each chemical (Table 3.2). The measured triclosan concentrations were used for modeling purpose until the minimum concentration was reached within the first 120 min. The subsequent increase of the triclosan concentration may indicate another process than just a diffusive exchange across cell membranes. This is why we did not modify the one-compartment toxicokinetic model to describe the triclosan concentration increase after 120 min of cumulative exposure.

The estimated uptake rate constants  $k_{in}$  normalized to the ratio of biomass volume to exposure volume ( $F$ ) varied over four orders of magnitude from  $640 \times 10^3 \text{ h}^{-1}$  for isoproturon to  $0.21 \times 10^3 \text{ h}^{-1}$  for metazachlor. The estimations of the uptake rate constants using all replicate measurements of one chemical globally were within the same order of magnitude to the predicted  $k_{in}$  using single measurement series each except for isoproturon (Table 3.2). The 95% confidence intervals of  $k_{in}$  for isoproturon and paraquat were wide indicating high uncertainty of  $k_{in}$ . The uptake rate for irgarol was 34-fold lower than  $k_{in}$  for triclosan and 230-fold lower than  $k_{in}$  for PNA. Isoproturon was estimated to be 3075-fold and 66-fold higher than  $k_{in}$  for metazachlor and paraquat, respectively. The kinetic uptake rate constants of irgarol and metazachlor were predicted to be lower in comparison to chemicals with similar hydrophobicity. The uptake rate constants were predicted to range over four orders and seemed to be related to an increase of the chemicals hydrophobicity (Figure 3.3). The application of a sufficiently high algae biomass in dependency of the chemical's hydrophobicity resulted in an uncorrelated relationship between the uptake rate constant and the cell density used in the toxicokinetic assay (Figure 3.4).

The overall elimination rate constant  $k_{out}$  spanned over five orders of magnitude from  $1852.70 \text{ h}^{-1}$  for isoproturon to  $0.22 \text{ h}^{-1}$  for metazachlor. The overall elimination kinetic rate constants predicted by using the single individual measurement series each differed by a minimum of one order of magnitude to the predictions using all replicate measurement series of one

**Table 3.2:** Estimated toxicokinetic parameters for each toxicokinetic experiment solely and for each chemical globally are given in dependency of the algae density used. The bioconcentration factors were calculated by the estimated toxicokinetic parameters ( $\log BCF_{kin}$ ) and by the hydrophobicity-derived equilibrium concentrations ( $\log BCF_{ss}$ ) and are comparable to  $\log BCF_{ss}$  predicted by using the QSAR (Geyer et al., 1984).

chemical	$C_m$ [ $\mu\text{mol}\cdot\text{L}^{-1}$ ]	Cell number [cells $\cdot\text{L}^{-1}$ ]	F [-]	$k_m \pm 95\%$ CI [ $\times 10^3 \text{h}^{-1}$ ]	$k_{out} \pm 95\%$ CI [ $\text{h}^{-1}$ ]	MAE [ $\mu\text{mol}\cdot\text{L}^{-1}$ ]	$R^2$ [%]	df [-]	$\log BCF_{kin}$ [ $\text{L}\cdot\text{kg}^{-1}$ ]	* $\log BCF_{ss}$ [-]	** $\log BCF_{ss}$ [-]	$t_{95}$ [h]
isoproturon	1.682	$2.11 \times 10^{12}$	$4.22 \times 10^{-3}$	$2.579 \pm 0.402$	$10.390 \pm 1.654$	0.041	99.9	19	2.395	1.51	2.118	0.288
	1.447	$1.23 \times 10^{12}$	$2.46 \times 10^{-3}$	$28.133 \pm 0.918 \times 10^5$	$74.247 \pm 2.565 \times 10^5$	0.042	99.73	61	2.579	1.68		0.04
global	0.652	$1.38 \times 10^{11}$	$2.77 \times 10^{-4}$	$639.690 \pm 1644.408 \times 10^5$	$1852.698 \pm 4.763 \times 10^8$	0.074	98.3	82	2.538			0.002
	0.652	$2.14 \times 10^{11}$	$4.29 \times 10^{-4}$	$2.163 \pm 0.131$	$0.528 \pm 0.061$	0.030	99.32	60	3.612	3.021	2.936	5.669
irgarol	0.652	$1.24 \times 10^{12}$	$2.48 \times 10^{-3}$	$1.078 \pm 0.076$	$0.010 \pm 0.030$	0.019	99.6	10	5.029	2.561		296.937
	1.373	$1.828 \pm 0.117$	$1.828 \pm 0.117$	$6.236 \pm 0.280$	$0.644 \pm 0.055$	0.037	98.91	72	3.708	1.861	1.61	8.372
metazachlor	1.352	$2.92 \times 10^{12}$	$5.84 \times 10^{-3}$	$0.179 \pm 0.001$	$0.177 \pm 0.003$	0.069	99.99	21	3.004	1.991		16.936
	1.373	$1.49 \times 10^{12}$	$2.98 \times 10^{-3}$	$0.226 \pm 0.007$	$0.088 \pm 0.014$	0.084	99.11	63	3.409	2.321		33.97
global	0.598	$7.11 \times 10^{10}$	$1.42 \times 10^{-4}$	$0.208 \pm 0.011$	$0.222 \pm 0.042$	0.106	97.74	126	2.971			13.464
	0.589	$2.90 \times 10^{10}$	$5.80 \times 10^{-5}$	$41.849 \pm 2.716$	$1.230 \pm 0.186$	0.050	94.35	60	4.532	3.531	3.405	2.436
triclozan	0.580	$2.20 \times 10^{10}$	$4.39 \times 10^{-5}$	$61.831 \pm 1.005$	$0.777 \pm 0.033$	0.018	99.65	54	4.901	3.921		3.856
	global	$62.747 \pm 2.317$	$97.987 \pm 1.101$	$0.922 \pm 0.082$	$1.390 \pm 0.092$	0.030	99.92	54	4.848	3.921		2.155
paraquat	700.7	$2.31 \times 10^{12}$	$4.63 \times 10^{-2}$	$5.646 \pm 2.337 \times 10^5$	$116.098 \pm 4.80 \times 10^6$	0.010	99.98	63	1.687	-0.29	-1.681	0.026
	719.7	$9.80 \times 10^{11}$	$1.96 \times 10^{-3}$	$8.958 \pm 0.623 \times 10^5$	$101.477 \pm 7.032 \times 10^5$	0.007	99.99	28	1.946	-0.06		0.029
global	715.2	$2.44 \times 10^{12}$	$4.89 \times 10^{-3}$	$2.248 \pm 0.283$	$21.505 \pm 2.776$	0.008	99.97	42	2.019	1.01		0.139
	0.762	$3.15 \times 10^{10}$	$3.15 \times 10^{-5}$	$9.674 \pm 4.362 \times 10^5$	$133.810 \pm 6.033 \times 10^6$	0.038	99.38	133	1.859			0.022
PNA				$415.688 \pm 91.295$	$8.356 \pm 2.390$	0.060	96.26	18	4.697	2.95	3.21	0.358

$C_m$  – initial concentration used in the toxicokinetic assay,  $F \hat{a} \hat{e}^{\hat{e}}$  – ratio of biovolume and exposure volume used in the toxicokinetic assay,  $k_m$  – uptake rate constant,  $k_{out}$  – overall elimination rate constant, CI – confidence interval, MAE  $\hat{a} \hat{e}^{\hat{e}}$  – mean absolute error,  $R^2$  – determination coefficient, df – degree of freedom,  $\log BCF_{kin}$  – kinetic bioconcentration factor, \* $\log BCF_{ss}$  – steady-state bioconcentration factor, predicted  $BCF_{ss} = 0.68 \times \log Kow + 0.164$  (N=41,  $R^2 = 90.2$ ) (Geyer et al., 1984),  $t_{95}$  – time to reach 95% of the equilibrium concentration, \*\* $\log BCF_{ss}$  based on the maximum accumulated amount of chemical in the algae biomass to the ambient concentration either at 30 min of triclosan exposure or at 240 min of metazachlor and irgarol exposure.

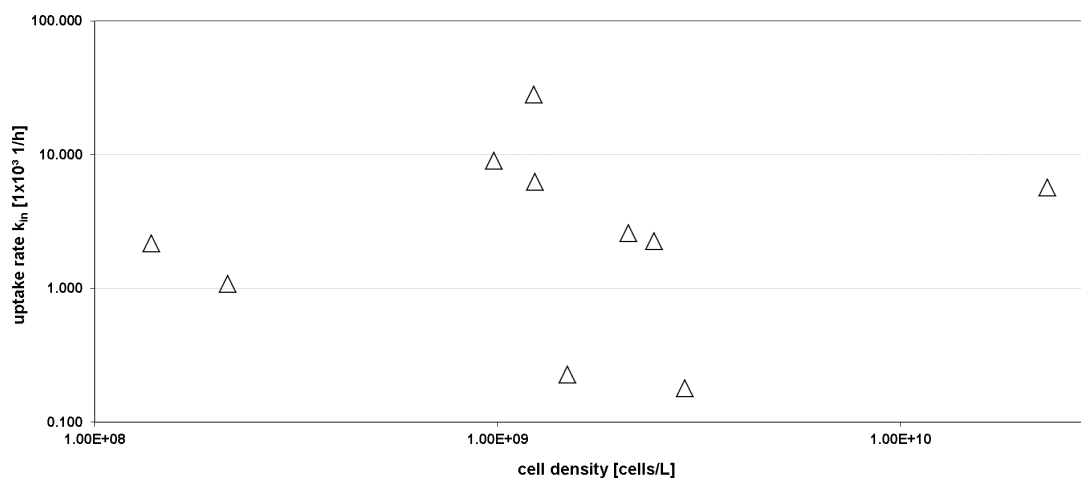


**Figure 3.4:** Estimated uptake rate constants related to the used cell densities.

chemical globally. A wide 95% confidence interval of  $k_{out}$  was again determined for isoproturon and paraquat. The overall elimination kinetic rate constants seemed to be uncorrelated with the hydrophobicity of the chemicals and cell densities used (Figure 3.5 and Figure 3.6), but decreased over time to reach the 95% of steady-state concentration in the following order: isoproturon > paraquat > PNA > triclosan > irgarol > metazachlor (Table 3.2).

The bioconcentration factors  $\log BCF_{ss}$  determined by the accumulated amount of the chemicals in the algae biomass to the ambient exposure concentration at equilibrium varied between -0.29 for paraquat and 2.95 for PNA (Table 3.2). Because equilibrium concentrations were not reached for triclosan, metazachlor, and irgarol, the calculated  $\log BCF_{ss}$  based on the maximum accumulated amount of chemical in the algae biomass to the ambient exposure concentration either at 30 min of triclosan exposure or at 240 min of metazachlor and irgarol exposure. The bioconcentration factor  $\log BCF_{kin}$  determined by the kinetic constant rates ranged from 1.86 for paraquat to 4.7 for PNA, which are about one order of magnitude higher than the  $\log BCF_{ss}$  of all chemicals (Table 3.2). These determined  $\log BCF$ -values were compared to steady state bioconcentration factors  $\log BCF_{ss}$  for *Chlorella fusca* estimated by quantitative structure-activity relationships (QSAR) (Geyer et al., 1984). According to this relationship, the chemicals' hydrophobicity linearly correlated to  $\log BCF_{ss}$  with a slope of 0.681 and an intercept of 0.164 which was derived from 41 chemicals spanning over five orders of magnitude in  $\log K_{OW}$  values (0.91 - 6.74). The determined  $\log BCF_{ss}$  were in the range of the  $\log BCF_{ss}$  predicted by QSAR, while the calculated  $\log BCF_{kin}$  of all chemicals were higher than the QSAR-based predicted  $\log BCF_{ss}$  (Figure 3.7). Logarithmic residuals between determined  $BCF_{kin}$  and QSAR-based predicted  $BCF_{ss}$  varied between 0.4 for isoproturon and 3.3 for the least hydrophobic chemical paraquat. It has to be noted that the estimated  $\log BCF_{ss}$  for paraquat is uncertain due to its  $\log K_{OW}$  of -2.71, which lies outside the  $\log K_{OW}$  domain of the applied QSAR model.

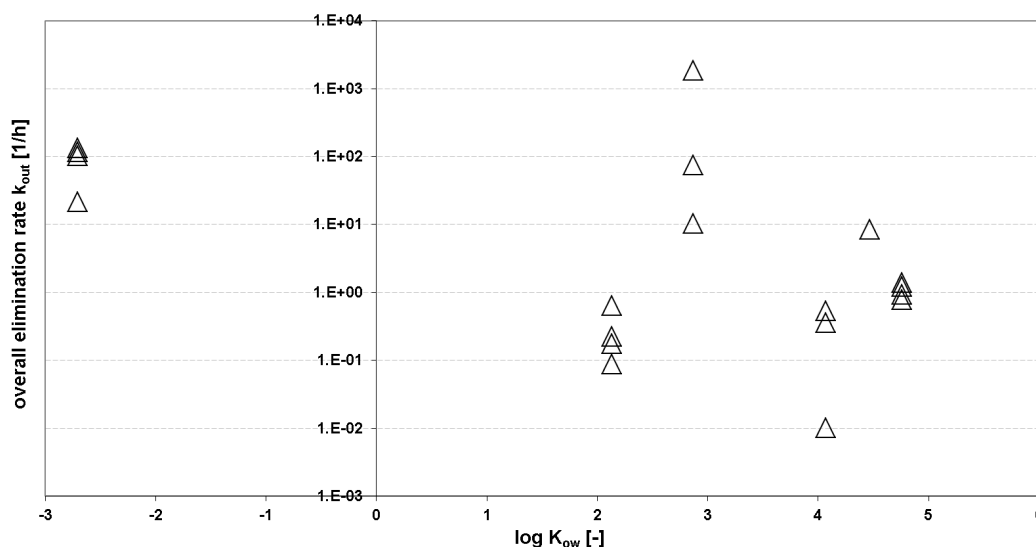


**Figure 3.5:** Estimated overall elimination rate constants for each independent experiment separately as well as for each chemical measurement series globally as a function of  $\log K_{OW}$  (paraquat  $\log K_{OW} = -2.71$ , metazachlor  $\log K_{OW} = 2.13$ , isotroturon  $\log K_{OW} = 2.87$ , irgarol  $\log K_{OW} = 4.07$ , PNA  $\log K_{OW} = 4.47$ , triclosan  $\log K_{OW} = 4.76$ ).

### 3.3.3 From measured external exposure concentration to predicted internal effect concentration

The effect concentrations varied over two orders of magnitude between  $0.781 \mu\text{mol L}^{-1}$  for paraquat (Faust et al., 2003) and  $0.0065 \mu\text{mol L}^{-1}$  for triclosan (Franz et al., 2008) and decreased in the following order: paraquat > metazachlor > PNA > isotroturon > irgarol > triclosan (Table 3.3). According to the quantitative relationship between  $EC_{50}$  for narcotic acting chemicals and their  $\log K_{OW}$  developed by Altenburger et al. (2004), the estimated baseline toxicity would systematically overestimate the effect concentrations by 100- to  $35 \times 10^6$ -fold. Thus, the chemicals are expected to provoke specific or reactive modes of toxic action. The estimated baseline toxicity is closer to the measured effect concentrations for chemicals with  $\log K_{OW} < 3$  than to the ones with  $\log K_{OW} > 4$ . Within the same mode of toxic action, the intrinsic potency seems to be driven by the chemicals' hydrophobicity: the PS II inhibitor irgarol is 3.3-fold more potent than isotroturon, the lipid biosynthesis inhibitor triclosan reached a 25.8-fold higher toxicity than metazachlor and PNA is 5.1-fold more potent than paraquat, which are both considered to be biologically active through intrinsic reactivity.

To predict the internal effect concentration  $IEC_{50}$ , the external exposure concentrations inhibiting 50% of population growth  $EC_{50}$  were linked to the  $BCF_{kin}$  (Equation 3.4). By considering differences in bioconcentration, the previous order of the intrinsic potency derived by the effect concentrations completely changed. The predicted  $IEC_{50}$  thus decreased within the range of  $7.61 \text{ mmol kg}_{\text{wet weight}}^{-1}$  ( $91722 \times 10^3 \text{ molecules cell}^{-1}$ ) to  $0.05 \text{ mmol kg}_{\text{wet weight}}^{-1}$  ( $573 \times 10^3 \text{ molecules cell}^{-1}$ ) in the following order: PNA > triclosan > metazachlor > irgarol > paraquat > isotroturon (Table 3.3). Chemicals with lower hydrophobicity show a higher intrinsic potency than chemicals with moderate hydrophobicity within the same mode of action class. This means that fewer molecules

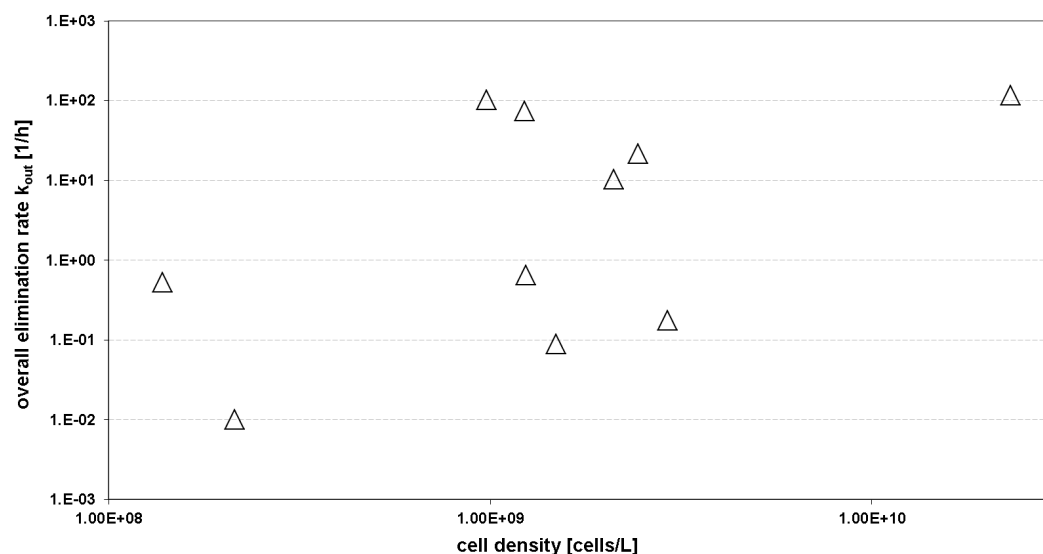


**Figure 3.6:** Estimated overall elimination rate constants related to the used cell densities.

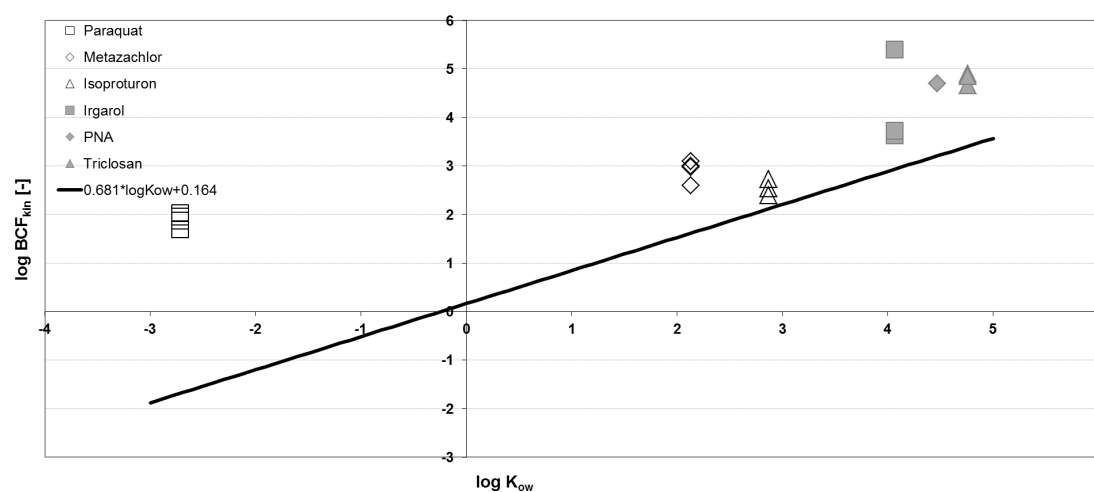


**Figure 3.7:** Calculated bioconcentration factor ( $\log BCF_{kin}$ ) as a function of  $\log K_{ow}$ . The relationship of the bioconcentration factor to the  $\log K_{ow}$  is depicted by the regression line according to Geyer et al. (1984)

of the chemicals with lower hydrophobicity were accumulated in algae cells than of the chemicals with moderate hydrophobicity in order to elicit the same effect level. According to the predicted  $IEC_{50}$  the photosystem II inhibitor isoproturon was 2.3-fold more potent than irgarol, the lipid biosynthesis inhibitor metazachlor was 2.9-fold more toxic than triclosan, and the reactive chemical paraquat was even 134.9-fold more potent than PNA. Moreover, the  $IEC_{50}$  for paraquat was in the same order of magnitude as the photosystem II inhibitor isoproturon.

**Table 3.3:** Estimated internal effect concentrations  $IEC_{50}$  [ $\text{mmol kg}_{\text{wet weight}}^{-1}$ ,  $1 \times 10^3$  molecules  $\text{cell}^{-1}$ ] based on literature-reported effect concentrations for  $EC_{50}$  of *S. vacuolatus* population growth. Even lower internal doses might potentially trigger median effect levels than the predicted  $IEC_{50}$ , because of an adsorption at the cell wall and/or biotransformation of the parent compound inside algae cells. Consequently, the chemicals' toxic potency may be underestimated.

	$EC_{50}$ [ $\mu\text{mol L}^{-1}$ ]	$BCF_{\text{kin}}$ [-]	$IEC_{50}(t_{24})$ [ $\text{mmol kg}_{\text{wet weight}}^{-1}$ ]	$IEC_{50}(t_{24})$ [ $1 \times 10^3$ molecules $\text{cell}^{-1}$ ]
isoproturon	0.138 <sup>1</sup>	345.14	0.0476	573
irgarol	0.022 <sup>2</sup>	5105.05	0.112	1353
metazachlor	0.168 <sup>3</sup>	935.40	0.157	1893
triclosan	0.0065 <sup>4</sup>	70469.31	0.458	5517
paraquat	0.781 <sup>3</sup>	72.28	0.056	680
PNA	0.153 <sup>5</sup>	49773.71	7.615	91722

<sup>1</sup>Manthey et al. (1993) <sup>2</sup>Arrhenius et al. (2006) <sup>3</sup>Faust et al. (2001) <sup>4</sup>Franz et al. (2008) <sup>5</sup>Altenburger et al. (2006)

## 3.4 DISCUSSION

### 3.4.1 Data quality assessment

A chemical depletion in the ambient medium was observed as a consequence of bioconcentration kinetics in algae cells by using the proposed experimental design. The estimated algae biomass was adequate to measure a substantial chemical decline. Consequently, bioconcentration kinetics were successfully determined for all analyzed chemicals in the described range of hydrophobicity and without reaching fully depleted concentration in the ambient medium. Maximum concentration decline was found at almost same cell densities for the independent experiments per chemical. This demonstrates that the experimental design with the previous determined algae biomass depending on the chemical hydrophobicity was suitable to achieve detectable concentration changes in the ambient medium and indicates good reproducibility. The relative standard deviation of the measured concentrations for each independent experiment separately ranged between 1.2% for paraquat and 12.83% for triclosan. The 95% confidence intervals are generally one to two orders of magnitude smaller than the predicted kinetic parameters (Table 3.2). Sijm et al. (1998) reported higher standard deviations for the predicted parameters in the same magnitude of order, which might be explained by the use of batch algae populations. Moreover, the median standard deviation of the bioconcentration factor  $\log BCF_{\text{kin}}$  was calculated to be 0.2 (relative 11%) which indicated high agreement of the results from the independent toxicokinetic experiments besides irgarol (Figure 3.7). In contrast, a higher median standard deviation of 2.9 (relative 59%) has been found for bioconcentration kinetic factors of hydrophobic chemicals in different algae densities (Sijm et al., 1998).

Kühnert et al. (2013) quantified time-dependent ambient and internal concentrations for several polycyclic aromatic hydrocarbons in zebrafish embryos by using a static exposure system and showed that the predicted internal concentration profiles in zebrafish embryo quantified by the chemical depletion in the ambient medium are comparable to the measured ones unless biotransformation impacts the time-course of the internal concentration. For the determination of the bioconcentration kinetics of specifically acting and reactive chemicals in algae, the indirect approach, however, has some shortcomings: In order to achieve concentration depletion in the ambient medium, a high algae biomass has to be achieved in the toxicokinetic assay depending on the hydrophobicity of the chemical. Moreover, very fast kinetics of bioconcentration, as here

observed for isoproturon and paraquat, cannot be captured very well. This resulted in higher parameter uncertainty of the predicted kinetic rate constants. Furthermore, the method used here does not allow for a distinction between adsorption at the cell wall or absorption in the algae cell. Low impact of adsorption at the algae surfaces on the overall bioconcentration process was observed for nonspecific, neutral organic chemicals (Jabusch and Swackhamer, 2004). Jabusch and Swackhamer (2004) explored subcellular accumulation for 13 polychlorinated biphenyls with high hydrophobicity ( $4.7 > \log K_{OW} > 8.1$ ) and found adsorption to the algae surface to be less than 10% of the total accumulated amount. Nevertheless, the impact of adsorption at the algae surface wall to the overall bioconcentration remains still to be investigated for ionized or specifically acting and reactive chemicals with a wide range of physicochemical properties. Chemical adsorption at the cell wall was therefore assumed to be negligible in the present study, which leads to the prediction of a maximum number of accumulated molecules. Consequently, the chemicals' toxic potency is likely to be underestimated and even lower internal doses might potentially trigger median effect levels.

### 3.4.2 Time for reaching chemical equilibration between ambient medium and algae biomass

The observed equilibrium's between extracellular and intracellular concentrations were reached within minutes to a few hours and are in agreement with reported toxicokinetic studies, e.g. for dichlordiphenyltrichlorethan in *Chlorella sp.* within 15 seconds (Södergren, 1968); for polychlorinated biphenyls, polybrominated biphenyls, hexachlorobenzene (Geyer et al., 1984) as well as sulfonyleurea herbicides in *S. vacuolatus* suspension within one hour (Fahl et al., 1995); and for polychlorinated biphenyls in *Chlorella pyrenoidosa* suspension within one hour (Sijm et al., 1998). Equilibrium concentrations of polychlorinated biphenyls were also observed in less than 25 hours for different species of marine phytoplankton (Gerofke et al., 2005). In contrast, other studies reported equilibrium concentrations of polychlorinated biphenyls within several days or weeks in different species of marine phytoplankton (Skoglund et al., 1996; Swackhamer and Skoglund, 1993). These differences between times needed to reach steady-state concentrations in algae cells may be caused either by physiological differences in growth stages, size, lipid content and lipid composition of different algae species (Gerofke et al., 2005) or by differences of physicochemical properties of the chemicals used such as ionic status or hydrophobicity (Escher et al., 2011; Könemann and van Leeuwen, 1980; Kühnert et al., 2013; Neuwoehner and Escher, 2011).

Hydrophobicity is the main key feature which drives the time needed to reach equilibrium concentrations when diffusion is the major process to be accounted for. Equilibrium concentrations are reached faster for isoproturon and paraquat with a  $\log K_{OW} < 3$  than for triclosan (approximately at 30 min) and PNA with a  $\log \log K_{OW} > 4$  which is in accordance to our expectations. This observation is generally explained by a longer time to reach equilibrium with an increase of the chemical's hydrophobicity (Escher et al., 2011; Könemann and van Leeuwen, 1980). In contrast to our expectations, equilibrium concentrations were not reached for metazachlor and irgarol within the exposure time period of four hours indicating a very slow kinetic of bioconcentration in comparison to the other analyzed chemicals. The unexpected slow kinetics for metazachlor and irgarol were moreover not justified by their hydrophobicity. Additionally, the observed increase of triclosan in the ambient medium after 120 min exposure is also not explainable by the hydrophobicity of  $\log K_{OW} = 4.76$ . In summary, the kinetics of bioconcentration observed for PNA, isoproturon and paraquat were expected according to

their hydrophobicity. We observed unexpected bioconcentration kinetics for triclosan, irgarol and metazachlor indicating that other processes besides hydrophobicity-driven uptake may be of relevance. The impact of other processes most potentially altering the hydrophobicity-driven bioconcentration kinetics in algae cells. The impact of ionization of the chemicals in the ambient medium, ion trapping mechanism and biotransformation on bioconcentration kinetics is therefore discussed in the following.

### **Ionization of the chemicals in the ambient medium**

Firstly, the amount of accumulated molecules inside algae cells depends on the bioavailable fraction of the neutral species in the ambient medium which primarily crosses the algae membranes by passive diffusion (Fahl et al., 1995; Neuwoehner and Escher, 2011). The charged species itself is not or only very poorly accessible through the membrane, which would lead to a reduced uptake of the total bioavailable molecules into the algae cells (Neuwoehner and Escher, 2011). In the present study, PNA, isoproturon and metazachlor are assumed to be completely bioavailable in their neutral forms according to the stable pH regime of 6.4 over the exposure time (Table B.4, B.5, B.6). Approximately 5% of the total triclosan molecules and 12% of the total irgarol molecules in the ambient medium exist as ionized fraction. Paraquat exists as a dissociated salt with two cationic quaternary ammonium substructures and it is fully charged in the aqueous medium at any pH ( $pK_a = pK_b = \infty$ ). The fraction of the charged triclosan, irgarol and paraquat species might hence not or only very poorly accessible through the algae membrane, which leads to a reduction of accumulated molecules in algae. Therefore, the chemicals' toxic potency is likely to be underestimated. Fahl et al. (1995) for instance explored the pH-dependent toxicity of the weak acids sulfonylurea herbicides to algae and showed that the toxicity decreases with a pH-increase in the ambient medium.

### **Ion trapping mechanism**

Secondly, the ion trapping mechanism changes the amount of accumulated molecules inside algae cells as a consequence of a pH shift from the ambient medium pH to the cytoplasmatic pH (Neuwoehner and Escher, 2011). In the algae cell, accumulated neutral molecules can dissociate to charged molecules depending on the internal algae pH, which leads to an additional flux of neutral molecules into algae cells or vice versa with a diffusion rate equal to the hydrophobicity-driven bioconcentration. A shift of the extracellular pH of 6.4 to the intracellular pH of 7.6 in the cytosol (Küsel et al., 1990) would lead to the dissociation of accumulated neutral molecules to charged molecules for triclosan (45%) and irgarol (1%) inside the algae cells, but not for PNA, isoproturon, paraquat and metazachlor (Table B.2 - B.6). Küsel et al. (1990) further showed that a change from aerobic to anaerobic conditions causes a decrease of intracellular pH from 7.6 to 7.0 within 6 min. Thus, the change of the intracellular pH would lead to an increase of the relative amount of neutral triclosan molecules inside the cells from 55% at pH 7.6 to 83% at pH 7.0 and to a decrease of neutral irgarol molecules from 99% at pH 7.6 to 95% at pH 7.0 (Table B.2 and B.4). The decrease of the pH in the algae cells might cause a direction change of the diffusion flux from the algae cell to the ambient medium mainly for triclosan as the ion trapping mechanism provides a reservoir of charged molecules. The pH dependent re-adjusted partitioning flux might explain the increase of the triclosan concentration in the ambient medium after 120 min of exposure.

## Biotransformation

Finally, biotransformation of the parent chemical in algae cells might alter the time-course of the internal concentration and the time needed to reach equilibrium. Information on biotransformation of chemicals in aquatic organisms other than fish is limited (Jeon et al., 2013). To our knowledge, no studies exist on biotransformation of irgarol, isoproturon, triclosan, metazachlor, paraquat and PNA in algae cells. On the basis of the unexpected slow bioconcentration kinetics observed for irgarol and metazachlor, we hypothesized that the toxicokinetic process is modified by biotransformation for these two chemicals. Chloroacetanilide herbicides such as metazachlor are known to be conjugated by glutathione *S*-transferase in corn (Lederer and Böger, 2005). Specific glutathione *S*-transferase enzymes have also been identified and characterized in algae cells which potentially enable the biotransformation for metazachlor (Tang et al., 1998). A metabolite of irgarol was found in *Phanerochaete chrysosporium* formed mainly via N-dealkylation at the cyclopropylamino group (Liu et al., 1997). Multiple biotransformation mechanisms of demethylation, hydroxylation and conjugation were further characterized for irgarol in the invertebrates *Daphnia magna* and *Gammarus pulex* (Jeon et al., 2013). To conclude, an unknown number of biotransformation products with different structures might be formed by multiphase enzymatic reactions of irgarol, metazachlor and other chemicals in algae cells. It is not known at which time point these biotransformation products are initiated during algae ontogenesis and to which magnitude of rates these biotransformation products are formed in order to understand whether biotransformation significantly impacts toxicokinetics in algae cells (Jeon et al., 2013). To this end, analytical detection limits have to be overcome for quantifying internal concentrations of different molecular structures in algae cells over time. Alternatively, transcriptional gene expression of phase I and II enzymes could provide indication of ongoing biotransformation.

### 3.4.3 Estimated toxicokinetic parameters

Analytical limits of quantifying the internal concentration in algae cells were overcome by the method presented here. The measurement of the chemical depletion in the ambient medium is a useful technique to indirectly determine the kinetics of bioconcentration of chemicals in algae cells. A one-compartment toxicokinetic model was successfully applied to estimate chemical uptake and overall elimination rate constants. So far, kinetic parameters have been estimated by fitting one-compartment toxicokinetic models to the time-dependent internal concentrations measured in batches of large algae biomass exposed to non-specific, organic chemicals with high hydrophobicities of  $4.46 < \log K_{OW} < 8.18$  (Skoglund et al., 1996) and of  $5.183 < \log K_{OW} < 6.9$  (Sijm et al., 1998). Sijm et al. (1998) predicted a range of uptake rate constants from  $0.008 \times 10^3$  to  $29.58 \times 10^3 \text{ L kg}^{-1} \text{ h}^{-1}$  which are similar to the uptake rate constants from  $0.21 \times 10^3$  to  $640 \times 10^3 \text{ h}^{-1}$  found in the present study. Sijm et al. (1998) moreover reported a relative standard deviation of 42% for the average uptake rate constant independent of the cell density and chemical's hydrophobicity. In this present study, the 95% confidence intervals were at least one order of magnitude smaller than the estimated uptake rate constants except for isoproturon and paraquat. The high parameter uncertainty for isoproturon and paraquat results from the fast bioconcentration kinetics which could not be captured in time by using the method used. Despite the broader range of chemicals' hydrophobicity in this present study, the lower uncertainty of kinetic uptake rates may result from the normalization of  $k_{in}$  to  $F$ . The uptake rates increased

with increasing hydrophobicity (Figure 3.3) and corroborate with those observations of Sijm et al. (1998). In contrast, Skoglund et al. (1996) reported that uptake rates were statistically independent of hydrophobicity for three different algae species and inversely related to the hydrophobicity for a fourth type of algae. Further experiments covering chemicals with diverse physicochemical properties and hydrophobicity for different algae species might be necessary to explore the relation between hydrophobicity and uptake rates.

A shorter interval to equilibrium between ambient medium concentration and intracellular concentration is generally associated with the prediction of a higher overall elimination rate constant  $k_{\text{out}}$  (Arnot and Gobas, 2006). In this present study,  $k_{\text{out}}$  ranged over five orders of magnitude but seemed to be unrelated to the chemical's hydrophobicity (Figure 3.5). In contrast to our study, Sijm et al. (1998) predicted a stable average overall elimination rate with a high standard deviation of  $0.649 \pm 1.892 \text{ h}^{-1}$  independent of the cell density and chemical's hydrophobicity. We predicted higher overall elimination rates for isoproturon, triclosan, paraquat, and PNA than determined by Sijm et al. (1998). The differences of  $k_{\text{out}}$  might be justified by a structured synchronized algae population used here while Sijm et al. (1998) exposed batch algae populations to hydrophobic chemicals with  $\log K_{\text{OW}} > 5.18$ . Nevertheless, Vogs et al. (2013) (**Chapter 2**) insert the overall elimination rate of  $0.649 \pm 1.892 \text{ h}^{-1}$  in a toxicokinetic-toxicodynamic model as a first guess to predict the time-course of internal effect concentrations for triclosan, PNA, and norflurazone. This approximation led to time estimates for reaching equilibrium concentrations in *S. vacuolatus* of five hours independent of the chemicals hydrophobicity, which would misfit the kinetics of bioconcentration observed for isoproturon, triclosan, paraquat, and PNA. Higher elimination rate constants for paraquat, PNA, triclosan and isoproturon seem therefore reasonable for the simulation of a faster equilibrium concentration. The predicted toxicokinetic time-courses using the elimination rate constant from the study of Sijm et al. (1998) would, however, lead to similar kinetics of bioconcentration for irgarol and metazachlor observed in this present study. This raises the question if biotransformation processes might play a role for polychlorinated biphenyls as well. However, the parameter  $k_{\text{out}}$  has to be interpreted carefully because of its character as a sum parameter integrating elimination and biotransformation processes in the whole organism as well as the inclusion of uncertainty on the parameter estimations due to the interference of uptake and elimination processes. The incorporation of a depuration experiment would lead to more confident estimation for kinetic parameters.

The estimation of the time to reach equilibrium concentrations is essential to understand and analyze time-dependent effects. Several studies reported time-dependent effects on individual cell growth or photosynthetic activity of *S. vacuolatus* caused by specifically acting and reactive chemicals (Altenburger et al., 2006; Franz et al., 2008; Vogs et al., 2013) (**Chapter 2**). In these studies, the observed steady-state effect levels needed hours to be reached. The here presented study, however, hypothesizes that toxicokinetic processes might not be solely responsible for those observed time-dependent toxicities. Rather it seems that toxicokinetic processes need minutes while toxicodynamic processes are progressed within hours. A wrong assumption of the toxicokinetic time-course might therefore lead to a misinterpretation of the time dependence of toxicity. Knowing the time-course of the internal concentration helps to understand and simulate toxicodynamic processes. Thus, toxicokinetic parameters have to be incorporated into toxicokinetic-toxicodynamic models in order to correctly interpret the observed effects over time caused by chemicals which specifically or reactive interact with the biological target site of action in algae cells.

### 3.4.4 From measured external exposure to predicted internal effect concentrations

Different CBR ranges have been found for chemicals with different modes of toxic action such as non-specific, specific and reactive (Escher and Hermens, 2002; McCarty and Mackay, 1993). Chemicals that non-specifically disturb the membrane's integrity and function showed equivalent intrinsic potencies reflected by a constant threshold of an effect concentration in the biological membrane (McCarty and Mackay, 1993; van Wezel and Opperhuizen, 1995). Studies reported critical body burdens in the average range of 2–8 mmol kg<sub>body weight</sub><sup>-1</sup> for non-polar, non-reactive organic chemicals in different organisms (McCarty and Mackay, 1993; van Wezel and Opperhuizen, 1995). Internal effect concentrations of polychlorinated biphenyl congeners in the green algae *Selenstrum capricornutum* were predicted to span between 6.7 to 14.3 mmol kg<sub>wet weight</sub><sup>-1</sup> (Mayer et al., 1998). We predicted CBRs in the range of 0.048 to 7.615 mmol kg<sub>wet weight</sub><sup>-1</sup> which are one to two orders of magnitude lower compared to the reported CBRs for narcotic acting chemicals except for PNA. This means that a lower number of molecules of specifically acting and reactive chemicals have to be accumulated in the whole body than narcotic acting chemicals in order to elicit the same effect level. Manthey et al. (1993) predicted *IEC*<sub>50</sub> in the range of 360 - 100 × 10<sup>3</sup> molecules cell<sup>-1</sup> for photosystem II inhibitors, which is in the range of the predicted *IEC*<sub>50</sub> for irgarol and isoproturon in the present study. Fahl et al. (1995) reported 45 to 63-fold lower *IEC*<sub>50</sub> for the more hydrophilic sulfonyleurea herbicides inhibiting the enzyme acetolactate synthase when compared to *IEC*<sub>50</sub> of photosystem II inhibitors (Manthey et al., 1993). In the present study, such a clear discrimination of *IEC*<sub>50</sub> values was not found for the different modes of toxic action. Interestingly, the predicted CBR of paraquat is two orders of magnitude lower than the reactive chemical PNA and is in the same CBR range of the specifically acting chemicals. Thus, the predicted CBR of paraquat indicates a specific interaction with the biological target site rather a reactive mode of action. It is known that paraquat is reduced by forming radicals when replacing the ferredoxin in the photosystem I (Hock et al., 1995). The CBRs found here are, however, non-equivalent for chemicals with the same mode of action, which might be caused by different affinities for and types of interaction with the target site (Escher et al., 2011). The predicted *IEC*<sub>50</sub> is a better dose descriptor than exposure-based dose metrics, but it does still not reflect the effective concentration at the target site. Therefore, more information about partitioning-driven distribution processes to the target site, target site locations as well as quantities of the target site, and mechanisms of toxic action have to be incorporated for characterizing target concentrations eliciting an effect (Escher and Hermens, 2002).

## 3.5 CONCLUDING REMARKS & OUTLOOK

The present study demonstrates that bioconcentration of chemicals in algae cells is a complex process as indicated by different kinetic patterns. Equilibrium concentrations were reached very fast within minutes for isoproturon, paraquat and PNA, if hydrophobicity-driven bioconcentration was the major process to be accounted for. Other processes such as ionization of the chemicals in the ambient medium, ion trapping mechanism, or the susceptibility for biotransformation potentially affected hydrophobicity-driven bioconcentration kinetics in algae cells. The amount of accumulated molecules inside algae cells depends on the bioavailability of neutral molecules in the ambient medium. The accumulation of molecules in algae cells might be reduced for triclosan, irgarol and paraquat due to the fraction of molecules which are charged in the ambient medium. According to the ion trapping mechanism, the amount of accumulated molecules inside algae cells might be changed for triclosan and irgarol as a consequence of different algae pH

compared to the ambient pH. In the specific case of triclosan, we suggested that that ion trapping causes a direction change of diffusion back to the ambient exposure medium. The present study further showed that equilibrium concentrations of irgarol and metazachlor were reached approximately after 180 min of exposure, because biotransformation processes potentially alter hydrophobicity-driven bioconcentration kinetics in algae cells. The internal change of exposure as a result of toxicokinetic processes can still not explain the time-delayed toxicity by cumulative exposure as reported by several studies for algae (Altenburger et al., 2006; Franz et al., 2008; Vogs et al., 2013) (**Chapter 2**). Rather additional, toxicodynamic processes impose a further time limiting step at which toxicity is progressed over hours. The implementation of mechanistic understanding of toxicokinetic processes may improve our understanding and the predictability of effects in algae.

Moreover, the assessment of combination effects on aquatic organisms from sequential exposures will be a challenging future task for which the understanding of toxicokinetic and toxicodynamic processes might help. Ashauer et al. (2007a) for instance modeled the combined effects of pulsed exposure to carabryl and chlorpyrifos on *Gammarus pulex* and showed that carry-over toxicity might be caused by either a slow elimination kinetic or by a slow recovery from internal damage. The consolidation of experimental design and toxicokinetic-toxicodynamic modeling has been demonstrated to be a promising framework for understanding and predicting combined effects on aquatic organisms from sequential exposures. However, the toxicity through more realistic exposure scenarios such as fluctuating concentrations and the corresponding carry-over toxicity after sequential pulses are rarely studied for other organisms like algae. Recently, Weber et al. (2012) assessed the biomass inhibition of time-variable isoproturon exposure on *Pseudokirchneriella subcapitata* and *Desmodesmus subspicatus* indicating the possibility for carry-over toxicity after a first exposure event when the populations were fully recovered. A study about carry-over toxicity has yet not been investigated for algae to our knowledge. A more systematic experimental design with defined concentration peaks, pulse durations and the potential for recovery between pulses would therefore help to explore carry-over toxicity of chemicals with different hydrophobicities, mechanisms of action, and the degree of reversibility on algae as shown for invertebrates (Ashauer et al., 2007a).

Joint effects based on ambient concentrations of simultaneous exposure are well studied for algae but not for fluctuating exposure. The incorporation of time-dependent body burdens or internal concentrations at the target site would, however, increase the predictability of toxicity on algae exposed to fluctuating concentrations of complex mixtures. The variability of joint toxicity could be expressed by the investigation of the affinity to the target site, mechanisms of action and the potential to interact between chemicals in the mixture.

# How toxicokinetic and toxicodynamic processes in *Scenedesmus vacuolatus* contribute to the time dependence of toxicity? - A modeling case study for different adverse outcome pathways

## ABSTRACT

The internal chemical concentration in unicellular algae cells reaches equilibrium within minutes due to hydrophobicity-driven partitioning processes. By contrast, damage in algae cells cumulatively increases over hours. The observed time-gap of hours between steady-state of internal exposure and damage development in algae cells might be explainable assuming a rate-limiting toxicodynamic step depending on the effect progression toward an adverse outcome (AOP). This study seeks to determine these rates quantifying the effect progression from an initiating molecular event over key events toward the adverse outcome on algae growth. To this end, *Scenedesmus vacuolatus* growth assays were conducted for six chemicals characterized by two different hydrophobicity groups and three different modes of action. The time-course of the estimated internal concentrations were related to the affected growth patterns of *Scenedesmus vacuolatus* through toxicokinetic-toxicodynamic modeling. As one result, the progress of an effect over time correlates with different AOPs independent of the time when equilibrium concentrations in the algae cells were reached. The effect progression rate constants ranged over six orders of magnitude in the following order: inhibitor of the photosystem II > reactive chemicals > inhibitor of lipid synthesis. By contrast, effect progression rate constants between chemicals representing one AOP varied less than one order of magnitude. Quantification of effect progression rates might thus help to characterize and distinguish between different types of AOPs.

## 4.1 INTRODUCTION

The occurrence of agricultural and industrial chemicals in the environment has likely caused effects on aquatic organism (Malaj et al., 2014). To estimate and assess the likelihood of effects on aquatic organisms exposed to fluctuating and sequential concentrations of a chemical cocktail, effect models could face two main challenges in current risk assessment: the extrapolation of combined effects on aquatic organisms exposed to sequential concentrations of a chemical mixture and the linkage of adverse outcomes across different levels of biological organization (Forbes and Calow, 2012; Hartung and Rovida, 2009; Villeneuve and Garcia-Reyero, 2011). The application of effect models, especially which describe toxicokinetic and toxicodynamic processes, has been discussed for their ability to compare and extrapolate the adverse outcomes on various response levels between different chemicals, species, exposure conditions and durations (Altenburger and Greco, 2009; Ashauer and Escher, 2010; Jager et al., 2006, 2011).

Toxicokinetic-toxicodynamic (TKTD) models link the accumulated concentration in the entire organism to the probability of survival over time. Thereby, toxicokinetic processes describe the time-course of the internal concentration in the entire body which are composed of the summed mass fluxes including chemical uptake in the organism, distribution to the target site, potential susceptibility for biotransformation, and chemical elimination back into the ambient exposure medium (Ashauer et al., 2007b, 2013; Jager et al., 2011). The toxicodynamic processes encompass the underlying mechanisms of biologically significant perturbations which are represented as the sum of the overall damage injury and damage recovery in order to describe the temporal dynamics of lethality (Ashauer et al., 2007b, 2013; Jager et al., 2011). To this end, TKTD studies have been developed for fish and vertebrates, where the time-course of toxicity was examined by integrating the information of overlapping toxicokinetic and toxicodynamic processes (Ashauer et al., 2013; Jager et al., 2011; Lee et al., 2002a; Legierse et al., 1999; McCarty and Mackay, 1993; Verhaar et al., 1999). Here, toxicity development has differently been interpreted depending on several factors like the chemical's hydrophobicity, organism size, mechanisms of action, exposure system or the type of effect model (Ashauer et al., 2007b; Ashauer and Brown, 2008; Jager et al., 2011). Thus, toxicity of chemicals to fish or invertebrates over time was dominated by either the rate-limiting processes of chemical's overall elimination or the chemical's degree of reversibility to bind at a biological target site as well as the ability to recover (Ashauer et al., 2007b; Ashauer and Brown, 2008; Jager et al., 2011). However, if the equilibrium of internal chemical exposure in an organism is reached fast compared with the time-course of the overall toxicity, damage development caused by the progress of an effect could be studied without bias of internal exposure changes over time (Forbes et al., 2006). Vogs et al. (2013) (**Chapter 2**) provided evidence that the unicellular algae system might be suitable to study rates of effect progression for toxicodynamic processes almost independent of internal concentration changes over time.

Toxicity has been shown to cumulatively increase over several hours in the unicellular green algae *Scenedesmus vacuolatus* (*S. vacuolatus*) (Altenburger et al., 2006; Franz et al., 2008; Vogs et al., 2013) (**Chapter 2**). By contrast, the internal concentration in the unicellular green algae are assumed to reach equilibrium within minutes due to hydrophobicity-depending partitioning processes (Fahl et al., 1995; Manthey et al., 1993; Vogs et al., 2015) (**Chapter 3**). Therefore, the bias of the chemical accumulation change over time is likely minimized in *S. vacuolatus* over time compared with the overall toxicity development. The hypothesized time-gap of hours between the time point of the steady-state internal exposure and the progressed toxicity in algae cells might be explained by assuming a rate-limiting toxicodynamic step that depends on the effect progression

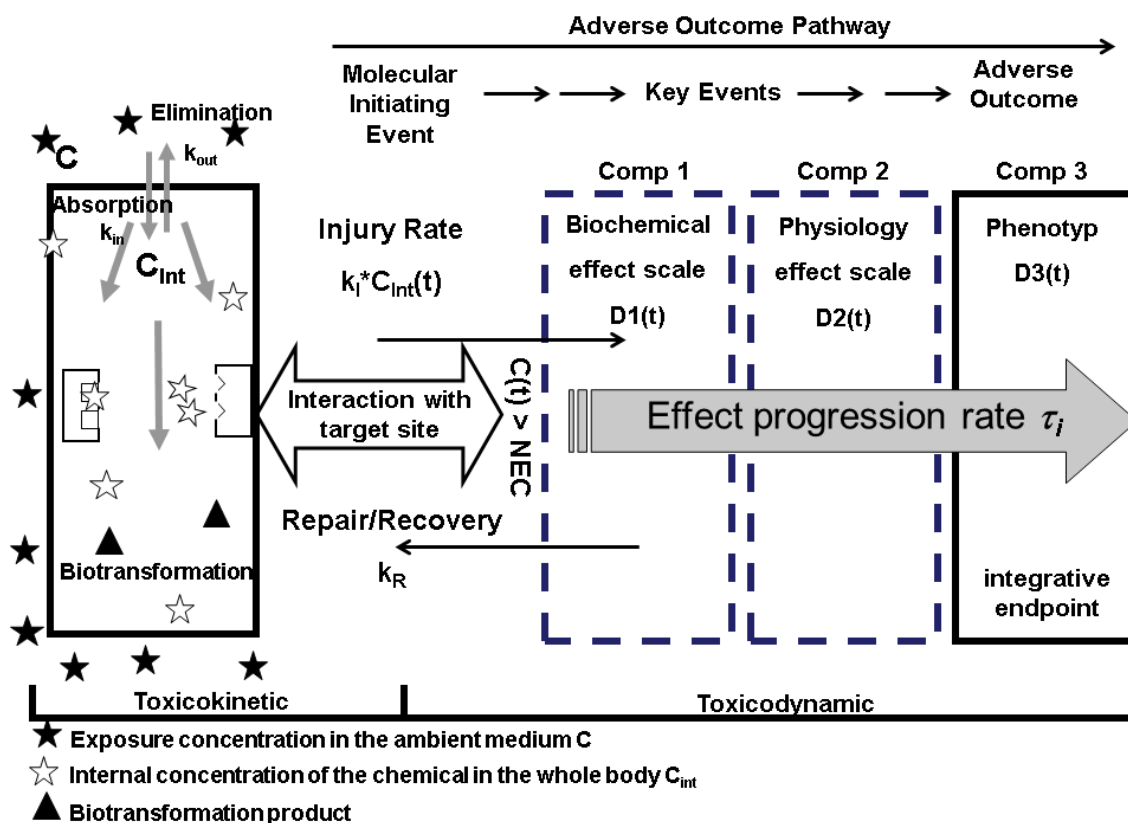


**Figure 4.1:** Conceptual scheme illustrating toxicokinetic and toxicodynamic processes for an adverse outcome pathway.

toward an adverse outcome. Rates of effect progression may be quantified by applying an algae TKTD model developed by Vogs et al. (2013) (**Chapter 2**), which abstracts different adverse outcome pathways (Ankley et al., 2010).

The adverse outcome pathway (AOP) is a theoretical framework that has been suggested to conceptualize a chain of events initiated by a chemical-molecular interaction that triggers a cascade of key events on multiple biological levels progressed toward an adverse outcome (Ankley et al., 2010). Various AOPs have been designed based on comprehensive information of critical toxicological endpoints organized for multiple biological levels of well-known mechanism (Ankley et al., 2010). However, it remains still challenging to fill the compartments with multivariate data of critical toxicological effects from chemicals with known and unknown AOPs. Apart from that, AOPs are theoretical frameworks without relating exposure to concentration-dependent responses that are progressed through multiple biological layers over time. Complementary, the cascade of disturbed processes after chemical-induced target stimulation could be abstracted by TKTD modeling that provides a quantitative linkage between internal exposure change and the effect progressed toward an adverse outcome on the organism level. Simeoni et al. (2004), for instance, successfully applied an indirect response pharmacokinetic-pharmacodynamic model that described a reduced tumor growth over time after the administration of various anticancer drugs by enabling the effect to progress toward the reduced tumor growth. Similarly, TKTD modeling of concentration-dependent response changes over time

might be able to characterize the rate-limiting toxicodynamic step of the progressed effect toward an adverse outcome on algae growth for chemicals between different types of AOPs (Figure 4.1). However, how toxicokinetic and toxicodynamic processes contribute to the overall time-course of toxicity of chemicals with different hydrophobicities and modes of action to algae growth has not been investigated in *S. vacuolatus* yet.

The first objective of the present study was to systematically investigate the contribution of toxicokinetic and toxicodynamic processes toward the adverse outcome on growth by providing a joint approach of experimentation and mathematical modeling. The second objective was to quantify rates which are hypothesized to be related to different key adverse outcome pathways in *S. vacuolatus*. To this end, dynamics of internal concentrations were linked to the growth of *S. vacuolatus* by applying an algae TKTD model. Therefore, the experiments were set up for six model chemicals which represent (i) two hydrophobicity groups ( $\log K_{OW} < 3$ : isoproturon, metazachlor, paraquat and  $\log K_{OW} > 4$ : irgarol, triclosan, n-phenyl-2-naphthylamine (PNA)) and (ii) three groups of different AOPs. Isoproturon and irgarol are known to inhibit photosynthesis functioning, metazachlor and triclosan block the lipid biosynthesis, and paraquat and PNA are reactive chemicals.

## 4.2 METHODOLOGY

### 4.2.1 Algae cultivation

Algae growth assays were performed with a synchronized culture of *S. vacuolatus* population (strain 211-215 SAG, Göttingen, Germany). The unicellular green algae were grown photoautotrophically in a modified inorganic, sterilized Grimme-Boardman medium (GB-medium) adjusted to pH 6.4 at  $28 \pm 0.5^\circ\text{C}$ . The *S. vacuolatus* culture was synchronized by a light/dark rhythm of 14/10h and periodic diluted to the standard cell density of  $1 \times 10^9$  cells  $\text{L}^{-1}$  after every 24 h generation cycle (Altenburger et al., 2004).

### 4.2.2 Modeling of the concentration-response relationship for different exposure times

The effects of six chemicals on algae growth were investigated over 24 h. CAS Registry Number, sources, the molecular structure, and relevant physicochemical properties for irgarol, isoproturon, triclosan, metazachlor, paraquat, and PNA are listed in Table 3.1, **Chapter 3**.

A homogeneous algae size distribution of cultured autospore suspensions with a starting cell density of approximately  $7.5 \times 10^7$  cells  $\text{L}^{-1}$  was harvested and transferred in closed 20 mL pyrex glass tubes. The GB-medium was enriched with  $1.9 \text{ mmol L}^{-1}$  of  $\text{NaHCO}_2$  in order to buffer the pH at  $6.9 \pm 0.2$ . The harvested algae cells continued to grow normally under permanent fluorescent light before the exposure experiment started. Irgarol, isoproturon, metazachlor, triclosan, and PNA were dissolved in dimethyl sulfoxide (DMSO, CAS RN: 67-68-5, Merck, Germany), whereas paraquat was dissolved in GB-medium. Chemicals were added to the algae suspension after six or eight hours of normal algae growth at  $t_6$  or  $t_8$ . Algae cells were continuously exposed to six concentrations of PNA during the last 16 h ( $t_8 - t_{24}$ ) and of the other chemicals during the last 18 h ( $t_6 - t_{24}$ ). Six suitable exposure concentrations for covering 0 to 100% inhibition of algae growth were chosen according to preliminary range-finding (according to the protocol

specified in Altenburger et al. (2004), exposure condition was identical to the algae growth assay). To determine the inhibition of algae growth over time, cell volume and cell number of aliquot samples were measured twice by an electronic particle counter (CASYII, Schärfe System, Reutlingen, Germany) every two hours. One experiment was performed by using two time-shifted synchronized algae cultures for capturing the 24 h cell cycle. Cell volume was determined between 2 h and 14 h for the first treated algae culture and between 14 h and 24 h for the second treated algae culture. Thus, measurements were four-fold at the time points of  $t_6$  or  $t_8$  and  $t_{14}$ . In parallel to the 24 h experiment, two negative controls and two DMSO controls for each experiment were performed in analogous manner.

The inhibition of cell growth for each time point was calculated by normalizing the measured cell volume data of the treated algae suspension to the results of the control growth. Concentration-effect relationships  $E$  were determined by fitting a four-parametric logistic model to the inhibited cell volume (OriginLab, OriginPro 8.5.1 G)

$$E = \frac{E_{\max} - E_{\min}}{1 + \left(\frac{C}{EC_{50}}\right)^{\theta}} + E_{\min} \quad (4.1)$$

where  $C$  [ $\mu\text{mol L}^{-1}$ ] is the exposure concentration in the ambient medium,  $EC_{50}$  [ $\mu\text{mol L}^{-1}$ ] represents the median effect concentration at which 50% of the algae growth is inhibited,  $\theta$  [-] indicates the slope of the logistic curve and  $E_{\min}$  [-] and  $E_{\max}$  [-] are the minimum and maximum effect levels, respectively. The parameters  $EC_{50}$  and  $\theta$  were inversely estimated by minimizing the residual sum of squares while  $E_{\min}$  and  $E_{\max}$  were fixed to 0 and 100%, respectively. A criterion to estimate  $\theta$  and  $EC_{50}$  values was that growth or reproduction were inhibited more than 50%.

### 4.2.3 Toxicokinetic and toxicodynamic modeling

Toxicokinetic and toxicodynamic processes were formulated by a TKTD model in order to describe and simulate the perturbed *S. vacuolatus* growth by chemical impact (Vogs et al., 2013) (Chapter 2). The conceptual scheme of the toxicokinetic-toxicodynamic processes is depicted in Figure 4.1. The effect model consisted of a system of ordinary differential equations including a total of eleven parameters. Unperturbed dynamic of algae growth was mathematically expressed for three growth phases, namely an exponential growth phase ( $\approx 0-8$  h), followed by a linear growth phase ( $\approx 8-16$  h), which passes into a limited growth phase at the end of the 24 h generation cell cycle. This is expressed as:

$$\frac{dV_{\text{Control}}(t)}{dt} = \frac{\mu_E \times V_{\text{Control}}(t)}{\left[1 + \left(\frac{\mu_E}{\mu_L} \times V_{\text{Control}}(t)\right)^{\Psi}\right]^{\frac{1}{\Psi}}} \times \left(1 - \mu_C \times \frac{V_{\text{Control}}(t)}{K_{\text{Crit}}}\right) \quad (4.2)$$

where the parameter  $\mu_E$  [ $\text{h}^{-1}$ ] represents the exponential growth rate,  $\mu_L$  [ $\text{fL h}^{-1}$ ] means the linear growth rate and  $\mu_C$  [ $\text{fL h}^{-1}$ ] is the cell-clock rate. The parameter  $\Psi$  [-] forces the switch from exponential to linear growth and  $K_{\text{Crit}}$  [ $\text{fL}$ ] is the critical size for a commitment point.  $V_0$  [ $\text{fL}$ ] represents the initial cell volume of the autospore cells (Altenburger et al., 2008). Furthermore, a simple one-compartment toxicokinetic model with a first-order kinetic was applied to simulate the internal effect concentration in algae cells. The time-course of the internal concentration in the whole body  $C_{\text{int}}(t)$  [ $\mu\text{mol L}_{\text{Biovolume}}^{-1}$ ] is mathematically expressed as:

$$\frac{dC_{\text{int}}(t)}{dt} = k_{\text{in}} \times C(t) - k_{\text{out}} \times C_{\text{int}}(t) \quad (4.3)$$

where  $C(t)$  [ $\mu\text{mol L}^{-1}$ ] means the ambient concentration over time. The parameters  $k_{\text{in}}$  [ $\text{h}^{-1}$ ] and  $k_{\text{out}}$  [ $\text{h}^{-1}$ ] represent the uptake rate constant and the overall elimination rate constant of the chemical, respectively. Kinetic rate constants for the six chemicals in *S. vacuolatus* have been determined by Vogs et al. (2015) (**Chapter 3**) and were implemented in the TKTD model. Finally, a pharmacodynamic model for analyzing the anticancer drug effect on cancer cell growth was adapted and modified to describe the affected algae cell growth (Simeoni et al., 2004; Vogs et al., 2013) (**Chapter 2**). To this end, the internal concentration  $C_{\text{int}}(t)$  was linked to a three compartment model simplifying the progressive degrees of damage over time. Damage was initiated by a molecular chemical-target interaction in a first damage stage  $D_1(t)$  [fL], if the exposure concentration exceeded a certain no-effect concentration ( $NEC$  [ $\mu\text{mol L}^{-1}$ ]). Otherwise, the growth of algae remained unperturbed ( $C(t) < NEC$ ):

$$\frac{D_1(t)}{dt} = \begin{cases} V_{\text{Control}}(t) & \text{for } C(t) \leq NEC \\ V_{\text{Control}}(t) - (k_E \times C_{\text{int}}(t) \times D_1(t) - k_R \times D_1) & \text{for } C(t) > NEC \end{cases} \quad (4.4)$$

where  $k_I$  [ $\text{L}_{\text{Biovolume}} \mu\text{mol}^{-1} \text{h}^{-1}$ ] is the chemical injury rate and  $k_R$  [ $\text{h}^{-1}$ ] represents the repair/recovery rate. Damage was further assumed to be progressed across different levels of biological organization over time abstracted by an effect progression rate constant  $\tau$  [ $\text{h}^{-1}$ ]. The second and third compartments represented further progressive degrees of damage on higher effect response levels such as the physiological and phenotypical response level, respectively (Figure 4.1). This degree of damage in the second compartments were quantified as:

$$\frac{D_2(t)}{dt} = (k_E \times C_{\text{int}}(t) \times D_1(t) - k_R \times D_1(t)) - D_2(t) \times \tau \quad (4.5)$$

$$\frac{D_3(t)}{dt} = \tau \times (D_2(t) - D_3(t)) \quad (4.6)$$

The sum of each damage stage led to the overall damage  $D(t)$  which represents the affected dynamic of algae growth.

#### 4.2.4 Model calibration and parameter estimation

Parameter estimations and the simulation runs of toxicokinetic and toxicodynamic processes were generated in the software Mathematica (Version 8.0, Wolfram Research). For model calibration purposes, cell volume measurements from the first generation cycle were used in order to predict parameters describing either the unperturbed algae growth by the growth parameters  $\mu_E$ ,  $\mu_L$ , and  $\mu_C$  ( $K_{\text{Crit}}$  and  $\Psi$  were fixed) or the perturbed growth by the toxicodynamic process parameters  $k_I$ ,  $k_R$ ,  $\tau$ , and  $NEC$ . Reported kinetics of bioconcentration  $k_{\text{in}}$  and  $k_{\text{out}}$  served as model input parameters, for details see Vogs et al. (2015) (**Chapter 3**). A global set of the four toxicodynamic process parameters was estimated for each chemical treatment by minimizing the least-squares objective function using the genetic algorithm "Differential Evolution" (described in **Chapter 2**). The errors of residuum were assumed to be normally distributed with a mean of zero and an unknown standard deviation according to the maximum-likelihood theory. The 95% confidence intervals  $CI$  and coefficient of variation  $CoV$  [%] were quantified for the best-fit

parameter values. Measures of fit accuracy and variances were given by the root mean squared error  $RMSE$  [fL], the mean absolute error  $MAE$  [fL], and the coefficient of determination  $R^2$  [%].

## 4.3 RESULTS

### 4.3.1 Unperturbed algae growth

The goal was to study the effect on algae growth impacted by chemicals compared to the unperturbed algae growth. In a first step, we analyzed the pattern of unperturbed algae growth for two negative controls and two DMSO treated controls per experiment. The observed cell volume did not significantly differ between the negative and the DMSO treated control and all data were pooled into one control group per experiment (Figure C.1). Mean values of cell volume are shown in Figure C.1. The unperturbed growth model (Equation 4.2) fitted the pooled growth data well as indicated by a  $MAE < 21.63$  fL and  $R^2 > 99.23\%$ . The estimated growth rates for each experiment are listed in Table 4.1. Similar parameter values for the unperturbed growth kinetics were derived for all six experiments. Thus, inverse modeling led to the average rate constants for exponential growth  $\mu_E$  of  $0.235 \pm 0.016$  h<sup>-1</sup>, for the linear growth  $\mu_L$  of  $78.24 \pm 36.22$  fL h<sup>-1</sup> and for the limited growth  $\mu_C$  of  $0.015 \pm 0.005$  fL h<sup>-1</sup>, while at the same time the parameters  $K_{Crit}$  and  $\Psi$  were fixed to 80 fL and 20, respectively.

The mathematical simplification of cellular mechanisms of algae growth provided an interpretation tool, which was used to set-up the exposure regime. As previously supposed from the studies Altenburger et al. (2008) and Vogs et al. (2013) (**Chapter 2**), algae growth was slower in the exponential growth phase than in the linear growth phase according to the estimated kinetic rate constants. To overcome the initially slow exponential growth phase, chemical exposure started after normal algae growth of six ( $t_6$ ) or eight hours ( $t_8$ ). Then, the exponential growth switched into the linear growth without exceeding the critical cell size for cell cycle commitment after which cells are committed to division. By using this exposure design, we aimed to detect earliest and most sensitive responses of the chemical impact within the linear growth phase.

### 4.3.2 Perturbed algae growth pattern in dependence of exposure concentration and exposure time

Algae growth assays were performed for six concentrations per chemical to study the concentration-dependent response over time. Previous to the algae growth assay, six concentrations were chosen based on preliminary concentration range-finding experiments in order to elicit the same levels of effect on growth at  $t_{14}$  (inhibition level of 0%, 20%, 40%, 60%, 80% and 100%) for irgarol, isoproturon, triclosan, paraquat, PNA or reproduction at  $t_{24}$  for metazachlor. Concentration-response curves as a result of the preliminary concentration range-finding experiments are depicted in Figure 4.2 for all chemicals used. Metazachlor did not impact growth more than 50% in any algae growth experiment independent of whether the exposure started at  $t_0$  (data not shown) or at  $t_6$ . As a result of the preliminary concentration range-finding experiments, the same levels of effect on growth or reproduction were elicited by one order of magnitude higher exposure concentrations of chemicals with a lower hydrophobicity of  $\log K_{OW} < 3$  (isoproturon  $\log K_{OW} = 2.87$ , metazachlor  $\log K_{OW} = 2.13$ , paraquat  $\log K_{OW} = -2.71$ ) compared to the exposure concentrations of the chemicals with a moderate hydrophobicity of  $\log K_{OW} > 4$  (irgarol  $\log K_{OW} = 4.07$ , triclosan  $\log K_{OW} = 4.76$ , PNA  $\log K_{OW} = 4.47$ ) (Table C.7 and Table C.8).

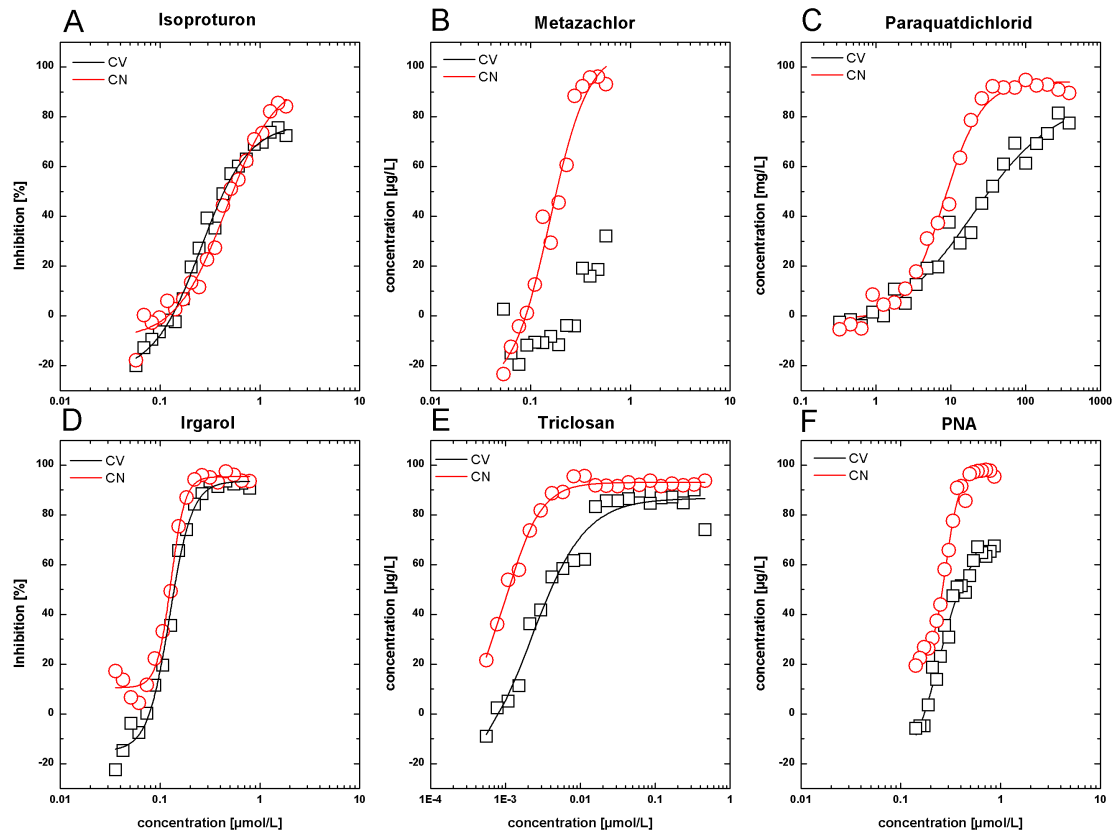


**Figure 4.2:** Inhibited cell volume measured at  $t_{14}$  (square) and cell number measured at  $t_{24}$  (circle) in dependency of various concentrations as result of the preliminary range-finding test for all chemicals (A–F). Exposure started at  $t_6$  or  $t_8$ . The four parametric log-logistic model was fitted to the concentration-depending responses on cell volume (black line) and cell number (red line). Please notice that minimum and maximum effect levels were estimated (Table C.7).

Although the exposure of six concentrations per chemical were assumed to elicit the same inhibition levels on algae growth at  $t_{14}$  as investigated by preliminary range-finding experiments (Figure 4.2), we observed different patterns of perturbed algae growth for the chemicals used (raw data C.1 – C.6, Figure 4.3). The use of two time-shifted algae cultures did not disturb the time-course of impacted growth as shown in Figure 4.3. Chemicals differently inhibited algae growth in a concentration and time-dependent relationship. Growth was affected for all six concentrations of irgarol and PNA, the five highest isoproturon and paraquat concentrations, the three highest triclosan concentrations and the highest metazachlor concentrations. Higher exposure concentrations generally disturbed the growth process faster than lower concentrations, as depicted in Figure 4.2. Compared with the unperturbed algae growth, effects on growth were approximately observed after exposure of (i) two hours for both photosystem II inhibitors, (ii) four hours for both reactive chemicals, (iii) six hours for triclosan, (iv) ten hours of the highest exposure concentration for metazachlor.

The adverse outcome on algae growth further led to effects on population growth (Figure C.3). We observed effects on reproduction in a concentration-dependent relationship at  $t_{24}$  for all chemicals used (Figure C.3). Median effect concentrations on reproduction  $EC_{50}$  ranged

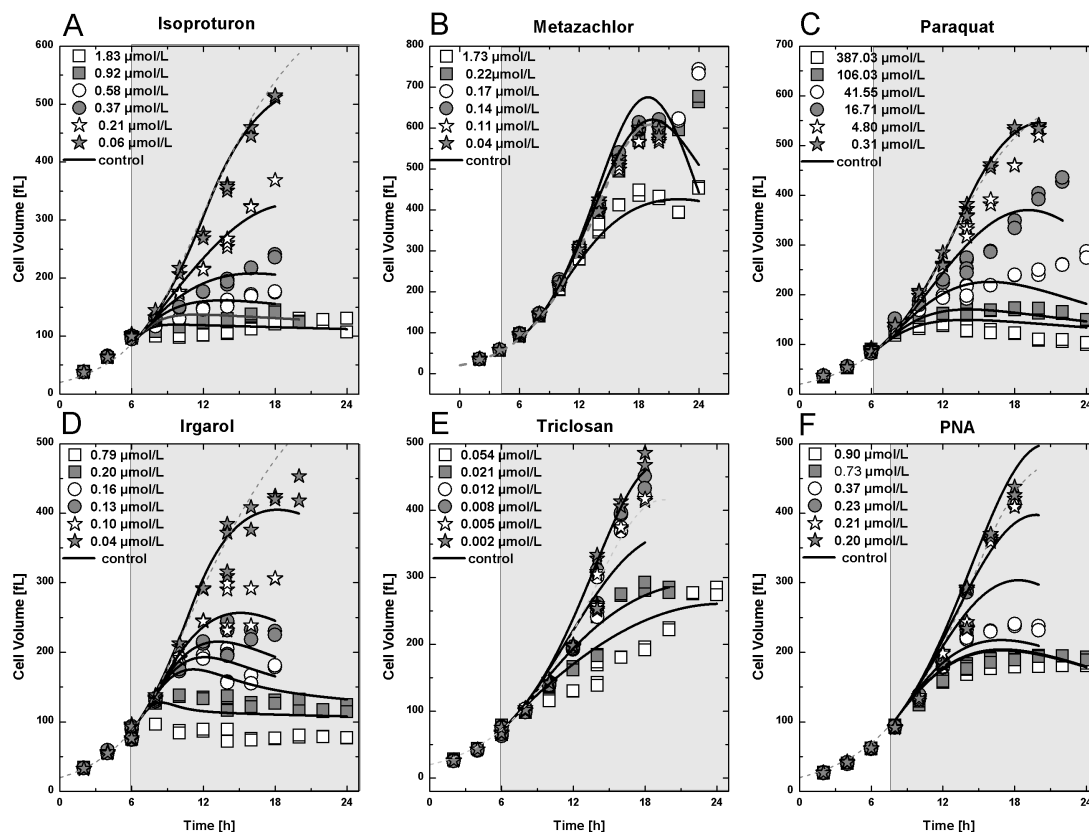


**Figure 4.3:** Measured cell volumes of the first-generation algae cycle at different time points affected by six different concentrations per chemical (symbols) and the respective simulated cell volumes described by the TKTD model (lines). Grey box represents the exposure time frame.

between  $0.0158 \mu\text{mol L}^{-1}$  for triclosan and  $7.24 \mu\text{mol L}^{-1}$  for paraquat at  $t_{24}$  (Table C.8). Exposure of triclosan, paraquat and PNA affected reproduction 2.55-fold, 4.12-fold and 2.21-fold more, respectively, than compared to the growth  $EC_{50}$  values at  $t_{14}$  (Table C.8). In contrast, exposure of isoprotruron was 0.69-fold less potent on reproduction  $t_{24}$  than compared to the growth  $EC_{50}$  value at  $t_{14}$  (Table C.8). Median effect concentration of irgarol inhibiting 50% reproduction was almost equal to the  $EC_{50}$  value of growth (Table C.8). Comparison with the cell division of the control group starting at  $t_{20}$ , a time-delayed cell division and a reduced number of daughter cells was observed for chemical exposed algae (Figure 4.3). By an increased exposure concentration, algae cells divided latter or did not divide during the measurement time frame as observed for the three highest concentrations of paraquat, the two highest concentrations of PNA and the highest concentration of irgarol, metazachlor, and triclosan.

### 4.3.3 Time dependence of toxicity

We aggregated the data of the observed growth pattern under chemical exposure for predicting the slope parameter ( $\theta$ ) and the median effect concentrations ( $EC_{50}$ ) of the concentration-response relationships over cumulative exposure time starting from  $t_6$  or  $t_8$  (Figure 4.4, Table C.8). Slope values generally increased over time except for triclosan (Table C.8). The increase of the slopes over the entire exposure time was smallest for paraquat (0.8-fold) and largest for isoprotruron

(22-fold). Moreover,  $\theta$  values were estimated to be higher than one except for irgarol at  $t_8$  and for paraquat between  $t_{10}$  and  $t_{18}$ . Median effect concentrations of each analyzed chemical decreased over exposure time except for metazachlor (Figure 4.4, Table C.8). The time-courses of median effect concentrations of algae growth differed considerably for the six chemicals used (e.g.,  $EC_{50}$  values of paraquat decreased from  $234.1 \mu\text{mol L}^{-1}$  to  $27.6 \mu\text{mol L}^{-1}$ , see Table C.8 for more details). The decrease of  $EC_{50}$  values over exposure time was smallest for isoprotruron (1.59-fold) and largest for paraquat (8.47-fold). Earliest responses of isoprotruron, irgarol and PNA exposure on growth were approximately detected for exposed algae cells after two hours and for triclosan and paraquat exposure after four hours. Steady state effect concentrations were reached at different time points between four hours and twelve hours in the following order: isoprotruron < PNA < paraquat. Steady state growth  $EC_{50}$  values were not reached for irgarol and triclosan within the time frame until  $t_{20}$  (Figure 4.4). The  $EC_{50}$  values of growth inhibition at  $t_{20}$  differed with the  $EC_{50}$  values for reproduction at  $t_{24}$  (Figure 4.4). Effects of triclosan, PNA and paraquat on reproduction at  $t_{24}$  were 3.12-fold, 1.36-fold and 3.82-fold higher, respectively, than the growth  $EC_{50}$  values at  $t_{20}$  (Figure 4.4, Table C.8). In contrast, the photosystem II inhibitors isoprotruron and irgarol were 0.66-fold and 0.54-fold less potent on reproduction at  $t_{24}$ , respectively, compared to the growth  $EC_{50}$  values at  $t_{20}$ .

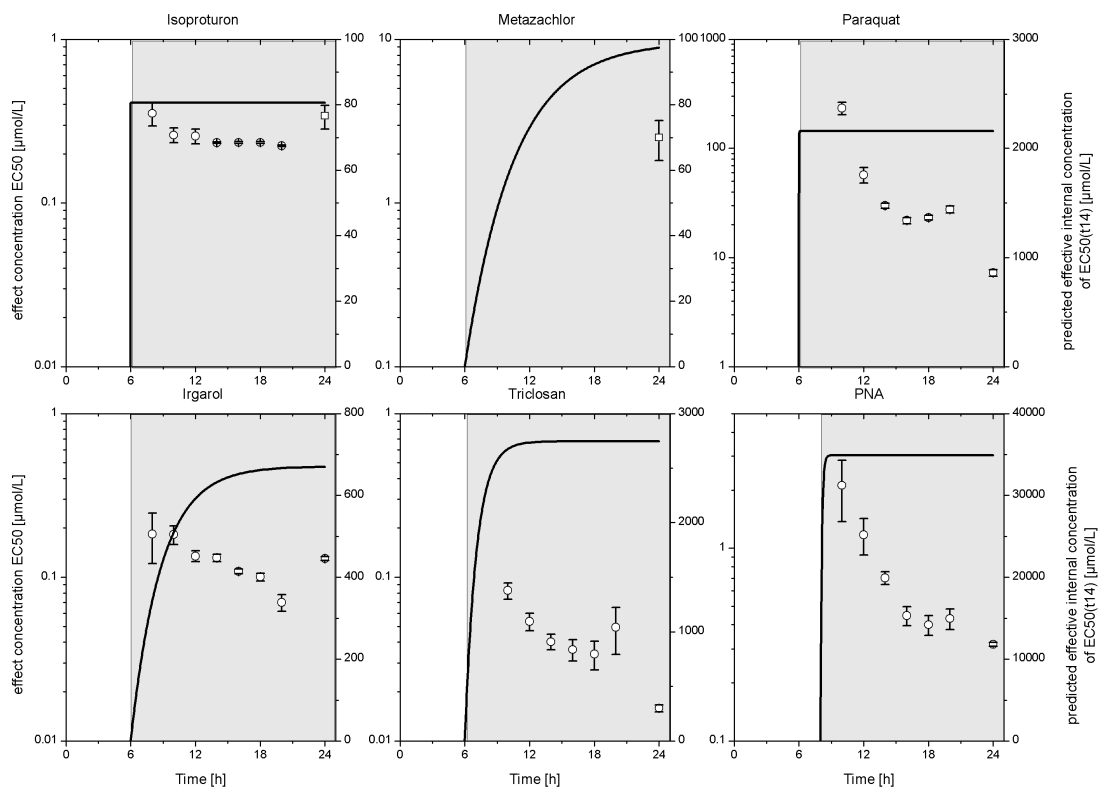


**Figure 4.4:** Effect concentrations  $EC_{50}$  ( $\pm$  standard error) describing affected algae growth over time ( $t_6$ – $t_{20}$ , circle symbol) and affected reproduction at  $t_{24}$  (square symbol) in comparison to the time-course of the estimated internal concentration  $IEC_{50}$  over time derived from  $EC_{50}(t_{14})$  values for the six model chemicals. Grey box represents the exposure time frame.

#### 4.3.4 Contribution of toxicokinetic processes to the toxicity development over time

The six exposure concentrations per chemical were linked to the adverse effect on algae growth via the predicted time-course of the internal concentrations. To this end, estimated kinetic parameters were implemented in the TKTD model that described bioconcentration kinetics of the six chemicals analyzed and discussed by Vogs et al. (2015) (**Chapter 3**). One simulation of the internal concentration over time was shown representative for each chemical in Figure 4.4 instead of depiction six simulations for each internal concentration curve. We assumed that the concentration-independent hydrophobicity-driven partitioning process resulted into equal time-courses but different accumulated concentrations in algae cells depending on the exposure concentration. Here, the median effect concentrations inhibiting 50% algae growth at  $t_{14}$  has been implemented in the one-compartment toxicokinetic model as one representative simulation that indicates the estimated internal concentrations over time for each chemical (Figure 4.4). The time point of steady state internal concentration was reached much faster than the stationary growth  $EC_{50}$  values. A time-gap of hours between the steady state of internal concentration and the continuous increase of toxicity was observed for all chemicals analyzed (Figure 4.4).

Furthermore, internal concentrations were estimated which inhibited growth at  $t_{14}$  and reproduction at  $t_{24}$  according to the effect measurements of this study (Table C.10). Internal concentrations inhibiting 50% of algae growth at  $t_{14}$  ranged from  $0.08 \text{ mmol kg}_{\text{wet weight}}^{-1}$  for isoproturon to  $34.91 \text{ mmol kg}_{\text{wet weight}}^{-1}$  for PNA (Figure 4.4, Table C.10). Reproduction was affected by the accumulated concentrations in the entire algae cells at  $t_{24}$  spanned from  $0.10 \text{ mmol kg}_{\text{wet weight}}^{-1}$  for metazachlor and  $15.75 \text{ mmol kg}_{\text{wet weight}}^{-1}$  for PNA (Table C.10). As calculated by the one-compartment toxicokinetic model, the internal concentrations inhibiting 50% of growth at  $t_{14}$  is higher than inhibiting reproduction at  $t_{24}$  for triclosan, paraquat, and PNA (Table C.10). Consequently, reproduction was affected by a 0.45- to 4.15-fold lower number of triclosan, paraquat, and PNA molecules than growth that elicit the same level of effect. By contrast, an equal number of irgarol molecules or 1.5-fold more isoproturon molecules caused the same level of adversity on growth and reproduction (Table C.10).

#### 4.3.5 Toxicokinetic-toxicodynamic modeling

The TKTD model fitted the pattern of disturbed algae growth well ( $R^2 \geq 98\%$ ) for all fits; see Figure 4.3. The residues between measurements and fit became slightly larger with higher cell volumes for all simulations (Figure 4.3). In some cases, the measured cell volume was still increasing at the end of one generation cycle, whereas the fit slowly decreased (Figure 4.3). A mean absolute error (MAE) value of 37.8 fL signified lowest accuracy for triclosan compared to the simulations for the other chemicals (Table 4.1). The greatest variance in the individual errors of fit was also denoted for triclosan, because of a 35.1% lower MEA value compared to the root mean squared error (RMSE) value (Table 4.1). In contrast, the fit for isoproturon affected growth pattern was characterized by the MAE value of 15.45 fL which was 17.7% lower than the RMSE (Table 4.1). That indicates lowest variance in the individual errors compared with all fits. The degrees of freedom ranged between 94 and 136 (Table 4.1). One global toxicodynamic parameter set (no-effect concentration, chemical injury rate constant, repair/recovery rate constant, effect progression rate constant) per chemical was estimated with reasonable precision, because most coefficient of variation values (CoV) were lower than 30% (Table C.9). At the same time, parameters of unperturbed algae growth and bioconcentration kinetics were fixed to the values listed in Table 4.1. Chemical injury rate constants spanned over one order of magnitude

**Table 4.1:** Estimated parameters and their 95% confidence interval to characterize unperturbed algae growth, toxicokinetic and toxicodynamic parameters as well as as goodness-of-fit indicators

	common name	isoprotruron	metazachlor	paraquat	
unperturbed algae growth	exponential growth rate	$\mu_E$ [h <sup>-1</sup> ]	0.246 ± 0.003	0.246 ± 0.002	0.235 ± 0.001
	linear growth rate	$\mu_L$ [FL h <sup>-1</sup> ]	55.47 ± 4.74	146.20 ± 162.67	62.95 ± 48.57
	cell-clock rate	$\mu_C$ [FL h <sup>-1</sup> ]	0.009 ± 0.002	0.020 ± 0.001	0.013 ± 0.001
toxicokinetic process	uptake rate	$k_{in}$ [1 × 10 <sup>3</sup> h <sup>-1</sup> ]	639.7 ± 1644.4 × 10 <sup>5</sup>	0.21 ± 0.01	9.67 ± 4.36 × 10 <sup>5</sup>
	overall elimination rate	$k_{out}$ [h <sup>-1</sup> ]	1852.70 ± 4.76 × 10 <sup>8</sup>	0.22 ± 0.04	133.81 ± 4.36 × 10 <sup>5</sup>
	injury rate	$k_I$ [1 × 10 <sup>3</sup> L <sub>Biov</sub> μmol <sup>-1</sup> h <sup>-1</sup> ]	2.97 ± 0.22	0.33 ± 0.11	0.15 ± 0.04
toxicodynamic process	repair/recovery rate	$k_R$ [h <sup>-1</sup> ]	0 ± 0.01	0 ± 0.01	8.88 × 10 <sup>-5</sup> ± 0.03
	effect progression rate	$\tau$ [h <sup>-1</sup> ]	2.22 ± 0.25	5.46 × 10 <sup>-6</sup> ± 0.18	0.52 ± 0.09
	no-effect concentration	NEC [μmol L <sup>-1</sup> ]	0 ± 0	0.19 ± 0	3.62 ± 0
goodness-of-fit	mean absolute error	MAE [FL]	15.45	37.76	24.59
	root mean square error	RMSE [FL]	19.53	58.17	35.36
	akaike information criterion	AIC [-]	976.05	1391.56	1286.00
	coefficient of determination	R <sup>2</sup> [-]	0.99	0.98	0.98
	degrees of freedom	df [-]	106	136	124
	common name	irgarol	trichosan	PNA	
unperturbed algae growth	exponential growth rate	$\mu_E$ [h <sup>-1</sup> ]	0.25 ± 0.006	0.22 ± 0.01	0.21 ± 0.01
	linear growth	$\mu_L$ [FL h <sup>-1</sup> ]	44.54 ± 5.15	84.93 ± 168.38	75.35 ± 79.01
	cell-clock rate	$\mu_C$ [FL h <sup>-1</sup> ]	0.01 ± 0.003	0.02 ± 0.004	0.02 ± 0.01
toxicokinetic process	uptake rate	$k_{in}$ [1 × 10 <sup>3</sup> h <sup>-1</sup> ]	1.83 ± 0.01	62.75 ± 2.32	415.69 ± 91.29
	overall elimination rate	$k_{out}$ [h <sup>-1</sup> ]	0.36 ± 0.05	0.92 ± 0.08	8.36 ± 2.34
	injury rate	$k_I$ [1 × 10 <sup>3</sup> L <sub>Biov</sub> μmol <sup>-1</sup> h <sup>-1</sup> ]	0.73 ± 0.07	0.68 ± 0.13	0.18 ± 0.02
toxicodynamic process	repair/recovery rate	$k_R$ [h <sup>-1</sup> ]	0.03 ± 0.02	0.38 ± 0.08	1.77 ± 0.15
	effect progression rate	$\tau$ [h <sup>-1</sup> ]	2.50 ± 0.18	2.50 × 10 <sup>-5</sup> ± 0.08	0.32 ± 0.05
	no-effect concentration	NEC [μmol L <sup>-1</sup> ]	0.01 ± 0	0.01 ± 0	0.13 ± 0
goodness-of-fit	mean absolute error	MAE [FL]	20.38	24.11	22.12
	root mean square error	RMSE [FL]	24.77	30.33	30.00
	akaike information criterion	AIC [-]	1102.33	1072.87	954.77
log K <sub>OW</sub> > 4	coefficient of determination	R <sup>2</sup> [-]	0.98	0.98	0.98
	degrees of freedom	df [-]	114	106	94

between  $0.153 \times 10^{-3} \text{ L}_{\text{Biovolume}} \mu\text{mol}^{-1} \text{ h}^{-1}$  and  $2.97 \times 10^{-3} \text{ L}_{\text{Biovolume}} \mu\text{mol}^{-1} \text{ h}^{-1}$  and decreased in the following order: paraquat < PNA < metazachlor < triclosan < irgarol < isoproturon. Repair/recovery rate constants spanned between  $0. \text{ h}^{-1}$  and  $1.77 \text{ h}^{-1}$  and followed the order isoproturon = metazachlor < paraquat < irgarol < triclosan < PNA. Values of  $k_R$  were thus lower for the chemical group with low hydrophobicity of  $\log K_{\text{OW}} < 3$  compared with the chemical group with moderate hydrophobicity of  $\log K_{\text{OW}} > 4$ . Moreover, estimated *NEC* values were higher than zero for all chemicals analyzed except for isoproturon. According to the respective *NEC* values, the lowest exposure concentration used for irgarol and paraquat, the three lowest exposure concentrations used for triclosan and the four lowest exposure concentrations used for metazachlor did not affect algae growth at any exposure time. All exposure concentrations of isoproturon and PNA exceeded the estimated *NEC* values. Effect progression rate constants spanned over six orders of magnitude in the following order  $\tau_{\text{irgarol}} \approx \tau_{\text{isoproturon}} > \tau_{\text{paraquat}} \approx \tau_{\text{PNA}} > \tau_{\text{triclosan}} > \tau_{\text{metazachlor}}$  and ranging from  $2.50 \text{ h}^{-1}$  and  $5.45 \times 10^{-6} \text{ h}^{-1}$ . Thus, the estimated  $\tau$  values for the chemicals affecting algae growth through similar types of AOPs were in the same order of magnitude and independent of the chemical' hydrophobicity: inhibitors of photosystem II > biological reactivity > inhibitors of lipid biosynthesis.

## 4.4 DISCUSSION

### 4.4.1 Data quality assessment

In the present study, we investigated the impact of specifically acting and reactive chemicals on algae growth by examining toxicokinetic and toxicodynamic processes over time. The effect estimations based on the algae growth responses were likely less robust than the traditionally determined  $EC_{50}$  values based on a series of concentrations spanning an entire response range. The growth  $EC_{50}$  values at  $t_{14}$  and reproduction  $EC_{50}$  values at  $t_{24}$  based on the algae growth assay corresponded to  $EC_{50}$  values at  $t_{14}$  and at  $t_{24}$  based on the preliminary range-finding experiments, respectively, except for triclosan (Table C.10). The averaged relative variance of  $37.68 \pm 48.28\%$  for the entire data pool was indicated to be very high. In particular, effect estimations derived from preliminary concentration range-finding experiments for triclosan were 15 to 18-fold lower than the effect indicators based on the algae growth bioassay. The high differences could be not explained by measurements or estimations error. However, the estimated values based on a series of concentrations spanning an entire response range seem to be more reasonable, because the measurements are more similar to the literature reported values for triclosan (Table C.10). By contrast,  $EC_{50}$  values of the photosystem II inhibitors were nearly equal between the preliminary range-finding experiments and the algae growth assay. The maximized effect difference was indicated for paraquat, because the growth  $EC_{50}$  value measured by the preliminary concentration-range finding was 0.65-fold higher than the  $EC_{50}$  value of the algae growth assay at  $t_{14}$  (Table C.10). That measurement variance of the maximized effect difference for paraquat is even 2.5-fold smaller than the smallest change of growth  $EC_{50}$  values over time determined for isoproturon.  $EC_{50}$  values of isoproturon decreased 1.59-fold over exposure time. Further support for characterizing robustness and quality of the measurements is given by measuring the algae growth responses over time. The time-courses of the estimated  $EC_{50}$  values followed a systematic trend as observed for all chemicals and were thus assumed to be not dominated by technical

or biological variance. Further technical and biological variance was evaluated to be marginal between the independent measurements of unperturbed algae growth over time for two untreated and two DMSO-treated samples per experiment. The mathematical model was suitable to describe unperturbed growth of unicellular organisms and growth kinetic rates, and to estimate parameters of growth kinetics corresponded to values reported from literature (Altenburger et al., 2008; Vogs et al., 2013) (**Chapter 2**). A 95% confidence interval of estimated growth kinetic parameters were one order of magnitude lower than mean values that indicated high parameter certainty (Table 4.1). However, linear growth rate constant was less robust compared to the exponential and limited growth kinetic parameters, because the linear growth rate constant varied between the independent experiments for each algae growth assay conducted per chemical (Table 4.1). To conclude, the measured  $EC_{50}$  values constituted high data quality and were robust.

In comparison to the literature-reported effect concentrations based on traditionally determined growth and reproduction responses of *S. vacuolatus*, chemicals were added to the algae cell suspension at  $t_6$  or  $t_8$  in this study. Thus, reproduction  $EC_{50}$  values at  $t_{24}$  determined in this study were between two- to nearly ten-fold higher than reported reproduction  $EC_{50}$  values at  $t_{24}$  (Table C.10). Here, Haber's rule may give an explanation for the differences between the observed and the literature-reported efficacy (Haber, 1924). According to Haber's rule, the time integral of the exposure concentration is equivalent to the produced effect (Rozman and Doull, 2000). That means that the exposure time needs to be prolonged in this study in order to achieve effect concentrations in reproduction comparable to the reported  $EC_{50}$  values at  $t_{24}$  reported in literature. The empirical model directly link exposure concentration and effect without considering toxicokinetic and toxicodynamic processes (Ashauer et al., 2007b). To this end, toxicokinetic and toxicodynamic processes to the overall effect on algae growth over time has been overlooked.

#### 4.4.2 Time dependence of median effect concentrations

The time-course of growth  $EC_{50}$  values integrates information on kinetics of bioconcentration as well as on the intrinsic toxicity (Escher and Hermens, 2002). In this study,  $EC_{50}$  values of algae growth decreased over time for all chemicals analyzed, except for metazachlor, before steady state of effect were reached (Figure 4.4). Böger et al. (2000) investigated that metazachlor affects the elongation of very-long-chain fatty acids (C20, C22, and C24) which are required for division processes in algae cells (Nobusaws and Umeda, 2012). Thus, rather cell division at  $t_{24}$  was specifically inhibited in a concentration-dependent relationship by metazachlor than algae growth over time. The observed time-courses of the effect on growth is consistent with other studies on algae toxicity that reported an increase in toxicity over time for algae photosynthesis activity exposed to triclosan and for algae growth exposed to norflurazon, triclosan and PNA (Altenburger et al., 2006; Franz et al., 2008; Vogs et al., 2013) (**Chapter 2**). Thereby, the increase of toxicity was likely not driven by toxicokinetic processes, because steady state concentrations in algae cells were reached within minutes due to hydrophobicity-driven partitioning process, as illustrated in Figure 4.4 (Vogs et al., 2015) (**Chapter 3**). Influential processes like the ionization of the chemical, ion trapping mechanism or the potential susceptibility for biotransformation alter hydrophobicity-driven partitioning process that prolong the time-course of internal concentrations (Vogs et al., 2015) (**Chapter 3**). However, the toxicokinetic processes resulting into the internal exposure changes over time in the algae cells did not explain the time-course of toxicity for specifically acting and reactive chemicals solely, as depicted in Figure 4.4. Rather, another rate-limiting step seems to cause the toxicity increase over hours in algae cells observed for all chemicals except for metazachlor (Figure 4.4). A rate-limiting step supposedly accounts for the

toxicodynamic processes according to pharmacological indirect response models that generalize the effect to be progressed across various biological level (Jusko et al., 1995; Jusko, 2013; Mager et al., 2003; Mager and Jusko, 2008; Simeoni et al., 2004). Effect progression is here defined as a chain of events starting from an initiating molecular chemical-target interaction, followed by key events on different biological levels of organization which led to an adverse outcome on growth and reproduction (Ankley et al., 2010). This is not a common finding, because time-dependent toxicity has been interpreted to be mainly driven by physicochemical and physiological factors like the hydrophobicity of the chemical, organism size, mechanism of action, mode of action and exposure pathway (Ashauer et al., 2007b; Escher and Hermens, 2002).

McCarty and Mackay (1993) firstly reported that responses over time of narcotic acting chemicals follow the kinetics of bioconcentration driven by hydrophobicity-dependent partitioning processes and reversible mechanism between baseline toxicants and the membrane. Internal concentrations of narcotic acting chemicals at steady state conditions have been reported to vary between 2–8 mmol kg<sub>wet weight</sub><sup>-1</sup> which is defined as the critical body burden. On the contrary, the time course of toxicity is likely related to the critical area under the curve of reactive chemicals and the critical target occupation of specifically activating chemicals due to the chemical's irreversible interaction with the biological target site (Legierse et al., 1999; Verhaar et al., 1999). Hence, toxicity over time is triggered by a certain time integral of the internal concentration which characterized the time-course of guppy mortality exposed to benzylic chemicals (Verhaar et al., 1999). Similarly, this has also been shown for guppy and pond snail mortality exposed to organophosphates (Legierse et al., 1999). For harmonizing different types of chemical interaction mechanisms with the biological target biomolecules, Lee et al. (2002a) introduced a rate-limiting toxicodynamic process by including damage injury and damage repair/recovery into the effect models. By incorporating the damage as dose surrogate into a TKTD modeling framework, the temporal patterns of survival probabilities of *Gammarus pulex* after sequential pulsed exposure to carbaryl could be explained by a slow elimination processes (Ashauer et al., 2007c). In the case of the sequential pulsed exposure of chlorpyrifos, the temporal patterns of survival probabilities was driven by a slow recovery process (Ashauer et al., 2007c). Subsequent research suggested that, on the one hand, the time course of survival can be directly linked to body residues, if the elimination process is much slower than the repair process (Jager et al., 2011). On the other hand, the time course of survival can be used to simulate the scaled internal concentration without differentiating of elimination and repair as the time-limiting steps, if measurements of internal concentrations over time do not exist (Ashauer et al., 2013). To conclude from the previously cited studies, time-dependent toxicity in organism has mainly been characterized by changes of internal exposure and the interaction mechanism of the chemical with the biological target site. However, the contribution of toxicodynamic processes on cumulative damage has been rarely analyzed without the influence of internal exposure alterations and interaction kinetics. In contrast, responses on algae growth over time are mainly time-limited by toxicodynamic processes with minimized bias of internal exposure changes as highlighted by the results of this study.

#### 4.4.3 Toxicokinetic-toxicodynamic modeling framework

We hypothesized that the algae system may provide a promising biological tool to study the progress of the effect across multiple key events of biological responses toward the adverse outcome on growth and reproduction. To this end, the TKTD model was calibrated to the perturbed growth pattern of exposed algae cells for characterizing the observed time lags between maximum internal effect concentrations and the time course of cumulative damages in

a quantitative manner. A key element in effect modeling is the distinction between parameters explaining chemical-specific properties and biological system-specific properties (Danhof et al., 2007, 2008). The experimental design in this study enabled that the impact of different chemical hydrophobicities as well as different modes of toxic action on cumulative damage was discriminate by a two-step approach. First, the time-limiting step of toxicodynamic processes was analyzed in dependence of various time-courses of the internal concentration resulted by hydrophobicity-driven partitioning processes. Thus, the uncertainty on parameter prediction was potentially reduced in order to increase the interpretation power of process-based toxicodynamic parameters. In a second step, we analyzed whether toxicodynamic processes in algae cells may be rate-specific for different adverse outcome pathways.

#### 4.4.4 Estimated no-effect concentration

The estimated *NEC* parameter of the algae TKTD model represents a threshold concentration below which no effect on algae growth was measured. Estimated *NEC* values ranged from  $0 \mu\text{mol L}^{-1}$  to  $3.62 \mu\text{mol L}^{-1}$  in the following order: isoproturon < irgarol  $\approx$  triclosan < PNA < metazachlor < paraquat. That result indicates that a lower number of molecules of photosystem II inhibitors and triclosan need to be bioavailable in the exposure media than PNA, metazachlor and paraquat molecules in order to produce any observable adverse outcome on growth. However, The *NEC* value is related to the exposure concentration in the ambient medium and disregards the differences in toxicokinetic processes as has been suggested by the body residue approach (Meador et al., 2008).

The critical threshold value for PNA causing an adverse outcome on algae growth was 1.75-fold lower than the reported threshold value of  $0.228 \mu\text{mol L}^{-1}$  PNA exposure that caused a response on the algae metabolome level (Sans-Piché et al., 2010). By anchoring concentration-changes of metabolomics to effects on photosynthesis and growth of *S. vacuolatus* under PNA exposure, Sans-Piché et al. (2010) could distinguish pharmacological effects on the metabolism level ( $0.00713 \mu\text{mol L}^{-1}$ –  $0.228 \mu\text{mol L}^{-1}$ ) from toxic effects on the phenotypic level ( $0.45 \mu\text{mol L}^{-1}$ –  $1.82 \mu\text{mol L}^{-1}$ ). Moreover, the *NEC* value for metazachlor has been estimated to be 19-fold higher than the no-observed effect concentration (*NOEC*) of  $0.0551 \mu\text{mol L}^{-1}$  statistically determined from concentration-dependent reproduction responses (Junghans et al., 2003). Furthermore, Jamers and De Coen (2010) reported a statistical diagnosed *NOEC* value for paraquat of  $0.1 \mu\text{mol L}^{-1}$  based on concentration-dependent effects on *C. reinhardtii* growth at  $t_{72}$  that is 36.2-fold lower compared to the estimated *NEC* value in this study. Threshold values might be highly variable depending on the exposure time and concentrations, the endpoint, or the estimation method. Nevertheless, the application of a higher *NEC* value in risk assessment approaches was considered to be more conservative due to the ability to incorporate uncertainties into the likelihood estimation of effects on non-target organisms in the environment.

#### 4.4.5 Estimated injury rate constant and repair/recovery rate constant

Specifically acting and reactive chemicals interact with the biological target sites such as membranes, proteins, transporters or macromolecules by different mechanisms of toxic action. The injury rate constant  $k_I$  characterizes the intrinsic activity to produce an effect normalized to a

concentration at the target site. In this study, the average injury rate constant was determined to be  $0.84 \times 10^{-3} \pm 0.98 \times 10^{-3} \text{ L}_{\text{Biovolume}} \mu\text{mol}^{-1} \text{ h}^{-1}$  that is two-fold higher than the average injury rate constant of  $0.40 \times 10^{-3} \pm 0.51 \times 10^{-3} \text{ mL ng}^{-1} \text{ d}^{-1}$  determined for cancer growth kinetics after drug administration in tumor-bearing mice (Simeoni et al., 2004; Magni et al., 2006). Nevertheless, average injury rate constants and the standard deviation were within the same range of magnitude. That finding is in contrast to our first study that introduced the algae TKTD model (Vogs et al., 2013) (**Chapter 2**). Vogs et al. (2013) (**Chapter 2**) reported that  $k_I$  values ranged six orders of magnitude for three chemicals analyzed (triclosan, PNA, norflurazon) that indicated a higher standard deviation compared with the standard deviation of one order of magnitude estimated in this study. One reason for the reduced data variability in this study likely relies in a more accurate and certain estimation of the internal concentration time-course of the chemicals. Chemical injury rate constants increased in the following order: reactive chemicals < lipid biosynthesis inhibitors < photosystem II inhibitors. A lower chemical injury rate constant might signify an unspecific mechanism with lower intrinsic affinity causing an effect as it would be reasonable in the cases for paraquat and PNA (Altenburger et al., 2006; Faust et al., 2003). By contrast, the high injury rate constants of irgarol and isotroturon potentially reflect the specific mechanism of the photosystem II inhibitors at the QB binding site of the D1 protein (Hock et al., 1995).

The repair/recovery rate constant characterizes the degree of reversibility at the target site by taking into account repair mechanisms and *de novo* synthesis of receptors (Ashauer and Brown, 2008). In the present study, an average  $k_R$  value of  $0.36 \pm 0.64 \text{ h}^{-1}$  was determined for all chemicals analyzed that was 1.9-fold higher than the average estimated rate reported from a previous study (Vogs et al., 2013) (**Chapter 2**). The high deviation of the repair/recovery rate constant is likely related to the potential correlation with the chemical's hydrophobicity. It has to be noted that  $k_I$  values were either larger than the  $k_R$  values for the chemical group with hydrophobicity of  $\log K_{\text{OW}} < 3$  or the  $k_I$  values were smaller than the  $k_R$  values for the chemical group with hydrophobicity of  $\log K_{\text{OW}} > 4$ . Thus, the estimated  $k_I$  and  $k_R$  values potentially correlated with the accumulated amount of chemicals in the entire organism  $C_{\text{int}}(t)$ . Chemicals with  $\log K_{\text{OW}} < 3$  accumulated less in organism than chemicals with  $\log K_{\text{OW}} > 4$  according to the estimated internal concentrations (Table 4.1). However, repair/recovery processes represent biological-specific processes for which chemical hydrophobicity is likely a wrong descriptor. Instead, repair/recovery processes might depend on biological-related parameters like the reversibility degree of the chemical to the target site, the *de novel* synthesis of target sites or other detoxification mechanisms (Escher and Hermens, 2002).

The estimated parameters  $k_I$  and  $k_R$  need to be interpreted carefully, although the variance of the parameter values between the samples was low and the coefficient of variance was mostly smaller than 30% (Table C.9). The TKTD model does not depict the more complicated mechanism of chemical-target interaction involving dynamics of receptor binding, aging processes or types of interaction. To adequately estimate  $k_I$  and  $k_R$  for characterizing the intrinsic affinity to produce an effect, *in vitro* assays representing the specific target sites could be used in addition to *in vivo* bioassays (Escher et al., 2011). Furthermore, information on target sites, target densities and types of interaction would improve the understanding of the mechanisms of action. However, there is still a lack of information on the various mechanisms of toxic action for chemical-target interactions. Alternatively, pulsed exposure experiments could provide indication of the intrinsic affinity as well as recovery/repair mechanism as shown by modeling the effects caused by sequential exposure of carbaryl, diazinon and chlorpyrifos on *Gammarus pulex* (Ashauer et al., 2007a, 2010).

#### 4.4.6 Estimated effect progression rate constants for different adverse outcome pathway

Chemical-target interaction may provoke a reaction which blocks or triggers an array of molecular and biochemical events progressed toward an adverse outcome on the physiological level (Danhof et al., 2007; Mager et al., 2003). In the present study, effect progression has been generalized by implementing three compartments into the TKTD model as proposed by Simeoni et al. (2004). Effect progression rate constants  $\tau$  were supposed to vary between different types of AOPs (Danhof et al., 2007; Jusko, 2013). In general, the progress of an effect has been discussed to operate with either rate constants on the order of milliseconds to seconds indicating a time-independent transduction function, or with rate constants on the order of hours to days being suggestive of a time-dependent transduction function (Danhof et al., 2007; Jusko, 2013). Toxicodynamic processes determine the time-course of effect in the case of time-dependent transduction functions. Then, effect progression *in vivo* is slow and the affected turnover processes in physiology are not rate-limiting as in the case of the observations in the present study (Danhof et al., 2008; Jusko, 2013). The observed time lags between steady state internal concentrations in algae cells and the ongoing effect toward the adverse outcome on algae growth were quantified by the effect progression rates spanning from  $2.5 \text{ h}^{-1}$  to  $5.46 \times 10^{-6} \text{ h}^{-1}$  in the following order  $\tau_{\text{irgarol}} \approx \tau_{\text{isoproturon}} > \tau_{\text{paraquat}} \approx \tau_{\text{PNA}} > \tau_{\text{triclosan}} > \tau_{\text{metazachlor}}$ . For the purpose of comparison, an average effect progression rate of  $0.025 \pm 0.016 \text{ h}^{-1}$  was reported from pharmacological studies on the effect of drug administration on tumor growth dynamics (Simeoni et al., 2004; Magni et al., 2006). That reported value is one to two orders of magnitude smaller than the estimated  $\tau$  values for photosystem II inhibitors and reactive chemicals, but three to four orders of magnitude larger than the  $\tau$  values for lipid synthesis inhibitors. Thus, the deviation of effect progression rate constants estimated for different drugs was relative constant (as indicated by a small standard deviation of  $0.016 \text{ h}^{-1}$ ) compared to the high data variability of estimated  $\tau$  values in this study. A reason might be that the turnover process of cancer growth measured as tumor weight over days in the studies of Simeoni et al. (2004); Magni et al. (2006) is a rate-limiting process that overlap the progress of effect. Furthermore, differences of effect progression rates between this study and the reported results of a previous study (Vogs et al., 2013) (**Chapter 2**) might be caused by uncertainty of toxicokinetic processes and the modification of the exposure time frame. In comparison with Vogs et al. (2013) (**Chapter 2**), we estimated a 40.72-fold higher  $\tau$  value for triclosan and a 5.44-fold lower  $\tau$  value for PNA in the present study. Estimated parameter values are therefore assumed to be sensitive toward an unknown time-course of the internal concentration eliciting an effect as in the case of triclosan. As indicated in the case of PNA, the time frame of exposure might as well be relevant especially for developing organisms with variable turn-over rates of physiology processes over the life-cycle. For instance, PNA exposure on algae autospores at  $t_0$  led to the development of two subpopulations of variable sensitivities on algae growth (Vogs et al., 2013) (**Chapter 2**). In contrast, a time-delayed PNA exposure used in this study starting in the linear growth phase did not differently affect algae growth.

A sensitivity analysis of the effect progression rate showed that a decrease of the toxicodynamic parameter value correlates to a prolonged time-delay and a reduced peak high of toxicodynamic responses within each compartment (Sun and Jusko, 1998). The time to progress an effect from the initiating event of chemical-target interaction to the adverse outcome on algae growth is therefore indicated to be fastest for photosystem II inhibitors and slowest for lipid synthesis inhibitors. Although  $\tau$  was estimated to range over six orders of magnitude for all chemicals used, effect progression rates were similar within the three groups of AOPs and

independent between the two hydrophobicity groups. This finding is supported by a previous study which reported that photosynthetic fluorescence quenching for atrazine was completely inhibited within 10 min of  $0.464 \mu\text{mol L}^{-1}$  atrazine exposure on  $t_{14}$  cells of *S. vacuolatus* (Altenburger et al., 2006). In contrast to the immediate response of photosystem II inhibitor, a time-lag for the inhibition of photosynthetic fluorescence quenching has been observed for *S. vacuolatus* ( $t_{14}$ ) exposed to  $1.46 \mu\text{mol L}^{-1}$  and  $0.73 \mu\text{mol L}^{-1}$  PNA until 100 min (Altenburger et al., 2006). Based on the results of this study, constants of effect progression rate indicated different time durations to progress an effect which were initiated from a molecular interaction with chemical molecules, followed by key events on different biological levels toward an adverse outcome on algae growth. Hence, effect progression rate constants might be related to the specific alteration of the central metabolisms by photosystem II inhibitors, the unspecific alteration of the central metabolisms by reactive chemicals and the specific perturbation on cell wall and lipid metabolisms.

## 4.5 CONCLUDING REMARKS & OUTLOOK

The present study provides a joint approach between experimentation and mathematical modeling for the systematic investigation of the impact of toxicokinetic and toxicodynamic processes toward the adverse outcome on growth through key toxicity pathways in *S. vacuolatus*. A previous study showed that the time of internal steady-state concentrations in *S. vacuolatus* was reached within minutes due to hydrophobicity-driven partitioning processes. Steady state concentrations were reached later when hydrophobicity-driven partitioning processes might be altered by other processes like biotransformation or ion-trapping (Vogs et al., 2015) (**Chapter 3**). However, toxicity continued to increase over hours until equilibrium of effect concentrations was reached. The time-course of cumulative damage on *S. vacuolatus* growth was thus not explainable by the change of the internal concentrations solely, but was rather dominated by a rate-limiting toxicodynamic processes. This simple unicellular system could consequently provide a useful tool for investigating key events on different biological levels which are independent from changes of internal concentrations. Dynamics of toxicogenomic responses like gene transcript, protein expressions or metabolic responses might therefore be characterized by effects to chemicals only and not due to changes of internal exposure (Forbes et al., 2006). That may provide the bases for the mechanistic linkage of molecular responses to the adverse outcome on different levels of biological organization such as physiological or phenotypical changes. Just recently, researchers causally linked toxicity and adaptive responses across the transcriptome, proteome, and phenotype of *Chlamydomonas reinhardtii* exposed to different concentrations of silver and thus provided detailed insights of the perturbations of the cells functional networks related to the time-dependent internal silver concentrations (Pillai et al., 2014). Additional, the progression of dose-dependent responses across molecular, cellular, and phenotypical levels in effect modeling would improve the capability to identify and estimate inaccessible system variables (Mager et al., 2003) as well as the ability to assess and predict likely impacts on organism and population for realistic multiple exposures prospectively (Forbes and Calow, 2012).

It was indicated in this study that the rate-limiting step of toxicodynamic processes differed between the analyzed AOPs as quantified by the effect progression rates. The rate of effect progression ranged between six orders of magnitude for all chemicals analyzed. The effect progression rate was highest for the photosystem II inhibitors isoproturon and irgarol, followed by the reactive chemicals paraquat and PNA and the lipid biosynthesis inhibitors metazachlor and triclosan. At the same time, variability of  $\tau$  within the chemicals of similar types of AOP

was less than one order of magnitude. This result denoted that the progression of an effect from the molecular initiating event over changes of biochemical responses and physiological dynamics toward the adverse outcome on growth may be specified for various AOPs that bases on the dose- and time-depended impact of a chemical on growth. Complementary to the investigations of effects on different levels of biological organization, toxicokinetic and toxicodynamic relevant processes might explain the system as a whole how the parts behave according to the holistic approach (Garcia-Reyero and Perkins, 2011). Thus, process parameters aggregate the function of an effect that is progressed toward an adverse outcome on the organism level. This holistic approach offers the scope for the characterization of AOPs as well as for the discrimination of chemicals.

# CHAPTER 5

## Synthesis

Organisms in the aquatic environment are exposed to sequential pulses of a numerous number of structurally diverse chemicals (Handy, 1994; Kolpin et al., 2002; Reinert et al., 2002; Schwarzenbach et al., 2010). Furthermore, aquatic organisms are likely exposed to complex mixtures of chemicals in the environment (Altenburger et al., 2015; Brack et al., 2015). Nevertheless, currently environmental risk assessment bases on standard toxicity tests of ecotoxicological model organisms that are continuously exposed to individual chemicals for a predefined duration. Predictive effect models are recommended to be one powerful tool for addressing the challenges toward a 21st century risk assessment of environmental exposure (Forbes and Calow, 2012; Villeneuve and Garcia-Reyero, 2011). The application of effect models, especially which describe toxicokinetic and toxicodynamic processes, has been discussed for their ability to compare and extrapolate the adverse outcomes on various response levels between different chemicals, species, exposure conditions and durations (Altenburger and Greco, 2009; Ashauer and Escher, 2010; Jager et al., 2006, 2011).

Nowadays, toxicokinetic-toxicodynamic (TKTD) models are the most advanced effect modeling frameworks that describe and interpret the toxicity dynamic in an aquatic organism over time (Ashauer et al., 2007b; Ashauer and Brown, 2008; Escher et al., 2011; Lee et al., 2002a). Thereby, toxicokinetic processes comprise the chemical accumulation in the organism, the distribution to the target site, the capability of biotransformation and the chemical elimination back in the ambient medium (Ashauer et al., 2006b; Escher and Hermens, 2002; Landrum et al., 1992; Nuutinen et al., 2003). The sum of these mass fluxes leads to the change of the internal concentration in the entire organism over time. Toxicodynamic processes describe the damage processes leading to an adverse response of an organism (Ashauer et al., 2007b; Lee et al., 2002a). The system variable damage consists of damage injury and damage recovery. Thus, TKTD models combine toxicokinetic and toxicodynamic processes by linking internal concentrations to the survival probability of an individual organism (Ashauer et al., 2007b,c,a; Lee et al., 2002a). Effects at the individual level are assumed to be caused only if a certain threshold concentration level is exceeded in the organism (Ashauer et al., 2007b).

In **Chapter 1** of this dissertation, an overview of various effect models including the toxicokinetic-toxicodynamic modeling is given that introduces their different hypothesis, assumptions and applicabilities. To summarize briefly, different effect models have been proposed to simulate temporal effect dynamics in guppy and pond snails of specifically acting and reactive chemicals (Legierse et al., 1999; Verhaar et al., 1999) and time-dependent polycyclic aromatic hydrocarbons toxicity in the amphipod *Hyalella azteca* (Lee et al., 2002b,a). Other TKTD models have been developed to describe the receptor-mediated toxicity of organophosphorus pesticides in invertebrates and fish (Kretschmann et al., 2011b,a; Jager and Kooijman, 2005).

Furthermore, TKTD models have been used to explain carry-over toxicity of sequential diazinon and propiconazole exposure in invertebrates (Ashauer et al., 2010; Nyman et al., 2012). Combined effects of pulsed exposure to carbaryl and chlorpyrifos were simulated by Ashauer et al. (2006a, 2007a). Other applications of TKTD models deal with the mechanistic explanation for differences in specie sensitivities between aquatic invertebrates (Kretschmann et al., 2012; Nyman et al., 2014). Interspecies variation in the dynamics of mortality and immobility responses in freshwater arthropods exposed to chlorpyrifos have been explained by differences in uptake and elimination process that accounted for 50% to 60% data variability (Rubach et al., 2010, 2011). To conclude from literature findings, modeling toxicokinetic and toxicodynamic processes is a powerful tool with the ability to improve our understanding about toxicological mechanisms and to extrapolate combined effects on different species exposed to sequential or fluctuating concentrations of a chemical mixture. **Thus, TKTD modeling is a promising tool for predictive environmental risk assessment.** The overview of TKTD approaches given in **Chapter 1** also pointed out that the major TKTD modeling approaches have been suggested to describe the survival probability of invertebrate and fish species related to the exposure of a few specifically acting and reactive chemicals. However, current effect assessment is based on the three model organisms fish, invertebrates, and unicellular algae species to cover a big rang of possible organism targets. So far, a TKTD model describing toxicity dynamics in the unicellular green algae has not been developed yet.

The presented thesis highlights a novel TKTD model that describes the perturbed unicellular green algae growth as a consequence of chemical exposure. To this end, experimental methods were developed in order to obtain information on the time-course of internal concentration in the algae cell and the related effect dynamic. An improved understanding of toxicokinetic and toxicodynamic processes of specifically acting and reactive chemicals with a broad range of physicochemical properties in the unicellular algae cell *Scenedesmus vacuolatus* was generated in this thesis by combining experimental and modeling methods. In the following, the individual results will be synthesized, the thesis research questions will be answered and the limitations of the studies will be discussed. A general conclusion will be derived at the end of this synthesis. Directions for future research are separately addressed in **Chapter 6**.

## **5.1 Developed tool: toxicokinetic-toxicodynamic modeling of *S. vacuolatus* growth**

In **Chapter 2**, a novel TKTD was introduced that describes growth pattern of the algae cell *Scenedesmus vacuolatus* over time exposed to various chemical concentrations. The model formulation was adapted from a pharmacological model that was proposed for simulating tumor growth kinetics after drug administration (Simeoni et al., 2004). Here, the pharmacological model was extended to account for the unperturbed growth pattern of the unicellular green algae according to Altenburger et al. (2008) and to meet the assumptions behind (eco)toxicodynamic processes as introduced in **Chapter 1**. The TKTD model included a total of eleven parameters that characterize the processes of unperturbed algae growth (five parameters), kinetics of bioconcentration (two parameters) and toxicodynamic processes (four parameters). For calibration purposes, unperturbed and perturbed algae growth were studied over one generation cell-cycle of 24 h. For this purpose, the standard *S. vacuolatus* bioassay has been modified to catch the algae growth over one generation-cycle. The algae cell volume was measured every 2 h for two untreated samples, two DMSO samples and six chemical treated samples, respectively. Algae samples were

exposed to six concentrations of norflurazone, triclosan, and n-phenyl-2-naphtylamine (PNA). To monitor the algae growth over one generation cell-cycle, two time-shifted synchronized algae cultures were handled in analogous manner. The cell volume was measured from  $t_0$  to  $t_{14}$  for the treated samples of the first synchronized algae culture and from  $t_{14}$  to  $t_{24}$  for the treated samples of the second synchronized algae culture. In general, six trajectories of algae growth were observed following a concentration-time-response pattern. Exposure of the highest concentration led to fastest response on algae growth as expected by Haber's rule (Rozman and Doull, 2000). Lowest exposure concentrations did generally not affect algae growth over the entire exposure time compared to the unperturbed algae growth. Here, a certain threshold concentration level triggering adverse outcome on growth might not have been exceeded which is in agreement to assumptions of toxicodynamic processes (Ashauer et al., 2006a, 2007b). Calculated effect concentrations inhibiting 50% *S. vacuolatus* growth decreased over hours for all chemicals until a steady state of effect was reached. That is in accordance to results of toxicity development in algae cells over time reported by other studies (Altenburger et al., 2006; Franz et al., 2008). Nevertheless, the pattern of the perturbed algae growth differed between the three analyzed chemicals that might be a result of different toxicokinetic and toxicodynamic processes of the three chemicals used. The algae TKTD model was tested on its applicability to the experimental observations and on its interpretation power of parameter estimations. ***The patterns of algae growth were matched well by the algae TKTD model. A global parameter set including four toxicodynamic parameters (no-effect concentration, injury rate constant, repair/recovery rate constant, effect progression rate constant) was successfully estimated for each chemical by using inverse modeling techniques.*** The estimated toxicodynamic parameters indicated high variability between the different chemicals with a low interpretation power of the biological meaning. At the same time, parameters characterizing the unperturbed algae growth and toxicokinetic processes were fixed. As a first guess, the time-course of internal concentrations in *S. vacuolatus* was estimated based on literature-reported parameters of bioconcentration kinetics for very hydrophobic ( $\log K_{OW} \geq 5$ ) and non-specifically acting chemicals (Sijm et al., 1998). Estimated internal concentrations reached steady state after five hours of exposure independent of the chemical used. In comparison with the bioconcentration kinetics for very hydrophobic chemicals observed by Sijm et al. (1998), equilibrium concentrations of chemicals with lower hydrophobicity as used in this study would likely be reached earlier in algae cells according to partitioning-driven distribution processes than estimated by a first guess (Fahl et al., 1995; Könemann and van Leeuwen, 1980; Kühnert et al., 2013; Manthey et al., 1993). However, an unknown time-course of the internal concentration in algae cells likely led to an high uncertainty of process parameters estimations and thus the scope of the model applicability.

The time-course of toxicity in algae cells has usually been characterized by descriptive models like concentration-response models (Altenburger et al., 2006; Franz et al., 2008). As shown in this thesis, concentration-response models would need more than 14 parameters to be optimized without improving the understanding of the toxicological mechanisms behind (Jager et al., 2006). By contrast, mechanism-based TKTD models could help to derive deeper insights in the underlying toxicological processes by distinguishing toxicokinetic and toxicodynamic processes of a chemical in a developing organism. Known toxicokinetic and toxicodynamic parameters would thus increase the applicability of TKTD models to estimate the adverse outcome on the organism or population level under real environmental conditions including sequential exposure of a chemical mixture. However, the procedures need to be speed up in order to obtain information on time-dependent toxicokinetic and toxicodynamic processes. Then, the optimization of TKTD parameters would be possible for a broad range of environmental relevant chemicals.

In addition, relevant time-consuming processes have to be determined and the uncertainty of parameter estimation has to be decreased. Therefore, the uncertainty of toxicokinetic processes of chemicals in algae cells were minimized in a next step (**Chapter 3** in order to increase the accuracy and robustness of toxicodynamic parameter estimations that allows the mechanism-based characterization and interpretation of the time-limiting processes behind the development of damage (**Chapter 4**).

## 5.2 ”How fast accumulate structurally diverse chemicals with different physicochemical properties in algae cells?”

In **Chapter 3**, bioconcentration kinetics for structurally diverse chemicals with different physicochemical properties are highlighted that influence time-dependent accumulation and toxicity to unicellular green algae. The determination of the time-concentration-profile in small-volume organisms like algae cells remains, however, challenging. A few studies investigated internal concentrations in algae cells by using radio-labeled chemicals (Gerofke et al., 2005; Geyer et al., 1984; Swackhamer and Skoglund, 1993). However, the concentration measurement of radio-labeled chemicals is restricted to the total amount without distinguishing of the parent chemical and potential biotransformation product(s) (Arnot and Gobas, 2006). Instead, analytical methods need to be developed in order to enable the easy and fast determination of the internal concentration of chemicals with different structures (Jeon et al., 2013). So far, bioconcentration kinetics of very hydrophobic and non-specifically acting chemicals ( $\log K_{OW} \geq 5$ ) have analytically been determined in batches of large algae volume by using solid-phase microextraction (Sijm et al., 1998). To overcome the analytical limitations for determining the internal concentrations for chemicals with low and moderate accumulation potential, an indirect method was successfully adapted and modified from literature in this thesis by the widely-used high-performance liquid chromatography (HPLC)-system (Fahl et al., 1995; Manthey et al., 1993). In this thesis, concentrations of six chemicals with either lower ( $\log K_{OW} \leq 3$ : isoproturon, metazachlor, paraquat) or moderate hydrophobicity ( $\log K_{OW} \geq 4$ : irgarol, triclosan, PNA) in a synchronized *S. vacuolatus* culture of low volume samples were analytical quantified (**Chapter 3**). To this end, concentrations in the ambient medium of a static exposure system were measured, which depleted as a consequence of the accumulated amount by a sufficient high algae biomass. The method established was very robust, because approximately 50% of the concentration in the ambient medium depleted for all chemicals used in this study as a result of the cell density adjustment that spanned from  $1 \times 10^{10}$  to  $1 \times 10^{12}$  cells  $L^{-1}$ . The adjustment of algae biomass was previously calculated in relation to the chemical's  $\log K_{OW}$ . In contrast, concentrations in GB-medium without algae remained stable confirming bioconcentration in algae cells is the only cause for the chemical depletion.

***Intracellular and extracellular equilibrium concentrations were reached within minutes supposedly driven by hydrophobicity-dependent partitioning processes.*** Observed altered bioconcentration kinetics of triclosan, irgarol and metazachlor cannot be explained by partitioning-driven distribution processes only. Instead, the time to reach steady state internal concentration were likely prolonged by other influential factors like ionization of chemicals, the ion trapping mechanism, or the potential susceptibility for biotransformation (Escher and Hermens, 2002, 2004; Jeon et al., 2013; Neuwoehner and Escher, 2011). Uptake rate constant and overall elimination rate constant were successfully estimated for all chemicals used by calibrating a one-compartment toxicokinetic model to the measured concentration depletion in the

ambient medium. The established toxicokinetic assay was suitable to determine bioconcentration kinetics of structurally diverse chemicals with low or moderate accumulation potential in algae cells. Nevertheless, it has to be noticed that the concentration depletion of isoproturon and paraquat was within the first seven minutes measurement window indicating a very fast bioconcentration kinetic which result in high parameter uncertainties. Moreover, this method does not allow for distinguishing between adsorption at the cell wall and absorption in the algae cell. Moreover, intracellular processes like pH-dependent dissociation and the potential susceptibility for biotransformation supposedly influence the time-course of the internal concentration. Here, analytical detection limits need to be overcome for enabling the quantification of the internal concentration of different molecular structures in algae cells. To account for the potential susceptibility for biotransformation in algae cells, alternatively, transcriptional gene expression of phase I and II could provide indication of ongoing biotransformation.

The internal concentration is assumed to better reflect the intrinsic toxic potency of a chemical by accounting for variability of toxicokinetic processes in comparison to the exposure concentration (Escher and Hermens, 2004; McCarty et al., 2011, 2013; Meador et al., 2008). Internal effect concentrations were determined by using the determined bioconcentration potentials for all chemicals used. Internal effect concentrations causing 50% reproduction inhibition at  $t_{24}$  were estimated by accounting for the variability of toxicokinetic processes. The internal effect concentration ranged between  $360 \times 10^3$  to  $2100 \times 10^3$  molecules per algae cell to elicit the same effect level on reproduction for all chemicals. A lower number of molecules were accumulated in the algae cells for the chemicals with lower hydrophobicity than for the chemicals with moderate hydrophobicity that inhibited 50% of algae reproduction at  $t_{24}$ . As the method does not allow for distinguishing between adsorption at the cell wall and absorption in the algae cell, the estimated number of accumulated molecules is likely overestimated and even lower internal concentrations are expected to cause 50% growth inhibition at  $t_{24}$ . Moreover, internal effect concentrations varied less than one order of magnitude and thus different mechanism of action could not be distinguished between the specifically acting and reactive chemicals as indicated by McCarty and Mackay (1993) or Fahl et al. (1995).

### **5.3 "How toxicokinetic and toxicodynamic processes contribute to the overall toxicity development in algae cells over time?"**

Two hypotheses were formulated according to the findings provided in **Chapter 2** and **Chapter 3**. First, damage increases over hours in algae cells, which is likely unexplainable by the increase of the internal concentration over time solely. Second, the rate-limiting process of damage supposedly varied between chemicals depending on the progressed effect from the molecular initiating event over key events toward an adverse outcome on the individual organism level. To test both hypotheses, a joint approach between experimentation and effect modeling was designed (**Chapter 4**). Algae growth assays were performed for the six model chemicals which were previously used in the toxicokinetic assay (**Chapter 3**). The chemical selection based on the expected time to reach equilibrium concentrations in algae cells according to the partitioning-driven distribution process combined with the suspected time to progress the effect from the initiating molecular event towards an adverse outcome on growth. Isoproturon and irgarol inhibit photosystem II, metazachlor and triclosan block the lipid biosynthesis, whereas paraquat and PNA are reactive chemicals. By contrast to the traditional exposure system used for algae toxicity testing, algae exposition started at  $t_6$  or  $t_8$  when algae cells were in a linear

growth phase according to the unperturbed growth model (Altenburger et al., 2008). It was assumed that responses on growth can be detected earliest and are most sensitive in the phase of fastest growth (as indicated by the growth parameters). The specific concentration-time-response patterns were assumed to depend on either the physicochemical properties of the chemical or the biological-specific properties of the effect functioning (Danhof et al., 2008). Estimated internal concentrations were linked to the respect algae growth changes through TKTD modeling. ***The joint approach showed that a time-lag of hours existed between the time point when chemical accumulation is supposed to be stationary and the continuous development of damage.*** Consequently, the partitioning-driven partition process is not the dominating time-limiting step for toxicity in algae cells. The results rather indicated that the time to progress an effect from the initiating molecular event over key events (e.g., toxicogenomic responses) towards an adverse outcome on growth is driving the toxicity over time. This process is generalized by the effect progression rate constant implemented in the TKTD model. ***The estimated rates of effect progression spanned over six orders of magnitude between all six chemicals, but less than one order of magnitude between chemicals with similar biological activity. Thus, the time to develop damage seemed to vary between chemicals depending on how effect is progressed across different key events towards an adverse outcome.***

It was highlighted that the compact information on toxicokinetic and toxicodynamic processes reduces the uncertainty of the parameter estimations. Therefore, a meaningful interpretation of aggregated process parameters likely gave a deeper insight in time process of toxicological mechanisms. In this study, effect progression indicates the relevant time-consuming processes that dominates the development of damage in algae cells. Effect progression rates varied over six orders of magnitude between different chemicals. Thus, the process parameter accounting for the effect progression has been shown to be more indicative to distinguish between the AOPs than the calculated internal effect concentration (**Chapter3**). However, toxicokinetic and toxicodynamic parameters need to be interpreted carefully, because these parameters aggregate different system variables which are not directly measurable. Especially, injury and recovery/repair rate constants might still be imprecise. Here, a step forward would be to measure the algae growth exposed to sequential concentrations as shown by Ashauer et al. (2007b).

#### **5.4 Implication of toxicokinetic-toxicodynamic modeling in current risk assessment**

Potential applications of effect models for the environmental risk assessment of chemicals have been summarized by Hommen et al. (2010) and Galic et al. (2010):

- extrapolation of organism-level effects to the population-level
- extrapolation of effects between different exposure profiles
- extrapolation of recovery processes
- analysis and prediction of indirect effects
- prediction of bioaccumulation within food chains

Toxicokinetic-toxicodynamic models have been shown to handle fluctuating concentrations of chemicals and to extrapolate effects to the population-level and of recovery processes (Ashauer

et al., 2011; Galic et al., 2010, 2014; Hommen et al., 2010; Martin et al., 2013). However, these days, model parameters are missing for a variety of species exposed to a broad range of chemicals which narrow the applicability of that approach (Ashauer et al., 2011). Moreover, we are currently dealing with process parameters that integrate several toxicological processes, showing high parameter uncertainties and are less robust. Therefore, we need to understand what the biological meaning of these parameters is in order to use toxicokinetic-toxicodynamic models as extrapolation tool. As highlighted in this thesis, one way forward is to test and optimize process parameters for a broad range of chemicals in order to improve the understanding of toxicological mechanism behind toxicokinetic-toxicodynamic frameworks. Moreover, the simple unicellular algae system seems to be a promising tool for studying the damage development without considering internal exposure changes. Therefore, further research is suggested in **Chapter 6** addressing several open issues by using the synchronized algae system as model organism.



## Implementation challenges

Based on this dissertations results, I would like to give three recommendations for future research. All recommendations generally aim to understand the development of toxicity in an organism exposed to a chemical and to characterize process parameters to increase the model applicability for extrapolating the adverse outcome on the organism or population level for untested scenarios.

### 6.1 Refinement and modeling of toxicokinetic processes in algae cells

Internal concentrations in the entire organism or at the target site are thought to be more suitable dose surrogates than exposure concentrations (Escher and Hermens, 2004; McCarty et al., 2013; Meador et al., 2008). Various studies showed that the use of internal concentrations reduced the data variability for a better interpretation of the intrinsic toxicity differences between various species and chemicals (Barron et al., 1990; Nyman et al., 2014). For instance, lethal membrane concentrations of nonspecific organic chemicals with different hydrophobicities are almost equivalent to elicit the same effect level, also known as critical body residue (Di Toro et al., 2000; McCarty and Mackay, 1993; van Wezel and Opperhuizen, 1995). The time to reach the steady state lethal membrane concentrations still differs between the nonspecifically acting chemicals due to partitioning-driven distribution processes (Escher and Hermens, 2002). In comparison with the nonspecifically acting chemicals, specifically acting and reactive chemicals are intrinsically more potent and cover a broad range of internal concentrations eliciting the same effect level (Escher and Hermens, 2002; McCarty and Mackay, 1993). This may be caused by variable chemical affinities to or the interaction types between different classes of lipids and proteins (Endo et al., 2011, 2012; Escher and Hermens, 2002). In addition, partitioning-driven distribution processes of the structurally diverse chemicals are likely altered by biotransformation processes (Ashauer et al., 2012) or speciation in regard to the extra- or intracellular pH (Escher and Schwarzenbach, 2002; Fahl et al., 1995; Neuwoehner and Escher, 2011). Those processes may significantly change the time-course of the internal concentration in the entire organism driven by the hydrophobicity-dominated distribution processes and thus the development of damage over time (Ashauer et al., 2012; Neuwoehner and Escher, 2011). As a consequence, the risk on algae might be underestimated for more complex molecular structures when using the exposure concentration as dose surrogate for toxicity (Escher and Hermens, 2004; Fahl et al., 1995; Neuwoehner and Escher, 2011). It has been reported that chemical accumulation across the cell membrane is hampered for dissociating species that resulted

into a lower estimated toxicity (Escher and Hermens, 2004; Fahl et al., 1995; Neuwoehner and Escher, 2011). Further, the toxicity of basic pharmaceuticals was explained with a toxicokinetic ion-trapping model that accounts for the capability of speciation inside the algae cell (Neuwoehner and Escher, 2011). These findings are confirmed by the results of the work presented in this dissertation indicating that partitioning-driven distribution processes might be altered by ionization, ion-trapping mechanism, or biotransformation (**Chapter 3**). Therefore, it is suggested to subsequently research toxicokinetic processes of diverse structural molecules (polar, ionizable, easily biotransformed) in algae cells. Simultaneously, the development of toxicokinetic models for those chemicals in algae cells would help to analyze time-dependent changes of internal exposure and damage in a mechanistic way.

Modeling toxicokinetic processes can be used to estimate the change of the internal concentration at the target site over time in order to overcome analytical detection limits. For this purpose, in a first instance, the simple one-compartment toxicokinetic model could be extended to three compartments for representation the three algae phases lipid, protein and water. Similarly, a three-phase equilibration partitioning model was suggested for fish (van Wezel and Opperhuizen, 1995). According to such a model formulation, chemical distribution to the representative algae compartments depends on partition properties of the chemical to the respect phase and is related to physicochemical properties of the chemical. However, biological parameters are still missing in such a partitioning model. A subsequent research step would therefore be the inclusion of biological parameters into the modeling framework as proposed by physiologically-based toxicokinetic modeling. Here, the influence of the physiology of subcellular algae compartments, the number/volume of target sites, the potential susceptibility for biotransformation, and dilution processes of the concentration due to growth can be investigated on partitioning-driven distribution processes. Stadnicka et al. (2012) demonstrated that at least 88% of the internal concentrations were correctly predicted within one order of magnitude using the physiologically-based toxicokinetic model for fish developed by Nichols et al. (1990). Whether the influence of biological parameters significantly impacts the internal concentration at the target site could then systematically be analyzed by a physiologically-based toxicokinetic model for algae.

## 6.2 Extrapolation concepts for dealing with multiple contamination

Toxicokinetic-toxicodynamic (TKTD) modeling has been suggested to provide a conceptual framework for extrapolating combined effects at the individual organism level exposed to sequential concentrations of a chemical cocktail (Ashauer et al., 2007b,a; Altenburger and Greco, 2009). Studies further reported carry-over toxicity following a sequential exposure (Ashauer et al., 2007c, 2010). Carry-over toxicity means that the effect is increased after a second exposure pulse compared with the previously not stressed organisms (Ashauer et al., 2010). By applying the TKTD model, carry-over toxicity on *Gammarus pulex* was explained by either the overall chemical elimination in the ambient medium (toxicokinetic) or the time needed to recover between two pulses (toxicodynamic) (Ashauer et al., 2007a). Hence, environmental risk assessment based on standard toxicity tests with continuous exposure conditions might underestimate the risk on organisms exposed to fluctuating concentrations in the environment (Ashauer et al., 2010).

So far, carry-over toxicity on algae has been implicitly described by observing the population recovery following pulse exposure. Repeated pulse exposures on *S. vacuolatus* have been

conducted for the photosystem II inhibitors isoproturon and atrazine as well as for S-metolachlor inhibiting the formation of very long chain fatty acids (Brain et al., 2012; Vallotton et al., 2008a,b, 2009). These studies reported that the recovery of population algae growth was immediate for photosystem II inhibitors, but a recovery was 29 h delayed after S-metolachlor pulse exposure. Recently, Weber et al. (2012) published a method to accomplish a time-variable exposure of fluctuating isoproturon concentration on the two algae species *Desmodesmus subspicatus* and *Pseudokirchneriella subcapitata*. Here, recovery has been found to be rapid which was explained by a fast chemical dissipation from the system. To conclude from the findings in literature, carry-over toxicity on algae is hypothesized to depend on hydrophobicity, chemical-target-interactions or degree of reversibility. However, afterward investigations need to be conducted to understand carry-over toxicity on algae cells.

Algae growth following sequential exposure of a structurally diverse chemical mixture could be measured and simulated for investigating combined effects and carry-over toxicity. To this end, an experimental set-up is suggested to consider different peak concentrations, exposure durations and recovery times between two pulses. Moreover, the model chemicals used in this dissertation provide a broad range of properties with regard to hydrophobicity, chemical-target-interactions addressing various target sites, and degrees of reversibility. Those chemicals may be further employed to increase the capability on covering all potential processes leading to carry-over toxicity and combined effects on algae growth. By applying the algae TKTD model, the understanding of damage processes including injury and recovery/repair processes in algae cells would be improved and the uncertainty of estimated TKTD parameters may be reduced. Additionally, the toxicodynamic assumptions of survival concepts ("individual tolerance" and "stochastic death") could be extended for graded endpoints like growth. By contrast to the "on" or "off" type of survival, the stopped growth of algae cells within an exposure phase may continue to growth again within the recovery phase between two pulse exposures (Ashauer et al., 2011).

### **6.3 Linkage of effects across multiple biological levels towards an adverse outcome at the individual or population level**

Adverse outcome pathways (AOPs) have been recommended as an analytical construct that portrays a sequential chain of causally linked responses from the initiating molecular event over key events toward an adverse health or ecotoxicological outcome (Ankley et al., 2010). The construction of AOPs for different toxicological mechanisms aims to support the assessment of chemical risk on the environment. However, the understanding of how a detected response on the molecular or cellular level is progressed to an adverse outcome on the individual or population level still remains a formidable research challenge (Altenburger et al., 2015). To face that research challenge, the application of predictive effect models might be a powerful tool for linking and extrapolating effects of concentration-time-response relationships for different endpoints in a mechanistic way (Forbes and Calow, 2012; Hartung and Rovida, 2009; Villeneuve and Garcia-Reyero, 2011). For this purpose, physiologic indirect response models have been proposed by pharmacological research in order to characterize various types of toxicodynamic effects (Danhof et al., 2008; Iyengar et al., 2012; Jusko et al., 1995; Jusko, 2013).

Toxicodynamic effects are described by the inhibition or stimulation of the production or loss of endogenous substances or mediators as a consequence of a chemical-target interaction according to the physiologic indirect response models (Mager et al., 2003). Jin et al. (2003), for

instance, modeled corticosteroid pharmacogenomics in rat liver and described time-patterns for each responsive gene. By using the fifth-generation pharmacokinetic-pharmacodynamic model developed by Ramakrishnan et al. (2002), observed clusters of the time-course of gene responses were explained by a limited array of different rate-limiting mechanisms of gene regulation. Adapting pharmacokinetic-pharmacodynamic model structures for simulating pharmacogenomics could quantitatively anchor phenotypic effects in ecotoxicology. By doing so, the mechanism of effects caused by long-term mixture exposure of low concentrations might be predictable. However, it has to be noted that observed effects and estimated process parameters need to be interpreted carefully.

The time-course of molecular responses likely interfere by other processes such as gene regulation due to organism development or the accumulation of chemicals over time. Knowing turnover rates for physiological system components therefore help to identify the rate-limiting process of toxicological mechanisms dominating the effect progression toward an adverse outcome at individual or population level (Mager and Jusko, 2008). Moreover, the detected responses on molecular or cellular level over time can supposedly be caused by the change of internal concentration of the chemical, but not by the effect itself (Forbes et al., 2006). Therefore, experiments need to be designed which carefully control toxicokinetic and toxicodynamic processes (Ankley et al., 2006). Reducing the bias of toxicokinetic processes likely improves the interpretation power of generated response data and the predictability power of the TKTD model (Forbes et al., 2006). As investigated in this dissertation, the simple unicellular algae systems provides a useful tool for facing the research challenge of phenotypic anchoring in ecotoxicology. The bias of internal concentration changes is minimized in algae cells. Therefore, the time-course of toxicity can be interpreted with regard to the effect progressed toward an adverse outcome at the individual organism level only. Subsequent research is suggested to analyze and model the sequential chain of causally linked events from the initiating molecular event over key events toward an adverse outcome on individual algae growth and algae reproduction by an extended algae TKTD model based on physiologic indirect response models.

# Bibliography

- Adler, N.E.; Schmitt-Jansen, M. and Altenburger, R. 2007. Flow cytometry as a tool to study phytotoxic modes of action. *Environmental Toxicology and Chemistry*, **26**(2), 297–306.
- Alford, R.A. and Richards, S.J. 1999. Global amphibian declines: a problem in applied ecology. *Annual review of Ecology and Systematics*, **30**, 133–165.
- Altenburger, R. and Greco, W.R. 2009. Extrapolation concepts for dealing with multiple contamination in environmental risk assessment. *Integrated Environmental Assessment and Management*, **5**(1), 62–68.
- Altenburger, R.; Walter, H. and Grote, M. 2004. What contributes to the combined effect of a complex mixture? *Environmental Science & Technology*, **38**(23), 6353–6362.
- Altenburger, R.; Brack, W.; Greco, W. R.; Grote, M.; Jung, K.; Ovari, A.; Riedl, J.; Schwab, K. and Küster, E. 2006. On the mode of action of N-phenyl-2-naphthylamine in plants. *Environmental Science & Technology*, **40**(19), 6163–6169.
- Altenburger, R.; Schmitt-Jansen, M. and Riedl, J. 2008. Bioassays with unicellular algae: Deviations from exponential growth and its implications for toxicity test results. *Journal of Environmental Quality*, **37**(1), 16–21.
- Altenburger, R.; Ait-Aissa, S.; Antczak, P.; Backhaus, T.; Barceló, D.; Seiler, T.-B.; Brion, F.; Busch, W.; Chipman, K.; de Alda, M.L.; de Aragão, U.G.; Escher, B.I.; Falciani, F.; Faust, M.; Focks, A.; K., H.; Hollender, J.; Hollert, H.; Jäger, F.; Jahnke, A.; Kortenkamp, A.; Krauss, M.; Lemkine, G. F.; Munthe, J.; Neumann, S.; Schymanski, E.L.; Scrimshaw, M.; Segner, H.; Slobodnik, J.; Smedes, F.; Kughathas, S.; Teodorovic, I; Tindall, A.J.; Tollefsen, K.E.; Walz, K.H.; Williams, T.D.; Van den Brink, P.J.; van Gils, J.; Vrana, B.; Zhang, X. and Brack, W. 2015. Future water quality monitoring - Adapting tools to deal with mixtures of pollutants in water resource management. *Science of the Total Environment*, **512**, 540–551.
- Ankley, G.T.; Erickson, R.J.; Phipps, G.L.; Mattson, V.R.; Kosian, P.A.; Sheedy, B.R. and Cox, J.S. 1995. Effects of light intensity on the phototoxicity of fluoranthene to a benthic macroinvertebrate. *Environmental Science & Technology*, **29**(11), 2828–2833.
- Ankley, G.T.; Daston, G.P.; Degitz, S.J.; Denslow, N.D.; Hoke, R.A.; Kennedy, S.W.; Miracle, A.L.; Perkins, E.J.; Snape, J. and Tillitt, D.E. 2006. Toxicogenomics in regulatory ecotoxicology. *Environmental Science & Technology*, **40**(13), 4055–4065.
- Ankley, G.T.; Bennett, R.S.; Erickson, R.J.; Hoff, D.J.; Hornung, M.W.; Johnson, R.D.; Mount, D.R.; Nichols, J.W.; Russom, C.L. and Schmieder, P.K. 2010. Adverse outcome pathways: A conceptual framework to support ecotoxicology research and risk assessment. *Environmental Toxicology and Chemistry*, **29**(3), 730–741.

- Ariffin, M.M. and Anderson, R.A. 2006. LC/MS/MS analysis of quaternary ammonium drugs and herbicides in whole blood. *Journal of Chromatography B*, **842**(2), 91–97.
- Arnot, J.A. and Gobas, F. 2006. A review of bioconcentration factor (BCF) and bioaccumulation factor (BAF) assessments for organic chemicals in aquatic organisms. *Environmental Reviews*, **14**(4), 257–297.
- Arrhenius, Å.; Backhaus, T.; Grönvall, F.; Junghans, M.; Scholze, M. and Blanck, H. 2006. Effects of three antifouling agents on algal communities and algal reproduction: mixture toxicity studies with TBT, Irgarol, and Sea-Nine. *Archives of Environmental Contamination and Toxicology*, **50**(3), 335–345.
- Ashauer, R. and Brown, C.D. 2008. Toxicodynamic assumptions in ecotoxicological hazard models. *Environmental Toxicology and Chemistry*, **27**(8), 1817–1821.
- Ashauer, R. and Escher, B.I. 2010. Advantages of toxicokinetic and toxicodynamic modelling in aquatic ecotoxicology and risk assessment. *Journal of Environmental Monitoring*, **12**(11), 2056–2061.
- Ashauer, R.; Boxall, A.B.A. and Brown, C.D. 2006a. Predicting effects on aquatic organisms from fluctuating or pulsed exposure to pesticides. *Environmental Toxicology and Chemistry*, **25**(7), 1899–1912.
- Ashauer, R.; Boxall, A.B.A. and Brown, C.D. 2006b. Uptake and elimination of chlorpyrifos and pentachlorophenol into the freshwater amphipod *Gammarus pulex*. *Archives of Environmental Contamination and Toxicology*, **51**(4), 542–548.
- Ashauer, R.; Boxall, A.B.A. and Brown, C.D. 2007a. Modeling combined effects of pulsed exposure to carbaryl and chlorpyrifos on *Gammarus pulex*. *Environmental Science & Technology*, **41**(15), 5535–5541.
- Ashauer, R.; Boxall, A.B.A. and Brown, C.D. 2007b. New ecotoxicological model to simulate survival of aquatic invertebrates after exposure to fluctuating and sequential pulses of pesticides. *Environmental Science & Technology*, **41**(4), 1480–1486.
- Ashauer, R.; Boxall, A.B.A. and Brown, C.D. 2007c. Simulating toxicity of carbaryl to *Gammarus pulex* after sequential pulsed exposure. *Environmental Science & Technology*, **41**(15), 5528–5534.
- Ashauer, R.; Hintermeister, A.; Caravatti, I.; Kretschmann, A. and Escher, B.I. 2010. Toxicokinetic and toxicodynamic modeling explains carry-over toxicity from exposure to diazinon by slow organism recovery. *Environmental Science & Technology*, **44**(10), 3963–3971.
- Ashauer, R.; Agatz, A.; Albert, C.; Ducrot, V.; Galic, N.; Hendriks, J.; Jager, T.; Kretschmann, A.; O'Connor, I. and Rubach, M.N. 2011. Toxicokinetic-toxicodynamic modeling of quantal and graded sublethal endpoints: A brief discussion of concepts. *Environmental Toxicology and Chemistry*, **30**, 2519–2524.
- Ashauer, R.; Hintermeister, A.; O'Connor, I.; Elumelu, M.; Hollender, J. and Escher, B.I. 2012. Significance of xenobiotic metabolism for bioaccumulation kinetics of organic chemicals in *Gammarus pulex*. *Environmental Science & Technology*, **46**, 3498–3508.

- Ashauer, R.; Thorbek, P.; Warinton, J.S.; Wheeler, J.R. and Maund, S. 2013. A method to predict and understand fish survival under dynamic chemical stress using standard ecotoxicity data. *Environmental Toxicology and Chemistry*, **32**(4), 954–965.
- Baas, J.; Jager, T. and Kooijman, B. 2009. Understanding toxicity as processes in time. *Science of the Total Environment*, **408**(18), 2735–3739.
- Bandow, N.; Altenburger, R. and Brack, W. 2010. Application of nd-SPME to determine freely dissolved concentrations in the presence of green algae and algae-water partition coefficients. *Chemosphere*, **79**(11), 1070–1076.
- Barron, M.G.; Stehly, G.R. and Hayton, W.L. 1990. Pharmacokinetic modeling in aquatic animals. 1. models and concepts. *Aquatic Toxicology*, **18**(2), 61–86.
- Böger, P.; Matthes, B. and Schmalfuss, J. 2000. Towards the primary target of chloroacetamides - new findings pave the way. *Pest Management Science*, **56**(6), 497–508.
- Brack, W.; Altenburger, R.; Schüürmann, G.; Krauss, M.; Herráez, D.L.; van Gils, J.; Slobodnik, J.; Munthe, J.; Gawlik, B.M.; van Wezel, A.; Schriks, M.; Hollender, J.; Tollefsen, K.E.; Mekenyan, O.; Dimitrov, S.; Bunke, D.; Cousins, I.; Posthuma, L.; van den Brink, P.J.; de Alda, M.L.; Barceló, D.; Faust, M.; Kortenkamp, A.; Scrimshaw, M.; Ignatova, S.; Engelen, G.; Massmann, G.; Lemkine, G. and Teodorovic, I. 2015. The SOLUTIONS project: challenges and responses for present and future emerging pollutants in land and water resources management. *Science of the Total Environment*, **503**, 22–31.
- Brain, R.A.; Arnie, J.R.; Porch, J.R. and Hosmer, A.J. 2012. Recovery of photosynthesis and growth rate in green, blue-green, and diatom algae after exposure to atrazine. *Environmental Toxicology and Chemistry*, **31**(11), 2572–2581.
- Brock, T.; Arts, G.H.P.; Maltby, L. and Van den Brink, P.J. 2006. Aquatic risks of pesticides, ecological protection goals, and common aims in European Union legislation. *Integrated Environmental Assessment and Management*, **2**(4), e20–e46.
- Carpenter, S.R.; Stanley, E.H. and Vander Zanden, M.J. 2011. State of the world's freshwater ecosystems: physical, chemical, and biological changes. *Annual Review of Environment and Resources*, **36**, 75–99.
- Chaisuksant, Y.; Yu, Q. and Connell, D. 1997. Internal lethal concentrations of halobenzenes with fish (*Gambusia affinis*). *Ecotoxicology and Environmental Safety*, **37**(1), 66–75.
- Colborn, T.; vom Saal, F.S. and Soto, A.M. 1993. Developmental effects of endocrine-disrupting chemicals in wildlife and humans. *Environmental Health Perspectives*, **101**(5), 378.
- Dahl, S.G.; Aarons, L.; Gundert-Remy, U.; Karlsson, M.O.; Schneider, Y.J.; Steimer, J.L. and Troconiz, I.F. 2010. Incorporating physiological and biochemical mechanisms into pharmacokinetic-pharmacodynamic models: A conceptual framework. *Basic & clinical pharmacology & toxicology*, **106**(1), 2–12.
- Danhof, M.; de Jongh, J.; De Lange, E.C.; Della Pasqua, O.E.; Ploeger, B.A. and Voskuyl, R.A. 2007. Mechanism-based pharmacokinetic-pharmacodynamic modeling: biophase distribution, receptor theory, and dynamical systems analysis. *Annual Reviews: Pharmacology And Toxicology*, **47**, 357–400.

- Danhof, M.; de Lange, E.; Della Pasqua, O.E.; Ploeger, B.A. and Voskuyl, R.A. 2008. Mechanism-based pharmacokinetic-pharmacodynamic (PK-PD) modeling in translational drug research. *Trends in pharmacological sciences*, **29**(4), 186–191.
- Dann, A.B. and Hontela, A. 2011. Triclosan: environmental exposure, toxicity and mechanisms of action. *Journal of Applied Toxicology*, **31**(4), 285.
- Daughton, C.G. and Ternes, T.A. 1999. Pharmaceuticals and personal care products in the environment: Agents of subtle change? *Environmental Health Perspectives*, **107**, 907–938.
- de Maagd, P.G.J.; van de Klundert, I.C.M.; van Wezel, A.P.; Opperhuizen, A. and Sijm, D.T.H.M. 1997. Lipid content and time-to-death-dependent lethal body burdens of naphthalene and 1,2,4-trichlorobenzene in fathead minnow (*Pimephales promelas*). *Ecotoxicology and Environmental Safety*, **38**(3), 232–237.
- Di Toro, D.M.; McGrath, J.A. and Hansen, D.J. 2000. Technical basis for narcotic chemicals and polycyclic aromatic hydrocarbon criteria. I. Water and tissue. *Environmental Toxicology and Chemistry*, **19**(8), 1951–1970.
- Eggen, R.I.L.; Behra, R.; Burkhardt-Holm, P.; Escher, B.I. and Schweigert, N. 2004. Peer reviewed: Challenges in ecotoxicology. *Environmental Science & Technology*, **38**(3), 58–64.
- Endo, S.; Escher, B. I. and Goss, K.-U. 2011. Capacities of membrane lipids to accumulate neutral organic chemicals. *Environmental Science & Technology*, **45**(14), 5912–5921.
- Endo, S.; Bauerfeind, J. and Goss, K.-U. 2012. Partitioning of neutral organic compounds to structural proteins. *Environmental Science & Technology*, **46**(22), 12697–12703.
- Eriksson, E.; Auffarth, K.; Henze, M. and Ledin, A. 2002. Characteristics of grey wastewater. *Urban water*, **4**(1), 85–104.
- Escher, B.I. and Hermens, J.L.M. 2002. Modes of action in ecotoxicology: Their role in body burdens, species sensitivity, QSARs, and mixture effects. *Environmental Science & Technology*, **36**(20), 4201–4217.
- Escher, B.I. and Hermens, J.L.M. 2004. Internal exposure: Linking bioavailability to effects. *Environmental Science & Technology*, **38**(23), 455A–462A.
- Escher, B.I. and Schwarzenbach, R.P. 2002. Mechanistic studies on baseline toxicity and uncoupling of organic compounds as a basis for modeling effective membrane concentrations in aquatic organisms. *Aquatic Sciences*, **64**(1), 20–35.
- Escher, B.I.; Ashauer, R.; Dyer, S.; Hermens, J.L.M.; Lee, J.H.; Leslie, H.A.; Mayer, P.; Meador, J.P. and Warne, M.S.J. 2011. Crucial role of mechanisms and modes of toxic action for understanding tissue residue toxicity and internal effect concentrations of organic chemicals. *Integrated Environmental Assessment and Management*, **7**(1), 28–49.
- European Commission. 2000. The Directive 2000/60/EC of the European Parliament and of the Council of 23 October 2000 establishing a framework for Community action in the field of water policy. *Official Journal of the European Union*.

- European Commission. 2012. A blueprint to safeguard Europe's water resources. Communication from the Commission to the European Parliament the Council, the European Economic and Social Committee and the Committee of the Regions, COM, 673 Final.
- European Environment Agency. 2012. European waters - Assessment of status and pressures. <http://www.eea.europa.eu/themes/water/publications-2012>.
- Fahl, G.M.; Kreft, L.; Altenburger, R.; Faust, M.I; Boedeker, W. and Grimme, L.H. 1995. pH-dependent sorption, bioconcentration and algal toxicity of sulfonylurea herbicides. *Aquatic Toxicology*, **31**(2), 175–187.
- Faust, M.; Altenburger, R.; Backhaus, T.; Blanck, H.; Boedeker, W.; Gramatica, P.; Hamer, V.; Scholze, M.; Vighi, M. and Grimme, L.H. 2001. Predicting the joint algal toxicity of multi-component s-triazine mixtures at low-effect concentrations of individual toxicants. *Aquatic Toxicology*, **56**(1), 13–32.
- Faust, M.; Altenburger, R.; Backhaus, T.; Blanck, H.; Boedeker, W.; Gramatica, P.; Hamer, V.; Scholze, M.; Vighi, M. and Grimme, L.H. 2003. Joint algal toxicity of 16 dissimilarly acting chemicals is predictable by the concept of independent action. *Aquatic Toxicology*, **63**(1), 43–63.
- Forbes, V.E. and Calow, P. 2002. Extrapolation in ecological risk assessment: Balancing pragmatism and precaution in chemical controls legislation. *BioScience*, **52**(3), 249–257.
- Forbes, V.E. and Calow, P. 2012. Promises and problems for the new paradigm for risk assessment and an alternative approach involving predictive systems models. *Environmental Toxicology and Chemistry*, **31**(12), 2663–2671.
- Forbes, V.E.; Palmqvist, A. and Bach, L. 2006. The use and misuse of biomarkers in ecotoxicology. *Environmental Toxicology and Chemistry*, **25**(1), 272–280.
- Franz, S.; Altenburger, R.; Heilmeyer, H. and Schmitt-Jansen, M. 2008. What contributes to the sensitivity of microalgae to triclosan? *Aquatic Toxicology*, **90**(2), 102–108.
- Galic, N.; Hommen, U.; Baveco, J.M. and van den Brink, P.J. 2010. Potential application of population models in the European ecological risk assessment of chemicals II: review of models and their potential to address environmental protection aims. *Integrated Environmental Assessment and Management*, **6**(3), 338–360.
- Galic, N.; Ashauer, R.; Baveco, H.; Nyman, A.M.; Barsi, A.; Thorbek, P.; Bruns, E. and Van den Brink, P.J. 2014. Modeling the contribution of toxicokinetic and toxicodynamic processes to the recovery of *Gammarus pulex* populations after exposure to pesticides. *Environmental Toxicology and Chemistry*, **33**(7), 1476–1488.
- Garcia-Reyero, N. and Perkins, E.J. 2011. Systems biology: Leading the revolution in ecotoxicology. *Environmental Toxicology and Chemistry*, **30**(2), 265–273.
- Gerofke, A.; Kömp, P. and McLachlan, M.S. 2005. Bioconcentration of persistent organic pollutants in four species of marine phytoplankton. *Environmental Toxicology and Chemistry*, **24**(11), 2908–2917.

- Geyer, H.; Politzki, G. and Freitag, D. 1984. Prediction of ecotoxicological behaviour of chemicals: Relationship between n-octanol/water partition coefficient and bioaccumulation of organic chemicals by alga. *Chemosphere*, **13**(2), 269–284.
- Haber, F. 1924. *Zur Geschichte des Gaskrieges*. Springer. pp. 76–92.
- Handy, R.D. 1994. Intermittent exposure to aquatic pollutants: assessment, toxicity and sublethal responses in fish and invertebrates. *Comparative Biochemistry and Physiology C-Pharmacology Toxicology & Endocrinology*, **107**(2), 171–184.
- Hartung, T. and Rovida, C. 2009. Chemical regulators have overreached. *Nature*, **460**(7259), 1080–1081.
- Heckmann, L.H.; Baas, J. and Jager, T. 2010. Time is of the essence. *Environmental Toxicology and Chemistry*, **29**(6), 1396–1398.
- Hock, B.; Fedtke, C. and Schmidt, R. 1995. *Herbicides: development, use, activities, side effects*. Georg Thieme Verlag.
- Hommen, U.; Baveco, J.M.; Galic, N. and van den Brink, P.J. 2010. Potential application of ecological models in the European environmental risk assessment of chemicals I: review of protection goals in EU directives and regulations. *Integrated Environmental Assessment and Management*, **6**(3), 325–337.
- Houlahan, J.E.; Findlay, C.S.; Schmidt, B.R.; Meyer, A.H. and Kuzmin, S.L. 2000. Quantitative evidence for global amphibian population declines. *Nature*, **404**(6779), 752–755.
- Iyengar, R.; Zhao, S.; Chung, S.-W.; Mager, D.E. and Gallo, J.M. 2012. Merging systems biology with pharmacodynamics. *Science translational medicine*, **4**(126), 126ps7.
- Jabusch, T.W. and Swackhamer, D.L. 2004. Subcellular accumulation of polychlorinated biphenyls in the green alga *Chlamydomonas reinhardtii*. *Environmental Toxicology and Chemistry*, **23**(12), 2823–2830.
- Jackson, R.B.; Carpenter, S.R.; Dahm, C.N.; McKnight, D.M.; Naiman, R.J.; Postel, S.L. and Running, S.W. 2001. Water in a changing world. *Ecological Applications*, **11**(4), 1027–1045.
- Jager, T. and Kooijman, S. 2005. Modeling receptor kinetics in the analysis of survival data for organophosphorus pesticides. *Environmental Science & Technology*, **39**(21), 8307–8314.
- Jager, T.; Heugens, E.H.W. and Kooijman, S.A.L.M. 2006. Making sense of ecotoxicological test results: Towards application of process-based models. *Ecotoxicology*, **15**(3), 305–314.
- Jager, T.; Albert, C.; Preuss, T.G. and Ashauer, R. 2011. General unified threshold model of survival - A toxicokinetic-toxicodynamic framework for ecotoxicology. *Environmental Science & Technology*.
- Jamers, A. and De Coen, W. 2010. Effect assessment of the herbicide paraquat on a green alga using differential gene expression and biochemical biomarkers. *Environmental Toxicology and Chemistry*, **29**(4), 893–901.

- Jeon, J.; Kurth, D.; Ashauer, R. and Hollender, J. 2013. Comparative toxicokinetics of organic micropollutants in freshwater crustaceans. *Environmental Science & Technology*, **47**(15), 8809–8817.
- Jin, J.Y.; Almon, R.R.; DuBois, D.C. and Jusko, W.J. 2003. Modeling of corticosteroid pharmacogenomics in rat liver using gene microarrays. *Journal of Pharmacology and Experimental Therapeutics*, **307**(1), 93–109.
- Junghans, M.; Backhaus, T.; Faust, M.; Scholze, M. and Grimme, L.H. 2003. Predictability of combined effects of eight chloroacetanilide herbicides on algal reproduction. *Pest Management Science*, **59**(10), 1101–1110.
- Jusko, W. J. 2013. Moving from basic toward systems pharmacodynamic models. *Journal of Pharmaceutical Sciences*, **102**(9), 2930–2940.
- Jusko, W.J.; Ko, H.C. and Ebling, W.F. 1995. Convergence of direct and indirect pharmacodynamic response models - response. *Journal of Pharmacokinetics and Biopharmaceutics*, **23**(1), 5–8.
- Kluender, C.; Sans-Piché, F.; Riedl, J.; Altenburger, R.; Hartig, C.; Laue, G. and Schmitt-Jansen, M. 2009. A metabolomics approach to assessing phytotoxic effects on the green alga *Scenedesmus vacuolatus*. *Metabolomics*, **5**(1), 59–71.
- Kolpin, D.W.; Furlong, E.T.; Meyer, M.T.; Thurman, E.M.; Zaugg, S.D.; Barber, L.B. and Buxton, H.T. 2002. Pharmaceuticals, hormones, and other organic wastewater contaminants in US streams, 1999-2000: A national reconnaissance. *Environmental Science & Technology*, **36**(6), 1202–1211.
- Könemann, H. 1981. Quantitative structure-activity-relationships in fish toxicity studies. 1. Relationship for 50 industrial pollutants. *Toxicology*, **19**(3), 209–221.
- Könemann, H. and van Leeuwen, K. 1980. Toxicokinetics in fish: Accumulation and elimination of six chlorobenzenes by guppies. *Chemosphere*, **9**(1), 3–19.
- Kooijman, S. and Bedaux, J.J.M. 1996. The analysis of aquatic toxicity data. VU University Press Amsterdam.
- Kooijman, SALM. 2000. Dynamic energy and mass budgets in biological systems. Cambridge University Press.
- Kretschmann, A.; Ashauer, R.; Hitzfeld, K.; Spaak, P.; Hollender, J. and Escher, B.I. 2011a. Mechanistic toxicodynamic model for receptor-mediated toxicity of diazoxon, the active metabolite of Diazinon, in *Daphnia magna*. *Environmental Science & Technology*, **45**(11), 4980–4987.
- Kretschmann, A.; Ashauer, R.; Preuss, T.G.; Spaak, P.; Escher, B.I. and Hollender, J. 2011b. Toxicokinetic model describing bioconcentration and biotransformation of diazinon in *Daphnia magna*. *Environmental Science & Technology*, **45**(11), 4995–5002.
- Kretschmann, A.; Ashauer, R.; Hollender, J. and Escher, B.I. 2012. Toxicokinetic and toxicodynamic model for diazinon toxicity-mechanistic explanation of differences in the

- sensitivity of *Daphnia magna* and *Gammarus pulex*. *Environmental Toxicology and Chemistry*, **31**(9), 2014–2022.
- Krupinska, K. and Humbeck, K. 1994. New trends in photobiology: Light-induced synchronous cultures, an excellent tool to study the cell cycle of unicellular green algae. *Journal of Photochemistry and Photobiology B: Biology*, **26**(3), 217–231.
- Kühnert, A.; Vogs, C.; Altenburger, R. and Küster, E. 2013. The internal concentration of organic substances in fish embryos A toxicokinetic approach. *Environmental Toxicology and Chemistry*, **32**(8), 1819–1827.
- Küsel, A.C.; Sianoudis, J.; Leibfritz, D.; Grimme, L.H. and Mayer, A. 1990. The dependence of the cytoplasmic pH in aerobic and anaerobic cells of the green algae *Chlorella fusca* and *Chlorella vulgaris* on the pH of the medium as determined by  $^{31}\text{P}$  *in vivo* NMR spectroscopy. *Archives of Microbiology*, **153**(3), 254–258.
- Laham, S. and Potvin, M. 1984. Comparative N-dephenylation of N-phenyl-2-naphthylamine in Sprague-Dawley rats and New Zealand white rabbits. *Chemosphere*, **13**(5-6), 657–667.
- Landrum, P.F.; Lee, H. and Lydy, M. . 1992. Toxicokinetics in aquatic systems: model comparisons and use in hazard assessment. *Environmental Toxicology and Chemistry*, **11**(12), 1709–1725.
- Landrum, P.F.; Steevens, J.A.; McElroy, M.; Gossiaux, D.C.; Lewis, J.S and Robinson, S.D. 2005. Time-dependent toxicity of dichlorodiphenyldichloroethylene to *Hyalomma azteca*. *Environmental Toxicology and Chemistry*, **24**(1), 211–218.
- Larsson, DG.J. and Förlin, L. 2002. Male-biased sex ratios of fish embryos near a pulp mill: temporary recovery after a short-term shutdown. *Environmental Health Perspectives*, **110**(8), 739.
- Lederer, B. and Böger, P. 2005. A ligand function of glutathione S-transferase. *Zeitschrift für Naturforschung 60c*, 166–171.
- Lee, J.H.; Landrum, P.F. and Koh, C.H. 2002a. Prediction of time-dependent PAH toxicity in *Hyalomma azteca* using a damage assessment model. *Environmental Science & Technology*, **36**(14), 3131–3138.
- Lee, J.H.; Landrum, P.F. and Koh, C.H. 2002b. Toxicokinetics and time-dependent PAH toxicity in the amphipod *Hyalomma Azteca*. *Environmental Science & Technology*, **36**(14), 3124–3130.
- Legierse, K.; Verhaar, H.J.M.; Vaes, W.H. J.; De Bruijn, J.H.M. and Hermens, J.L.M. 1999. Analysis of the time-dependent acute aquatic toxicity of organophosphorus pesticides: The critical target occupation model. *Environmental Science & Technology*, **33**(6), 917–925.
- Liu, D.; Maguire, R.J.; Lau, Y.L.; Pacepavicius, G.J.; Okamura, H. and Aoyama, I. 1997. *Water Research*, **31**(9), 2363–2369.
- Mager, D. E. and Jusko, W. J. 2001. General pharmacokinetic model for drugs exhibiting target-mediated drug disposition. *Journal of Pharmacokinetics and Pharmacodynamics*, **28**(6), 507–532.

- Mager, D.E. and Jusko, W.J. 2008. Development of translational pharmacokinetic-pharmacodynamic models. *Clinical Pharmacology & Therapeutics*, **83**(6), 909–912.
- Mager, D.E.; Wyska, E. and Jusko, W.J. 2003. Diversity of mechanism-based pharmacodynamic models. *Drug Metabolism and Disposition*, **31**(5), 510–518.
- Magni, P.; Simeoni, M.; Poggesi, I.; Rocchetti, M. and De Nicolao, G. 2006. A mathematical model to study the effects of drugs administration on tumor growth dynamics. *Mathematical Biosciences*, **200**(2), 127–151.
- Malaj, E.; von der Ohe, P.C.; Grote, M.; Kühne, R.; Mondy, C. P.; Usseglio-Polatera, P.; Brack, W.r and Schäfer, R.B. 2014. Organic chemicals jeopardize the health of freshwater ecosystems on the continental scale. *Proceedings of the National Academy of Sciences*, **111**(26), 9549–9554.
- Manthey, M.; Faust, M.I; Smolka, S. and Grimme, H.L. 1993. Herbicide bioconcentration in algae: studies on lipophilicity-sorption-activity relationships (LSAR) with *Chlorella fusca*. *Science of the Total Environment*, **134**, 453–459.
- Martin, B.T.; Jager, T.; Nisbet, R.M.; Preuss, T.G. and Grimm, V. 2013. Predicting population dynamics from the properties of individuals: a cross-level test of Dynamic Energy Budget theory. *The American Naturalist*, **181**(4), 506–519.
- Martin, B.T.; Jager, T.; Nisbet, R.M.; Preuss, T.G.; Hammers-Wirtz, M. and Grimm, V. 2013b. Extrapolating ecotoxicological effects from individuals to populations: a generic approach based on Dynamic Energy Budget theory and individual-based modeling. *Ecotoxicology*, **22**(3), 574–583.
- Mayer, P.; Halling Sørensen, B.; Sijm, D.T. and Nyholm, N. 1998. Toxic cell concentrations of three polychlorinated biphenyl congeners in the green alga *Selenastrum capricornutum*. *Environmental Toxicology and Chemistry*, **17**(9), 1848–1851.
- McCarty, L.S. 1986. The relationship between aquatic toxicity QSARs and bioconcentration for some organo-chemicals. *Environmental Toxicology and Chemistry*, **5**(12), 1071–1080.
- McCarty, L.S. and Mackay, D. 1993. Enhancing ecotoxicological modeling and assessment. *Environmental Science & Technology*, **27**(9), 1719–1728.
- McCarty, L.S.; Landrum, P.F.; Luoma, S.N.; Meador, J.P.; Merten, A.A.; Shephard, B.K. and van Wezel, A.P. 2011. Advancing environmental toxicology through chemical dosimetry: External exposures versus tissue residues. *Integrated Environmental Assessment and Management*, **7**, 7–27.
- McCarty, L.S.; Arnot, J.A. and Mackay, D. 2013. Evaluation of critical body residue data for acute narcosis in aquatic organisms. *Environmental Toxicology and Chemistry*, **32**(10), 2301–2314.
- Meador, J.P.; McCarty, L.S.; Escher, B.I. and Adams, W.J. 2008. 10th Anniversary Critical Review: The tissue-residue approach for toxicity assessment: concepts, issues, application, and recommendations. *Journal of Environmental Monitoring*, **10**(12), 1486–1498.
- Mittag, M.; Kiaulehn, S. and Johnson, C.H. 2005. The circadian clock in *Chlamydomonas reinhardtii*. What is it for? What is it similar to? *Plant physiology*, **137**(2), 399–409.

- Mortimer, M.R. and Connell, D.W. 1994. Critical internal and aqueous lethal concentrations of chlorobenzenes with the crab *Portunus pelagicus* (L). *Ecotoxicology and Environmental Safety*, **28**(3), 298–312.
- Munkittrick, K.R.; Miller, P.A.; Barton, D.R. and Dixon, D.G. 1991. Altered performance of white sucker populations in the Manitowadge chain of lakes is associated with changes in benthic macroinvertebrate communities as a result of copper and zinc contamination. *Ecotoxicology and Environmental Safety*, **21**(3), 318–326.
- Neuwoehner, J. and Escher, B.I. 2011. The pH-dependent toxicity of basic pharmaceuticals in the green algae *Scenedesmus vacuolatus* can be explained with a toxicokinetic ion-trapping model. *Aquatic Toxicology*, **101**(1), 266–275.
- Neuwoehner, J.; Junghans, M.; Koller, M. and Escher, B.I. 2008. QSAR analysis and specific endpoints for classifying the physiological modes of action of biocides in synchronous green algae. *Aquatic Toxicology*, **90**(1), 8–18.
- Nichols, J.W.; McKim, J.M.; Andersen, M.E.; Gargas, M.L.; Clewell, H.J. and Erickson, R.J. 1990. A physiologically based toxicokinetic model for the uptake and disposition of waterborne organic chemicals in fish. *Toxicology and Applied Pharmacology*, **106**(3), 433–447.
- Nisbet, R.M.; Muller, E.B.; Lika, K. and Kooijman, SALM. 2000. From molecules to ecosystems through dynamic energy budget models. *Journal of animal ecology*, **69**(6), 913–926.
- Nobusaws, T. and Umeda, M. 2012. Very-long-chain fatty acids have an essential role in plastid division by controlling Z-ring formation in *Arabidopsis thaliana*. *Genes Cells*, **17**(8), 709–719.
- Nuutinen, S.; Landrum, P.F.; Schuler, L.J.; Kukkonen, J.V.K. and Lydy, M.J. 2003. Toxicokinetics of organic contaminants in *Hyalella azteca*. *Archives of Environmental Contamination and Toxicology*, **44**(4), 467–475.
- Nyman, A.-M.; Schirmer, K. and Ashauer, R. 2012. Toxicokinetic-toxicodynamic modelling of survival of *Gammarus pulex* in multiple pulse exposures to propiconazole: model assumptions, calibration data requirements and predictive power. *Ecotoxicology*, **21**(7), 1828–1840.
- Nyman, AM.; Schirmer, K. and Ashauer, R. 2014. Importance of toxicokinetics for interspecies variation in sensitivity to chemicals. *Environmental Science & Technology*, **48**(10), 5946–5954.
- Ohe, T.; Watanabe, T. and Wakabayashi, K. 2004. Mutagens in surface waters: a review. *Mutation Research/Reviews in Mutation Research*, **567**(2), 109–149.
- Péry, A.R.R.; Bedaux, J.J.M.; Zonneveld, C. and Kooijman, SALM. 2001. Analysis of bioassays with time-varying concentrations. *Water Research*, **35**(16), 3825–3832.
- Péry, A.R.R.; Flammarion, P.; Vollat, B.; Bedaux, J. J. M.; Kooijman, SALM and Garric, J. 2002. Using a biology-based model (DEBtox) to analyze bioassays in ecotoxicology: Opportunities and recommendations. *Environmental Toxicology and Chemistry*, **21**(2), 459–465.
- Pillai, S.; Behra, R.; Nestler, H.; Suter, M.; Sigg, L. and Schirmer, K. 2014. Linking toxicity and adaptive responses across the transcriptome, proteome, and phenotype of *Chlamydomonas reinhardtii* exposed to silver. *Proceedings of the National Academy of Sciences*, **111**(9), 3490–3495.

- Ramakrishnan, R.; DuBois, D.C.; Almon, R.R.; Pyszczynski, N.J. and Jusko, W.J. 2002. Fifth-Generation Model for Corticosteroid Pharmacodynamics: Application to Steady-State Receptor Down-Regulation and Enzyme Induction Patterns During Seven-Day Continuous Infusion of Methylprednisolone in Rats. *Journal of Pharmacokinetics and Pharmacodynamics*, **29**(1), 1–24.
- Reinert, K.H.; Giddings, J.A. and Judd, L. 2002. Effects analysis of time-varying or repeated exposures in aquatic ecological risk assessment of agrochemicals. *Environmental Toxicology and Chemistry*, **21**(9), 1977–1992.
- Richardson, B.J.; Lam, P.K.S. and Martin, M. 2005. Emerging chemicals of concern: pharmaceuticals and personal care products (PPCPs) in Asia, with particular reference to Southern China. *Marine Pollution Bulletin*, **50**(9), 913–920.
- Ritter, K.S.; Sibley, P.; Hall, K.; Keen, P.; Mattu, G. and Len, B.L. 2002. Sources, pathways, and relative risks of contaminants in surface water and groundwater: a perspective prepared for the Walkerton inquiry. *Journal of Toxicology and Environmental Health Part A*, **65**(1), 1–142.
- Ritz, C. and Streibig, J.C. 2005. Bioassay analysis using R. *Journal of Statistical Software*, **12**(5), 1–22.
- Rockström, J.; Steffen, W.; Noone, K.; Persson, Å.; Chapin, F.S.; Lambin, E.F.; Lenton, T.M.; Scheffer, M.; Folke, C. and Schellnhuber, H.J. 2009. A safe operating space for humanity. *Nature*, **461**(7263), 472–475.
- Rotter, S.; Heilmeier, H.; Altenburger, R. and Schmitt-Jansen, M. 2013. Multiple stressors in periphyton—comparison of observed and predicted tolerance responses to high ionic loads and herbicide exposure. *Journal of applied ecology*, **50**(6), 1459–1468.
- Rozman, K.K. and Doull, J. 2000. Dose and time as variables of toxicity. *Toxicology*, **144**(1-3), 169–178.
- Rubach, M.N.; Ashauer, R.; Maund, S.J.; Baird, D.J. and Van den Brink, P.J. 2010. Toxicokinetic variation in 15 freshwater arthropod species exposed to the insecticide chlorpyrifos. *Environmental Toxicology and Chemistry*, **29**(10), 2225–2234.
- Rubach, M.N.; Crum, S.J.H. and Van den Brink, P.J. 2011. Variability in the dynamics of mortality and immobility responses of freshwater arthropods exposed to chlorpyrifos. *Archives of Environmental Contamination and Toxicology*, **60**(4), 708–721.
- Rubach, M.N.; Baird, D.J.; Boerwinkel, M.C.; Maund, S.J.; Roessink, I. and Van den Brink, P.J. 2012. Species traits as predictors for intrinsic sensitivity of aquatic invertebrates to the insecticide chlorpyrifos. *Ecotoxicology*, **21**(7), 2088–2101.
- Sans-Piché, F.; Kluender, C.; Altenburger, R. and Schmitt-Jansen, M. 2010. Anchoring metabolic changes to phenotypic effects in the chlorophyte *Scenedesmus vacuolatus* under chemical exposure. *Marine Environmental Research*, **69**(1), 28–30.
- Schuler, L.J.; Landrum, P.F. and Lydy, M.J. 2004. Time-dependent toxicity of fluoranthene to freshwater invertebrates and the role of biotransformation on lethal body residues. *Environmental Science & Technology*, **38**(23), 6247–6255.

- Schwarzenbach, R.P.; Escher, B.I.; Fenner, K.; Hofstetter, T.B.; Johnson, C.A.; von Gunten, U. and Wehrli, B. 2006. The challenge of micropollutants in aquatic systems. *Science*, **313**(5790), 1072–1077.
- Schwarzenbach, R.P.; Egli, T.; Hofstetter, T.B.; von Gunten, U. and Wehrli, B. 2010. Global water pollution and human health. *Annual Review of Environment and Resources*. pp. 109–136.
- Sijm, D.T.; Broersen, K.W.; de Roode, D.F. and Mayer, P. 1998. Bioconcentration kinetics of hydrophobic chemicals in different densities of *Chlorella pyrenoidosa*. *Environmental Toxicology and Chemistry*, **17**(9), 1695–1704.
- Simeoni, M.; Magni, P.; Cammia, C.; De Nicolao, G.; Croci, V.; Pesenti, E.; Germani, M.; Poggesi, I. and Rocchetti, M. 2004. Predictive pharmacokinetic-pharmacodynamic modeling of tumor growth kinetics in xenograft models after administration of anticancer agents. *Cancer Research*, **64**(3), 1094–1101.
- Skoglund, R. S.; Stange, K. and Swackhamer, D. L. 1996. A kinetics model for predicting the accumulation of PCBs in phytoplankton. *Environmental Science & Technology*, **30**(7), 2113–2120.
- Södergren, A. 1968. Uptake and accumulation of C 14-DDT by *Chlorella sp.* (Chlorophyceae). *Oikos*, **19**, 126–138.
- Spacie, A. and Hamelink, J.L. 1982. Alternative models for describing the bioconcentration of organics in fish. *Environmental Toxicology and Chemistry*, **1**(4), 309–320.
- Stadnicka, J.; Schirmer, K. and Ashauer, R. 2012. Predicting concentrations of organic chemicals in fish by using toxicokinetic models. *Environmental Science & Technology*, **46**(6), 3273–3280.
- Steffen, W.; Richardson, K.; Rockström, J.; Cornell, S.E.; Fetzer, I.; Bennett, E.M.; Biggs, R.; Carpenter, S.R.; de Vries, W. and de Wit, C.A. 2015. Planetary boundaries: Guiding human development on a changing planet. *Science*, DOI: 10.1126/science.1259855.
- Storn, R. and Price, K. 1995. Differential evolution—a simple and efficient adaptive scheme for global optimization over continuous spaces. Vol. 3. ICSI Berkeley.
- Sun, Y. N. and Jusko, W. J. 1998. Transit compartments versus gamma distribution function to model signal transduction processes in pharmacodynamics. *Journal of Pharmaceutical Sciences*, **87**(6), 732–737.
- Swackhamer, D.L. and Skoglund, R.S. 1993. Bioaccumulation of PCBs by algae: kinetics versus equilibrium. *Environmental Toxicology and Chemistry*, **12**(5), 831–838.
- Taher, S.A. and Afsari, S.A. 2012. Optimal location and sizing of UPQC in distribution networks using differential evolution algorithm. *Mathematical Problems in Engineering*, **2012**.
- Tang, J.; Hoagland, K.D. and Siegfried, B.D. 1998. Uptake and bioconcentration of atrazine by selected freshwater algae. *Environmental Toxicology and Chemistry*, **17**(6), 1085–1090.
- Thies, F.; Backhaus, T.; Bossmann, B. and Grimme, L.H. 1996. Xenobiotic Biotransformation in Unicellular Green Algae. Involvement of Cytochrome P450 in the Activation and Selectivity of the Pyridazinone Pro-Herbicide Metflurazon. *Plant physiology*, **112**(1), 361.

- Vallotton, N.; Ilda, R.; Eggen, L.; Escher, B.I.; Krayenbuhl, J. and Chèvre, N. 2008a. Effect of pulse herbicidal exposure on *Scenedesmus vacuolatus*: A comparison of two photosystem II inhibitors. *Environmental Toxicology and Chemistry*, **27**(6), 1399–1407.
- Vallotton, N.; Moser, D.; Eggen, R.I.; Junghans, M. and Chèvre, N. 2008b. S-metolachlor pulse exposure on the alga *Scenedesmus vacuolatus*: Effects during exposure and the subsequent recovery. *Chemosphere*, **73**(3), 395–400.
- Vallotton, N.; Eggen, R.I.L. and Chèvre, N. 2009. Effect of sequential isoproturon pulse exposure on *Scenedesmus vacuolatus*. *Archives of Environmental Contamination and Toxicology*, **56**(3), 442–449.
- Van Hoogen, G. and Opperhuizen, A. 1988. Toxicokinetics of chlorobenzenes in fish. *Environmental Toxicology and Chemistry*, **7**(3), 213–219.
- van Straalen, N.M. and Feder, M.E. 2011. Ecological and evolutionary functional genomics- How can it contribute to the risk assessment of chemicals? *Environmental Science & Technology*, **46**(1), 3–9.
- van Wezel, A. P. and Opperhuizen, A. 1995. Narcosis due to environmental pollutants in aquatic organisms: residue-based toxicity, mechanisms, and membrane burdens. *Critical Reviews in Toxicology*, **25**(3), 255–279.
- Veith, G.D.; Call, D.J. and Brooke, LT. 1983. Structure-toxicity relationships for the fathead minnow, *Pimephales promelas*: narcotic industrial chemicals. *Canadian Journal of Fisheries and Aquatic Sciences*, **40**(6), 743–748.
- Verhaar, H.J.M.; Vanleeuwen, C.J. and Hermens, J.L.M. 1992. Classifying environmental-pollutants .1. Structure-activity-relationships for prediction of aquatic toxicity. *Chemosphere*, **25**(4), 471–491.
- Verhaar, H.J.M.; de Wolf, W.; Dyer, S.; Legierse, K.C.H.M.; Seinen, W. and Hermens, J.L.M. 1999. An LC50 vs time model for the aquatic toxicity of reactive and receptor-mediated compounds. Consequences for bioconcentration kinetics and risk assessment. *Environmental Science & Technology*, **33**(5), 758–763.
- Villeneuve, D.L. and Garcia-Reyero, N. 2011. Vision & strategy: Predictive ecotoxicology in the 21st century. *Environmental Toxicology and Chemistry*, **30**(1), 1–8.
- Vogs, C.; Bandow, N. and Altenburger, R. 2013. Effect propagation in a toxicokinetic/toxicodynamic model explains delayed effects on the growth of unicellular green algae *Scenedesmus vacuolatus*. *Environmental Toxicology and Chemistry*, **32**(5), 1161–1172.
- Vogs, C.; Kühnert, A.; Hug, C.; Küster, E. and Altenburger, R. 2015. A toxicokinetic study of specifically acting and reactive organic chemicals for the prediction of internal effect concentrations in *Scenedesmus vacuolatus*. *Environmental Toxicology and Chemistry*, **34**(1), 100–111.
- von der Ohe, P.C.; De Deckere, E.; Prü[ss, A.; Munoz, I.; Wolfram, G.; Villagrasa, M.; Ginebreda, A.; Hein, M. and Brack, W. 2009. Toward an integrated assessment of the ecological

- and chemical status of European river basins. *Integrated Environmental Assessment and Management*, **5**(1), 50–61.
- Vörösmarty, C.J.; McIntyre, P.B.; Gessner, M.O.; Dudgeon, D.; Prusevich, A.; Green, P.; Glidden, S.; Bunn, S.E.; Sullivan, C.A. and Liermann, C. R. 2010. Global threats to human water security and river biodiversity. *Nature*, **467**(7315), 555–561.
- Ševčovičová, A.; Hamzová, A.; Gálová, E. and Vlček, D. 2008. Use of algae in the study of essential cell processes. *Biologia*, **63**(6), 952–957.
- Weber, D.; Schäffer, D.; Dorgerloh, M.; Bruns, E; Görlitz, G.; Hammel, K.; Greuss, T. G. and Ratte, H. T. 2012. Combination of a higher-tier flow-through system and population modeling to assess the effects of time-variable exposure of isoproturon on the green algae *Desmodesmus subspicatus* and *Pseudokirchneriella subcapitata*. *Environmental Toxicology and Chemistry*, **31**(3), 899–908.
- Weiner, J.A.; DeLorenzo, M.E. and Fulton, M.H. 2004. Relationship between uptake capacity and differential toxicity of the herbicide atrazine in selected microalgal species. *Aquatic Toxicology*, **68**(2), 121–128.
- Whitehorn, P.R.; O'Connor, S.; Wackers, F.L. and Goulson, D. 2012. Neonicotinoid pesticide reduces bumble bee colony growth and queen production. *Science*, **336**(6079), 351–352.
- Wittmer, I.K.; Bader, H.P.; Scheidegger, R.; Singer, H.; Luck, A.; Hanke, I.; Carlsson, C. and Stamm, C. 2010. Significance of urban and agricultural land use for biocide and pesticide dynamics in surface waters. *Water Research*, **44**(9), 2850–2862.
- World Health Organization. 2004. IPCS risk assessment terminology. IPCS Harmonization Project.
- Yu, Q.; Chaisuksant, Y. and Connell, D. 1999. A model for non-specific toxicity with aquatic organisms over relatively long periods of exposure time. *Chemosphere*, **38**(4), 909–918.

APPENDIX **A**

## Supplementary information for Chapter 2

**Table A.1:** Measured cell number for two untreated algae cell cultures (c1/c2), two DMSO-treated algae cell cultures (DMSO1/DMSO2) and norflurzon-treated algae cultures exposed to six concentrations over two hours. Grey highlighted boxes represent the cell volumes of the second algae generation which were excluded for calibrating purposes.

Time h	c1	c2	DMSO1	DMSO2	2.18 $\mu\text{g L}^{-1}$	3.37 $\mu\text{g L}^{-1}$	3.96 $\mu\text{g L}^{-1}$	4.75 $\mu\text{g L}^{-1}$	5.74 $\mu\text{g L}^{-1}$	14.85 $\mu\text{g L}^{-1}$
2a	0.7968	0.8888	0.8628	0.8567	0.8492	0.8567	0.8431	0.8413	0.8413	0.8335
2b	0.8188	0.8425	0.8454	0.8350	0.8683	0.8147	0.7892	0.8570	0.8332	0.8425
4a	1.0110	0.9528	0.9259	0.9383	0.9244	0.9010	0.9013	0.9551	0.9320	0.9424
4b	0.9893	0.9522	0.9760	0.9517	0.8738	0.9027	0.8596	0.9282	0.9323	0.9737
6a	1.0420	1.0070	1.0070	0.9569	0.9027	0.9140	0.9664	0.9745	0.9337	0.9464
6b	0.9511	0.9427	0.9311	0.9855	0.9195	0.9653	0.9010	0.8683	0.9291	0.9569
8a	0.9291	0.9742	0.9441	0.9065	0.8992	0.9560	0.9019	0.9676	0.9812	0.9357
8b	0.9670	0.9754	0.9357	0.9444	0.9158	0.9152	0.8683	0.9557	0.9731	0.9682
10a	0.8975	0.8700	0.8807	0.7843	0.8230	0.8929	0.9033	0.7832	0.8929	0.9143
10b	0.9074	0.9320	0.9047	0.7710	0.9021	0.8822	0.9030	0.7947	0.9114	0.9360
12a	0.8248	0.8772	0.8405	0.7669	0.8468	0.8373	0.8509	0.8607	0.8567	0.8790
12b	0.8127	0.9317	0.8584	0.7875	0.8587	0.8205	0.9091	0.8515	0.8486	0.8665
14a	0.6893	0.6841	0.6433	0.6181	0.6268	0.6769	0.6581	0.7212	0.7655	0.7510
14b	0.6875	0.6728	0.6291	0.6248	0.6340	0.6451	0.6340	0.6543	0.7273	0.8321
14a	0.8790	0.8202	0.8283	0.8069	0.8489	0.7988	0.8384	0.7748	0.7360	0.8431
14b	0.9007	0.8292	0.8066	0.8136	0.8202	0.7982	0.7907	0.8292	0.6340	0.8576
16a	0.6804	0.6320	0.6705	0.6164	0.6222	0.6572	0.6517	0.6697	0.6572	0.7157
16b	0.6940	0.6520	0.5602	0.5883	0.6109	0.6604	0.6523	0.7096	0.6711	0.7400
18a	0.6552	0.5220	0.6584	0.6384	0.6462	0.6546	0.6844	0.7215	0.6830	0.8350
18b	0.6569	0.6039	0.6702	0.6034	0.6068	0.6688	0.6972	0.6810	0.7195	0.7279
20a-Peak1	0.5712	0.3004	0.6540	0.6097	0.6511	3.2450	1.1230	0.8845	0.7475	0.7475
20a-Peak2	0.6002	0.6283	0.6199	0.5790	0.5845	0.3772	0.5368	0.6349	0.5414	
20b-Peak1	0.5877	0.3599	0.6427	0.6847	0.5828	3.3070	1.1310	0.8373	0.9638	0.7568
20b-Peak2	0.6584	0.6563	0.5924	0.5732	0.5452	0.3995	0.5814	0.5695	0.5938	
22a	6.6360	6.4500	7.2350	6.6000	6.7130	6.8890	6.9210	5.1390	4.7000	0.9062
22b	7.1790	6.2390	7.0840	6.2300	6.7940	7.0320	6.9430	5.1940	4.7300	0.8202
24a	10.6900	7.8890	10.9800	9.8680	9.9320	6.9680	7.3190	6.2800	6.4330	0.8063
24b	10.6700	8.6400	10.9000	9.6090	10.3700	7.3890	7.5450	5.8570	6.4500	0.7264

**Table A.2:** Measured cell volume for two untreated algae cell cultures (c1/c2), two DMSO-treated algae cell cultures (DMSO1/DMSO2) and norflurazon-treated algae cultures exposed to six concentrations every two hours. Grey highlighted boxes represent the cell volumes of the second algae generation which were excluded for calibrating purposes.

	Time h	c1	c2	DMSO1	DMSO2	2.18 $\mu\text{g L}^{-1}$	3.37 $\mu\text{g L}^{-1}$	3.96 $\mu\text{g L}^{-1}$	4.75 $\mu\text{g L}^{-1}$	5.74 $\mu\text{g L}^{-1}$	14.85 $\mu\text{g L}^{-1}$
culture 1	2a	33.06	33.83	33.08	33.33	33.89	33.28	32.69	32.86	33.30	33.06
	2b	31.86	32.20	33.18	32.73	35.06	33.36	32.46	33.39	33.83	34.78
	4a	53.30	54.67	54.46	54.67	56.54	55.93	57.14	55.63	54.33	54.10
	4b	53.35	54.46	54.45	55.04	54.30	57.18	58.54	56.23	55.71	58.57
	6a	84.94	84.61	83.98	82.02	84.07	100.40	83.56	84.87	85.39	75.50
	6b	83.42	81.89	83.30	83.00	84.37	99.36	84.80	87.29	86.32	75.72
	8a	132.60	130.50	131.40	129.70	130.10	133.50	117.30	125.10	120.30	82.94
	8b	130.00	130.60	131.20	129.40	129.60	130.90	118.40	126.90	119.40	86.43
	10a	178.90	183.90	183.40	181.70	177.70	178.30	140.40	153.10	134.00	85.95
	10b	180.70	180.20	183.60	177.80	177.80	180.90	136.00	156.20	137.90	82.74
	12a	255.20	256.20	249.10	247.70	239.00	240.70	150.40	175.20	147.10	78.83
	12b	246.10	256.40	247.50	243.90	245.70	232.70	154.10	177.80	143.90	77.33
	14a	372.50	375.30	380.30	376.60	387.40	321.20	342.60	271.00	223.90	82.48
	14b	375.60	378.70	374.50	381.10	386.30	311.40	345.00	257.70	223.70	83.79
culture 2	14a	347.60	345.40	337.20	337.30	335.50	306.90	161.60	206.70	163.70	79.82
	14b	343.80	346.20	335.40	336.20	332.20	310.90	165.10	202.40	163.00	80.34
	16a	498.20	490.10	508.30	497.40	504.20	330.40	379.20	308.30	278.70	87.02
	16b	498.90	492.80	496.10	502.30	515.00	328.60	385.70	320.10	286.20	82.39
	18a	570.30	539.10	570.60	570.30	593.20	352.10	400.50	324.60	328.20	79.79
	18b	567.80	540.50	565.70	568.30	586.40	346.20	402.20	328.40	310.50	84.50
	20a-Peak1	32.52	30.03	31.30	31.21	32.40	28.99	29.74	28.48	26.09	80.34
	20a-Peak2	635.90	583.60	634.40	596.10	637.10	338.60	421.60	328.20	366.10	
	20b-Peak1	30.12	33.37	31.93	29.71	30.75	29.28	30.06	27.68	26.99	82.23
	20b-Peak2	622.10	576.10	635.00	619.10	615.90	337.00	417.70	337.20	357.80	
	22a	34.28	32.24	33.10	33.15	33.51	35.65	32.34	33.38	32.88	70.10
	22b	33.93	31.93	33.34	33.22	33.27	35.54	32.37	33.18	32.67	75.16
	24a	35.75	33.68	38.31	36.81	36.68	38.60	37.63	46.37	44.28	70.00
	24b	35.97	33.11	36.71	35.27	37.65	41.49	40.29	41.31	44.23	74.49

**Table A.3:** Measured cell number for two untreated algae cell cultures (c1/c2), two DMSO-treated algae cell cultures (DMSO1/DMSO2) and PNA-treated algae cultures exposed to six concentrations every two hours. Grey highlighted boxes represent the cell volumes of the second algae generation which were excluded for calibrating purposes.

Time h	c1	c2	DMSO1	DMSO2	44.47 $\mu\text{g L}^{-1}$	44.47 $\mu\text{g L}^{-1}$	47.23 $\mu\text{g L}^{-1}$	47.23 $\mu\text{g L}^{-1}$	50.16 $\mu\text{g L}^{-1}$	50.16 $\mu\text{g L}^{-1}$	80.30 $\mu\text{g L}^{-1}$	159.58 $\mu\text{g L}^{-1}$	198.81 $\mu\text{g L}^{-1}$	
culture 1	2a	0.8228	0.8049	0.8746	0.9039	0.8772	0.8463	0.8813	0.8538	0.8098	0.8329	0.6786	0.7383	0.7950
	2b	0.8660	0.8301	0.8312	0.8431	0.8156	0.8495	0.8104	0.8709	0.8008	0.7140		0.7712	0.7791
	4a	0.9369	1.0180	0.9638	0.9427	0.9696	0.9887	0.8555	0.9476	0.9928	0.9421	0.6653	0.7927	0.7897
	4b	0.9450	0.9858	0.9650	0.9343	0.9563	0.9036	0.8616	0.9172	0.9540	0.9641		0.8421	0.8097
	6a	0.9960	0.9360	0.9372	0.9239	0.9835	0.9294	0.9922	0.9450	0.9739	0.9682	0.6375	0.7505	0.7377
	6b	0.9786	0.9574	0.9252	0.9531	0.9175	0.9323	0.9198	0.9276	0.9609	0.9268		0.7696	0.7865
	8a	0.7982	7.5960	0.9548	0.8822	0.9129	0.7884	0.9615	0.8819	0.8720	0.9123	0.6016	0.6943	0.7443
	8b	0.7713	8.0820	0.8827	0.7675	0.7878	0.8906	0.8964	0.8712	0.8411	0.9233		0.7279	0.7587
	10a	0.9100	0.8816	0.8891	0.8877	0.8686	0.7947	0.6500	0.8179	0.8964	0.8660	0.5843	0.6899	0.6406
	10b	0.9270	0.9126	0.9253	0.8654	0.8541	0.8118	0.6621	0.7846	0.9878	0.8738		0.5129	0.6801
	12a	0.8746	0.9314	0.8966	0.8327	0.8222	0.8072	0.9227	0.8547	0.9062	0.9227	0.7226	0.7151	0.6510
	12b	0.9131	0.9389	0.8955	0.8454	0.8315	0.7866	0.9598	0.9030	0.9433	0.9160		0.6345	0.6614
	14a	0.6841	0.7053	0.7418	0.7099	0.2759	0.3208	0.4459	0.5078	0.4351	0.5263	0.7698	0.7270	0.6950
	14b					0.5431	0.5032	0.3654	0.3196	0.3671	0.2203		0.6867	0.7166
culture2	14a	0.6943	0.7296	0.7050	0.7056	0.2241	0.3124	0.4433	0.4734	0.4270	0.5624	0.7415	0.6609	0.6833
	14b					0.5443	0.5287	0.3602	0.3251	0.3020	0.2467		0.7038	0.7567
	16a-Peak1	0.7171	0.7397	0.7264	0.7197	0.3092	0.3636	0.4806	0.5214	0.4896	0.6063	0.7762	0.3967	0.7620
	16a-Peak2					0.5330	0.4655	0.3318	0.3266	0.3442	0.2244			
	16b-Peak1	0.7241	0.6946	0.7058	0.6960	0.2894	0.3648	0.4673	0.5521	0.4713	0.6013		0.7806	0.7497
	16b-Peak2					0.5394	0.4980	0.3199	0.3017	0.3466	0.2283			
	18a-Peak1	0.6980	0.7053	0.6749	0.6589	0.2823	0.3555	0.4687	0.5452	0.4635	0.6135	0.7858	0.7332	0.7538
	18a-Peak2					0.5098	0.4716	0.3023	0.2999	0.2878	0.2273			
	18b-Peak1	0.6723	0.6691	0.6401	0.6485	0.2785	0.3477	0.4792	0.5246	0.4557	0.5026		0.7407	0.7879
	18b-Peak2					0.4951	0.4349	0.2782	0.2884	0.2918	0.1228			
	20a-Peak1	1.0830	1.1210	1.1310	1.2340	0.7719	0.7704	0.9340	0.7693	0.6477	0.6103	0.7209	0.7980	0.8051
	20a-Peak2	0.5996	0.6118	0.6036	0.5753	0.4331	0.4045	0.2438	0.1908	0.2455	0.1604			
	20b-Peak1	1.0670	1.1210	1.1330	1.2410	0.8179	0.7087	1.0140	0.9383	0.6225	0.6317		0.8181	0.8175
	20b-Peak2	0.5069	0.6118	0.5721	0.5394	0.4111	0.4013	0.2461	0.2189	0.2250	0.1065			
22a	7.8810	7.6960	6.8400	7.3840	4.8360	4.6350	3.4780	3.2010	3.0480	2.3670	0.7030	0.7549	0.8908	
22b	8.3540	7.2270	6.4660	7.5110	4.6970	4.1600	3.3460	3.1160	2.9160	2.4710		0.7100	0.7087	
24a	8.6970	8.2430	8.6910	9.0820	5.7840	5.2040	3.7140	3.5260	3.6820	2.9130	0.8442	0.7023	0.6580	
24b	8.8520	8.0040	8.4200	8.6380	5.8010	5.6620	4.1830	3.7310	3.7060	2.8580		0.6839	0.6852	

**Table A.4:** Measured cell volume for two untreated algae cell cultures (c1/c2), two DMSO-treated algae cell cultures (DMSO1/DMSO2) and PNA-treated algae cultures exposed to six concentrations every two hours. Grey highlighted boxes represent the cell volumes of the second algae generation which were excluded for calibrating purposes.

Time h	c1	c2	DMSO1	DMSO2	44.47 $\mu\text{g L}^{-1}$	44.47 $\mu\text{g L}^{-1}$	47.23 $\mu\text{g L}^{-1}$	47.23 $\mu\text{g L}^{-1}$	50.16 $\mu\text{g L}^{-1}$	50.16 $\mu\text{g L}^{-1}$	80.30 $\mu\text{g L}^{-1}$	159.58 $\mu\text{g L}^{-1}$	198.81 $\mu\text{g L}^{-1}$
2a	32.45	33.61	33.15	34.12	34.19	32.93	34.28	33.30	33.62	33.96	32.86	26.01	25.40
2b	32.38	33.05	33.03	33.80	33.60	32.64	33.57	35.14	34.93	33.88		25.78	25.08
4a	57.04	56.69	55.37	54.12	55.81	54.84	55.47	54.17	58.08	55.82	46.01	29.27	28.50
4b	54.04	56.39	56.05	54.49	56.21	54.14	53.94	54.16	55.94	56.27		29.19	28.52
6a	78.93	81.29	82.15	81.61	81.73	80.71	81.07	81.81	83.41	80.33	51.19	29.25	28.54
6b	80.91	85.05	83.55	82.73	79.72	81.76	82.57	82.88	81.67	78.25		29.45	28.34
8a	124.10	40.13	123.70	124.70	115.40	120.10	114.30	119.80	107.00	105.70	50.57	29.35	28.52
8b	119.60	40.72	126.60	116.80	115.70	114.50	110.00	111.80	107.50	101.00		29.86	28.66
10a	179.10	184.90	178.12	198.60	163.90	159.20	152.60	161.10	137.50	113.90	48.82	25.37	27.88
10b	179.90	181.80	180.50	200.30	158.70	162.50	147.80	165.70	137.90	110.50		26.47	27.33
12a	249.40	258.80	250.40	253.20	208.60	218.80	174.30	209.80	156.00	113.30	51.30	30.91	26.22
12b	245.00	255.30	251.40	247.80	202.10	210.00	182.30	213.70	154.50	114.70		26.92	26.21
14a	313.80	329.70	317.20	323.50	71.31	70.95	70.43	73.88	70.56	72.64	52.60	28.09	27.84
14b					312.90	317.50	276.40	303.00	287.90	299.10		28.03	27.78
14a	308.10	330.50	316.90	329.90	68.85	67.85	77.90	68.91	74.63	68.28	51.37	38.42	38.18
14b					316.50	307.40	283.40	287.50	293.10	297.10		36.48	35.98
16a-Peak1	403.60	413.60	421.20	418.20	72.40	78.38	79.08	76.23	74.29	76.04	64.20	41.23	39.91
16a-Peak2					400.40	395.70	375.60	409.50	390.50	419.20			
16b-Peak1	400.20	425.40	405.60	414.70	67.04	74.73	80.78	77.53	76.04	77.04		40.24	38.53
16b-Peak2					403.50	400.10	377.80	395.00	419.20	392.80			
18a-Peak1	459.90	474.50	480.30	474.60	76.33	78.03	76.19	73.83	74.47	76.81	63.42	40.95	41.40
18a-Peak2					475.20	475.60	437.40	432.50	481.60	449.80			
18b-Peak1	451.20	469.40	486.10	475.80	76.43	80.01	78.86	81.70	78.46	75.26		40.33	38.16
18b-Peak2					473.00	468.40	451.40	457.10	486.20	424.90			
20a-Peak1	32.21	28.87	32.36	31.90	35.91	38.61	43.25	40.14	54.97	58.56	64.06	45.04	43.43
20a-Peak2	469.40	462.20	495.70	468.20	496.30	478.70	433.90	440.70	514.20	488.90			
20b-Peak1	30.96	30.88	31.85	31.61	39.08	38.01	47.59	46.26	54.53	59.90		42.88	45.48
20b-Peak2	456.10	458.00	487.70	479.90	477.50	492.20	438.20	454.80	504.00	509.70			
22a	34.67	35.58	34.04	32.67	36.71	38.63	32.73	34.56	41.47	38.24	61.03	39.30	37.09
22b	34.47	34.28	32.20	34.25	37.48	35.81	31.15	35.74	40.36	40.71		39.52	38.62
24a	41.40	42.06	45.31	43.32	47.65	44.45	35.71	39.31	46.75	45.46	65.27	38.72	36.19
24b	41.80	42.39	44.10	43.66	49.46	46.41	38.56	41.50	45.79	43.71		40.62	39.42

**Table A.5:** Measured cell number for two untreated algae cell cultures (c1/c2), two DMSO-treated algae cell cultures (DMSO1/DMSO2) and triclosan-treated algae cultures exposed to six concentrations every two hours. Grey highlighted boxes represent the cell volumes of the second algae generation which were excluded for calibrating purposes.

	Time h	c1	c2	DMSO1	DMSO2	0.72 $\mu\text{g L}^{-1}$	1.47 $\mu\text{g L}^{-1}$	2.32 $\mu\text{g L}^{-1}$	3.56 $\mu\text{g L}^{-1}$	5.12 $\mu\text{g L}^{-1}$	15.66 $\mu\text{g L}^{-1}$
culture 1	2a	0.8144	0.7837	0.7695	0.8066	0.7881	0.8370	0.8072	0.7687	0.8289	0.7985
	2b	0.8118	0.8683	0.7840	0.8063	0.7889	0.7701	0.8034	0.8590	0.8709	0.7464
	4a	0.7409	0.7053	0.7377	0.7513	0.7154	0.6549	0.7374	0.6891	0.7058	0.6812
	4b	0.7284	0.7302	0.6911	0.7632	0.7114	0.6731	0.7140	0.7212	0.7528	0.6798
	6a	0.7371	0.7745	0.7559	0.7846	0.7302	0.7745	0.7261	0.7910	0.7863	0.7325
	6b	0.7478	0.7690	0.7406	0.7250	0.7449	0.7365	0.7192	0.7449	0.7568	0.7064
	8a	0.7635	0.7481	0.7533	0.7629	0.7169	0.6943	0.7562	0.7713	0.7247	0.7336
	8b	0.7600	0.7548	0.7684	0.7736	0.6778	0.7224	0.7238	0.7409	0.7030	0.7305
	10a	0.6741	0.6578	0.6395	0.6320	0.6048	0.6416	0.6251	0.6523	0.6320	0.6196
	10b	0.7024	0.7012	0.6746	0.6856	0.6879	0.6766	0.6642	0.6833	0.6630	0.6262
	12a	0.6283	0.6251	0.2740	0.6071	0.6274	0.5353	0.6364	0.6028	0.6459	0.6401
	12b	0.6508	0.6575	0.6019	0.6700	0.6106	0.5417	0.6126	0.6312	0.6873	0.6723
	14a	0.7186	0.7281	0.7079	0.7218	0.7229	0.7070	0.7467	0.7907	0.7944	0.8784
	14b	0.7200	0.7076	0.7273	0.7348	0.6801	0.6998	0.6934	0.7988	0.7832	0.7652
culture 2	14a	0.5469	0.5834	0.6228	0.6118	0.6057	0.5744	0.6019	0.5602	0.5996	0.6436
	14b	0.6482	0.6109	0.5831	0.5947	0.5843	0.5814	0.5382	0.5964	0.6314	0.9178
	16a	0.6896	0.5850	0.6850	0.7006	0.6766	0.7255	0.7360	0.7884	0.7869	0.8295
	16b	0.7299	0.6633	0.6986	0.7241	0.6905	0.7319	0.7284	0.7843	0.7137	0.9111
	18a	0.6830	0.6372	0.6144	0.6572	0.6410	0.6702	0.6818	0.7895	0.7823	0.8422
	18b	0.6259	0.6410	0.6326	0.6361	0.6390	0.6326	0.6815	0.7600	0.7273	0.8321
	20a-Peak1	0.9401	1.0120	1.1830	1.1600	1.3960	1.4520	0.9490	0.2111	0.7643	0.8031
	20a-Peak2	0.5585	0.6158	0.6228	0.6242	0.5498	0.6306	0.6019	0.7061		
	20b-Peak1	1.0280	0.9818	1.1850	1.1640	1.2970	1.4070	0.9852	0.1699	0.7473	0.8191
	20b-Peak2	0.6097	0.6259	0.5631	0.5909	0.5950	0.5738	0.6358	0.7516		
	22a-Peak1	7.2860	7.3190	7.3210	7.0720	6.9730	7.3270	4.9440	0.9818	0.7429	0.7762
	22a-Peak2	0.5159	0.8098	0.5529	0.5602	0.5252	0.6352	0.7186	0.7099		
	22b-Peak1	7.2140	6.9970	7.2450	6.7740	6.7340	7.1670	4.9900	0.9331	0.7794	0.8222
	22b-Peak2	0.5203	0.5081	0.5565	0.5921	0.5255	0.5834	0.5950	0.7611		
	24a-Peak1	8.0520	8.3000	8.3980	7.5590	7.1170	7.5960	5.4900	1.2860	0.7157	0.6236
	24a-Peak2								0.7811		
	24b-Peak1	7.9140	8.0910	8.5900	7.9210	7.2720	7.9950	7.2760	1.4440	0.6995	0.6462
	24b-Peak2								0.6786		
	26a-Peak1	9.0690	8.5530	9.2400	8.1630	8.3380	7.5810	6.5500	1.5690	0.4163	0.1766
	26a-Peak2								0.8730	0.7024	0.6097
	26b-Peak1	8.9800	8.6120	8.9070	8.3830	8.1610	8.2390	6.8690	1.5580	0.4149	0.1763
	26b-Peak2								0.7076	0.7177	0.5284

**Table A.6:** Measured cell volume for two untreated algae cell cultures (c1/c2), two DMSO-treated algae cell cultures (DMSO1/DMSO2) and triclosan-treated algae cultures exposed to six concentrations every two hours. Grey highlighted boxes represent the cell volumes of the second algae generation which were excluded for calibrating purposes.

	Time h	c1	c2	DMSO1	DMSO2	0.72 $\mu\text{g L}^{-1}$	1.47 $\mu\text{g L}^{-1}$	2.32 $\mu\text{g L}^{-1}$	3.56 $\mu\text{g L}^{-1}$	5.12 $\mu\text{g L}^{-1}$	15.66 $\mu\text{g L}^{-1}$
culture 1	2a	30.57	29.25	29.73	31.43	32.81	32.70	30.96	32.24	34.13	33.90
	2b	31.02	30.48	29.66	31.98	30.77	31.40	32.10	33.43	32.88	34.40
	4a	44.28	44.57	45.78	45.67	43.61	42.36	44.40	43.81	41.76	38.28
	4b	43.68	42.62	43.54	43.70	44.38	45.48	43.68	44.45	41.78	38.55
	6a	66.41	70.86	70.51	74.10	70.87	68.80	66.25	67.30	60.35	49.32
	6b	66.40	68.74	67.52	68.84	69.67	70.87	68.72	67.80	61.29	48.47
	8a	105.00	110.00	108.10	106.70	107.90	106.80	98.65	90.49	73.49	56.12
	8b	102.00	106.00	107.40	108.10	110.50	109.00	97.99	89.39	72.50	54.16
	10a	146.30	150.80	151.30	148.80	150.30	156.30	128.20	150.06	79.62	61.15
	10b	152.40	154.20	154.60	157.90	150.70	153.10	127.70	105.00	78.70	59.20
	12a	208.20	211.80	212.00	220.80	217.50	210.90	263.70	123.80	90.20	61.49
	12b	197.50	214.50	216.10	213.10	216.90	213.70	169.60	116.10	86.24	59.80
	14a	285.60	290.30	289.50	281.20	277.30	282.10	262.10	199.80	148.20	74.08
	14b	278.40	287.10	288.30	274.20	280.10	281.10	264.60	206.00	146.40	74.18
14a	299.40	292.10	289.40	296.10	288.90	290.30	151.10	134.30	96.23	65.81	
14b	271.20	290.80	290.50	289.70	286.70	290.00	190.10	140.20	95.07	67.88	
16a	373.50	383.00	371.60	361.50	364.50	364.30	342.20	243.90	178.30	80.94	
16b	370.40	297.40	320.50	362.00	362.80	371.10	340.10	242.80	167.90	80.84	
18a	431.40	455.40	458.70	440.20	439.10	457.80	412.60	278.80	193.50	96.58	
18b	444.20	458.50	454.80	454.60	438.80	453.80	407.90	280.70	199.90	95.26	
20a-Peak1	31.18	33.15	32.03	35.21	33.16	32.87	34.86	37.46	217.40	105.20	
20a-Peak2	471.20	475.40	464.90	440.00	449.40	462.10	423.40	322.10			
20b-Peak1	32.11	32.36	33.03	31.85	32.59	34.57	36.58	34.79	221.30	107.20	
20b-Peak2	477.00	487.30	467.80	455.80	463.10	458.90	400.50	314.20			
22a-Peak1	36.45	38.19	34.86	35.56	36.25	37.19	38.59	47.74	245.10	119.50	
22a-Peak2	284.80	303.50	294.80	290.30	276.50	277.70	296.20	285.50			
22b-Peak1	35.76	36.68	37.40	35.06	35.08	36.32	40.29	49.37	247.10	109.30	
22b-Peak2	305.80	311.30	270.60	291.50	275.70	270.00	294.00	279.40			
24a-Peak 1	45.58	46.06	44.85	44.31	43.18	45.34	50.50	54.43	248.30	144.70	
24a-Peak2								272.20			
24b-Peak1	43.54	45.00	44.90	44.32	45.02	46.05	51.05	52.62	253.30	138.70	
24b-Peak 2								264.50			
26a-Peak1	60.77	59.46	59.72	57.30	57.69	60.22	74.44	59.79	43.62	44.80	
26a-Peak2								235.50	261.50	162.00	
26b-Peak1	55.26	58.36	56.86	58.37	57.15	59.58	75.92	62.83	49.53	43.65	
26b - Peak 2								246.60	264.70	160.30	

**Table A.7:** Analytical determined PNA concentrations in GB-medium without algae and in algae suspension over 256 minutes.

Time [min]	concentration in GB-medium			in algae suspension	
	C1 [ $\mu\text{g L}^{-1}$ ]	C2 [ $\mu\text{g L}^{-1}$ ]	C3 [ $\mu\text{g L}^{-1}$ ]	C1 [ $\mu\text{g L}^{-1}$ ]	C2 [ $\mu\text{g L}^{-1}$ ]
0	162.08	189.40	150.19		
1				114.00	132.00
2				142.31	78.30
4				116.81	96.03
8				73.58	56.87
16				77.21	77.62
32				61.14	83.04
64				42.97	57.23
128				64.43	71.04
256	200.37	187.63	171.69	59.37	56.29

**Table A.8:** Estimated effect concentrations ( $EC_{50}$  values) and slopes ( $\theta$ ), their 95% confidence interval [95% CI], and goodness-of-fit characterizations (RMSE – root mean squared error,  $R^2$ – regression coefficient) of the concentration-response relationship of inhibited cell volume (CV) and cell number (CN) for various exposure times.

Time [h]	$\theta$ [-]	triclosan				norflurazon				PNA			
		$EC_{50}$ [ $\mu\text{g L}^{-1}$ ]	RMSE [-]	$R^2$ [%]	$\theta$ [-]	$EC_{50}$ [ $\mu\text{g L}^{-1}$ ]	RMSE [-]	$R^2$ [%]	$\theta$ [-]	$EC_{50}$ [ $\mu\text{g L}^{-1}$ ]	RMSE [-]	$R^2$ [%]	
CV 4		n.d.				n.d.			2.42 [1.77, 3.07]	185.31 [166.96, 203.66]	0.05	93.06	
CV 6		n.d.				n.d.			2.54 [1.87, 3.22]	136.37 [118.26, 154.48]	0.08	91.96	
CV 8	1.18 [0.90, 1.47]	14.77 [10.77, 18.76]	0.06	87.71					19.25 [-153.25, 191.76]	80.23 [73.13, 87.32]	0.20	85.84	
CV 10	1.29 [0.75, 1.83]	9.13 [5.38, 12.89]	0.11	76.75	1.56 [1.15, 1.97]	13.13 [10.23, 16.03]	0.06	85.83	4.98 [1.09, 8.88]	68.48 [54.11, 82.85]	0.11	93.95	
CV 12	2.05 [-0.39, 4.49]	5.16 [1.98, 8.35]	0.16	80.64	1.64 [1.04, 2.24]	7.98 [6.00, 9.96]	0.09	81.17	4.88 [1.76, 8.00]	62.70 [52.66, 72.72]	0.10	94.36	
CV 14	1.67 [1.25, 2.08]	6.60 [5.37, 7.83]	0.06	94.67	2.06 [1.30, 2.81]	6.80 [5.45, 8.15]	0.13	76.43	8.09 [5.58, 10.60]	65.61 [60.19, 71.04]	0.06	98.24	
CV 16	2.04 [1.13, 2.96]	5.83 [4.23, 7.43]	0.09	91.45	2.03 [1.43, 2.63]	6.40 [5.44, 7.36]	0.08	90.49	9.94 [6.22, 13.67]	66.10 [60.11, 72.09]	0.06	98.41	
CV 18	2.06 [1.17, 2.95]	5.08 [3.99, 6.18]	0.08	94.48	2.06 [1.31, 2.82]	5.95 [4.92, 6.98]	0.09		14.14 [-6.14, 34.42]	70.40 [56.74, 84.05]	0.05	98.78	
CV 20	1.76 [1.29, 2.23]	5.71 [4.73, 6.70]	0.06	95.60	1.90 [1.90, 1.11]	5.70 [4.56, 6.85]	0.11	80.16		n.d.			
CV 22	2.03 [1.63, 2.44]	12.50 [11.08, 13.91]	0.04	96.66		n.d.				n.d.			
CN 24	6.07 [3.67, 9.35]	2.85 [2.60, 3.10]	0.07	97.57	6.31	2.39	0.07	91.87	10.82	45.93	0.03	94.67	

APPENDIX **B**

Supplementary information for Chapter 3

**Table B.1:** Analytical concentrations measured in the ambient medium with algae and without algae (C) for irgarol, isotroturon, triclosan, metazachlor, paraquat, and n-phenyl-2-naphthylamine (red numbers indicate outliers which were not used for modeling purpose, n.d.-not determined).

Time [min]	C measured in algae suspension [ $\mu\text{mol L}^{-1}$ ]	C measured in GB-medium only [ $\mu\text{mol L}^{-1}$ ]	Time [min]	C measured in algae suspension [ $\mu\text{mol L}^{-1}$ ]	C measured in GB-medium only [ $\mu\text{mol L}^{-1}$ ]
irgarol			isotroturon		
cell density: $1.38 \times 10^{11}$ cells $\text{L}^{-1}$			cell density: $2.113 \times 10^{12}$ cells $\text{L}^{-1}$		
14.02	0.4718	0.6590	7.14	0.8831	1.6889
14.02	0.4959	0.6188	7.14	0.8737	1.7013
14.02	n.d.	0.6414	7.14	0.8954	1.6558
14.02	0.6033	0.6932	13.08	0.8602	1.6977
14.02	0.5712	0.6671	13.08	0.8740	1.6920
14.02	0.5892	0.6614	13.08	0.8911	1.7014
14.02	0.6402	0.6509	21.09	0.8776	1.7138
14.02	0.6075	0.6255	21.09	0.8300	1.7016
20	0.4947	0.6529	21.09	0.8274	1.6833
20	0.4976	0.6406	36	0.8460	1.7230
20	0.4892	0.6328	36	0.8629	1.6902
20	0.5039	0.6488	36	0.8521	1.7278
20	0.5943	0.6440	68	0.8235	1.6789
20	0.5484	0.6487	68	0.8240	1.7148
20	0.5453	0.6362	68	0.8191	1.7001
20	0.5870	0.6376	126	0.6942	1.7130
20	0.6026	0.6285	126	0.7808	1.7159
20	0.6236	0.6407	126	0.7909	1.6761
27	0.4846	0.7043	246	0.7256	n.d.
27	0.5011	0.6623	246	0.7087	n.d.
27	0.4797	0.6584	246	0.7028	n.d.
			cell density: $1.228 \times 10^{12}$ cells $\text{L}^{-1}$		
27	0.5272	0.5867	7.24	0.7711	1.4629
27	0.5204	0.6207	7.24	0.7785	1.3624
27	0.5322	0.6238	7.24	0.7606	1.4735
27	0.5768	0.6636	7.24	0.7037	1.4294
27	0.5618	0.6532	7.24	0.7038	1.4747
27	0.5981	0.6230	7.24	0.7052	1.4800
35	0.4816	0.6737	7.24	0.6047	n.d.
35	0.4785	0.6261	7.24	0.5951	n.d.
35	0.4572	0.6236	7.24	0.5339	n.d.
35	0.4379	0.6463	13.3	0.7907	1.5079
35	0.4566	0.6024	13.3	0.7892	1.5142
35	0.4770	0.6369	13.3	0.7882	1.4962
35	0.5131	0.6146	13.3	0.7050	1.4803
35	0.5222	0.6381	13.3	0.7115	1.4805
35	0.5079	0.5807	13.3	0.6987	1.4657
65	0.3754	0.6289	13.3	0.7793	n.d.
65	0.4058	0.6054	13.3	0.7735	n.d.
65	0.3965	0.6208	13.3	0.7799	n.d.
65	0.3476	0.6406	22	0.7775	1.5439

Table B.1 continued from previous page

Time [min]	C measured in algae suspension [ $\mu\text{mol L}^{-1}$ ]	C measured in GB-medium only [ $\mu\text{mol L}^{-1}$ ]	Time [min]	C measured in algae suspension [ $\mu\text{mol L}^{-1}$ ]	C measured in GB-medium only [ $\mu\text{mol L}^{-1}$ ]	
65	0.3542	0.6331	22	0.7787	1.5088	
65	0.3635	0.6297	22	0.7793	1.5205	
65	0.4315	0.6509	22	0.7138	1.4570	
65	0.4205	0.6541	22	0.7184	1.4338	
65	0.4072	0.6453	22	0.7080	1.4652	
126.43	0.3489	0.6243	22	0.7583	n.d.	
126.43	0.3428	0.6132	22	0.7806	n.d.	
126.43	0.3347	0.5543	22	0.7727	n.d.	
126.43	0.3277	0.6362	36	0.7779	1.4869	
126.43	0.3273	0.6357	36	0.7695	1.4953	
126.43	0.3302	0.5831	36	0.7776	1.4902	
126.43	0.3903	0.6521	36	0.6986	1.4803	
126.43	0.3412	0.6391	36	0.7133	1.4605	
126.43	0.3775	0.6333	36	0.7013	1.4855	
245	0.3179	0.6106	36	0.7781	n.d.	
245	0.3301	0.6500	36	0.7786	n.d.	
245	0.3286	0.6248	36	0.7744	n.d.	
245	0.2608	0.6484	66	0.7583	1.5065	
245	0.2768	0.6156	66	0.7795	1.5162	
245	0.2785	0.6724	66	0.7830	1.5158	
245	0.3276	0.6795	66	0.7133	1.4667	
245	0.3352	0.6431	66	0.7443	1.4830	
245	0.3193	0.6733	66	0.7450	1.4585	
	cell density: $2.114 \times 10^{11}$ cells $\text{L}^{-1}$		66	0.8063	n.d.	
22	0.5688	0.073	66	0.8063	n.d.	
22	0.6114	0.069	66	0.7687	n.d.	
36	0.4820	0.826	66	0.7438	n.d.	
36	0.4880	0.817	127	0.7547	1.5183	
66	0.3752	0.814	127	0.7367	1.5184	
66	0.3642	0.800	127	0.7658	1.5391	
127.44	0.2580	0.819	127	0.7203	1.4682	
127.44	0.2553	0.774	127	0.7339	1.4791	
187.33	0.1762	0.821	127	0.7148	1.4819	
187.33	0.1516	0.822	127	0.7150	n.d.	
247	0.0840	0.794	127	0.7360	n.d.	
247	0.1196	0.804	127	0.7401	n.d.	
			247	0.6686	1.5166	
			247	0.6798	1.5048	
			247	0.6889	1.5317	
			247	0.6988	1.4625	
			247	0.6948	1.4812	
			247	0.6822	1.4860	
			247	0.6624	n.d.	
			247	0.6533	n.d.	
			247	0.6633	n.d.	
	triclosan			metazachlor		
	cell density: $7.107 \times 10^{10}$ cells $\text{L}^{-1}$			cell density: $1.242 \times 10^{12}$ cells $\text{L}^{-1}$		
7.4	0.3204	0.6318	7.49	1.2858	1.4074	

Table B.1 continued from previous page

Time [min]	C measured in algae suspension [ $\mu\text{mol L}^{-1}$ ]	C measured in GB-medium only [ $\mu\text{mol L}^{-1}$ ]	Time [min]	C measured in algae suspension [ $\mu\text{mol L}^{-1}$ ]	C measured in GB-medium only [ $\mu\text{mol L}^{-1}$ ]
7.4	0.3238	0.6363	7.49	1.2703	1.4055
7.4	0.3052	0.6181	7.49	1.2907	1.3955
7.4	0.3345	0.5767	7.49	1.2693	1.3621
7.4	0.3022	0.5752	7.49	1.2586	1.3328
7.4	0.3191	0.5714	7.49	1.2551	1.3376
7.4	0.3302	n.d.	13.5	1.1488	1.4068
7.4	0.3319	n.d.	13.5	1.1884	1.4322
7.4	0.3350	n.d.	13.5	1.1711	1.3876
14.25	0.1769	0.5876	13.5	1.1903	1.3287
14.25	0.1677	0.6242	13.5	1.2025	1.3308
14.25	0.1749	0.6090	13.5	1.1886	1.3365
14.25	0.1854	0.5208	22	1.1087	1.3925
14.25	0.1877	0.5053	22	1.1108	1.3679
14.25	0.1798	0.5247	22	1.1118	1.4032
14.25	0.1513	n.d.	22	1.1193	1.3357
14.25	0.1530	n.d.	22	1.0938	1.3569
14.25	0.1354	n.d.	22	1.1111	1.3255
22	0.1144	0.5570	34	1.0076	1.4159
22	0.1103	0.5559	34	1.0314	1.4150
22	0.1051	0.5805	34	1.0160	1.4177
22	0.1133	0.5069	34	1.0551	1.3451
22	0.1348	0.4992	34	1.0432	1.3363
22	0.1377	0.5134	34	1.0481	1.3755
22	0.1346	n.d.	105	0.7932	1.4406
22	0.1364	n.d.	105	0.7894	1.4138
22	0.1332	n.d.	105	0.7895	1.4066
37	0.0778	0.5509	105	0.9522	1.3658
37	0.0643	0.5693	105	0.9280	1.3955
37	0.0788	0.5781	105	0.9338	1.3667
37	0.0723	0.5358	126	0.6659	1.4487
37	0.0807	0.5196	126	0.6859	1.4547
37	0.0801	0.5424	126	0.6747	1.4195
37	0.0759	n.d.	126	0.7588	1.3906
37	0.0815	n.d.	126	0.7614	1.3739
37	0.0779	n.d.	126	0.7556	1.3695
67	n.d.	0.5955	242	0.3982	1.4445
67	n.d.	0.5883	242	0.4094	1.4201
67	0.0497	0.6173	242	0.3639	1.4435
67	0.0726	0.5502	242	0.4840	1.3774
67	0.0766	0.5505	242	0.4880	1.3758
67	0.0695	0.5555	242	0.4994	1.3704
cell density: $2.920 \times 10^{12}$ cells $\text{L}^{-1}$					
67	0.0566	n.d.	6.3	1.2728	1.3449
67	0.0590	n.d.	6.3	1.3081	1.3588
67	n.d.	n.d.	6.3	1.2577	1.3529
126.24	0.1029	0.5886	12.3	1.0994	1.3327
126.24	0.1120	0.6054	12.3	1.0759	1.3528
126.24	0.1029	0.5943	12.3	1.0824	1.3401
126.24	0.0636	0.5368	20	0.9655	1.3542

Table B.1 continued from previous page

Time [min]	C measured in algae suspension [ $\mu\text{mol L}^{-1}$ ]	C measured in GB-medium only [ $\mu\text{mol L}^{-1}$ ]	Time [min]	C measured in algae suspension [ $\mu\text{mol L}^{-1}$ ]	C measured in GB-medium only [ $\mu\text{mol L}^{-1}$ ]
126.24	0.0642	0.5451	20	0.9660	1.3547
126.24	0.0822	0.5373	20	0.9655	1.3715
126.24	0.1295	n.d.	35	0.8373	1.3628
126.24	0.1281	n.d.	35	0.8223	1.3534
126.24	0.1377	n.d.	35	0.8273	1.3698
245.18	0.3068	0.6491	66	0.6602	1.3423
245.18	0.3206	0.6045	66	0.6686	1.3707
245.18	0.3245	0.5960	66	0.6872	1.3305
245.18	0.2394	0.5851	128	0.4282	1.3248
245.18	0.2422	0.5619	128	0.4432	1.3620
245.18	0.2489	0.5767	128	0.4595	1.3515
245.18	0.3303	n.d.	246	0.2042	1.3686
245.18	0.3535	n.d.	246	0.2032	1.3096
245.18	0.3299	n.d.	246	0.2033	1.3686
cell density: $2.899 \times 10^{10}$ cells $\text{L}^{-1}$			cell density: $1.489 \times 10^{12}$ cells $\text{L}^{-1}$		
7.25	0.3744	0.6291	7.4	1.2144	1.3545
7.25	0.3649	0.6331	7.4	1.2152	1.3482
7.25	0.3565	0.6305	7.4	1.1669	1.3505
7.25	0.3715	0.5696	7.4	1.1774	1.3962
7.25	0.3523	0.5649	7.4	1.2255	1.3951
7.25	0.3467	0.5270	7.4	1.2212	1.3965
7.25	0.3730	n.d.	7.4	0.8041	n.d.
7.25	0.3339	n.d.	7.4	1.1832	n.d.
7.25	0.3631	n.d.	7.4	1.1550	n.d.
13.3	0.2843	0.5949	14	1.0532	1.3294
13.3	0.2929	0.6023	14	1.0695	1.3910
13.3	0.3011	0.6057	14	1.0484	1.3455
13.3	0.2657	0.5196	14	1.0606	1.4165
13.3	0.2818	0.5294	14	1.0684	1.4069
13.3	0.2560	0.5389	14	1.0650	1.2969
13.3	0.2228	n.d.	14	0.9917	n.d.
13.3	0.2548	n.d.	14	0.9687	n.d.
13.3	0.2475	n.d.	14	0.9838	n.d.
21	0.1992	0.5706	21	0.9715	1.3668
21	0.2008	0.5612	21	0.9476	1.3346
21	0.1943	0.5612	21	0.9721	1.3808
21	0.2019	0.5240	21	0.9512	1.3565
21	0.1862	0.5286	21	0.9433	1.4222
21	0.1750	0.5239	21	0.9197	1.4062
21	0.2207	n.d.	21	0.9215	n.d.
21	0.2170	n.d.	21	0.9144	n.d.
21	0.2176	n.d.	21	0.8866	n.d.
37	0.1450	0.5436	35.15	0.8142	1.3588
37	0.1411	0.5516	35.15	0.7990	1.3717
37	0.1424	0.5436	35.15	0.8233	1.3459
37	0.1302	0.4997	35.15	0.8221	1.4690
37	0.1288	0.5110	35.15	0.8648	1.4699
37	0.1384	0.4987	35.15	0.8452	1.4763
37	0.1702	n.d.	35.15	0.7675	n.d.

Table B.1 continued from previous page

Time [min]	C measured in algae suspension [ $\mu\text{mol L}^{-1}$ ]	C measured in GB-medium only [ $\mu\text{mol L}^{-1}$ ]	Time [min]	C measured in algae suspension [ $\mu\text{mol L}^{-1}$ ]	C measured in GB-medium only [ $\mu\text{mol L}^{-1}$ ]
37	0.1458	n.d.	35.15	0.8256	n.d.
37	0.1349	n.d.	35.15	0.8523	n.d.
67	0.0851	0.5527	66	0.6500	1.3800
67	0.1028	0.5775	66	0.6459	1.3202
67	0.0999	0.5537	66	0.6627	1.3655
67	0.1039	0.5018	66	0.6305	1.4203
67	0.1110	0.4988	66	0.6685	1.4197
67	0.1072	0.5075	66	0.6590	1.4086
67	0.1043	n.d.	66	0.6385	n.d.
67	0.0998	n.d.	66	0.6514	n.d.
67	0.1044	n.d.	66	0.6517	n.d.
127.3	0.1244	0.5108	128	0.4208	1.3364
127.3	0.1167	0.4979	128	0.4242	1.2988
127.3	0.1369	0.5016	128	0.4220	1.2897
127.3	0.1008	0.4406	128	0.4142	1.4184
127.3	0.1038	0.5025	128	0.4108	1.3971
127.3	0.0810	0.4639	128	0.4099	1.3706
127.3	0.1239	n.d.	128	0.4114	n.d.
127.3	0.1316	n.d.	128	0.3993	n.d.
127.3	0.1458	n.d.	128	0.3989	n.d.
248	0.3750	0.5323	246	0.1983	1.3406
248	0.3618	0.5331	246	0.1934	1.3355
248	0.3771	0.5116	246	0.1837	1.3342
248	0.2734	0.4717	246	0.1960	1.3020
248	0.2903	0.4559	246	0.1927	1.4087
248	0.2978	0.4709	246	0.1994	1.3739
248	0.3423	n.d.	246	0.1854	n.d.
248	0.3596	n.d.	246	0.1890	n.d.
248	0.3619	n.d.	246	0.1837	n.d.
390	0.4715	0.4759			
390	0.4805	0.4649			
390	0.4743	0.4695			
390	0.3544	0.5324			
390	0.3652	0.5470			
390	0.3659	0.5230			
390	0.4831	n.d.			
390	0.4825	n.d.			
390	0.4695	n.d.			
	cell density: $2.195 \times 10^{10}$ cells $\text{L}^{-1}$				
7.44	0.3345	0.5629			
7.44	0.3219	0.5928			
7.44	0.3174	0.5919			
7.44	0.3590	0.5930			
7.44	0.3592	0.5780			
7.44	0.3595	0.5820			
7.44	0.3273	n.d.			
7.44	0.3175	n.d.			
7.44	0.3226	n.d.			
14.2	0.3087	0.5894			

Table B.1 continued from previous page

Time [min]	C measured in algae suspension [ $\mu\text{mol L}^{-1}$ ]	C measured in GB-medium only [ $\mu\text{mol L}^{-1}$ ]	Time [min]	C measured in algae suspension [ $\mu\text{mol L}^{-1}$ ]	C measured in GB-medium only [ $\mu\text{mol L}^{-1}$ ]
14.2	0.2999	0.5891			
14.2	0.3041	0.6081			
14.2	0.3633	0.5296			
14.2	0.3379	0.5736			
14.2	0.3548	0.4853			
14.2	0.2431	n.d.			
14.2	0.2573	n.d.			
14.2	0.2525	n.d.			
21.42	0.2536	0.5659			
21.42	0.2532	0.5703			
21.42	0.2615	0.5645			
21.42	0.2163	0.5467			
21.42	0.2075	0.5580			
21.42	0.2088	0.5436			
21.42	0.2698	n.d.			
21.42	0.2662	n.d.			
21.42	0.2699	n.d.			
37.09	0.2076	0.6240			
37.09	0.1992	0.5802			
37.09	0.2078	0.5633			
37.09	0.2000	0.5514			
37.09	0.1883	0.5590			
37.09	0.1896	0.5596			
37.09	0.1806	n.d.			
37.09	0.1707	n.d.			
37.09	0.1848	n.d.			
66.02	0.1451	0.5547			
66.02	0.1375	0.5160			
66.02	0.1319	0.5736			
66.02	0.1546	0.5609			
66.02	0.1484	0.5607			
66.02	0.1546	0.5536			
66.02	0.1248	n.d.			
66.02	0.1265	n.d.			
66.02	0.1313	n.d.			
127.17	0.1220	0.5683			
127.17	0.1210	0.5557			
127.17	0.1237	0.5786			
127.17	0.1239	0.5573			
127.17	0.1005	0.5640			
127.17	0.1233	0.5651			
127.17	0.1326	n.d.			
127.17	0.1449	n.d.			
127.17	0.1469	n.d.			
249	0.2023	0.5966			
249	0.2213	0.5743			
249	0.2327	0.5740			
249	0.2243	0.5154			
249	0.2338	0.4925			

Table B.1 continued from previous page

Time [min]	C measured in algae suspension [ $\mu\text{mol L}^{-1}$ ]	C measured in GB-medium only [ $\mu\text{mol L}^{-1}$ ]	Time [min]	C measured in algae suspension [ $\mu\text{mol L}^{-1}$ ]	C measured in GB-medium only [ $\mu\text{mol L}^{-1}$ ]
249	0.2523	0.5123			
249	0.3048	n.d.			
249	0.2992	n.d.			
249	0.3142	n.d.			
367	0.3782	0.4747			
367	0.3667	0.4749			
367	0.3712	0.4674			
paraquat			PNA		
cell density: $2.314 \times 10^{12}$ cells $\text{L}^{-1}$			cell density: $3.15 \times 10^{10}$ cells $\text{L}^{-1}$		
7.15	530.4700	693.8484	0		0.7397
7.15	562.7814	703.1797	0	1.2342	0.8645
7.15	563.5393	695.8675	0	1.1411	0.6855
7.15	557.7832	696.1878	1	0.5203	
7.15	571.1475	705.2041	1	0.6024	
7.15	556.3996	709.9137	2	0.6495	
7.15	560.2361	n.d.	2	0.3574	
7.15	569.1323	n.d.	4	0.5331	
7.15	573.1460	n.d.	4	0.4383	
13.45	556.2909	695.9801	8	0.3358	
13.45	554.0572	716.4117	8	0.2596	
13.45	582.0483	709.1715	16	0.3524	
13.45	571.0187	694.7741	16	0.3543	
13.45	587.1638	727.0148	32	0.2791	
13.45	580.8772	716.2877	32	0.3790	
13.45	577.3808	n.d.	64	0.1961	
13.45	571.0833	n.d.	64	0.2612	
13.45	575.1852	n.d.	128	0.2941	
20.3	548.6338	687.1090	128	0.3242	
20.3	583.3123	712.9463	256	0.2710	0.9145
20.3	570.0528	722.9974	256	0.2569	0.8564
20.3	573.1343	712.0919	256		0.7836
20.3	586.2159	722.3612			
20.3	585.0830	715.4281			
20.3	571.8085	n.d.			
20.3	576.1107	n.d.			
20.3	573.4565	n.d.			
37	530.2338	708.7401			
37	562.5358	716.5306			
37	574.3164	708.0489			
37	543.7546	702.3186			
37	579.7134	743.0054			
37	563.4796	722.7382			
37	580.0188	n.d.			
37	580.5293	n.d.			
37	574.2526	n.d.			
68.09	557.6598	703.0137			
68.09	568.7175	708.7564			
68.09	570.3833	685.3403			

Table B.1 continued from previous page

Time [min]	C measured in algae suspension [ $\mu\text{mol L}^{-1}$ ]	C measured in GB-medium only [ $\mu\text{mol L}^{-1}$ ]	Time [min]	C measured in algae suspension [ $\mu\text{mol L}^{-1}$ ]	C measured in GB-medium only [ $\mu\text{mol L}^{-1}$ ]
68.09	558.6621	716.9279			
68.09	571.5078	723.0388			
68.09	541.2882	705.4790			
68.09	570.6433	n.d.			
68.09	576.6359	n.d.			
68.09	576.8837	n.d.			
126	555.6385	692.4739			
126	570.7230	712.3869			
126	568.5798	704.9813			
126	568.7986	718.5569			
126	569.8183	731.3708			
126	577.5230	713.6306			
126	530.5270	n.d.			
126	580.4240	n.d.			
126	578.3818	n.d.			
246	548.5857	706.0053			
246	554.8471	715.6800			
246	576.9937	710.7094			
246	554.2667	717.5397			
246	556.4056	724.7657			
246	563.3969	744.4280			
246	555.5096	n.d.			
246	553.7472	n.d.			
246	566.3863	n.d.			
	cell density: $9.801 \times 10^{11}$ cells $\text{L}^{-1}$				
7.15	606.7990	719.0085			
7.15	623.2668	735.3585			
7.15	603.0333	714.3526			
7.15	609.4390	710.2192			
13.45	616.5195	706.2538			
13.45	631.2538	730.5307			
13.45	600.4773	717.9617			
13.45	614.1643	724.8613			
20.3	615.1681	709.9964			
20.3	622.0106	719.9980			
20.3	617.2259	719.2363			
20.3	618.9784	726.8796			
37	621.5690	721.2739			
37	619.7451	717.8523			
37	632.0898	724.0907			
37	619.4058	719.6041			
68.09	609.5451	714.2593			
68.09	621.6384	721.3079			
68.09	612.8849	725.6423			
68.09	612.2818	718.5728			
126	606.2858	709.6806			
126	625.7664	729.4472			
126	613.0358	731.4766			
126	608.0802	724.8342			

Table B.1 continued from previous page

Time [min]	C measured in algae suspension [ $\mu\text{mol L}^{-1}$ ]	C measured in GB-medium only [ $\mu\text{mol L}^{-1}$ ]	Time [min]	C measured in algae suspension [ $\mu\text{mol L}^{-1}$ ]	C measured in GB-medium only [ $\mu\text{mol L}^{-1}$ ]
246	604.6981	718.1953			
246	595.5272	717.6420			
246	610.4511	716.0143			
246	608.1127	724.2137			
	cell density: $2.443 \times 10^{12}$ cells $\text{L}^{-1}$				
6.07	456.3837	713.9924			
6.07	478.2567	721.2339			
6.07	492.6727	717.5238			
6.07	482.4303	704.4079			
6.07	489.1516	721.4758			
6.07	477.0260	712.5496			
13.1	483.8952	701.3428			
13.1	465.9932	715.8169			
13.1	482.6042	710.1248			
13.1	476.3190	704.4242			
13.1	478.8927	697.9124			
13.1	487.5262	721.8388			
21	460.8505	701.3830			
21	488.2351	710.7428			
21	491.0231	719.5217			
21	469.5177	705.0478			
21	486.7354	705.6997			
21	493.8113	708.3686			
35.33	462.2693	690.3499			
35.33	469.7690	710.1114			
35.33	477.5303	710.9517			
35.33	473.2532	698.1492			
35.33	486.7294	709.7426			
35.33	478.7698	715.9570			
65.3	464.0003	692.5339			
65.3	477.8726	710.4264			
65.3	475.6190	717.2514			
65.3	465.6104	695.0860			
65.3	482.5390	712.8340			
65.3	481.5379	715.6349			
126.4	463.8998	708.0748			
126.4	475.8176	719.6765			
126.4	467.1913	715.6045			
126.4	463.1228	699.0764			
126.4	472.1455	722.0326			
126.4	477.1970	717.7141			
245.35	458.2636	726.8315			
245.35	469.5131	741.0063			
245.35	469.8560	720.0692			
245.35	463.8334	708.2322			
245.35	475.0650	726.4471			
245.35	477.0937	718.8805			

**Table B.2:** Calculated fraction of neutral irgarol species ( $pK_b$  5.68) in dependency of measured ambient medium pH as well as in dependency of cytoplasmatic pH measured under aerobic and anaerobic conditions (Küsel et al., 1990).

Time [min]	GB medium without algae		GB medium with algae cells	
	measured pH	neutral fraction	measured pH	neutral fraction
0	6.41	0.842	6.49	0.865
30	6.42	0.845	6.53	0.875
60	6.43	0.848	6.55	0.880
120	6.42	0.845	6.54	0.878
240	6.42	0.845	6.54	0.878
360	6.42	0.845	6.59	0.890
intracellular ionization potential				
	Cytoplasmatic pH	neutral fraction		
under aerobic conditions	7.6	0.988		
under anaerobic conditions	7.0	0.954		

**Table B.3:** Calculated fraction of neutral isotruturon species ( $pK_a$  13.78) in dependency of measured ambient medium pH as well as in dependency of cytoplasmatic pH measured under aerobic and anaerobic conditions (Küsel et al., 1990).

Time [min]	GB medium without algae		GB medium with algae cells	
	measured pH	neutral fraction	measured pH	neutral fraction
0	6.41	1	6.45	1
30	6.45	1	6.51	1
60	6.44	1	6.54	1
120	6.44	1	6.58	1
240	6.44	1	6.62	1
360	6.45	1	6.68	0.999
intracellular ionization potential				
	Cytoplasmatic pH	neutral fraction		
under aerobic conditions	7.6	0.999		
under anaerobic conditions	7.0	0.999		

**Table B.4:** Calculated fraction of neutral triclosan species ( $pK_a$  7.68) in dependency of measured ambient medium pH as well as in dependency of cytoplasmatic pH measured under aerobic and anaerobic conditions (Küsel et al., 1990).

Time [min]	GB medium without algae		GB medium with algae cells	
	measured pH	neutral fraction	measured pH	neutral fraction
0	6.46	0.943	6.46	0.944
30	6.44	0.946	6.45	0.944
60	6.46	0.943	6.46	0.943
120	6.45	0.944	6.45	0.944
240	6.43	0.947	6.44	0.946
360	6.47	0.942	6.44	0.946
intracellular ionization potential				
	Cytoplasmatic pH	neutral fraction		
under aerobic conditions	7.6	0.546		
under anaerobic conditions	7.0	0.827		

**Table B.5:** Calculated fraction of neutral metazachlor species ( $pK_b$  1.84) in dependency of measured ambient medium pH as well as in dependency of cytoplasmatic pH measured under aerobic and anaerobic conditions (Küsel et al., 1990).

Time [min]	GB medium without algae		GB medium with algae cells	
	measured pH	neutral fraction	measured pH	neutral fraction
0	6.41	0.999	6.43	0.999
30	6.43	0.999	6.49	0.999
60	6.43	0.999	6.52	0.999
120	6.43	0.999	6.57	0.999
240	6.42	0.999	6.65	0.999
360	6.43	0.999	6.7	0.999
intracellular ionization potential				
	Cytoplasmatic pH	neutral fraction		
under aerobic conditions	7.6	0.999		
under anaerobic conditions	7.0	0.999		

**Table B.6:** Calculated fraction of neutral PNA species ( $pK_b$  0.517) in dependency of measured ambient medium pH as well as in dependency of cytoplasmatic pH measured under aerobic and anaerobic conditions (Küsel et al., 1990).

Time [min]	GB medium without algae		GB medium with algae cells	
	measured pH	neutral fraction	measured pH	neutral fraction
0	6.35	0.999	6.70	0.999
30	6.43	0.999	6.83	1
60	6.43	0.999	6.92	1
120	6.42	0.999	7.02	1
240	6.42	0.999	7.15	1
360	6.42	0.999	7.18	1
intracellular ionization potential				
	Cytoplasmatic pH	neutral fraction		
under aerobic conditions	7.6	0.999		
under anaerobic conditions	7.0	0.999		



APPENDIX **C**

Supplementary information for Chapter 4

**Table C.1:** The cell volume measured every two hours for two untreated algae cell cultures (c1/c2), two DMSO-treated algae cell cultures (DMSO1/DMSO2) and PNA-treated algae cultures exposed to six concentrations. Exposure started at  $t_8$ . Grey highlighted boxes represent the cell volumes of the second algae generation which were excluded for calibrating purposes.

	Time h	c1	c2	DMSO1	DMSO2	0.90 $\mu\text{mol L}^{-1}$	0.73 $\mu\text{mol L}^{-1}$	0.37 $\mu\text{mol L}^{-1}$	0.23 $\mu\text{mol L}^{-1}$	0.21 $\mu\text{mol L}^{-1}$	0.20 $\mu\text{mol L}^{-1}$
culture 2	2a	26.44	25.8	24.66	25.45	26.04	27.33	26.54	27.27	27.33	27.23
	2b	25.21	24.17	24.37	25.98	26.51	27.53	26.4	26.91	26.98	26.29
	4a	42.07	40.1	41.05	40.48	40.39	40.01	41.4	39.63	41.67	42.47
	4b	41.67	41.52	40.29	40.69	39.92	40.61	40.28	41.63	41.06	41.39
	6a	64.15	61.3	63.58	60.37	61.01	62.19	61.66	61.18	61.39	62.04
	6b	64.33	61.82	62.39	60.45	62.47	62.56	61.8	62	62.22	61.95
	8a	90.63	89.28	90.63	88.88	91.54	92.93	92.73	94.02	92.82	90.86
	8b	90.19	90.92	91.02	88.45	95.29	93.7	91.91	93.73	90.8	91.24
	10a	137.7	137	134.3	136.5	129.3	123.9	132.5	139.3	135.4	130.7
	10b	134.1	136.8	135.3	139	129.6	129.6	135.4	139.3	136.9	133.4
	12a	187.5	183.6	184.1	188	161.4	161.8	177.9	184.2	200.7	182
	12b	186.9	186.4	185.1	189.2	156.7	158.3	179.2	186.4	198.2	183.6
	14a	318.1	318.3	296.3	298.2	179.3	183.4	232.1	288.6	290	293.1
	14b	318.1	318.3	296.3	298.2	175.4	180.2	218.2	286.4	293.3	292.2
culture 2	14a	247.1	239.7	239	245.6	168	175	223.3	238.2	235.2	233.1
	14b	242.2	237.5	235	239.8	168.1	176.6	220.9	240	243.5	233.9
	16a	402.1	403.5	383.3	386.3	177.2	191	231.1	365.3	361.7	365.1
	16b	395	404.2	391.3	399.6	176.6	185.6	230	364.1	358.3	369.7
	18a	487.8	473.7	455.8	464.7	179	189.9	237.6	412.2	420.1	438
	18b	469.3	474.5	450.2	469.3	192.6	188.9	240.6	413.2	409	426
	20a-Peak1	34.13	34.88	30.62	33.23				32.75	33.06	31.91
	20a-Peak2	460.1	441	395	410.6	181.4	195.5	237.6	390.4	397.2	398.5
	20b-Peak1	32.65	33.79	31.48	32.82				31.64	32.22	32.19
	20b-Peak2	464.5	455.6	394.9	421.2	179.5	193.5	231.8	380	392.1	410.9
	22a-Peak1	35.39	33.99	33.09	34.52	184.8	194.6	20.29	29.71	30.53	31.55
	22a-Peak2							169.3			
	22b-Peak1	34.48	34.81	33.38	34.1	180.8	195.2	20.32	29.68	31	31.13
	22b-Peak2							159.3			
	24a	44.1	44.64	43.06	44.84	180.6	193.2	20.12	34.2	36.65	38.1
	24b	43.84	44.71	43.29	44.82	184	188.7	19.97	34.35	37.73	38.31

**Table C.2:** The cell volume measured every two hours for two untreated algae cell cultures (c1/c2), two DMSO-treated algae cell cultures (DMSO1/DMSO2) and irgarol-treated algae cultures exposed to six concentrations. Exposure started at  $t_6$ . Grey highlighted boxes represent the cell volumes of the second algae generation which were excluded for calibrating purposes.

	Time h	c1	c2	DMSO1	DMSO2	0.79 $\mu\text{mol L}^{-1}$	0.20 $\mu\text{mol L}^{-1}$	0.16 $\mu\text{mol L}^{-1}$	0.13 $\mu\text{mol L}^{-1}$	0.10 $\mu\text{mol L}^{-1}$	0.04 $\mu\text{mol L}^{-1}$
culture 1	2a	34.22		32.95			33.71		34.3		32.16
	2b	32.91		32.44			34.72		33.25		32.8
	4a	56.72		53.42			56.46		55.2		56.55
	4b	54.65		55.52			54.88		59.13		54.54
	6a	87.17	88.32	86.02	87.26	90.65	90.96	88.5	89.73	93.79	96.11
	6b	86.05	87.87	88.22	91.08	86.59	91.06	89.38	93.28	95.38	93.4
	8a	185.5	196.1	132.9	138.1	96.47	126.3	133.6	129.6	133.1	135.3
	8b	134.8	158	131.6	137.6	96.45	132.3	130.2	131.8	134.1	138.4
	10a	204.7	208.3	210.1	212.9	87.28	136.4	183.3	172.7	190.5	207.1
	10b	211.9	201.8	206.1	218.7	83.66	138.8	174.1	175.5	191.8	212.7
	12a	299.9	298.7	300.6	313.5	86.05	135.5	196.2	212.2	245.6	290.9
	12b	297.9	299	294	302.7	89.08	133.3	191	215.3	244.7	291.7
	14a	384.6	388.5	388.1	392.1	80.28	133.2	204.5	231.7	290.2	384.6
	14b	378.1	396.4	385.7	391.5	89.39	137.3	205	244.6	298.3	371.7
culture 2	6a	74.45		75.13			76.6		74.43		74.62
	6b	75.85		74.54			74.64		74.67		76.62
	14a	341.9	326.5	324.2	328.9	72.15	117.5	157.9	197.4	238.7	309.2
	14b	337.6	325.6	322.5	319.8	72.16	116.4	156.4	194.9	231	315.6
	16a	433.6	420.8	419.9	422.3	75.96	128	166.5	231.9	238.2	375.7
	16b	429.9	428.8	411.3	414.1	73.72	121.8	155.2	218.1	292	408.4
	18a	498.6	495.2	480.5	486.8	75.68	131.1	178.8	230.6	305.9	424.5
	18b	512	492.5	479.7	486	76.66	126.5	180.9	225.2	306.3	419.9
	20a-Peak1	35.23	38.14	38.48	36.46	78.18	118.9	24.29	25.56	33.17	31.72
	20a-Peak2	518.3	518.1	494.1	506			140.4	149.4		418.2
	20b-Peak1	35.74	38.15	36.75	39.12	80.78	132.4	24.78	23.78	26.9	32.95
	20b-Peak2	518.4	531	502.1	504.1			135.8	131.4		453.1
	22a-Peak1	36	35.36	35.83	34.92	79.26	19.1	22.1	23.93	24.25	29.84
	22a-Peak2						114.3	113			
	22b-Peak1	35.98	36.46	36.16	35.11	78.58	18.69	22.29	23.03	23.92	29.2
	22b-Peak2						117.2	108.4			
	24a-Peak1	49.85	48.51	49.22	46.18	76.87	23.2	22.42	32.05	32.58	34.83
	24a-Peak2						124.8	99.76			
	24b-Peak1	46.27	47.25	46.95	48.28	77.14	20.9	22.58	29.26	32.7	34.34
	24b-Peak1						114.7	101.2			

**Table C.3:** The cell volume measured every two hours for two untreated algae cell cultures (c1/c2), two DMSO-treated algae cell cultures (DMSO1/DMSO2) and isotreturon-treated algae cultures exposed to six concentrations. Exposure started at  $t_6$ . Grey highlighted boxes represent the cell volumes of the second algae generation which were excluded for calibrating purposes.

	Time h	c1	c2	DMSO1	DMSO2	1.83 $\mu\text{mol L}^{-1}$	0.92 $\mu\text{mol L}^{-1}$	0.58 $\mu\text{mol L}^{-1}$	0.37 $\mu\text{mol L}^{-1}$	0.21 $\mu\text{mol L}^{-1}$	0.06 $\mu\text{mol L}^{-1}$
culture 1	2a	38.07		38.12			37.83		37.83		37.89
	2b	38.07		38.45			38.75		38.66		37.57
	4a	64.56		64.02			62.5		65.78		64.29
	4b	62.21		64.75			62.82		64.05		63.24
	6a	96.32	97.53	97.47	98.72	97.52	95.99	100.6	98.53	99.34	101.4
	6b	97.53	97.47	96.21	95.56	95.93	99.15	97.78	100.1	103.5	101.5
	8a	147	148.4	146.6	145.2	101.4	108.5	116.7	128.1	131.3	144.3
	8b	148.4	149.5	148.8	145.5	99.4	107.4	117	131.3	132.6	144.8
	10a	224.5	232.4	224.8	213.9	97.6	116	130.1	148.6	176.2	206.8
	10b	228	234.4	222.4	212.1	99.99	115.5	130	149.7	172.9	217.5
	12a	291.1	298.6	303.1	296.8	101.3	123.1	148.5	176.1	215.9	276.5
	12b	295.4	300.5	298.6	295.1	101.4	128.5	145.8	176.4	214.5	268.8
	14a	386.1	395.4	380.9	374.3	104.4	128.2	158.3	197	253.3	350.5
	14b	373.3	385	369.6	379.5	108.5	129.9	162.5	197.9	259.6	350.8
culture 2	6a	100.9		95.73				97.3	97.67		97.68
	6b	100.4		96.42				97.77	94.56		99.47
	14a	407.7	400.5	394.7	395.7	103.9	125	151.2	189	266.9	361.1
	14b	395.7	387.9	384	396.4	105.9	124.4	150.8	194.2	267.6	356.9
	16a	495.5	496.3	488.5	485.4	113.6	134.5	171.3	217.3	324.1	445
	16b	490.5	492.1	488.7	487	112.1	137.6	168.9	217.9	322.6	460.2
	18a	556.5	557.3	550.2	557.3	120.2	144.8	175.5	240.8	368.9	511.5
	18b	551.9	562.4	550.4	559.8	120.5	141.6	176.4	235.5	368.3	515.1
	20a-Peak1	32.06	35.5	33.62	33.37	127.7	26.28	26.25	28.13	33.74	32.55
	20a-Peak2	570.6	581.7	575.4	583		125.7	112.1	134.4		466.8
	20b-Peak1	33.07	35.9	34.02	33.75	130.4	25.63	27.05	28.41	34.83	32.98
	20b-Peak2	569.6	594	572.1	566		123.8	121.2	125.1		460.2
	22a-Peak1	34.96	36.07	34.74	34.73	29.19	29.68	30.5	37.84	37.84	33.93
	22a-Peak2					124.2					
	22b-Peak1	36.07	36.01	34.81	34.8	28.76	30.47	31.02	33.26	38.6	34.64
	22b-Peak2					128.4					
	24a-Peak1	43.37	48.66	44.55	44.99	36.5	42.86	41.03	39.76	48.47	46.86
	24a-Peak2					106.5					
	24b-Peak1	42.35	47.69	43.38	45.8	33.67	37.98	39.5	41.38	48.58	46.59
	24b-Peak1					130.5					

**Table C.4:** The cell volume measured every two hours for two untreated algae cell cultures (c1/c2), two DMSO-treated algae cell cultures (DMSO1/DMSO2) and metazachlor-treated algae cultures exposed to six concentrations. Exposure started at  $t_6$ . Grey highlighted boxes represent the cell volumes of the second algae generation which were excluded for calibrating purposes.

	Time h	c1	c2	DMSO1	DMSO2	1.73 $\mu\text{mol L}^{-1}$	0.22 $\mu\text{mol L}^{-1}$	0.17 $\mu\text{mol L}^{-1}$	0.14 $\mu\text{mol L}^{-1}$	0.11 $\mu\text{mol L}^{-1}$	0.04 $\mu\text{mol L}^{-1}$
culture 1	2a	34.46		34.97			34.72		34.64		36.92
	2b	34.66		35.3			34.66		36.15		34.78
	4a	60.92		55.09			55.95		58.65		57.85
	4b	57.45		54.78			56.35		57.97		57.39
	6a	93.8	93.78	87.09	94.16	92.75	91.53	94.38	95.93	91.01	94.55
	6b	93.78	96.32	89.39	92.62	93.52	96.96	97.04	98.54	95.91	95.45
	8a	141.1	144	141.6	143.7	139.6	140	147.3	141.9	145.4	144
	8b	144.1	148.8	137.5	141.5	139.9	143.5	145	146	143.2	146.8
	10a	220.4	217.3	209.1	230	204	217.6	216.4	229.6	215.8	220.2
	10b	215	219.2	208.8	229	206.8	218.2	227.3	223.4	219.8	220
	12a	317	315.3	301.7	311.8	279.3	296.8	309.9	301.7	308.9	302.4
	12b	319.3	313.5	307.5	309.1	279.7	308.2	304.1	306.3	296.4	302.3
	14a	418.2	410.6	400.2	402.4	370.6	403.2	401.2	399.4	396.3	399.4
	14b	421.8	405.3	397.3	393.3	345.3	403.3	415.5	401.9	395.7	397
6a	95.71		98.62			94.29		95.41		96.92	
6b	95.99		95.6			94.42		96.33		96.74	
culture 2	14a	416.6	417.2	416	404	350.6	403.1	410.8	414.2	396.1	425.5
	14b	419.1	417.5	418.5	408.9	364.2	409.5	411.5	413	400.2	417.3
	16a	537	535.8	518.7	493.6	412.9	506.7	529.7	540.2	497.5	526.5
	16b	539.5	540.7	508	502	411.1	494.3	522.1	520.5	506.4	515
	18a	600.5	604.4	585.9	561.1	434.9	569	594.8	598.7	564.5	597.7
	18b	595.5	624.9	578.9	567.7	448	580.7	612.7	613.9	566	600.9
	20a-Peak1	32.99	35.49	33.774	35.34	426.7	577.9	613.2	31.55	41.77	38.67
	20a-Peak2	614.5	620.3	603.1	606.5				620.8	565.6	596.4
	20b-Peak1	32.88	36.53	35.62	36.88	433.2	592.5	601.1	38.38	35.31	37.51
	20b-Peak2	605.3	655.5	606.1	570				602.1	571.1	579.5
	22a-Peak1	36.8	36.79	36.67	35.36	393.4	38.9	39.62	43.48	42.83	37.44
	22a-Peak2						609.4	618.1			
	22b-Peak1	36.79	36.44	35.85	35.48	394	34.99	37.8	44.79	42.81	37.07
	22b-Peak2						595	623.2			
	24a-Peak1	47.06	50.88	48.99	48.05	456.7	51.94	52.72	64.96	65.45	50.49
	24a-Peak2						663.9	743.6			
	24b-Peak1	47.65	48.67	50.05	49.47	452.7	51.54	50.53	77.39	75.59	49.95
	24b-Peak1						676.5	733			

**Table C.5:** The cell volume measured every two hours for two untreated algae cell cultures (c1/c2), two DMSO-treated algae cell cultures (DMSO1/DMSO2) and paraquat-treated algae cultures exposed to six concentrations. Exposure started at  $t_6$ . Grey highlighted boxes represent the cell volumes of the second algae generation which were excluded for calibrating purposes.

Time h	c1	c2	DMSO1	DMSO2	387.03 $\mu\text{mol L}^{-1}$	106.03 $\mu\text{mol L}^{-1}$	41.55 $\mu\text{mol L}^{-1}$	16.71 $\mu\text{mol L}^{-1}$	4.80 $\mu\text{mol L}^{-1}$	0.31 $\mu\text{mol L}^{-1}$
2a	34.19		35.71			34.05		36.27		36.19
2b	33.44		35.54			34.95		36.9		36.47
4a	55.65		54.42			53.25		54.29		54.68
4b	52.21		52.69			52.6		55.34		53.35
6a	86.55	88	83.53	84.73	86.24	85.68	89.05	89.12	89.11	91.1
6b	88	88.21	86.13	86.76	90.45	83.07	88.15	86.92	92.1	90.66
8a	131.6	141.4	128.9	131.5	118.1	124.1	135	134.4	131.8	139.5
8b	130	135.4	126.9	135.6	123.2	123.2	134.8	151.6	138.3	138.6
10a	198.2	197.3	197.4	197.3	131.4	153.1	171.8	187.2	197.4	207.5
10b	191.8	194.5	190.1	197	135.1	158.5	169.1	179.3	204.1	203.6
12a	284.1	276.6	271.8	293.4	137.5	162.1	198.5	223.8	262.2	258.9
12b	284.2	293	277.8	285	140.4	161.2	193.9	230.6	259.2	284.5
14a	381.2	378.3	371.7	381	135.6	173.3	218.6	269.8	337.2	372
14b	381.2	380.6	373.3	378.9	134.4	169.3	217.3	274.2	331.3	382
6a	84.12		84.38			86.5		81.87		86.72
6b	82.75		84.6			84.1		85.53		84.22
14a	370.4	354.8	351.3	365.2	126.5	160.7	191.6	252.7	317.4	359.1
14b	360.3	355.5	358.9	356.5	127.4	160.2	197.6	243.8	316.5	357.8
16a	470.3	451.7	458.9	452.9	129.8	167.7	218.9	287.8	381.7	455.2
16b	460.9	450.7	459.2	452	123.3	168.9	219.1	286	391.1	462.3
18a	530.2	524.2	530.1	522.7	121.6	169.4	238.5	348.9	459.9	531.2
18b	524.4	518	534	528.7	122.6	173.6	239.5	333.9	459.1	536.8
20a-Peak1	33.98	31.38	37.91	35.98	108.1	162.1	239.5	403.6	538.2	34.17
20a-Peak2	558.3	562	554.3	545.1						541.3
20b-Peak1	37.33	35.91	38.36	37.68	110.3	172.6	249.9	392	518.8	33.25
20b-Peak2	553.5	551.01	546.8	543.2						533.8
22a-Peak1	34.32	33.72	33.96	34.27	105.3	161.5	260.9	34.51	36.54	34.43
22a-Peak2								426.7		
22b-Peak1	33.72	33.91	33.76	33.85	109.6	165.5	260	32.85	35.56	35.06
22b-Peak2								435.3		
24a-Peak1	44.75	43.26	47.16	46.18	99.38	147.3	286.8	35.95	42.73	49.34
24a-Peak2								342.1		
24b-Peak1	43.42	46.76	44.79	44.37	103.5	149.9	274.3	36.54	43.72	47.21
24b-Peak1								358.4		

**Table C.6:** The cell volume measured every two hours for two untreated algae cell cultures (c1/c2), two DMSO-treated algae cell cultures (DMSO1/DMSO2) and triclosan-treated algae cultures exposed to six concentrations. Exposure started at  $t_6$ . Grey highlighted boxes represent the cell volumes of the second algae generation which were excluded for calibrating purposes.

	Time h	c1	c2	DMSO1	DMSO2	0.054 $\mu\text{mol L}^{-1}$	0.021 $\mu\text{mol L}^{-1}$	0.012 $\mu\text{mol L}^{-1}$	0.008 $\mu\text{mol L}^{-1}$	0.005 $\mu\text{mol L}^{-1}$	0.002 $\mu\text{mol L}^{-1}$
culture 1	2a	26.96		27.26			26.55		27.42		26.47
	2b	25.74		26.25			28.75		25.69		26.03
	4a	41.36		44.42			43.83		40.77		42.73
	4b	42.46		42.99			43.79		42.58		42.58
	6a	64	63.78	65.02	67.03	64.53	64.83	66.17	62.94	67.88	66.05
	6b	63.78	64.41	65.32	64.67	65.18	65.71	65.97	65.89	66.54	66.95
	8a	90.41	96.77	99.44	102.5	97.85	100.4	100.9	98.55	100.8	100
	8b	95.8	101.5	99.32	100.4	101.5	99.97	103.2	98.49	104.3	101.8
	10a	143.1	144.9	145.4	142.4	117.5	136.7	143.7	137.9	147	143.9
	10b	140.4	144.1	140	140.2	115	138	140.6	139.3	144.9	141.6
	12a	193	168.5	195.3	199.1	129.7	166.7	192.2	193.7	199	195.8
	12b	191	200.3	196	197.8	130.6	161.6	196.4	196.3	199.1	197.6
	14a	259.9	262.8	252.9	254.2	142.5	184.8	248.2	261.3	259.6	250.3
	14b	253.4	271.4	253.2	257.2	138.3	183	241	255.6	257.4	253
culture 2	6a	76.41		79.23			79.03		76.68		75.35
	6b	77.74		75.28			74.24		75.59		75.33
	14a	306.7	314.2	305.4	309.1	169.3	241	302	310.1	307.6	327.8
	14b	312	315.2	307	304	173.1	241.7	300.2	311	303.9	333.5
	16a	394.9	386.1	382.9	383.1	180.8	272.7	374.5	393.9	372.5	413.4
	16b	393.8	380.3	390.1	386	180.4	275.2	369	396	374.7	405.9
	18a	442	438.2	429.9	441.3	196.1	280	421.7	451	414.2	486
	18b	431.6	425.7	429.1	448.3	191.3	292.5	421.9	433.2	417	467.7
	20a-Peak1	33.42	34.2	36.12	33.43	224.7	48.84	36.25	34.01	34.9	33.55
	20a-Peak2	390.4	382.5	411.1	397.8		285.2	367.3	385.2		334.6
	20b-Peak1	34.27	34.95	34.73	32.05	221.7	51.66	36.17	33.02	34.98	31.88
	20b-Peak2	356.5	396.2	382.7	370.3		277	355.3	366.5		321.1
	22a	34.2	34.35	33.37	34.26	275	58.2	37.9	34.77	34.77	33.88
	22b	34.35	34.09	32.88	33.48	277	62.58	35.8	33.72	33.78	35.63
24a	39.55	41.46	40.15	41.58	284.8	66.08	47.51	41.68	41.11	38.97	
24b	40.14	42.65	40.92	41.47	273.6	72.14	47.3	39.59	42.08	38.94	

**Table C.7:** Mean values and standard errors of median effect concentration ( $EC_{50}$ ), slope of the curve ( $\theta$ ), minimum effect level ( $E_{\min}$ ) and maximum effect level ( $E_{\max}$ ) estimated by fitting the four-parametric log-logistic model to the concentration-dependent responses on algae growth at  $t_{14}$  and on reproduction at  $t_{24}$ . The parameter estimations bases on the results of the preliminary range-finding test (df–degree of freedom, SSE–sum of squared errors).

	Time h	$EC_{50}$ [ $\mu\text{mol L}^{-1}$ ]	$\theta$ [-]	$E_{\min}$ [%]	$E_{\max}$ [%]	df	SSE
isoproturon	$t_{14}$	$0.25 \pm 0.01$	$1.82 \pm 0.20$	$-23.05 \pm 4.08$	$77.35 \pm 0.20$	16	154.46
	$t_{24}$	$0.46 \pm 0.04$	$1.74 \pm 0.29$	$-9.22 \pm 3.84$	$95.17 \pm 7.11$		312.76
irgarol	$t_{14}$	$0.12 \pm 0.004$	$3.89 \pm 0.41$	$-14.90 \pm 2.80$	$93.53 \pm 1.87$	14	256.67
	$t_{24}$	$0.13 \pm 0.003$	$6.10 \pm 0.69$	$10.54 \pm 1.73$	$95.36 \pm 1.33$		175.37
metazachlor	$t_{14}$		n.d.			10	
	$t_{24}$	$0.16 \pm 0.02$	$2.26 \pm 0.70$	$-30.20 \pm 15.46$	$107.18 \pm 11.62$		663.11
triclosan	$t_{14}$	$0.00219 \pm 6.25 \times 10^{-4}$	$1.20 \pm 0.25$	$-26.31 \pm 16.09$	$86.68 \pm 2.42$	17	571.09
	$t_{24}$	$0.001 \pm 1.66 \times 10^{-4}$	$1.84 \pm 0.24$	$-0.62 \pm 12.25$	$93.05 \pm 0.71$		96.75
paraquat	$t_{14}$	$19.13 \pm 4.15$	$0.77 \pm 0.15$	$-7.56 \pm 4.71$	$87.88 \pm 7.47$	18	347.85
	$t_{24}$	$8.17 \pm 0.52$	$1.71 \pm 0.17$	$-1.44 \pm 2.12$	$94.17 \pm 1.75$		298.09
PNA	$t_{14}$	$0.24 \pm 12.43$	$3.00 \pm 0.67$	$-23.43 \pm 12.43$	$68.50 \pm 3.56$	16	277.91
	$t_{24}$	$0.28 \pm 0.005$	$6.37 \pm 0.59$	$20.79 \pm 1.96$	$97.34 \pm 1.14$		123.84

**Table C.8:** Mean values and their standard errors of median effect concentrations ( $EC_{50}$ ) and slopes of the curve ( $\theta$ ) were estimated by fitting the two-parametric log-logistic model to the concentration-dependent responses on algae growth over exposure time and on reproduction at  $t_{24}$ . Minimum effect levels ( $EC_{\min}$ ) and maximum effect level ( $EC_{\max}$ ) were fixed to 0 and 100%, respectively due to a limited number of data per time point. The parameter estimations bases on the results of the algae growth.

Time [h]	isoproturon				metazachlor				paraquat			
	$EC_{50}$ [ $\mu\text{mol L}^{-1}$ ]	SE	$\theta$ [-]	SE	$EC_{50}$ [ $\mu\text{mol L}^{-1}$ ]	SE	$\theta$ [-]	SE	$EC_{50}$ [ $\mu\text{mol L}^{-1}$ ]	SE	$\theta$ [-]	SE
8	0.353	0.057	1.386	0.426								
10	0.260	0.027	2.975	1.378					234.099	29.734	0.705	0.067
12	0.257	0.027	2.905	1.333					57.437	9.134	0.563	0.064
14	0.234	0.003	19.309	4.880					29.844	1.635	0.739	0.034
16	0.234	0.003	22.837	8.438					21.839	1.477	0.832	0.050
18	0.234	0.003	23.246	8.221					23.198	1.161	0.981	0.049
20	0.224	0.003	30.620	7.636	–				27.642	2.010	1.323	0.125
24	0.339	0.056	2.600	1.085	0.106	0.012	2.502	0.687	7.237	0.539	1.963	0.243
Time [h]	irgarol				triclosan				PNA			
	$EC_{50}$ [ $\mu\text{mol L}^{-1}$ ]	SE	$\theta$ [-]	SE	$EC_{50}$ [ $\mu\text{mol L}^{-1}$ ]	SE	$\theta$ [-]	SE	$EC_{50}$ [ $\mu\text{mol L}^{-1}$ ]	SE	$\theta$ [-]	SE
8	0.183	0.062	0.703	0.305								
10	0.183	0.024	2.129	0.805	0.083	0.009	1.613	0.242	2.117	0.740	1.042	0.264
12	0.135	0.010	2.194	0.554	0.054	0.007	1.768	0.365	1.174	0.252	1.861	0.677
14	0.131	0.007	3.437	0.752	0.040	0.004	1.766	0.299	0.702	0.054	1.802	0.252
16	0.108	0.003	2.623	0.252	0.036	0.005	2.027	0.499	0.447	0.051	2.044	0.417
18	0.100	0.005	2.246	0.298	0.034	0.007	2.015	0.654	0.400	0.047	2.183	0.488
20	0.070	0.008	2.795	0.505	0.049	0.016	1.329	0.531	0.432	0.053	2.107	0.476
24	0.130	0.004	4.910	0.694	0.016	0.001	7.941	1.526	0.317	0.008	3.960	0.309

**Table C.9:** Coefficient of variation (CoV) calculated for the estimated algae growth parameters ( $\mu_E$  – exponential growth rate,  $\mu_L$  – linear growth rate,  $\mu_C$  – cell-clock growth rate) and toxicodynamic parameters ( $k_I$  – injury rate,  $k_R$  – repair/recovery rate,  $\tau$  – effect progression rate,  $NEC$  – no-effect concentration).

parameter	isoproturon	metazachlor	paraquat	irgarol	triclosan	PNA
$\mu_E$	0.65	0.46	0.33	1.27	1.66	2.66
$\mu_L$	4.29	56.05	3.88	5.81	99.65	52.78
$\mu_C$	8.63	2.52	4.80	13.40	9.34	21.63
$k_I$	3.81	16.65	12.75	4.63	9.71	4.98
$\mu_R$	n.d.	n.d.	$1.58 \times 10^4$	29.97	10.98	4.3
$\tau$	5.94	$0.16 \times 10^{-6}$	8.84	3.65	161449.10	7.63
$NEC$	0	0	0	0	0	0

**Table C.10:** Values of measured effect concentrations and predicted internal effect concentrations for algae growth at  $t_{14}$  and algae reproduction at  $t_{24}$  from this study compared to values from literature summarized by Vogs et al. (2015) for all six model chemicals.

chemical	time	<sup>a</sup> EC <sub>50</sub> [ $\mu\text{mol L}^{-1}$ ]	<sup>b</sup> EC <sub>50</sub> [ $\mu\text{mol L}^{-1}$ ]	<sup>c</sup> EC <sub>50</sub> [ $\mu\text{mol L}^{-1}$ ]	<sup>d</sup> IEC <sub>50</sub> [mmol kg <sub>wet weight</sub> <sup>-1</sup> ]	<sup>e</sup> IEC <sub>50</sub> [mmol kg <sub>wet weight</sub> <sup>-1</sup> ]
isoproturon	$t_{14}$	0.25	0.23		0.08	
	$t_{24}$	0.46	0.34	0.138	0.12	0.0476
irgarol	$t_{14}$	0.12	0.13		0.67	
	$t_{24}$	0.13	0.13	0.022	0.67	0.112
metazachlor	$t_{14}$	n.d.	n.d.			
	$t_{24}$	0.16	0.11	0.168	0.10	0.157
triclosan	$t_{14}$	0.00219	0.040		2.74	
	$t_{24}$	0.001	0.0158	0.0065	1.08	0.458
paraquat	$t_{14}$	19.13	29.844		2.16	
	$t_{24}$	8.17	7.24	0.781	0.52	0.056
PNA	$t_{14}$	0.24	0.702		34.91	
	$t_{24}$	0.28	0.316	0.153	15.75	7.615

a – EC<sub>50</sub> values derived from preliminary concentration range-finding experiments, exposure started at  $t_6$  and  $t_8$ ;

b – EC<sub>50</sub> values derived from algae growth assay by using six measurements per time point, exposure started at  $t_6$  and  $t_8$

c – Vogs et al. (2015) reported EC<sub>50</sub> values summarized from literature, EC<sub>50</sub> values based on chemical exposure starting at  $t_0$ ,

d – estimated internal effect concentrations for algae growth at  $t_{14}$  by  $BCF_{kin} \cdot EC_{50}(t_{14})$  and for algae reproduction at  $t_{24}$  by  $BCF_{kin} \cdot EC_{50}(t_{24})$

e – Vogs et al. (2015) reported kinetic bioconcentration factors ( $BCF_{kin}$ ) and internal effect concentrations (IED<sub>50</sub>) for the six model chemicals

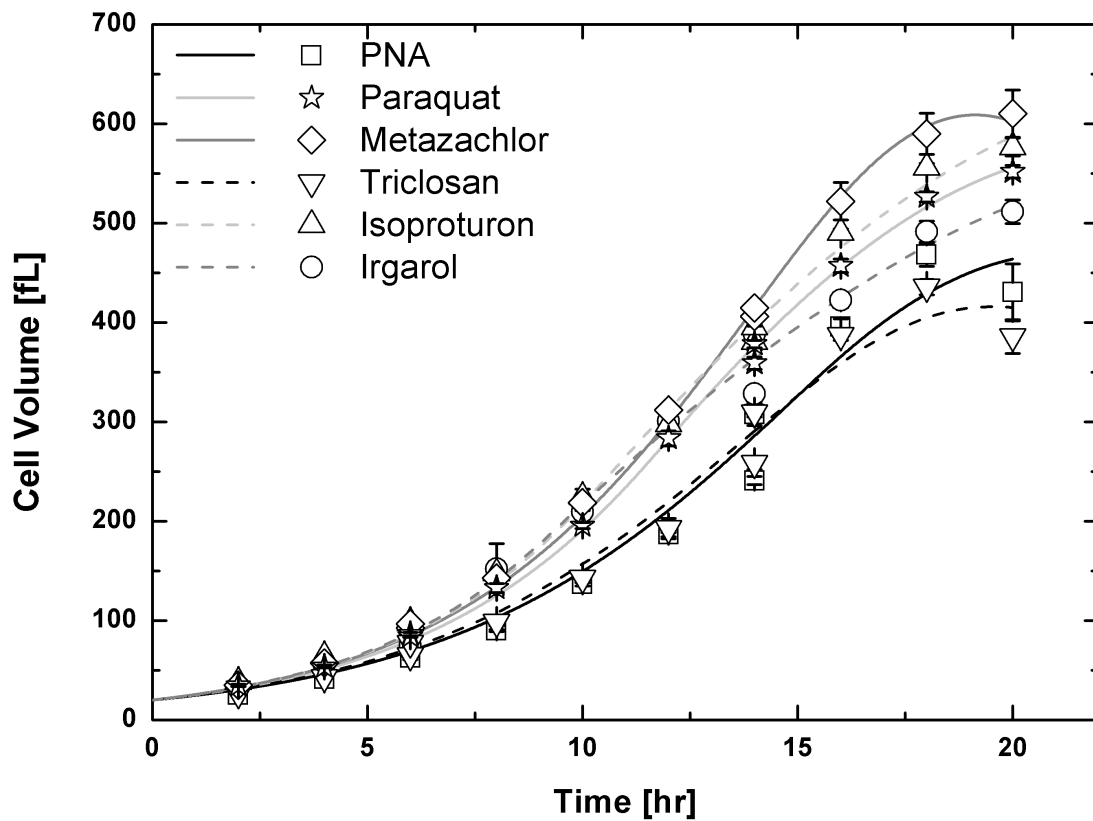


**Figure C.1:** The unperturbed growth of *S. vacuolatus* synchronized cultures was measured in parallel to each algae growth assay with PNA, paraquat, metazachlor, triclosan, isoproturon, and irgarol. The symbols represent the mean cell volumes ( $\pm 95\%$  CI) for the control group of the first generation (measurements from two untreated and two DMSO-treated cultures). Each control group consists of eight measurements per time point except  $t_6$  or  $t_8$  and  $t_{14}$  with 16 measurements. The lines show the simulations of the predicted time-course of the first generation cell volume.

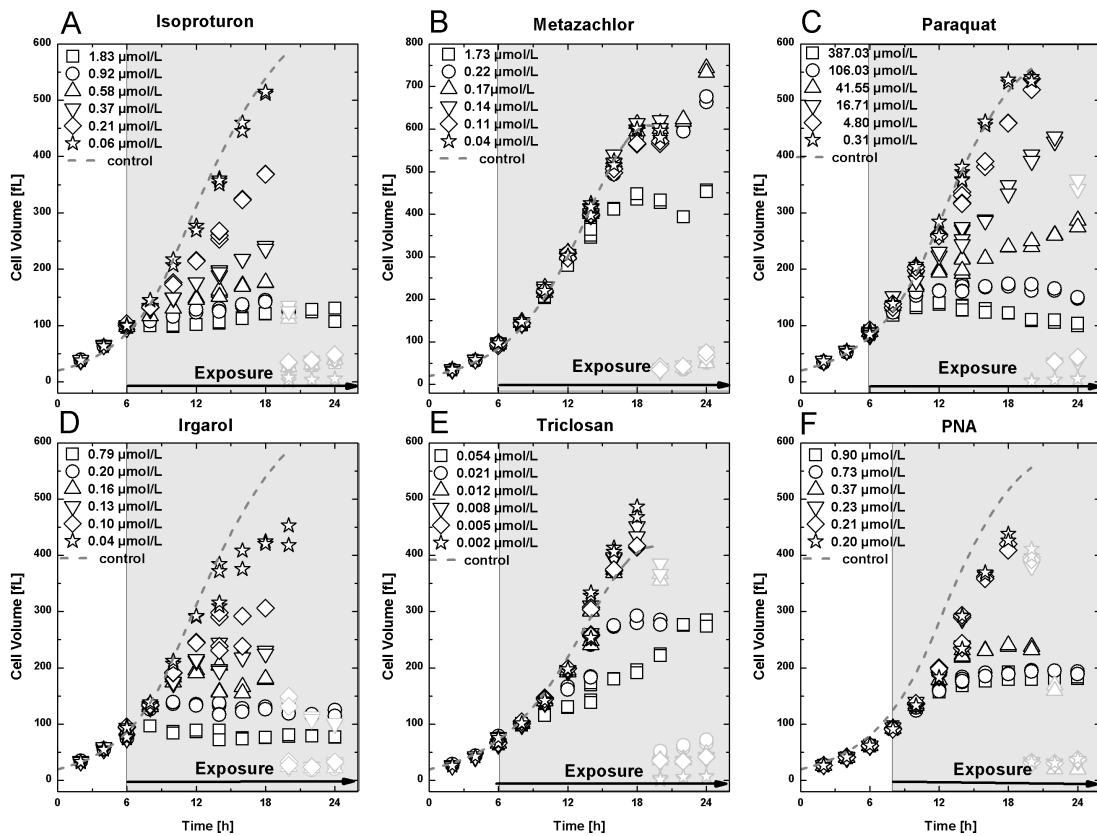


**Figure C.2:** Measured cell volumes of the first (open symbols) - and second-generation (closed symbols) algae cycle at different time points affected by six different concentrations per chemical. The unperturbed algae growth is simulated (dashed line). Grey box represents the exposure time frame.

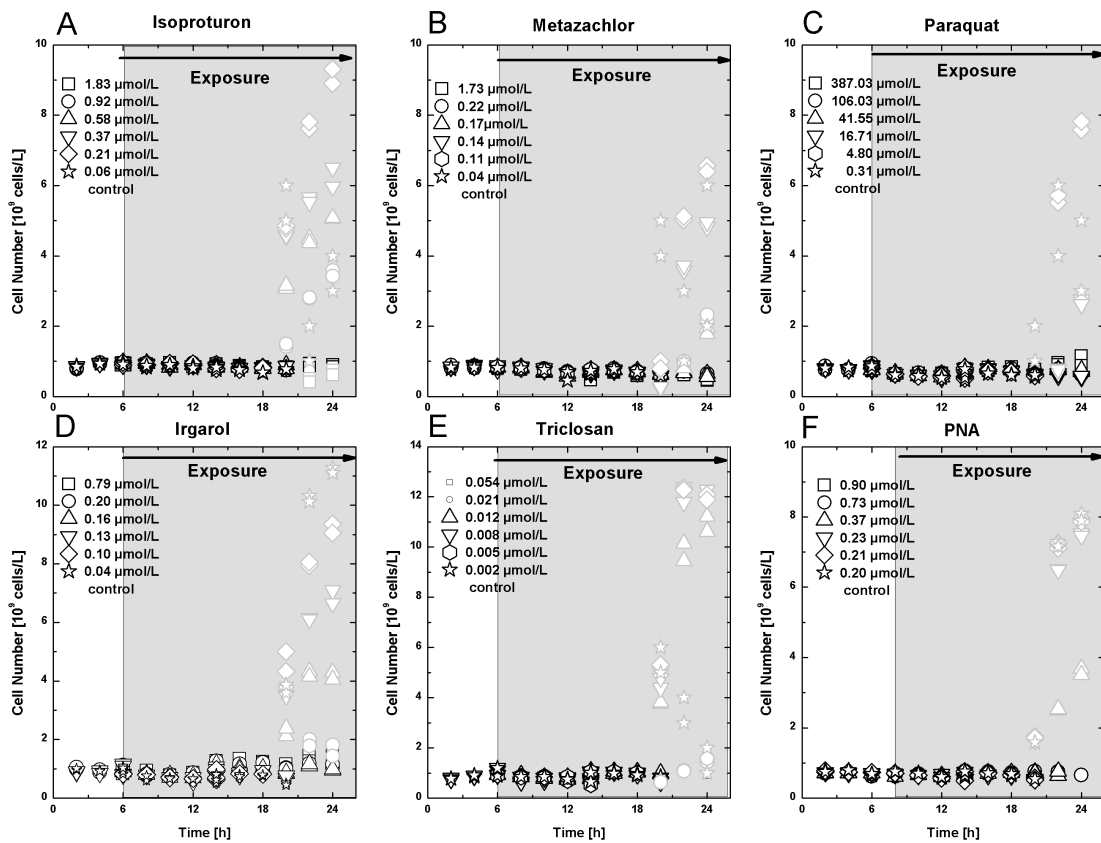


**Figure C.3:** Measured cell numbers of the first (open symbols) - and second-generation (closed symbols) algae cycle at different time points affected by six different concentrations per chemical. Grey box represents the exposure time frame.

# Acknowledgment

I would like to express my gratitude to Prof. Dr. Rolf Altenburger who provided the exciting topic in the Department Bioanalytical Ecotoxicology and advised my PhD work all the years. Thank you so much Rolf for trusting my ideas and for accompanying me on this rocky way. Prof. Dr. Henner Hollert is greatly acknowledged for accepting me as an external PhD student in RWTH Aachen and for evaluating this manuscript.

This PhD work was financed by the German Federal Ministry of Education and Research project "ProDarT" (FKZ 0315399) led by Dr. Eberhard Küster. Thank you Eberhard for welcoming me in your team and giving me some space to conduct my own research, meanwhile working on the ProDarT project goals. This work was further supported by The Helmholtz Research Program "Chemicals in the Environment" and the Helmholtz Interdisciplinary Graduate School for Environmental Research—"HiGrade".

I further want to express my appreciation to the technical assistance of Janet Krüger and Silke Ahlhorn in the laboratories. I am thankful to you guys, because you trusted a "modeler" being in your labs and introduced me how to use a pipette. I guess it was quite adventurous for all of us. Special thanks go to Janet. The quality of this PhD thesis is partly owed your exhaustless support in the lab work and the sharing hours of the nearly 24 hours experiments. Thanks also goes to Karen Herold, Christine Hug and Thomas G. Nicholls for their help in the lab.

Thanks to all members of the Department Bioanalytical Ecotoxicology, who created an inspiring and motivating atmosphere. I specifically would like to express my sincere appreciation to Agnes, Janet R., Jule, Steph and Wibke. Thank you so much for considering me as a discussion partner on exciting topics and for being open to the modeling world. The beauty to share ideas and knowledge is what I love most in science. Further, I would like to express my deepest thanks to the Leipziger Crew Christine, Egina & Brock, Fred, Steffi & Sven. All you guys are amazing and influenced me in many ways. I will miss our great discussions and laughs around life and science, especially around 4 p.m.. Nevertheless, I have the impression that this won't be the end of our journey in Leipzig but more a beginning of another great chapter dealing with Saxony exile lives within "Captain Planet". Thanks so much for being there!

I am also grateful to my "normal" friends Annika, Julia, Katja, Mira, Sabine, Sharon and all my fantastic friends from home. But to let you know: To my knowledge, the definition of "normal" or "adverse" is still under discussion in (eco)toxicology ... so let's hope! Unbelievable that you are still my friends talking to me while I have become a "science zombie" over the years.

At the end, I would like to draw the attention to my family. Thank you so much for supporting me with all your interests and concerns! Ich weiss, dass der von mir gewählte Weg für euch faszinierend ist und doch gleichzeitig ein Mysterium darstellt. Danke für eure Akzeptanz meiner Leidenschaft zur Wissenschaft, wo ich bisher meine Kreativität auslebte. Aber ich danke euch auch zutiefst, dass ihr meine Entwicklung mit allen veränderten Persönlichkeitszügen während dieser Zeit mitgetragen habt. Eine Freundin hat erst kürzlich zu mir gesagt, dass die 30er eines Menschen das intellektuelle Zeitfenster repräsentieren. Macht euch also auf mehr gefasst. Und ich kann es mir nicht verkneifen meine Danksagung mit diesen letzten Worten zu schließen: Wissenschaft ist nicht wie in der Serie "Big Bang Theory" dargestellt.



# Curriculum Vitae

Name: Carolina Vogs  
Date of Birth: 22.06.1983  
Place of Birth: Wernigerode  
Citizenship: German

## Education

---

currently: Guest scientist at UFZ – Helmholtz-Centre for Environmental Research, Department Bioanalytical Ecotoxicology

2011 – 2015: External PhD at the Institute for Environmental Research, RWTH Aachen University realization of work at UFZ – Helmholtz-Centre for Environmental Research, Department Bioanalytical Ecotoxicology  
Project funded PhD entitled **”Understanding toxicity as processes in time – Analyzing and modeling effects on algae cell cycle process exposed to organic chemicals”**

2003 – 2009: **Study of geoecology** at the Technical University of Braunschweig, Germany; course specializations: ecotoxicology, geochemistry, environmental system analyses, agricultural ecology, and soil physics

2008 – 2009: Diploma thesis **”Modelling and sensitivity analysis of water flow and colloid transport in an undisturbed Hanford sediment”**  
A cooperation between the Technical University of Braunschweig, Institute of Geoecology (Prof. Dr. Wolfgang Durner) and the Washington State University, Department of Crop and Soil Sciences (Prof. Dr. Markus Flury)

1996 – 2003: **Grammar school**, Wernigerode

## Work experiences

---

- 2012 – 2014: Research scientist in the project **”Establishment of a concept for comparative risk assessment of plant protection products with special focus on the risks to the environment”** financed by the German Environmental Agency
- 2009 – 2012: Research scientist in the project **”The fish embryo (*Danio rerio*) as replacement tool for the acute fish test: Determination of bioconcentration, the effective dose and the chemical potency of lipophilic organic substances by using chemical-analytical tools and proteomics”** (ProDarT) financed by the Federal Ministry of Education and Research
- 2007 – 2008: **Internship** at Washington State University (USA) to provide assistance to the project **”Long-term colloid mobilization and colloid-facilitated transport of radionuclides in a semi-arid vadose zone”**

# List of Publications

## The thesis is based on the following publications:

---

- **Vogs, C.**, Altenburger, R., (2015): How toxicokinetic and toxicodynamic processes in *Scenedesmus vacuolatus* contribute to the time dependence of toxicity? - A modeling case study for different adverse outcome pathways. (In prep.)
- **Vogs, C.**, Kühnert, A., Hug, C., Küster, E., Altenburger, R., (2015): A toxicokinetic study of specifically acting and reactive organic chemicals for the prediction of internal effect concentrations in *Scenedesmus vacuolatus*. Environ. Toxicol. Chem., 32(5), 1161 - 1172
- **Vogs, C.**, Bandow, N., Altenburger, R., (2013): Effect propagation in a toxicokinetic/ toxicodynamic model explains delayed effects on the growth of unicellular green algae *Scenedesmus vacuolatus*. Environ. Toxicol. Chem. 32 (5), 1161 - 1172

## Co-authored peer-reviewed publications

---

- Massei, R., **Vogs, C.**, Renner, P., Altenburger, R.: Differential sensitivity in embryonic stages of the zebrafish (*Danio rerio*): the role of toxicokinetics for stage-specific susceptibility for azinphos-methyl lethal effects. (submitted).
- Faust, M., **Vogs, C.**, Rotter, S., Wöltjen, J., Höllrigl-Rosta, A., Altenburger, R., (2014): Comparative assessment of plant protection products: how many cases will regulatory authorities have to answer?. Env. Sci. Eur. online.
- Kühnert, A., **Vogs, C.**, Altenburger, R., Küster, E., (2013): The internal concentration of organic substances in fish embryos – a toxicokinetic approach. Environ. Toxicol. Chem. 32 (8), 1819 - 1827
- Liu, Z., Flury, M., Harsh, J.B., Mathison, J.B., **Vogs, C.**, (2013): Colloid mobilization in an undisturbed sediment core under semiarid recharge rates. Water Resour. Res. 49 (8), 4985 - 4996

## Platform presentations

---

- **Vogs C**, Krüger J, Altenburger R. 2013. Predicting the effect progression time affecting growth of the green algae *Scenedesmus vacuolatus* - A Toxicokinetic/toxicodynamic modeling case study. Platform Presentation CREAM Meeting in Leipzig, Germany
- **Vogs C**. 2012. Toxicokinetic/toxicodynamic modeling of synchronized *Scenedesmus vacuolatus* growth using a model for cancer cell growth. Platform Presentation HiGrade Conference in Leipzig, Germany
- **Vogs C**, Bandow N, Altenburger R. 2012. Toxicokinetic/toxicodynamic modeling of synchronized *Scenedesmus vacuolatus* growth using a model for cancer cell growth. Platform Presentation SETAC World 6th Meeting in Berlin, Germany
- Kühnert, A, **Vogs C**, Küster, E. 2012. Determination of internal chemical concentration in zebrafish (*Danio rerio*) embryos – a toxicokinetic approach. Platform Presentation SETAC World 6th Meeting in Berlin, Germany
- **Vogs C**, Bandow N, Altenburger R. 2012. Toxicokinetic/toxicodynamic modeling of synchronized *Scenedesmus vacuolatus* growth by using a model for cancer cell growth. Poster Presentation SETAC GLB 2012 in Leipzig, Germany
- **Vogs C**, Bandow N, Altenburger R. 2011. Modeling of the time-dependent kinetic of green algae growth exposed to N-Phenyl-2-naphthylamine. Poster Presentation HiGrade Evaluation 2011 in Leipzig, Germany
- **Vogs C**, Bandow N, Altenburger R. 2010. Modeling of the time-dependent kinetic of green algae growth exposed to N-Phenyl-2-naphthylamine. Poster Presentation SETAC GLB 2010 in Dessau, Germany

”Ich bin immer noch verwirrt, aber auf einem höheren Niveau.”

Enrico Fermi (1901 – 1954)

